MASTER

MND-P-2352

FINAL SAFETY ANALYSIS REPORT— SNAP 1A RADIOISOTOPE FUELED THERMOELECTRIC GENERATOR

By
George P. Dix

June 30, 1960

Nuclear Division
Martin Company
Baltimore, Maryland

UNITED STATES ATOMIC ENERGY COMMISSION • OFFICE OF TECHNICAL INFORMATION

DISCLAIMER

This report was prepared as an account of work sponsored by an agency of the United States Government. Neither the United States Government nor any agency Thereof, nor any of their employees, makes any warranty, express or implied, or assumes any legal liability or responsibility for the accuracy, completeness, or usefulness of any information, apparatus, product, or process disclosed, or represents that its use would not infringe privately owned rights. Reference herein to any specific commercial product, process, or service by trade name, trademark, manufacturer, or otherwise does not necessarily constitute or imply its endorsement, recommendation, or favoring by the United States Government or any agency thereof. The views and opinions of authors expressed herein do not necessarily state or reflect those of the United States Government or any agency thereof.

DISCLAIMER

Portions of this document may be illegible in electronic image products. Images are produced from the best available original document.

LEGAL NOTICE

This report was prepared as an account of Government sponsored work. Neither the United States, nor the Commission, nor any person acting on behalf of the Commission:

A. Makes any warranty or representation, expressed or implied, with respect to the accuracy, completeness, or usefulness of the information contained in this report, or that the use of any information, apparatus, method, or process disclosed in this report may not infringe privately owned rights; or

B. Assumes any liabilities with respect to the use of, or for damages resulting from the use of any information, apparatus, method, or process disclosed in this report.

As used in the above, "person acting on behalf of the Commission" includes any employee or contractor of the Commission, or employee of such contractor, to the extent that such employee or contractor of the Commission, or employee of such contractor prepares, disseminates, or provides access to, any information pursuant to his employment or contract with the Commission, or his employment with such contractor.

This report has been reproduced directly from the best available copy.

Printed in USA. Price $3.00. Available from the Office of Technical Services, Department of Commerce, Washington 25, D. C.

USAEC Office of Technical Information Extension
Oak Ridge, Tennessee

MND-P-2352

PHYSICS

FINAL SAFETY ANALYSIS REPORT-- SNAP 1A RADIOISOTOPE FUELED THERMOELECTRIC GENERATOR

June 30, 1960

This report is prepared under
Contract AT (30-3)-217 with the
United States Atomic Energy
Commission

Prepared by:

George P. Dix
Nuclear Safety Analysis Unit

Approved by:

Douglas G. Harvey
Project Engineer

Nuclear Division
Martin Company
Baltimore, Maryland

page blank

FOREWORD

This is the final safety analysis report prepared by The Martin Company for the Task 2 Radioisotope Powered Thermoelectric Generator under U.S. Atomic Energy Commission Contract AT(30-3)-217. It presents analyses, tests and evaluation of the operational safety criteria for the generator.

page blank

CONTENTS

		Page
	Foreword	iii
	Summary	vii
I.	Introduction	1
II.	Description of Task 2 Thermoelectric Generator	3
	A. Generator Design	3
	B. Radiocerium Fuel	5
	C. Fuel Core	10
III.	Transport of Generator to Launch Site	17
	A. Shipping Cask	17
	B. Shipping Procedures	19
	C. Shipping Hazards	21
IV.	Ground Handling and Vehicle Integration	25
	A. Preparation for Transfer	25
	B. Transfer of Fuel Core to Generator	25
	C. Mating of Generators to Final Stage	27
	D. Mating of Final Stage to Booster	30
	E. Auxiliary Support Equipment	30
V.	Flight Vehicle	33
	A. Booster-Sustainer Stage	33
	B. Final Stage	33
	C. Propellants	36
	D. Safety Systems	36

CONTENTS (continued)

		Page
VI.	Missile Range	37
	A. Launch Complex	37
	B. Range Safety	37
VII.	Biological Shield	43
	A. Bare Core Source	43
	B. Shielded Generator	43
	C. Fuel Transfer	49
	D. Burial in Soil and Marine Immersion	49
VIII.	Successful Mission	53
	A. Radiocerium Inventory Prior to Re-Entry	53
	B. Re-Entry of Generators	53
IX.	Aborted Missions	59
	A. Definition of Aborted Missions	59
	B. Definition of Forces Imposed by Aborted Missions	67
X.	Summary and Conclusion	79
	A. Successful Mission	79
	B. Aborted Missions	79
	C. Fallout Pattern	90
XI.	References	99
	Appendix A--Safety Test Program	A-1
	Appendix B--Aerodynamics	B-1

SUMMARY

This report describes the safety aspects involved in utilizing the Task 2 Radioisotope Powered Thermoelectric Generator in a terrestrial satellite. It is based upon a generalized satellite mission having a 600-day orbital lifetime.

A description of the basic design of the generator is presented in order to establish the analytical model. This includes the generator design, radiocerium fuel properties and the fuel core.

The transport of the generator to the launch site is examined, including the shipping cask, shipping procedures and shipping hazards.

A description of ground handling and vehicle integration is presented including preparation for fuel transfer, transfer, mating of generators to final stage, mating final stage to booster, and auxiliary support equipment.

The flight vehicle is presented to complete the analytical model. Contained in this chapter are descriptions of the booster-sustainer, final stage, propellants and built-in safety systems.

The typical missile range is examined with respect to the launch complex and range safety characteristics.

The shielding of the fuel is discussed and includes both dose rates and shield thicknesses required. The bare core, shielded generator, fuel transfer operation and dose rates for accidental conditions are treated.

The mechanism of re-entry from the successful mission is covered. Radiocerium inventories with respect to time and the chronology of re-entry are specifically treated.

The multiplicity of conditions for aborted missions is set forth. The definition of aborted missions is treated first in order to present the initial conditions. Following this, a definition of the forces imposed upon the generator is presented.

The fate of the radiocerium fuel following both successful and aborted missions is presented. A large number of initial vehicle failure cases is narrowed down into categories of consequences. Since stratospheric injection of fuel results in cases where the fuel is not contained after re-entry, an extensive discussion of the fallout mechanism is presented.

I. INTRODUCTION*

This report summarizes the safety aspects associated with the use of the Task 2 nuclear thermoelectric generators as auxiliary power units for satellite vehicles. Two generators, each fueled with 0.88 megacurie of Cerium-144, produce thermal energy from beta decay which is thermoelectrically converted to 250 watts of electrical power. The Task 2 generator and its application have provided an ideal analytical model for defining radiological consequences and developing countermeasures for nuclear energy supplies used in space.

The safety of this application has been under examination for the past three years and has been supplemented by experimentation in areas where solution by theoretical means would have been difficult. The delineation of safety problems has led to the development of certain design countermeasures to enhance the safety of the mission. Though statistical data on operational failures is quite variable at present, an attempt has been made to relate statistical frequency of various failures with their consequences.

The Task 2 generator has been designed to be ablated and the fuel dispersed as an aerosol above 100,000 feet on re-entry from orbital decay, as recommended by the SNAP Hazards Subcommittee. This has been the basis of aerothermodynamic design criteria. A typical satellite has a lifetime of 600 days, and this time span is used to obtain data conditions of re-entry from successful missions.

Fifty-five cases of vehicle abort are evaluated, including launch, ascent and final stage failures, and the consequences are described.

This report is a refinement and revision of the preliminary safety report, MND-P-2184, submitted to the Commission in December 1959.

---

* Aerodynamics by W. Hagis and R. Oehrli; tests by T. J. Dobry

page blank

II. DESCRIPTION OF TASK 2 THERMOELECTRIC GENERATOR

Two Task 2 thermoelectric generators are designed to power certain electrical equipment in a satellite system. Each generator is designed to supply 125 electrical watts, 28 volts, and 4.46 amperes into a matched impedance load for a period of one year. A single generator produces 6500 thermal watts initially from the decay heat of the radioisotope core fueled with 0.88 megacurie of Cerium-144. To provide a constant power level, 4000 watts of the initial thermal output are radiated to the environment. During the one-year life span, this rejected radiant heat is gradually decreased by a built-in servomechanism to compensate for radioisotope decay.

A. GENERATOR DESIGN

1. Complete Unit

The generator is cylindrical with hemispherical ends and is 34.1 inches long by 24.0 inches in diameter. The unit weighs approximately 200 pounds during operation, and 4200 pounds when the mercury shield is present during prelaunch preparations. As shown in Fig. 1, the unit consists of a fuel core and core support structure and an outer shell. The biological shield, fuel core and core support structure are discussed in more detail in the following paragraphs.

A biological shield consisting of 4000 pounds of mercury fills the internal volume of the outer shell. The mercury is pumped into the generator for prelaunch ground handling and is drained five minutes before launch.

The outer shell of the generator consists of a sandwich of aluminum outer skin 0.051 inch thick, a meat of Min-K 1301 insulation 1.5 inches thick which encloses 554 lead telluride thermoelectric elements (277 pairs), and an inner skin of Type 316 stainless steel 0.063 inch thick. The outer skin is at 335° F and the inner skin is at 1075° F during steady-state operation in a space environment. The thermoelectric system is designed for rated output at hot and cold junction temperatures corresponding to the skin temperatures.

An internal radiant heat reflector is designed into the generator. This serves a twofold purpose:

(1) It redirects the high intensity thermal radiation from the fuel core toward the thermal shutter area where the heat is eventually dumped in a regulated fashion.

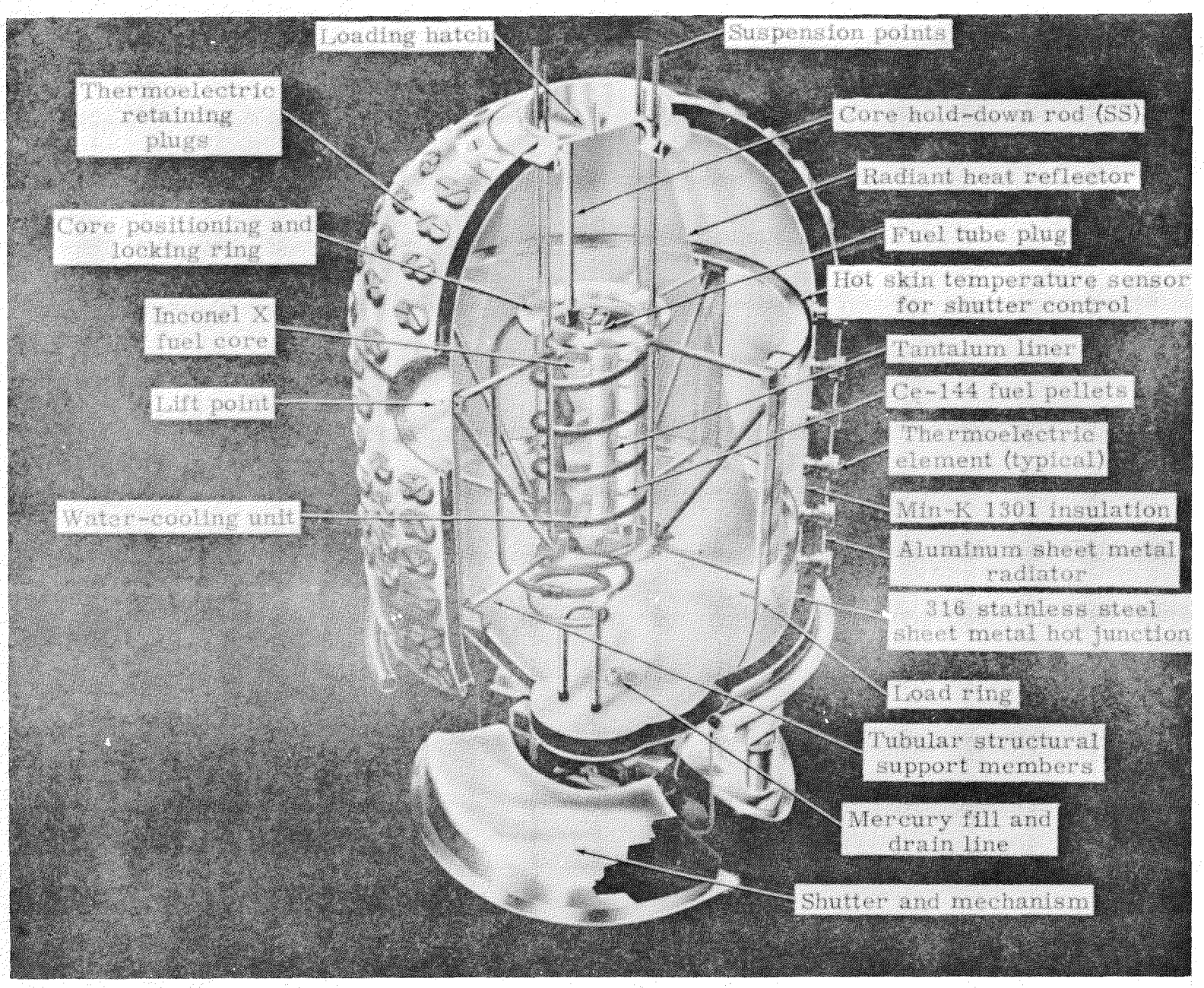

Fig. 1. Task 2 Nuclear Thermoelectric Generator

(2) It equalizes the temperatures on the inner skin of the unit.

The reflector consists of a two-layer stainless steel cone and is installed in the annular space between the fuel core support structure and the inner skin. A thermal shutter is located on the bottom of the unit and is activated by a servomechanism. The latter senses and regulates the hot skin temperature of the unit by controlling the amount of the inner skin that is exposed to space.

2. Core Support Structure

The Type 316 stainless steel core support and internal frame structures of the generator contribute to the overall integrity of the generator. As shown in Fig. 1, the core support structure consists of an upper core positioning and locking ring, a lower core support ring and four guide struts connecting the two rings. A Type 316 stainless steel hold-down positioning rod, attached to the loading hatch cover located in the upper part of the generator, is provided to ensure a positive indication that the fuel core is properly positioned within the generator. The loading hatch is bolted down after the fuel core is inserted.

The internal frame structure, also shown in Fig. 1, consists of a top and bottom load ring, four tubular trusses connecting the core support structure and load rings, and four lateral lift points attached to the upper core support ring. The core support and internal frame structures provide a rigid structure with eight mounting points for handling the unit and attaching it to the vehicle support members.

B. RADIOCERIUM FUEL

The amount of radiocerium fuel is predicated upon a required initial thermal output of 6500 watts. Given the constant power activity of Cerium-144 as 0.0074 watt/curie, a loading of 0.88 megacurie is required. This is approximately 3320 grams or 615 cubic centimeters of the fuel compound per generator. After screening various cerium compounds for the optimum fuel form, ceric oxide with certain additives was selected. Oak Ridge National Laboratory (ORNL) fuel material is formed into ceramic pellets containing 89% CeO_2, 10% SiC and 1% CaO by weight.

This fuel form readily disintegrates and disperses when subjected to intense re-entry heating, a prime safety criterion of the overall program. The properties of various radiocerium compounds are discussed in other reports (Refs. 1, 2, 3, 4). Table 1 summarizes properties of the fuel.

TABLE 1

Properties of the Ce-144 O_2 and CeO_2-SiC_2 Fuel Forms

	Ce-144 O_2	Ce-144 O_2 + 10% SiC
Chemical		
Solubility	Insoluble	--
Concentrated H_2SO_4, HNO_3	Soluble	--
Dilute acid	Insoluble	--
Stability in air	Stable	--
Physical		
Molecular weight	140.13	--
Color	Yellow-white	Gray-green
Melting point (°C)	2600	1800 (D)*
Boiling point (°C)	3800	--
Theoretical density (gm/cc)	7.3	6.44
Pellet bulk density (gm/cc)	5.6	5.4
Crystalline structure	Face-centered cubic	--
Thermal		
Thermal conductivity (cal/sec/cm/°C)	0.01	--
Specific heat (cal/gm/°C)	0.1	--
Thermal coefficient of expansion (cm/cm/°C)	12.1×10^{-6}	--
Specific activity (curies/gm)		
Theoretical	2.6×10^3	2.34×10^3
ORNL process	295	265
Specific power (watts/gm)		
Theoretical	19.2	17.3
ORNL process	2.18	1.96
Power activity--ORNL process (watt/curie)	0.0074	0.0074
Power density--ORNL process (watts/cc)	12.2	10.6

*(D) decomposes

Nuclear Properties of Cerium-144 and Its Daughters

Radionuclide	Half Life	Mode of Decay	Specific Activity (curies/gm)
$_{58}Ce^{144}$	285 days	β^-	3.2×10^3
$_{59}Pr^{144}$	17.5 minutes	β^-	7.5×10^7
$_{60}Nd^{144}$	1.5×10^{15} years	α	5.0×10^{-13}

Radionuclide	Energy of Decay Particles (mev)	Relative Abundance (%)	Gamma Energy (mev)	Relative Abundance (%)	Other Radiation
$_{58}Ce^{144}$	0.327 0.258 0.16	75 5 20	0.054 0.080 0.134	3.0 3.0 7.5	X from bremsstrahlung
$_{59}Pr^{144}$	3.01 2.30 0.79	~98 1.3 1.0	0.69 1.50 2.18	1.6 0.25 0.8	X from bremsstrahlung
$_{60}Nd^{144}$	1.9	100	None	--	--

1. Chemical Properties

Cerium and its daughters, praseodymium and neodymium, are members of the rare earth series of elements. Ceric oxide, the basic ingredient of the fuel mixture, is insoluble in hot water and dilute acid solutions, but is soluble in sulfuric and nitric acids. The addition of 10% silicon carbide to the ceric oxide fuel lowers the effective melting point of the fuel pellets. Some Ce_2O_3, CeC_2 and $CeSi_2$ will be formed in the fuel pellets at elevated temperatures. The fuel form (CeO_2 + 10% SiC) is compatible with Inconel X, the primary encapsulating material.

Because of the difference in oxidation states between cerium and its decay products, praseodymium and neodymium, an evolution of oxygen within the fuel occurs during decay according to the following equation:

$$12\ CeO_2 \xrightarrow{\beta^-} 2\ Pr_6O_{11} + O_2 \uparrow \xrightarrow{\beta^-} 6\ Nd_2O_3 + 2\ O_2 \uparrow$$

The maximum evolution of oxygen from 0.88 megacurie of ceric oxide is 152 grams over an infinite decay time. This oxygen would be evenly distributed in the seven fuel cavities. The maximum internal pressure would occur after 450 days and would be 9400 psi if all of the oxygen were liberated into the free volume of the individual fuel cavities. This is a maximum approximation of pressure because much of the evolved oxygen would remain in the lattices of the fuel material instead of migrating to the free volume.

To prevent this pressure buildup within the fuel core, tantalum liners could be placed around the fuel to combine with the free oxygen.

2. Physical Properties

The ceric oxide-silicon carbide fuel mixture has a bulk density of 5.4 gm/cc corresponding to a cerium density of 4.0 gm/cc. Pure ceric oxide melts at 2600° C and boils at 3800° C, but the 10% SiC additive produces decomposition of the fuel at 1800° C. When subjected to a plasma arc heat input of 180 Btu/ft^2-sec, the measured ablation rate was 30 seconds per linear inch of fuel; effluent particles were measured at well below 10 microns.

3. Thermal Properties

Ceric oxide has a thermal conductivity of 0.01 cal/cm-sec-°C, a specific heat of 0.1 cal/gm-°C, and a thermal coefficient of expansion of 12.1×10^{-6} cm/cm/°C. The theoretical specific activity of pure Ce-144 O_2 is 2.6 kc/gm, corresponding to a specific power of 19.2 watts/gm. The ceric oxide-silicon carbide fuel has a specific activity of 265 curies/gm corresponding to a specific power of 1.96 watts/gm. The difference between the theoretical values and predicted fuel value is caused by impurities, additives and radioactive decay, all arising as a result of the fuel reclamation and fabrication process.

4. Nuclear Properties

Cerium-144 is a fission product which is separated from reactor wastes at ORNL. Some of the radiation and resultant thermal power associated with radiocerium originates in the beta decay of Ce-144 to Pr-144, but most of the thermal power is derived from the decay of Pr-144 to Nd-144. Aside from the decay gamma radiation emitted, a large portion of the photons emitted are X-rays resulting from the slowing down of beta decay particles by electron shells (bremsstrahlung). Figure 2 shows the decay scheme of Ce-144.

Cerium-144 has the following genetic relationships.

$$\text{Xe-144}\ (\beta^-) \rightarrow \text{Cs-144}\ (\beta^-) \rightarrow \text{Ba-144}\ (\beta^-) \rightarrow \text{La-144}\ (\beta^-) \rightarrow \text{Ce-144}\ (\beta^-) \rightarrow$$

$$\text{Pr-144}\ (\beta^-) \rightarrow \text{Nd-144}$$

$$\uparrow \text{U-235}\ (n, \gamma)\ \text{Fission}$$

Cerium-144 has a half life of 285 days and decays through beta emission to Pr-144. The Ce-144 beta energies, given in mev, are 0.30 (75%), 0.25 (~5%), and 0.16 (20%). The decay gammas vary from 0.012 to 0.134 mev.

Praseodymium-144 has a half life of 17.5 minutes and decays through beta emission to Nd-144. The praseodymium beta energies, given in mev, are 3.0 (98%), 2.3 (~1.3%) and 0.79 (0.6%). It is readily apparent that the 3-mev beta is a major source of thermal power and high energy bremsstrahlung from the radiocerium fuel. The Pr-144 decay gammas vary from 2.18 to 0.69 mev.

Neodymium-144 has a half life of 1.5×10^5 years and decays through emission of a 1.5 mev alpha particle. Because of its long half life, Nd-144 is considered to be stable.

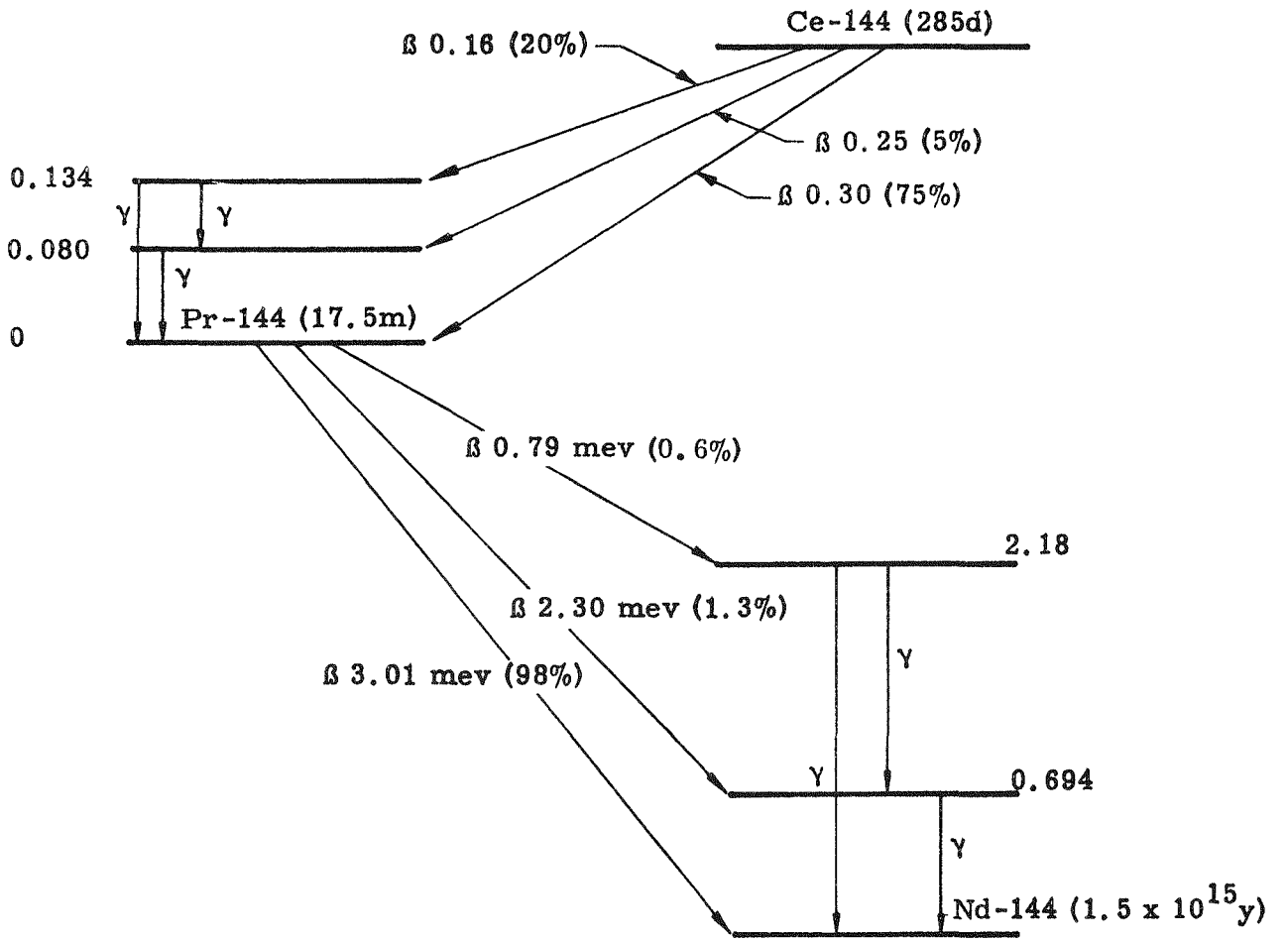

Fig. 2. Decay Scheme of Cerium-144

The spectral distribution of decay gamma radiation from Ce-144 to Nd-144 is well known. However, the spectrum for X-radiation from bremsstrahlung is somewhat obscure because of the lack of experimental data. The bremsstrahlung covers a broad range of energies with a maximum energy approaching that of the impinging beta particles and an average energy which is much lower. The bremsstrahlung is an important factor in shielding the generator.

5. Radiobiological Properties (Refs. 5 and 6)

The direct external radiation doses from the fuel are discussed in Chapter VII, Shielding, so the following discussion is limited to internal radiation hazards only.

Because of its relative insolubility, cerium would not be expected to be conducive to biological uptake. Though Ce-144 does not occur in natural abundance, more than 100 megacuries of it have been produced from weapons testing and dispersed throughout the world. A composite sample of milk from the New York area was found to contain about 1 d/m/liter (4.5×10^{-13} curie/liter), Ref. 10. This observed value is about a million times less than the maximum permissible concentration in drinking water (10^{-7} curie/liter). Since it is an insoluble material, the maximum permissible concentrations applying to the lungs and large lower intestine are of particular interest. The radiobiological properties of Ce-144 and its daughters, Pr-144 and Nd-144, are shown in Table 2.

C. FUEL CORE

The radiocerium is encapsulated in a right cylindrical core. The basis of the design of the core was dictated by the following requirements:

(1) Ability to withstand impact and shock at elevated temperatures.

(2) Corrosion resistance in sea water.

(3) Resistance to oxidation at high temperatures.

(4) Burnup on re-entry into the earth's atmosphere after orbital decay.

Inconel X was selected over a number of potential core materials because it met these requirements.

TABLE 2

Radiobiological Properties of Cerium-144

Form	Organ of Preference	Maximum Permissible Body Burden (μc)	Maximum Permissible Concentration: 40-hr Week Water (μc/cc)	40-hr Week Air (μc/cc)	168-hr Week Water (μc/cc)	168-hr Week Air (μc/cc)
Soluble	GI tract	-	3×10^{-4}	8×10^{-8}	10^{-4}	3×10^{-8}
	Bone	5	0.2	10^{-8}	0.08	3×10^{-9}
	Liver	6	0.3	10^{-8}	0.1	4×10^{-9}
	Kidney	10	0.5	2×10^{-8}	0.2	7×10^{-9}
	Total body	20	0.7	3×10^{-8}	0.3	10^{-8}
Insoluble	Lung	-	-	6×10^{-9}	-	2×10^{-9}
	GI tract	-	3×10^{-4}	6×10^{-8}	10^{-4}	2×10^{-8}

Organ of Reference	Half Life (days): Physical	Biological	Effective	Fraction from GI Tract to Blood	Fraction in Organ of Reference to That in Total Body	Fraction from Blood to Organ of Reference	Fraction Reaching Organ of Reference: By Ingestion	By Inhalation
Liver (1.7×10^3 gm) (soluble)	285	293	146	10^{-4}	0.19	0.25	2×10^{-5}	0.06
Kidneys (300 gm) (soluble)	285	563	191	10^{-4}	0.02	0.02	2×10^{-6}	5×10^{-3}

1. Configuration

The cylindrical core has a diameter of 4.25 inches and a length of 11 inches. Six 1-inch diameter fuel channels are drilled on a diameter center of 2.47 inches with an additional 1-inch diameter fuel channel in the center of the core. Prior to placement in the fuel core, the Ce-144 is sealed in seven tubular tantalum liners. The seven tantalum capsules are held in place in the fuel channels by threaded screw plugs. Each plug is welded into position to provide a mechanical and leaktight seal.

Impact depressors are located at both ends of the cylinder to absorb the energy of high impact and shock. The depressors are 4.75 inches in diameter and 2.125 inches in length. Figure 3 shows the fuel core and depressors.

This configuration was selected as the result of tests performed at the Aberdeen Proving Ground (APG) by The Martin Company. The tests of various fuel core configurations are reported in Appendix A, where the bases for selecting the core design are described.

2. Thermal Characteristics (Ref. 7)

The thermal characteristics of the fuel core have been determined by theoretical and empirical methods with the following identical results. At a thermal output of 6500 watts, the temperature at the centerline of the core when operating in the generator is approximately 1890° F and decreases to 1670° F at the surface of the core. This is well below the melting point of the core material, which varies from 2540° to 2600° F. The thermal conductivity of Inconel X is 7.8 Btu/ft-hr-°F and the specific heat is 0.10 to 0.11 Btu/lb-°F.

The fuel core must have desirable burnup characteristics upon reentering the earth's atmosphere after orbital decay. Such characteristics are dependent upon the recession rate of the core material. The recession rates of the core material were obtained for varying heat fluxes by plasma jet tests[8]. At a heat flux of 300 Btu/sec-ft^2, a recession rate of 0.055 in./sec was determined for Inconel X. A detailed analysis of core burnup is reported in a later section.

3. Physical Properties

Inconel X has good mechanical integrity at the operating surface temperature of the core, 1670° F. Figure 4 shows the ultimate tensile strength of Inconel X at various temperatures. Rocket sled tests and simulated missile failure tests prove that the core would withstand mechanical shock and impact forces on sea water, unconsolidated and consolidated rock, at or near its operating temperature.

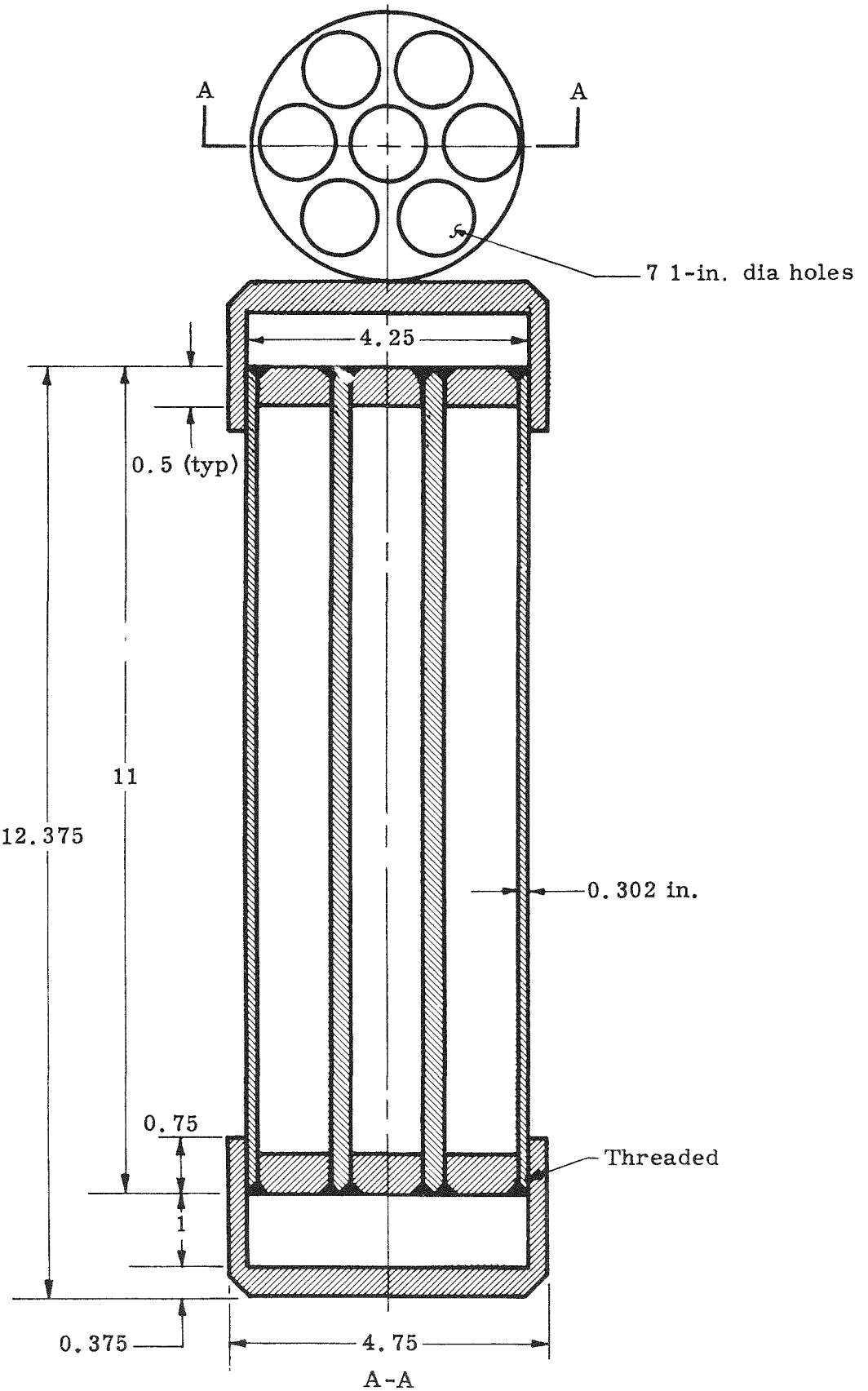

Fig. 3. Core Configuration

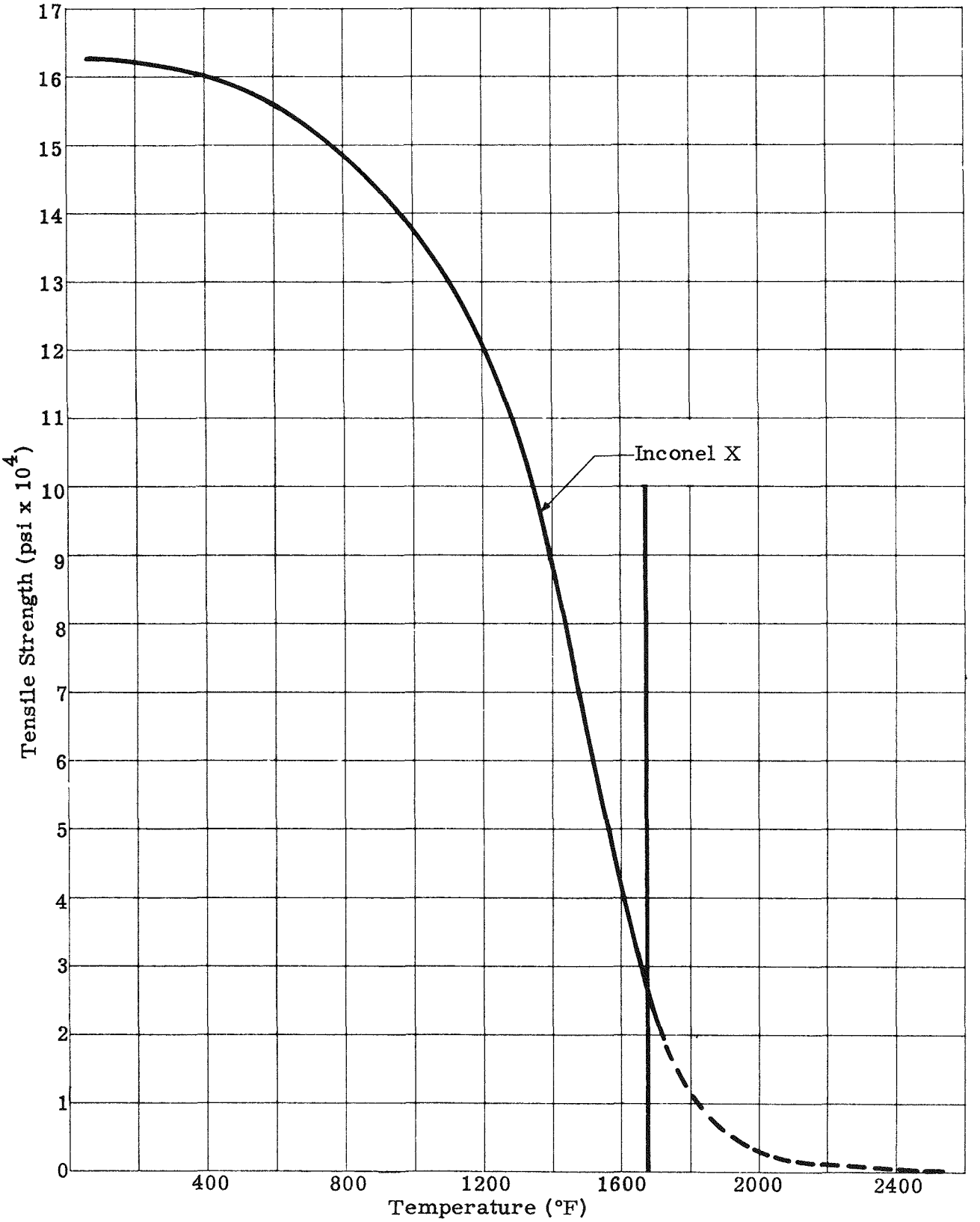

Fig. 4. Ultimate Tensile Strength of Inconel X as a Function of Temperature

Inconel X is a nickel alloy containing approximately 73% Ni, 15% Cr, 7% Fe, 2.5% Ti, 1% Cb and 0.9% Al by weight. It has a density of 8.3 gm/cc. The fully loaded core weighs 22.6 kilograms based upon a bulk density of 6.82 gm/cc.

4. Chemical Properties

Inconel X has good oxidation and corrosion resistance at the operating temperatures of the core. It has a maximum pitting rate in quiescent sea water of 0.0236 inch per year for a 32-month exposure[9]. Its corrosion rate in flowing sea water is estimated at less than 0.002 inch per year. If the core became immersed in sea water, the radioisotope would be contained for a minimum of 12.8 years until the fuel had decayed to an insignificant level of less than 20 curies.

Since one of the characteristics of the cerium fuel is the evolution of oxygen gas in the sealed core, tantalum fuel liners serve to collect the evolved oxygen by chemical combination. Inconel X is subject to corrosion by fuming nitric acid should such a propellant be used for the satellite vehicle, The tantalum fuel liners are impervious to nitric acid attack.

page blank

III. TRANSPORT OF GENERATOR TO LAUNCH SITE

The shipment of the generators to the launch site is divided into two specific operations:

(1) Shipment of the radioactive fuel cores.

(2) Shipment of nonradioactive hardware, including empty generators, field handling equipment and auxiliary components.

The fuel cores and the generator components will be assembled at the launch site as described in Chapter IV. Shipment of nonradioactive hardware from Baltimore to the launch site, the second operation, is governed by conventional shipping procedures and need not be given further consideration. Point of origin for the fuel core shipment will be Oak Ridge National Laboratory (ORNL) located near Knoxville, Tennessee, and the destination will be the Pacific Missile Range near Santa Maria, California.

A system has been devised for handling, loading and shipping the fuel core, and transferring the fuel core to the thermoelectric generator. Equipment has been designed to effect the transfer without using a hot cell.

The following discussion includes a description of the major equipment involved in the handling and transportation of the core, including the shipping procedures, and an examination of possible shipping hazards.

A. SHIPPING CASK

The major piece of handling equipment used for transport of the fuel core is the shipping cask. It is designed to provide shielding of the fuel, adequate cooling of the fuel core during shipment, and containment of the fuel core during credible transport accidents. A photo and a cutaway drawing of the shipping cask are shown in Fig. 5.

1. Shielding

The shipping cask is designed for a dose rate of 10 milliroentgen/hr or less at 3 feet from the surface. This is achieved by using a 13-inch thick lead wall around the fuel core to attenuate the gamma activity.

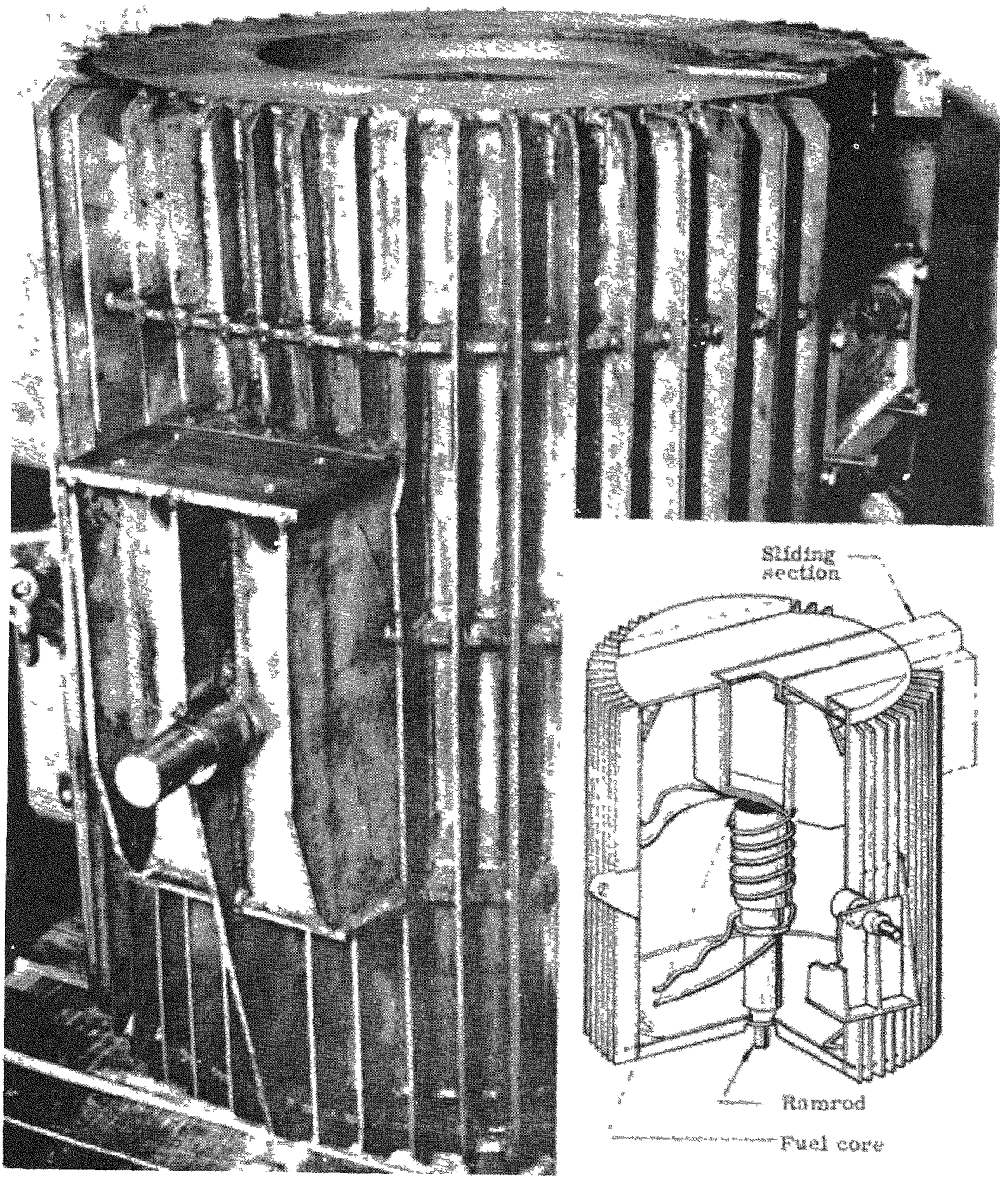

Fig. 5. Shipping Cask (inverted during fuel transfer)

2. Cooling

During transport, na ural convection cools the cask. Cooling fins placed around the outside of the container provide the necessary convective surface. Wood's metal, a low melting point alloy, fills the cavity around the fuel core and provides a dense fluid path for the conduction of heat from the fuel core to the walls of the shipping cask. Calculations show that the surface temperature of a loaded cask will be approximately 270° F. At the request of the Bureau of Explosives, a protective cage will be placed around the cask to prevent accidental contact of personnel with the hot exterior.

3. Cask Design

The lead shield of the transport cask is completely encased in a stainless steel shell fitted with cooling fins and supported by tension straps to ensure the structural integrity of the cask during transport. An inner stainless steel container supports the fuel core. The bottom of the cask is fitted with a loading ram and coupling device. The latter also serves as a locking device to secure the fuel core to the built-in transfer mechanism during shipment. The top of the cask is fitted with an access plug designed to slide to the side. These features are provided to facilitate transfer of the fuel core to the generator. During shipment, a steel plate bolted to the cask, and fitted with wire seals, covers the slide plug and prevents access to the fuel core. Each cask weighs approximately 15,000 pounds. Bureau of Explosives Permit No. 898 has been issued for shipment of this cask.

Because of shielding considerations, the weight of the cask is concentrated in a relatively small area. A skid approximately 6 x 8 feet is provided to distribute the cask weight over the floor of the conveying vehicle. Tiedowns are provided to secure the cask to the skid, and the skid, in turn, to the transporting vehicle. Figure 6 shows the protective cage-transport cask-shipping skid assembly.

B. SHIPPING PROCEDURES

The cask will be shipped by rail, in a gondola car, from Oak Ridge National Laboratory (ORNL) located near Knoxville, Tennessee, to the Pacific Missile Range near Santa Maria, California.

1. Preparation for Shipment

The fuel core will be loaded remotely at ORNL and welded. ORNL personnel will decontaminate the surface of the core to prevent contamination of the shipping cask and generator. Due to the high radiation field associated with the contained fuel, the core must be loaded into the transport cask in a hot cell using remote handling procedures. The core will

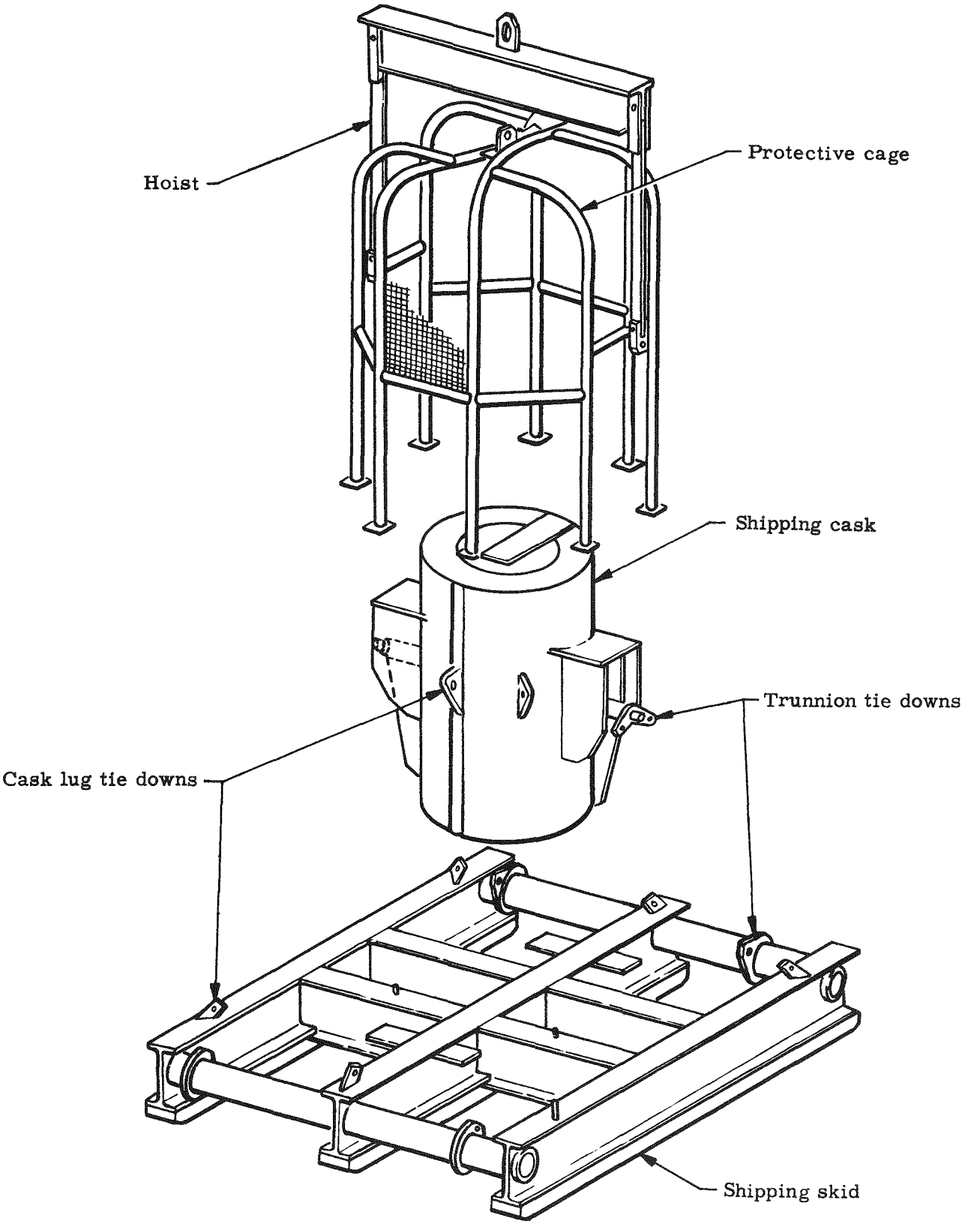

Fig. 6. Shipping Equipment

be placed in the shipping cask with remote handling equipment and locked in place. The sliding plug will be closed; Wood's metal will be added and the seal affixed to the sliding plug cover. After decontamination and monitoring procedures on the cask have been satisfactorily completed, it will be removed from the hot cell by a 10-ton crane and positioned on the skid. The protective cage will then be placed over the cask and attached to the skid, and the cask will be firmly secured to the skid with six turnbuckles.

2. Shipment

The shipment will move by truck from the hot cell at ORNL to the plant site railroad siding. The cask will be shipped by rail to the launch site in a gondola car. The four steel walls of the car afford additional protection of the shipment. "Preferred Rail Handling" will be requested for all shipments involving the cask so that humping and dynamic coupling are minimized. For rail shipment, the skid will probably be blocked to prevent shifting of the load during shipment. Since a forward or aft load of 1-1/2g would upend a blocked skid, the skid will be secured to the floor of the car by means of tiedown rings located along the sides of the skid.

C. SHIPPING HAZARDS

The potential hazards associated with the shipment of the radiocerium fuel core are:

(1) Direct external radiation exposure from the fuel.

(2) Internal radiation exposure from ingestion or inhalation of the fuel in particulate form.

The countermeasures inherent in the fuel core and shipping cask designs to prevent or minimize exposure are the following:

(1) Multiple containment.

(2) Biological shielding.

Since the multiple containment materials and biological shield components have good structural properties, high thermal capacity, and are resistant to corrosion, containment cannot be lost due to forces imposed by credible rail transport accidents. The following analysis describes certain credible accidents and maximum credible accidents*; the latter are beyond the scope of normal accidents.

---

* A hypothetical accident based upon the coincident occurrence of several credible events.

1. Transport Accidents

The frequency and magnitude of transport accidents involving the generator can be significantly diminished by the selection of shipping routes, optimization of shipping procedure, proper location of the cask on the carrier, regulation of shipping time, and by utilization of an escort. The cask will be shipped by truck and rail to its destination.

Truck accidents. Truck accidents that could be postulated are collision (impact), explosions, and fire. The frequency of truck accidents is estimated to be 1/230 based upon the number of accidents per 1000-mile shipment.[11] It is also estimated that 1 accident in 500 would involve an explosion and, therefore, the frequency of truck accidents involving explosions would be 1/115,000 per 1000-mile shipment. Statistics for truck accidents involving fires are not available, but they would probably have a frequency of 1/10,000 per 1000-mile shipment. It should be pointed out that the above statistics are for 1000-mile shipments in the Continental U.S., whereas the shipment under consideration is to be shipped by truck a total distance of less than 20 miles over controlled routes at PMR and ORNL.

Within the framework of the planned movements of the Task 2 generator, a credible impact accident could be postulated. In this accident, the carrier moving at 30 mph (44 fps) could collide with an immovable object to yield a maximum impact pressure of 290 psi on the cask. This pressure would not result in mechanical failure of the cask structure. Should the fuel of the carrier become ignited, insufficient thermal energy is available to melt the cask. For example, a carrier fuel tank containing 100 gallons of gasoline would have a thermal energy potential of about 4×10^9 calories. Assuming 0.1% of this, or 4×10^6 calories, would be imparted to the cask, it would not be sufficient to melt the lead shield, which requires 3.5×10^7 calories under adiabatic conditions.

Truck movements involved in this shipment are of a type that would preclude the possibility of a major accident. The shipment will move by truck from the hot cell at ORNL to the plant railroad siding. At PMR the shipment will move by truck from the siding to the launch complex. The above movements will be executed by qualified personnel under controlled conditions at low speeds.

Rail accidents. The shipment will move by rail from ORNL near Knoxville, Tennessee, to PMR near Santa Maria, California. Transportation will be accomplished by scheduling the shipment on a through train with a minimum number of stops en route.

Rail accidents that could be considered are derailment, explosions and fire. The frequency of rail accidents is estimated at 1/3300 per 1000 miles traveled. Whereas the frequency for gasoline fires per 1000 miles is 1/22,000, the frequency of accidents involving explosives is 1/87,000. Approximately 50% of all freight car derailments occur at speeds greater than 35 mph with 24% at speeds greater than 45 mph.

Both the cask skid and the tiedown structure are designed to withstand the high g loads encountered in rail transport. The skid is attached to the gondola car in such a manner that it will absorb an ultimate vertical load of 5 g before failure. Braces attaching the cask trunnions to the skid will absorb an ultimate fore and aft load of 15 g before failure.[12] Blocking the skid against both ends of the car will prevent shifting of the load and will provide additional energy absorption upon impact.

Assuming a derailment speed of 80 mph (118 fps) wherein the cask attachments absorb none of the impact force, an impact pressure of less than 2000 psi would be exerted on the cask. This would result in considerable plastic deformation of the cask without brittle structural failure.*

Involving the cask with a tank car containing a large quantity of gasoline could be eliminated by proper positioning of the cask shipment on the train. However, it is evident that a fire arising from the involvement of the cask with a tank car carrying 10,000 gallons of gasoline (a potential heat release of 4×10^{11} calories) could result in loss of shielding. However, proper handling of the shipment would preclude this type of incident.

Various administrative controls will be employed to lower the statistical probability of accidents below the values previously stated and also to prevent the occurrence of accidents of sufficient magnitude to provide marginal integrity of the cask. Requiring that the shipment be placed in the middle of the train and that adjacent cars may not contain explosives or inflammable materials will minimize the safety problems inherent in the transcontinental shipment of a radioactive source of this magnitude. Railroad personnel consulted on this problem state that the gondola car will contain the mounted cask under any circumstance short of complete overturning of the car.

---

* Cast lead has a compressive stress of 2120 psi.

page blank

IV. GROUND HANDLING AND VEHICLE INTEGRATION

The ground support system for preparing the nuclear APU for flight has been designed to permit loading of a flight generator without requiring a hot cell at the launch complex. This system provides cooling, monitoring and shielding of the fuel capsule during its transfer from the shipping cask into the generator, during ground handling of the fueled generator, and during installation in the missile.

The following sequence of operations is performed:

(1) Preparation for transfer.

(2) Transfer of the fuel capsule to the generator.

(3) Mating of the generator and the final stage.

(4) Mating of the final stage and the booster.

A. PREPARATION FOR TRANSFER

When shipping casks containing the fuel cores arrive at their destination, tiedowns between the skid and gondola will be removed, the shipment inspected, and then towed from the transport vehicle onto a flat bed trailer for movement to the launch complex. At the launch complex each cask will be inverted, hoisted onto a field transfer structure, positioned by a portable crane and bolted in place. Simultaneously, a dolly containing the generators and a collar shield will be positioned in the transfer structure beneath the cask as shown in Fig. 7. The collar shield is a tank of single unit construction and, when filled with mercury, it maintains biological shield continuity between the lead cask and the generator.

The dolly is used for field installation of the isotope block into the power conversion unit, for short term storage of the loaded units and for installation of the power units in the missile. Included on the dolly are support fixtures which hold the power units each containing 4000 pounds of mercury biological shield. Adjustments are provided on the base of the dolly to permit fine alignment of the power unit with the loading fixture and the missile structure.

B. TRANSFER OF FUEL CORE TO GENERATOR

A feature in the design of the shipping cask and fuel core transfer equipment is that the transfer of the fuel core to the generator does not require the use of a hot cell and may be accomplished at any convenient location. If required, the reverse operation can also be accomplished with this equipment.

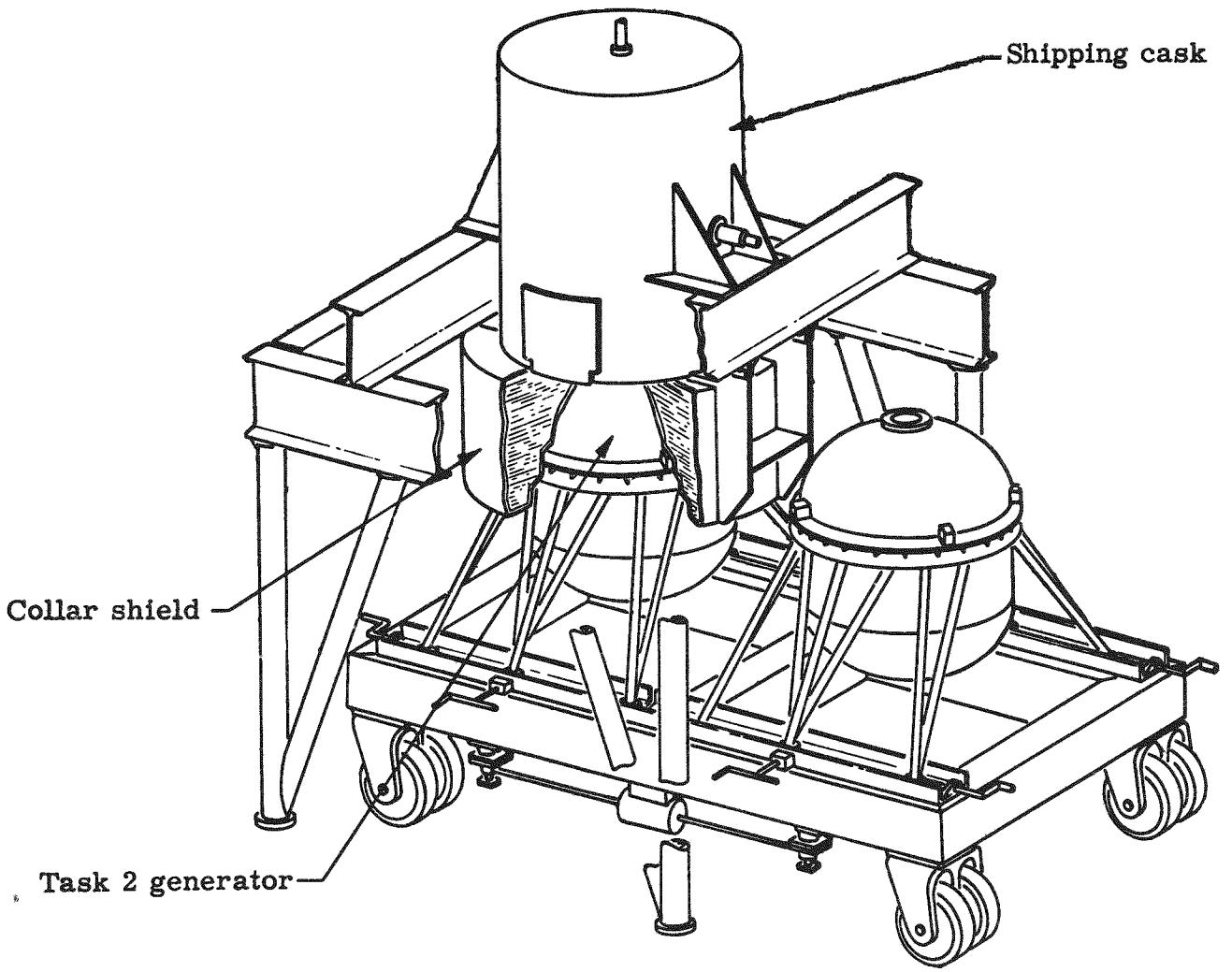

Fig. 7. Arrangement of Field Transfer Equipment

The shipping cask is fitted with two devices to facilitate transfer. First, one end of the cask is fitted with a stepped sliding plug, which is driven by a screw jack and which retracts to clear the fuel core for passage into the generator. This design permits close coupling of the cask to the generator. Second, the core is attached to a stepped, hand-operated ramrod which is fitted with a remote connect and disconnect mechanism and which is actuated to insert and seat the core in the generator. The connect-disconnect mechanism is manually operated.

At the start of the fuel transfer operation, the cask is inverted, positioned and bolted onto the loading stand. The dolly carrying the generator and collar shield is rolled under the stand, raised via its built-in jacks and positioned so that generator, collar shield and cask are in proper alignment. The collar shield is then bolted to the loading stand and both shield and generator are filled with mercury. Figure 8 shows an internal view of this arrangement.

An extension is fitted to the loading ramrod on the cask and water is circulated through cooling coils in the cask and in the generator. After the core has cooled, the Wood's metal heat transfer medium is drained, the sliding plug is opened and the core lowered into the generator and locked in place. The ramrod is released from the core and withdrawn; the collar shield is drained and the dolly lowered and removed from the loading stand. Once the loading hatch on top of the generator is seated and secured, the transfer operation is complete. Water must be circulated through the cooling coils of the generator to dissipate the heat generated in the fuel core.

C. MATING OF GENERATORS TO FINAL STAGE

After the dolly-mounted generators are fueled, the dolly is moved underneath the final stage mating structure as shown in Fig. 9. Since the generator is designed for tension loads, it must be loaded onto the final stage vehicle in a vertical position.

A representative satellite vehicle is shown in a vertical position on a support fixture with the rocket engine and nozzle extending below the platform. Clearance below the platform allows the power unit dolly to be moved under the vehicle structure. Once the dolly is in position, the power units are jacked vertically into position, final lateral adjustments are made with hand cranks provided on the support dolly, and the power conversion units are bolted onto the support structure of the vehicle. After servicing and electrical lines are attached, the complete satellite assembly is ready to be hoisted by gantry crane and fitted to the top of the booster. The mercury shield is maintained within the generators throughout this operation.

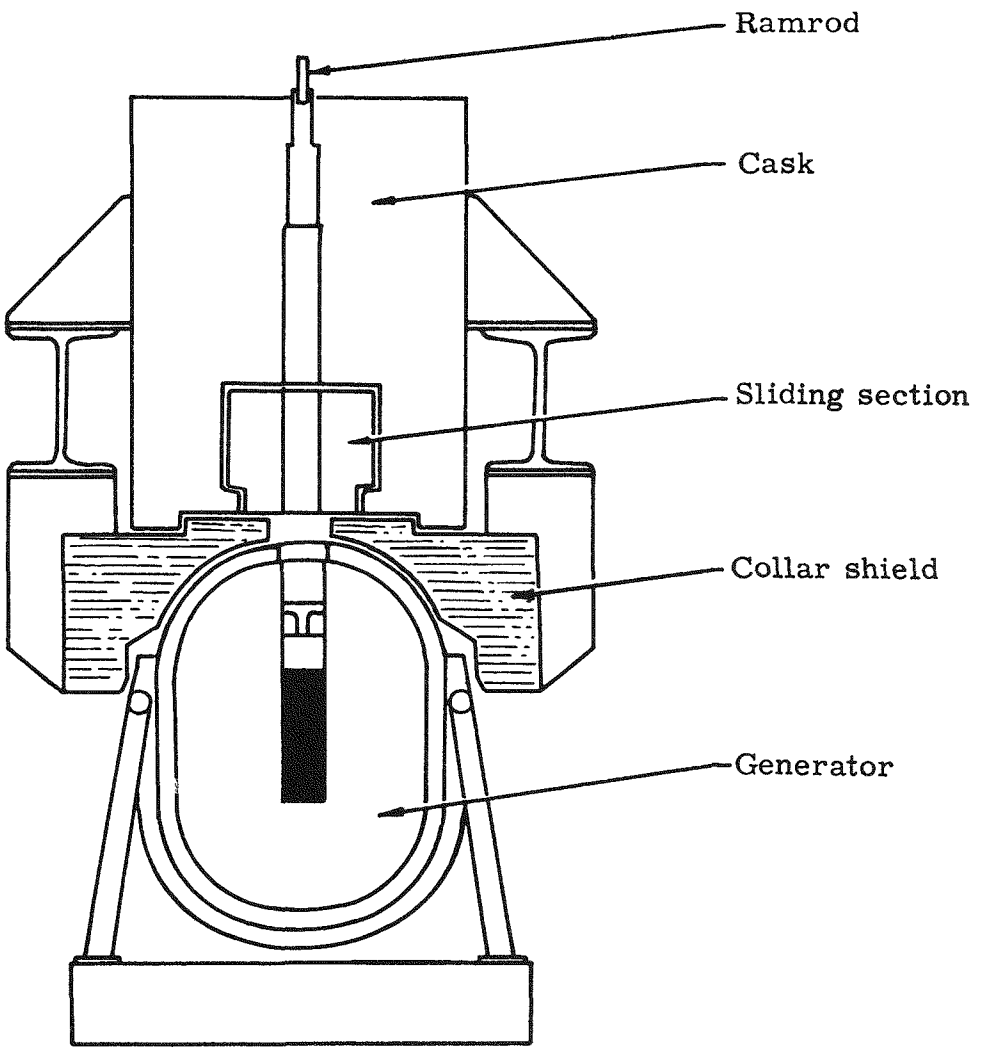

Fig. 8. Internal View of Fuel Transfer Operation

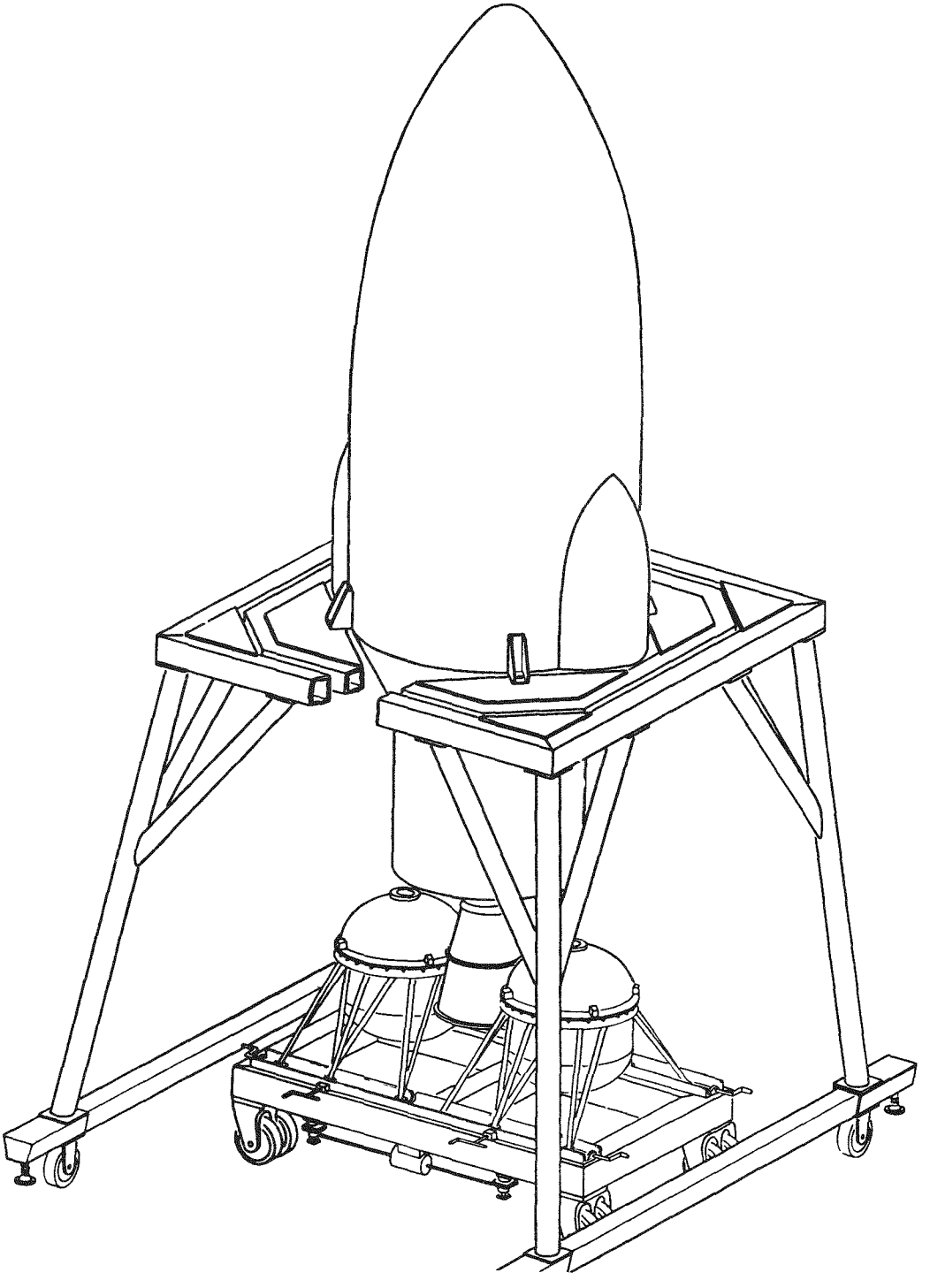

Fig. 9. Mating of Task 2 Generators to Satellite Vehicle

The two Task 2 generators will add approximately 8400 pounds to the weight of the satellite vehicle of which 8000 pounds is the mercury shield material which is removed prior to launch.

D. MATING OF FINAL STAGE TO BOOSTER

The water cooling and biological shield systems operate from the umbilical tower from the time the gantry is removed up to launch. At T = -300 seconds the mercury shield material is drained from the generator. At T = -60 seconds, the mercury drainage is complete and the temperature of the generator will begin to rise. Under normal launch conditions, operating temperature in the generator should be approached in orbit at T = +3300 seconds. Service lines do not disconnect until the vehicle lifts off the pad. If any hold occurs in the prelaunch countdown, the mercury may be returned to the shield to facilitate work in and around the vehicle.

E. AUXILIARY SUPPORT EQUIPMENT

Certain auxiliary support equipment must be provided to facilitate field handling, core transfer, mating of the final stage and generators, and servicing of the generator on the booster. In addition, certain modifications will have to be made to existing equipment for remote servicing and monitoring of the generators.

1. Auxiliary Systems

Handling, transfer and mating system. A packaged servicing system will accompany the generators to provide cooling of the cores, a mercury shield system, radiation monitoring and control of temperature and mercury levels. This system specifically provides:

(1) Cask cooling of core prior to transfer (water).

(2) Generator cooling of core (water).

(3) Compressed gas for pumping mercury (nitrogen).

(4) A mercury fill and drain system for the collar shield and generators (mercury).

(5) Gamma radiation monitors on the cask, collar shield and generators.

Umbilical tower system. When the generator-loaded satellite vehicle is prepared for final installation atop the booster, the tower system becomes operative. Specifically, the system includes:

(1) Core cooling (water).

(2) Compressed gas for filling and purging the mercury shield (nitrogen).

(3) A shield fill and drain system and reservoir (mercury).

(4) Radiation monitors.

These services are provided with quick disconnect lines to expedite launch operations. Heavy components are located on the pad with service lines through the umbilical tower to the generators.

2. Equipment Modification or Additions

To supplement the above systems, modifications or additions will be made to the following existing facilities at the launch site to facilitate the servicing and handling of the generators.

Launch operations building. The launch operations building will house the additional consoles required for the testing of the generator coolant servicing equipment, consoles for operating the remote control equipment for vehicle removal from the booster, and for the shield and cooling line coupling and disconnect. Coolant pressure and temperature recorders, television viewers, and all necessary instrumentation recorders will also be housed in the launch operations building.

TV cameras. TV cameras will be located on the umbilical mast or elsewhere in the pad area, so that remotely operated equipment and vehicle components can be observed during prelaunch countdowns. This equipment will also be utilized in the operation and servicing of the generators.

Umbilical mast. The umbilical mast used to service nonnuclear satellite vehicles will be utilized with certain modifications to service the Task 2 generators. Required modifications to the mast will consist of additional stainless steel piping, valves and fittings for pumping the coolant, mercury shielding and nitrogen gas. A provision will be made for running the necessary wiring to the unit for electrically operated valves, sensors and instrumentation. The mast will be fitted with safety devices to prevent the accidental release of the service lines by the vehicle before liftoff.

page blank

V. FLIGHT VEHICLE

The purpose of this section is to describe a typical vehicle used for satellite injection in order to establish the analytical model in general terms. The vehicle configuration assumed is shown in Fig. 10. This vehicle is considered as a two and one-half stage missile with booster-sustainer and final stages. The final stage injects itself into a 300 statute mile circular orbit and carries the payload.

A. BOOSTER-SUSTAINER STAGE

The booster-sustainer stage consists of two main booster engines and a sustainer engine which are fed from common propellant tankage. From launch, the engines boost the vehicle to an altitude of about 250,000 feet and a velocity of about 10,000 feet per second. At this point, the outboard booster engines and skirt separate from the vehicle, and the single remaining sustainer engine continues to provide thrust until the propellants are expended. At this point (altitude $\sim$ 860,000 feet, velocity $\sim$18,500 feet per second), the vernier rockets apply flight attitude correction which terminates after approximately 10 seconds of operation. After this alignment, the injection stage separates from the remainder of the booster-sustainer vehicle.

B. FINAL STAGE

The achievement of the desired flight profile requires that the injection stage coast for about five minutes before it starts up almost at orbital altitude. From this point, it provides thrust for about 100 seconds before it injects itself and the payload into the desired orbit. The final stage is joined to the basement booster stage by an adapter section. It is assumed that the final stage is powered by a single liquid-fueled rocket engine which protrudes from the aft section of the stage. The satellite or final stage is divided into forward, midbody, and aft sections. The forward section bears the structural loads and houses the payload and, beneath this, the propellant tanks. The separation point between the stages is located at the lower load ring of the midbody, where separation is accomplished by explosive bolts. The Task 2 generators are located in the aft section and are hung from the load ring on either side of the engine nozzle as shown in Fig. 11.

The satellite structure is typically about 700 pounds of magnesium and consists of skins up to 0.1 inch thick and structural members up to 0.25 inch thick. Magnesium melts at 651° C and has a specific heat of about 0.25 Btu/lb/°F.

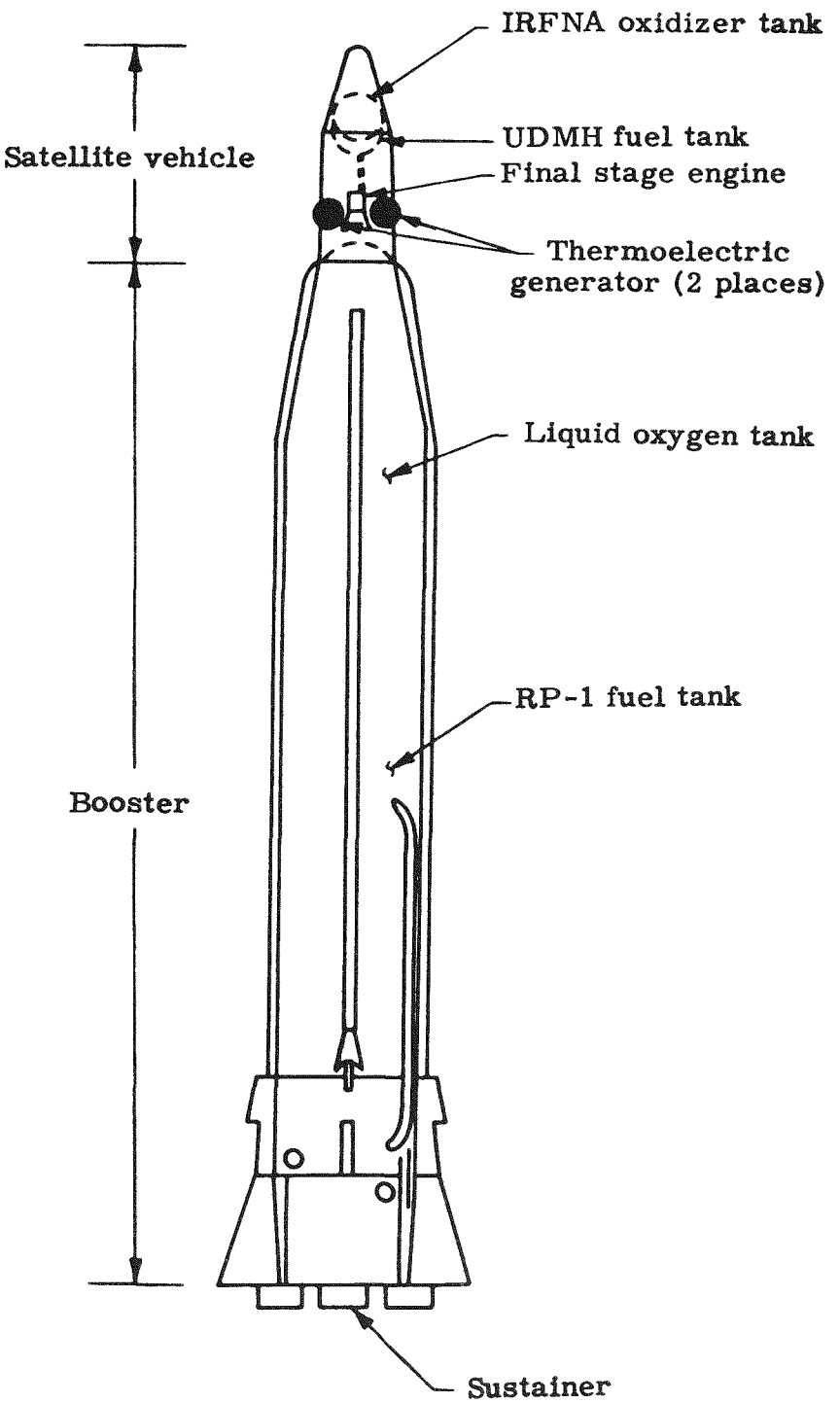

Fig. 10. Typical Vehicle Configuration

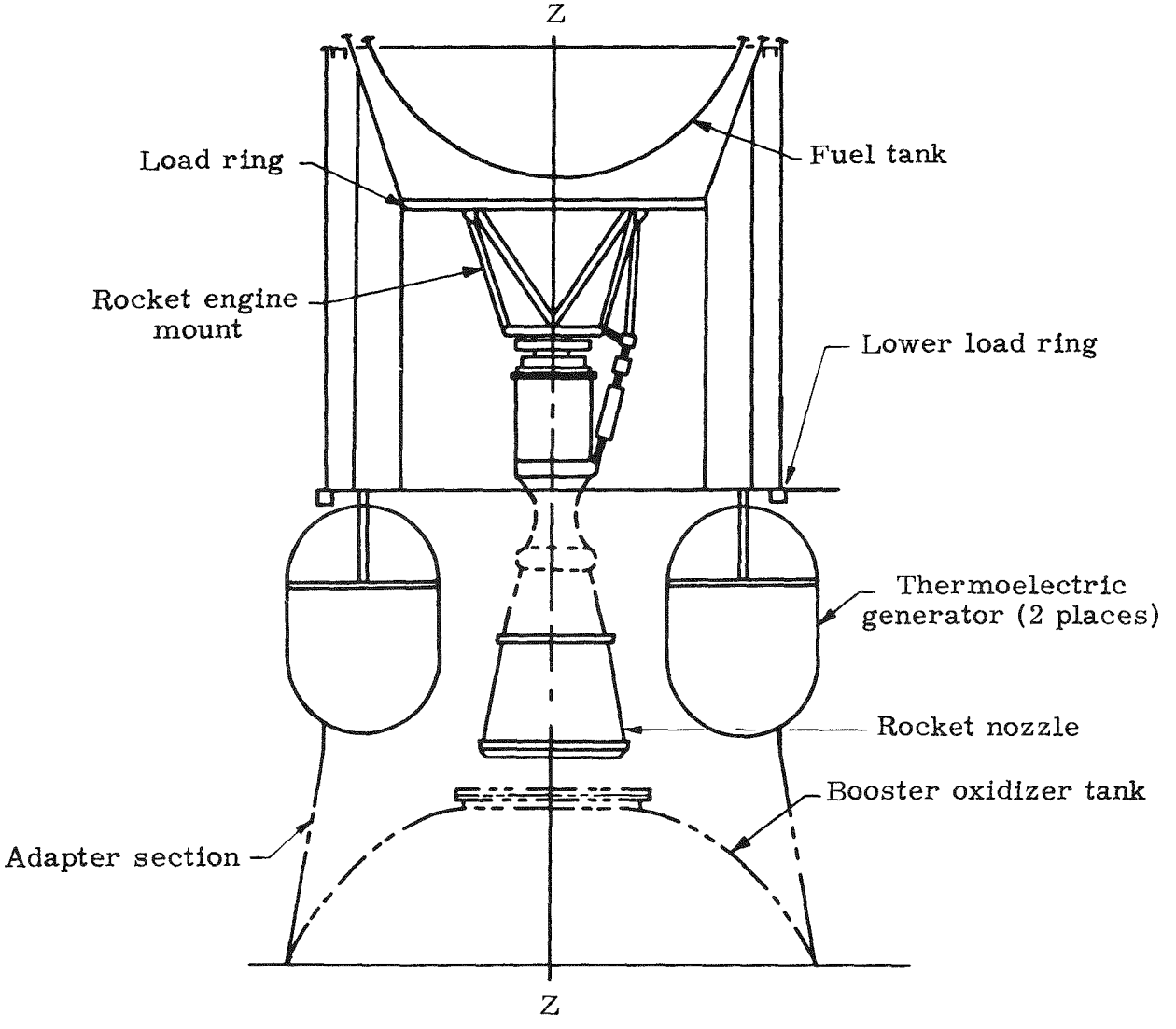

Fig. 11. Aft Section of Typical Satellite Vehicle

C. PROPELLANTS

The propellants for the typical basement booster stage are liquid oxygen and RP-1 (a kerosene) having a gross weight of about 260,000 pounds. The liquid oxygen tank, mounted above the fuel tank, contains about 177,000 pounds of the oxidizer. The bottom RP-1 tank contains about 83,000 pounds of fuel. When ignited, the propellant mixture reacts to release primarily thermal energy when not retained as an intimate mixture by secondary structures.

The final-stage propellants are inhibited red fuming nitric acid (IRFNA) as the oxidizer and unsymmetrical dimethylhydrazine (UDMH) as the fuel. The total propellant load, about 6640 pounds, consists of 1870 pounds of UDMH and 4770 pounds of IRFNA. These propellants are hypergolic, i.e., they ignite spontaneously when mixed and yield only thermal energy when reacting.

D. SAFETY SYSTEMS

Each stage is equipped with a missile safety subsystem which provides (1) a means of determining location, behavior, and projected missile impact point to the range safety officer, and (2) a means of terminating powered flight and destroying the missile. The safety subsystem hardware consists of a transponder and command receivers associated with shutdown and destruct circuitry. Vehicle destruct is achieved with explosive charges placed to destroy the propellant tanks, thus terminating the rocket thrust.

VI. MISSILE RANGE

The Task 2 generators are assumed to be an integral part of a satellite vehicle which will be launched from the Pacific Missile Range (PMR) at the Point Arguello Complex. The launch azimuth will allow the tracking facilities of the Pacific Missile Range to be utilized. The Point Arguello Complex is located at 120 degrees 35 minutes West longitude and 35 degrees 45 minutes North latitude;[13] a launching vehicle will traverse approximately 8 miles of Government and private land before it reaches the ocean. The geographical location is shown in Figs. 12 and 13. A polar orbit launch from this site due south has the advantage that shortly after leaving the pad, the vehicle follows a trajectory that is entirely over water or the Antarctic Continent. It will be shown that aborted conditions will result in impact or high altitude dispersion of the radiocerium fuel in geographical zones that are either very sparsely populated or are not inhabited at all (i.e., Pacific and Indian Oceans, Antarctica). The first orbit passes over Madagascar, but the last downrange re-entry will result in burnup of the isotope fuel above 234,000 feet at a point approximately midway between Antarctica and Madagascar. The range is, therefore, ideal for this mission.

A. LAUNCH COMPLEX

The Point Arguello Launch Complex consists of a Launch Operations Building, two launch pads, and associated service buildings. The blockhouse, approximately 1000 feet from the launch pads, is the only location in the fallback area in which personnel are present at time of launch. The launch complex is shown in Fig. 14. The fallback area consists of a 25 square mile area surrounding the launch facilities and extending downrange to the ocean. The terrain downrange is extremely rugged and consists mostly of sand or unconsolidated soil with very little vegetation. Use of vehicles in this area is limited only to those capable of climbing grades of at least 35%. Figure 15 shows the range safety zone.

B. RANGE SAFETY

During missile firings at the Point Arguello Complex, a Missile Accident Emergency Team (MAET) stands by just outside the fallback area. The team's equipment requires some revision to enable it to adequately retrieve fuel cores. Presently, the equipment consists of an M-246 wrecker, a 20-ton crane, a D-8 tractor and a H-19 helicopter.[14] Recovery of the aborted generators will dictate the need for airborne

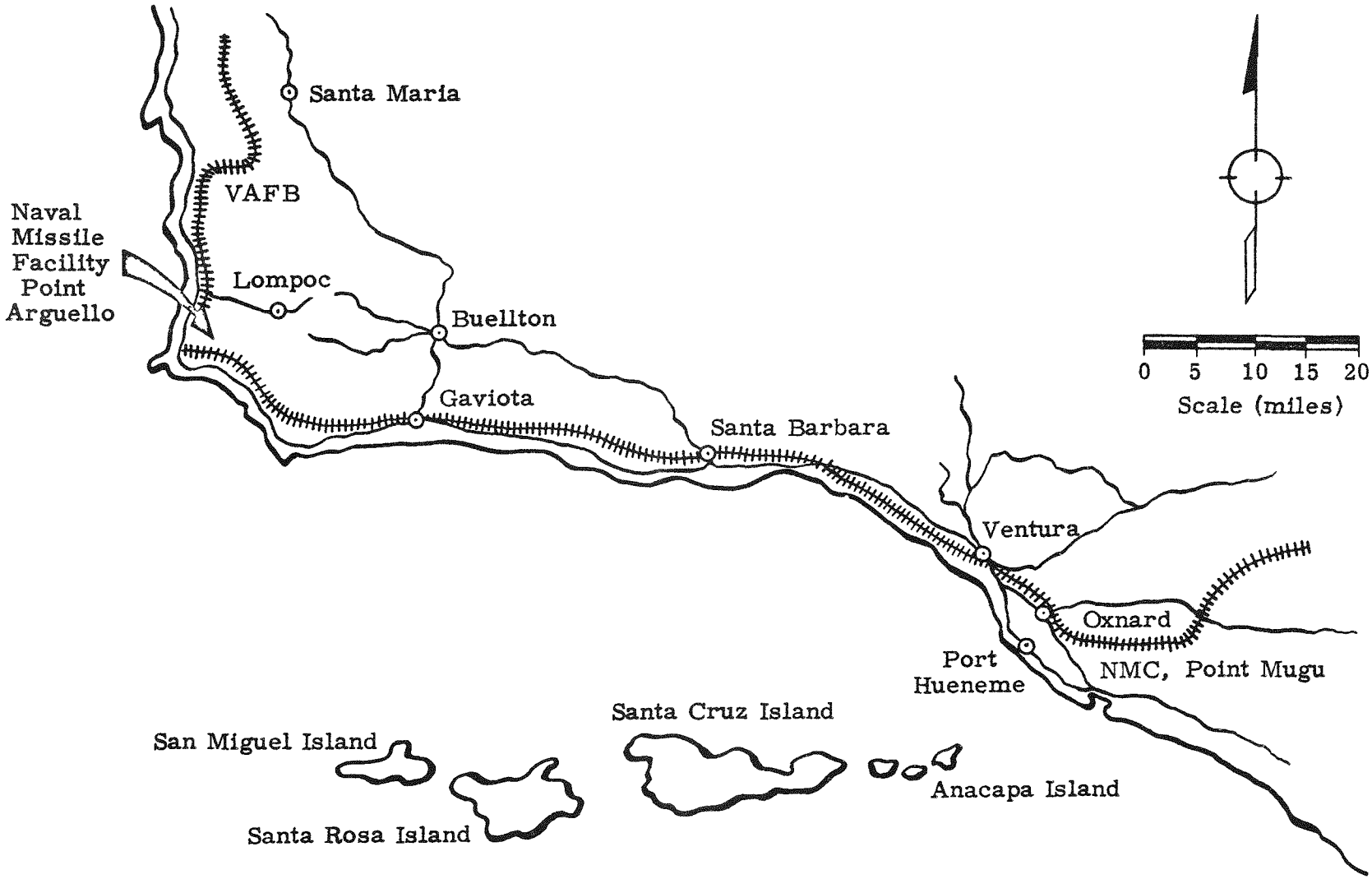

Fig. 12. Area Map of Point Mugu and Point Arguello

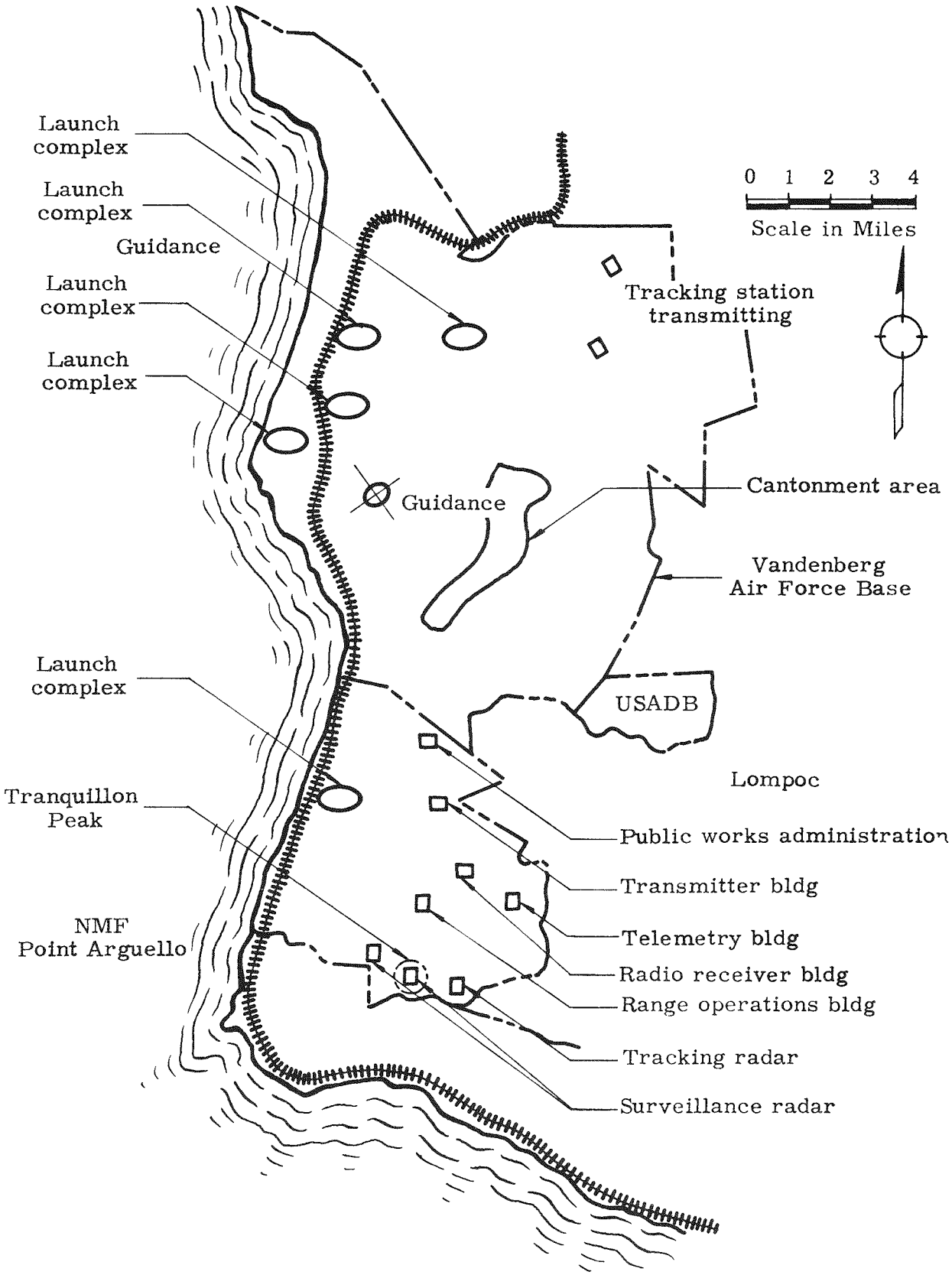

Fig. 13. NMFPA/VAFB Complex

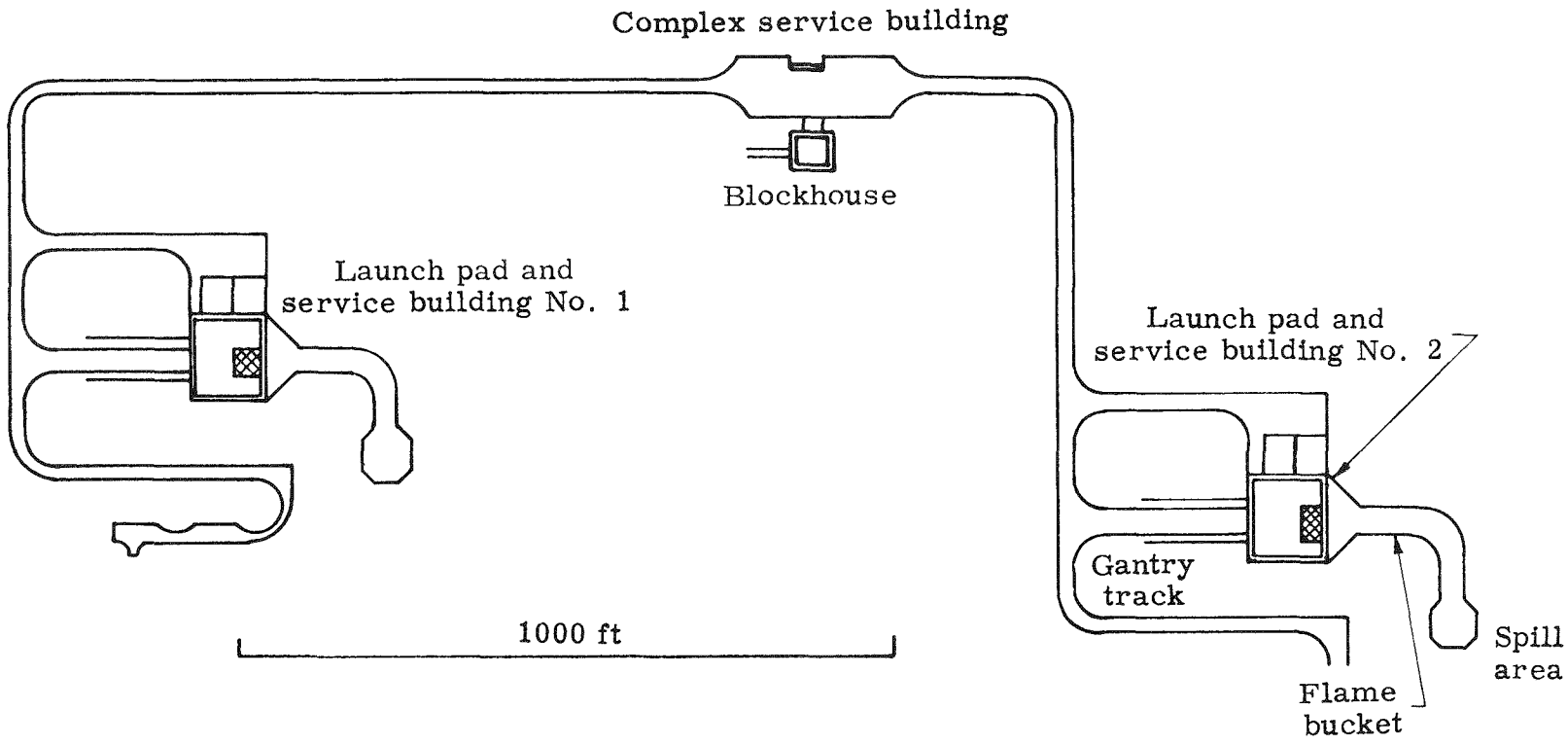

Fig. 14. Point Arguello Launch Complex

Point Arguello Launch Area

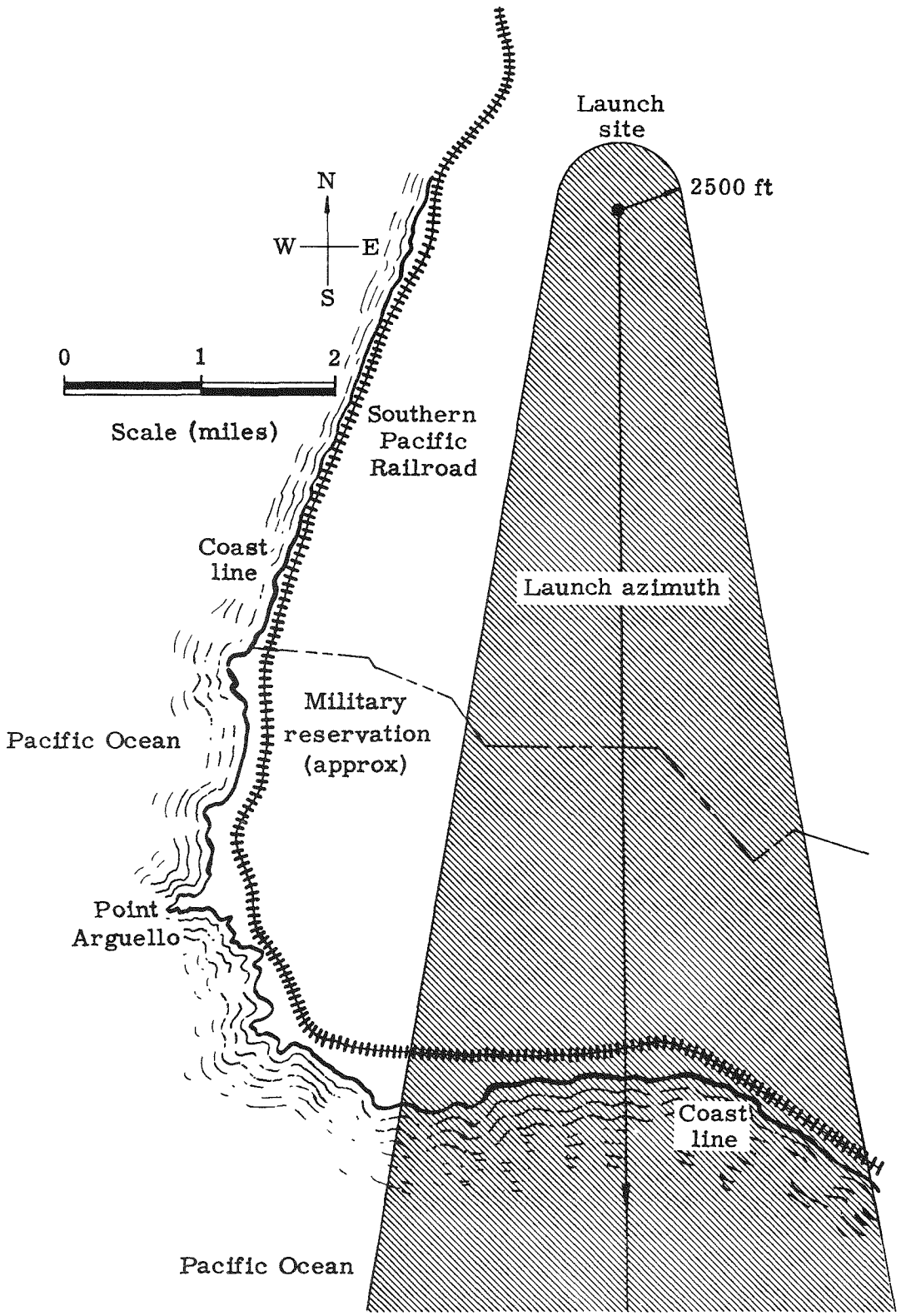

Fig. 15. Range Safety Zone

search equipment with radiation detectors and remotely operated, shielded handling vehicles. Additional equipment required are TV systems and a nearby water pool or other shielded facility for safe storage of the aborted fuel cores.

It is highly desirable to recover the Task 2 fuel cores if the debris from an abort is scattered on land areas. These cores will best be located by aircraft equipped with radiation detectors; recovery can be handled by the aforementioned special equipment.

If the capsule or generator falls into shallow water, the Inconel X material, because of its good corrosive resistance, will contain the radioisotope long enough to permit intact recovery. The ocean on the launch azimuth is 72 feet deep one mile from the shore line. At four miles out the water is 240 feet deep; the bottom is relatively smooth and sandy. It is anticipated that salvage operations might be conducted in water up to depths of 500 feet. Recovery of aborted vehicles impacting in shallow waters is normally carried out as a matter of course.

VII. BIOLOGICAL SHIELD*

During the ground handling operation each Task 2 unit is filled with approximately 4000 pounds of shield mercury. This mercury is drained at launch and would be pumped back into the unit in the case of an extended hold in the countdown. The following discussion includes listings of the dose rates from a bare unshielded source, with the biological shield in place, during the field transfer operation, and after accidents where the fuel core is either buried in soil or immersed in water.

A. BARE CORE SOURCE

Radiation dose rates were calculated for two cores at zero decay (1.7 megacuries), for one core at zero decay or two cores after one half life (0.88 megacurie), and for one core after one half life (0.44 megacurie). The dose rates 3 and 100 feet from the above sources are:

	Dose Rates (r/hr)	
(curies)	3 feet	100 feet
1.7×10^6 (2 cores)	5×10^4	46
0.88×10^6 (1 core)	2×10^4	22
0.44×10^6 (1 core after 1 half life)	10^4	11

Figure 16 shows the dose rate as a function of distance from the three bare core sources, neglecting air attenuation and including self-absorption.

B. SHIELDED GENERATOR

Figures 17, 18, 19 and Table 3 show the dose rates at various points around a generator with the mercury shield in place. Because of the geometry of the biological shield container, the dose rates vary from point to point. At the surface of the unit, for instance, the dose rates vary from 11 to 750 milliroentgens/hour. At 1 meter from the surface of the unit, the dose rates vary from 2 to 95 milliroentgens/hour.

---

* A. M. Spamer, Shield Analysis Unit

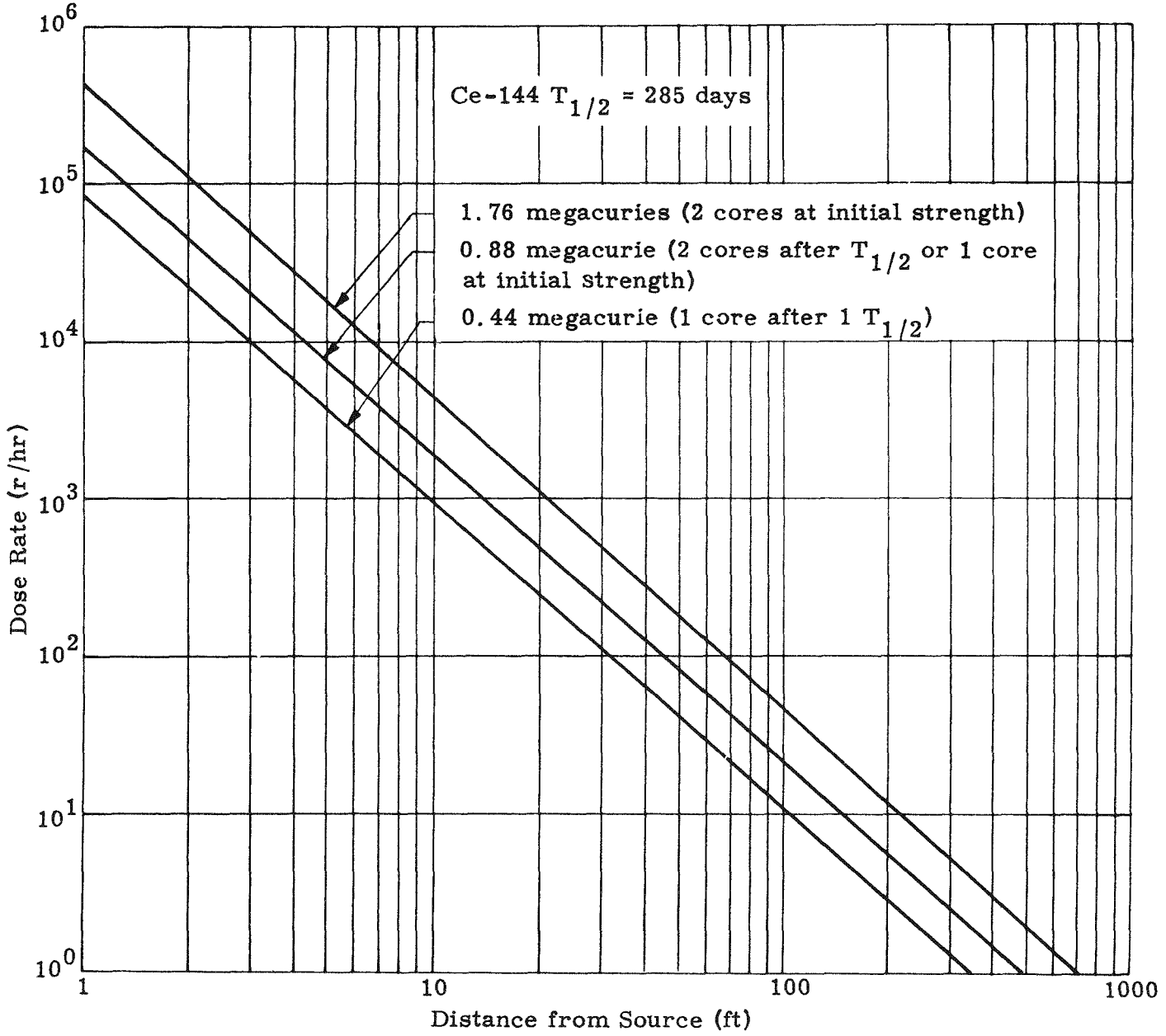

Fig. 16. Dose Rate Versus Distance from Unshielded Fuel Cores

NOTE: Dose rates are given in Table 3

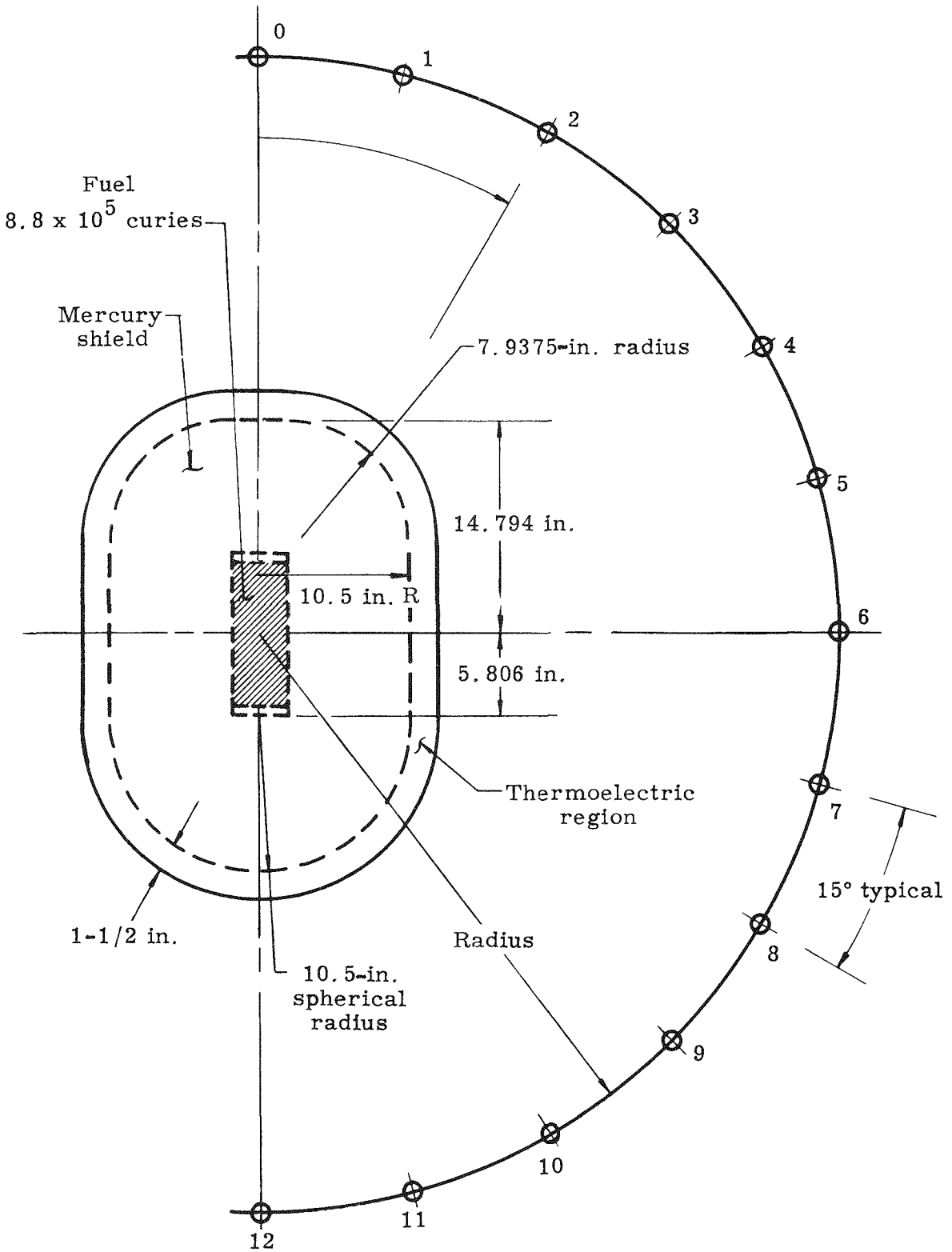

Fig. 17. Location of Dose Points in Vertical Plane Through Generator

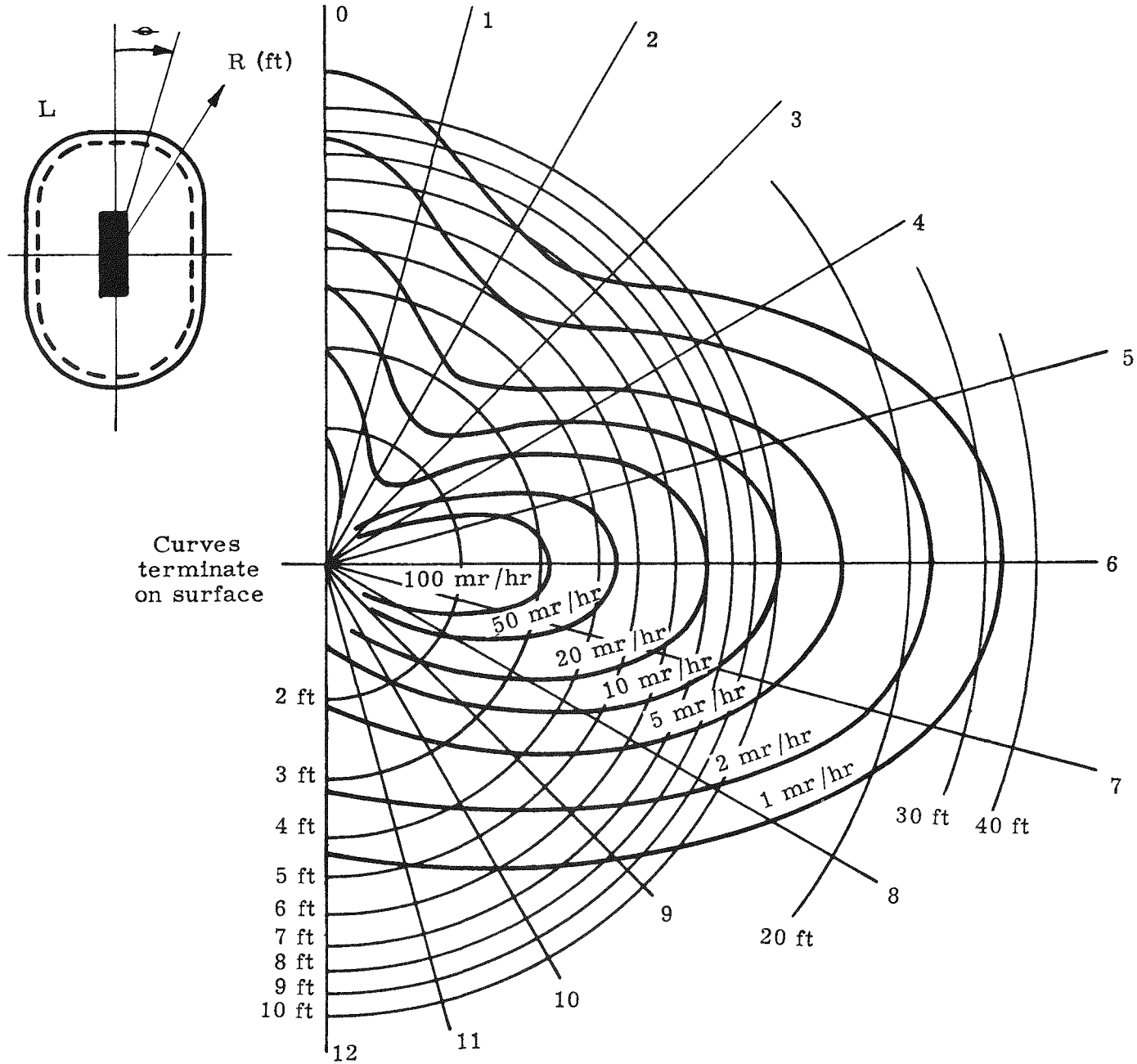

Fig. 18. Isodose Contours in Vertical Plane Through Shielded Generator

All dimensions given in inches

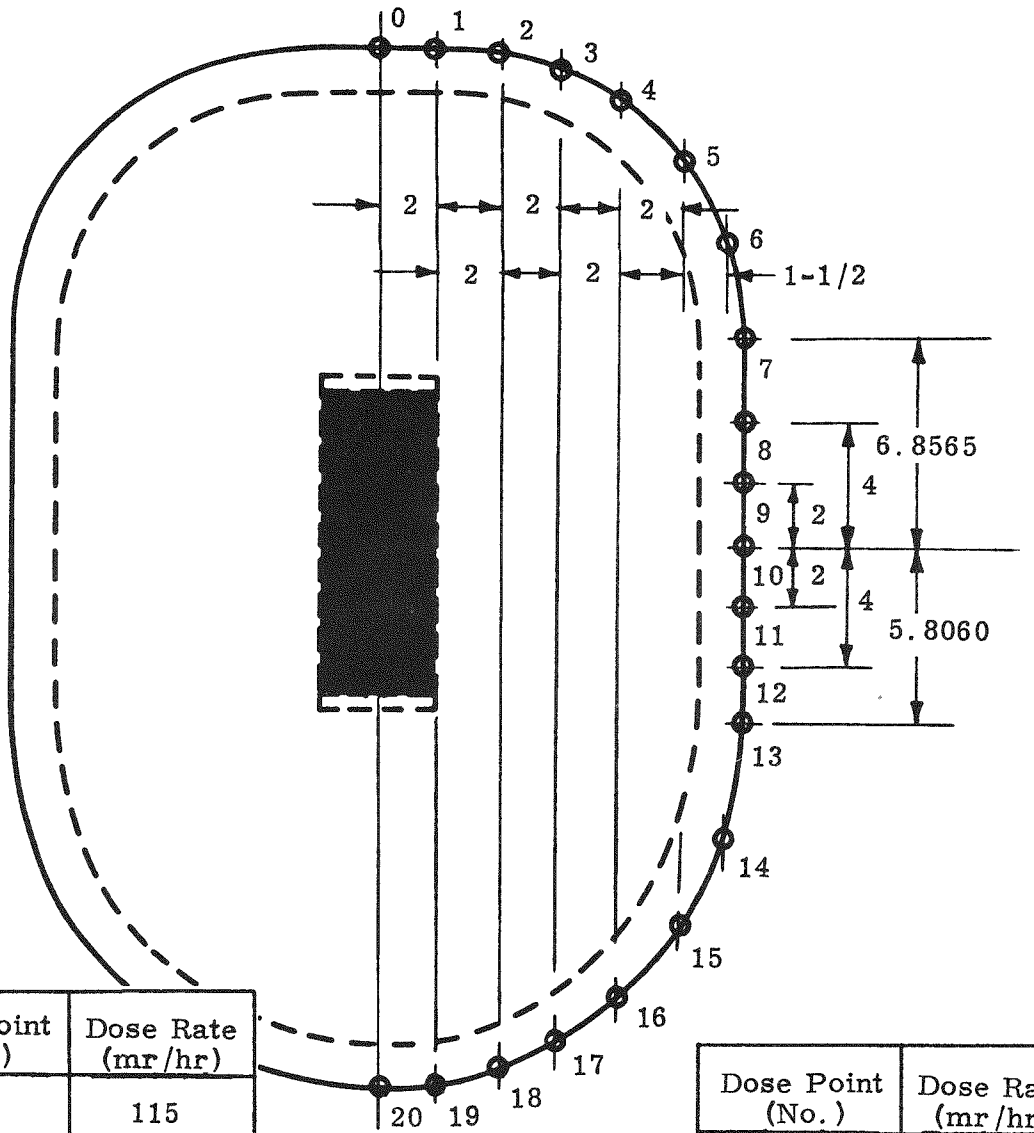

Dose Point (No.)	Dose Rate (mr/hr)
0	115
1	95
2	60
3	41
4	35
5	39
6	72
7	225
8	525
9	690
10	750

Dose Point (No.)	Dose Rate (mr/hr)
11	690
12	525
13	330
14	115
15	50
16	28
17	19
18	14
19	12
20	11

Fig. 19. Dose Rates on Surface of Shielded Generator

TABLE 3

Dose Rates at Various Distances from Center of Generator with Shield Filled with Mercury

Dose Point	0	1	2	3	4	5
	0°	15°	30°	45°	60°	75°
Radius	Dose Rate (mr/hr)					
(on surface)	116	55	35	48	210	600
2.5 ft	28	15	9	10	29	106
1 meter	15	8.8	5	5.5	16	62
5.0 ft	6.2	3.6	2	2.2	6.7	26
10.0 ft	1.5	0.88	0.5	0.5	1.7	6.6
25.0 ft	0.23	0.14	0.077	0.083	0.27	1.1
100.0 ft	0.014	0.0086	0.0048	0.0051	0.017	0.066

Dose Point	6	7	8	9	10	11	12
	90°	105°	120°	135°	150°	165°	180°
Radius	Dose Rate (mr/hr)						
(on surface)	750	600	230	74	31	15	11
2.5 ft	160	106	34	13	7	4.3	3.4
1 meter	95	62	19	7	4	2.3	2
5.0 ft	42	26	8	2.8	1.5	0.95	0.77
10.0 ft	10	6.6	2	0.64	0.34	0.22	0.18
25.0 ft	2	1.1	0.31	0.10	0.052	0.035	0.029
100.0 ft	0.1	0.066	0.02	0.006	0.003	0.002	0.002

NOTE: Locations of dose points in relation to generator are shown in Fig. 17.

C. FUEL TRANSFER

The shipping and field loading cask is designed to meet the requirement that the maximum dose rate at 3 feet from the source will be 10 milliroentgens/hour. Figure 20 shows the total directional doses received at 3 feet during the fuel transfer operation which lasts for 15 to 20 seconds. Significant directional doses are received in specific areas such as around the sliding plug at the bottom of the cask, around the collar shield, and below the collar shield. Though the doses go as high as 5 roentgens, they are of a radial beam type geometry and do not represent steradian doses. Therefore, these doses cannot be interpreted as equivalent total body doses. Precautions will be taken to minimize personnel doses from this source of direct radiation.

D. BURIAL IN SOIL AND MARINE IMMERSION*

After an abort during launching, the fuel core falls in the proximity of the launching area. The three probable resulting conditions are:

(1) The fuel core will penetrate the surface of the earth (maximum burial depth in earth of a bare fuel core is 110 inches).

(2) The fuel core will immerse in a body of water.

(3) The fuel core will be on the surface of the ground in vehicle debris.

Dose rates from a 0.88 megacurie fuel core versus thickness of soil and thickness of water are shown in Fig. 21. The dose rate will not exceed the maximum permissible operational exposure of 900 mrem for 1 hour if the fuel core is buried or immersed, respectively, under 3 feet of soil or 4-1/3 feet of water. By use of radiation monitoring devices in the accident area, exposure to retrieving personnel can be controlled.

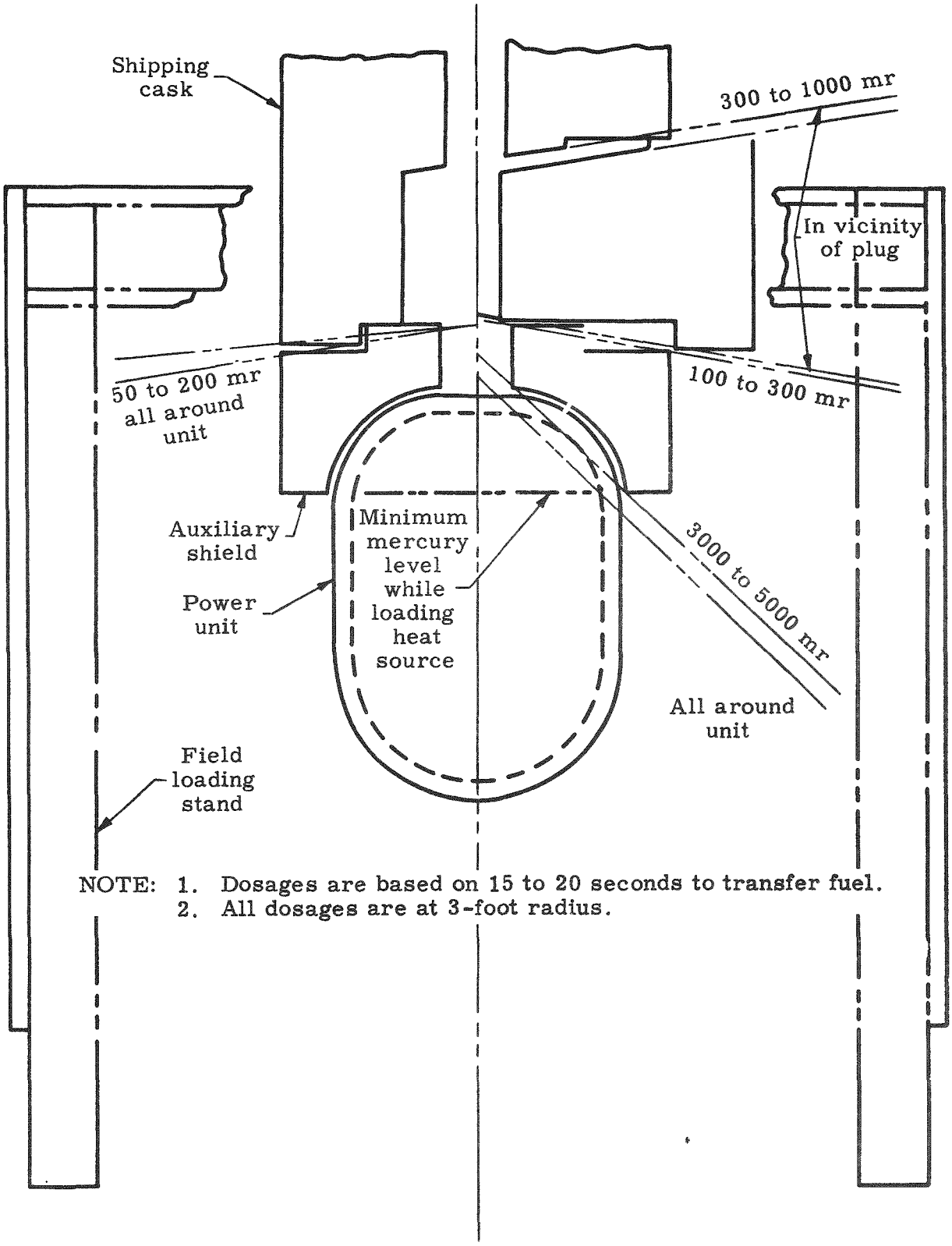

NOTE: 1. Dosages are based on 15 to 20 seconds to transfer fuel.
2. All dosages are at 3-foot radius.

Fig. 20. Transfer of Fuel Core to Generator

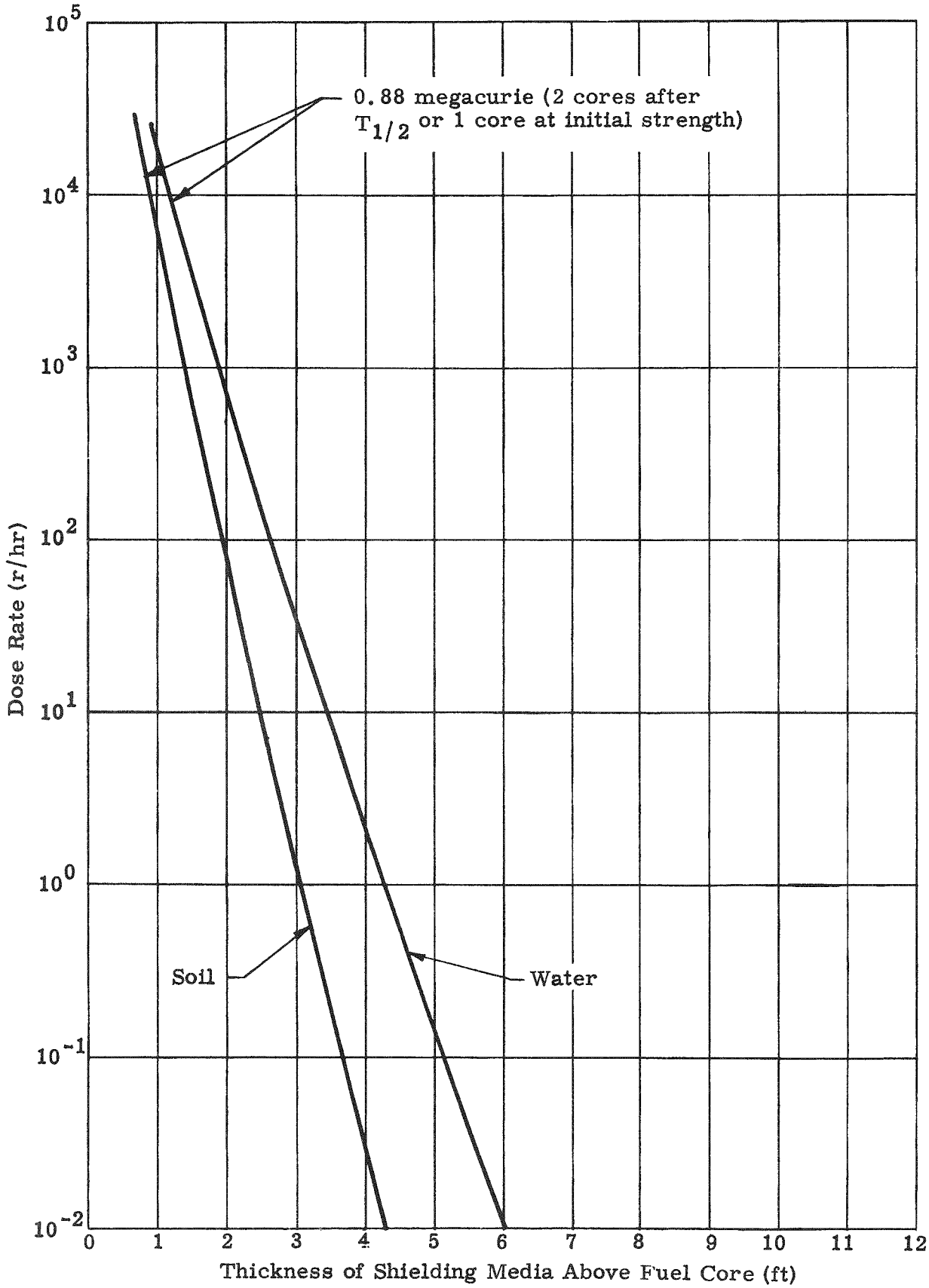

Fig. 21. Dose Rate Versus Thickness of Soil and Water Above Fuel Core

page blank

VIII. SUCCESSFUL MISSION

The successful mission is defined as one in which the satellite is placed into a terrestrial orbit of 600 days or more. This minimum orbital lifetime is based upon a 300-statute mile circular orbit. The three factors affecting the safety of the successful mission are:

(1) Satellite lifetime.

(2) Re-entry burnup characteristics (altitude of release, particle size of radiocerium fuel, etc.).

(3) The mean residence time of the radiocerium fuel released on re-entry.

The following safety evaluation discusses the radiocerium inventory of the satellite with respect to satellite lifetime, the re-entry characteristics of the Task 2 generators, and the fallout characteristics of the fuel.

A. RADIOCERIUM INVENTORY PRIOR TO RE-ENTRY

Figure 22 shows the radiocerium inventory of the satellite as a function of time after launch. At the 600 day minimum datum time, the original 1.76 megacuries has decayed to 0.409 megacurie. Longer satellite lifetimes will yield a more significant decrease in the radiocerium inventory. For example, a 5-year satellite lifetime would yield 20,800 curies, and, at 10 years, 246 curies*. Our datum inventory, however, remains at 0.409 megacurie and is the basis for calculations in this section.

B. RE-ENTRY OF GENERATORS

Existing satellite tracking stations can observe the history of the satellite bearing the Task 2 generators. Once orbit is established and altitude reduction rates are determined, the orbital lifetime can be estimated. Toward the end of the mission, after many tracking observations, it will be possible to approximate the projected geographical location of re-entry. This is somewhat academic in that the safety of the mission cannot be appreciably affected by virtue of this knowledge at this time. The re-entry of the satellite will occur at a random geographical location, but the radiocerium will be dispersed as aerosols at acceptable safe altitudes.

*Considered to be a negligible amount of radiocerium for atmospheric dispersion.

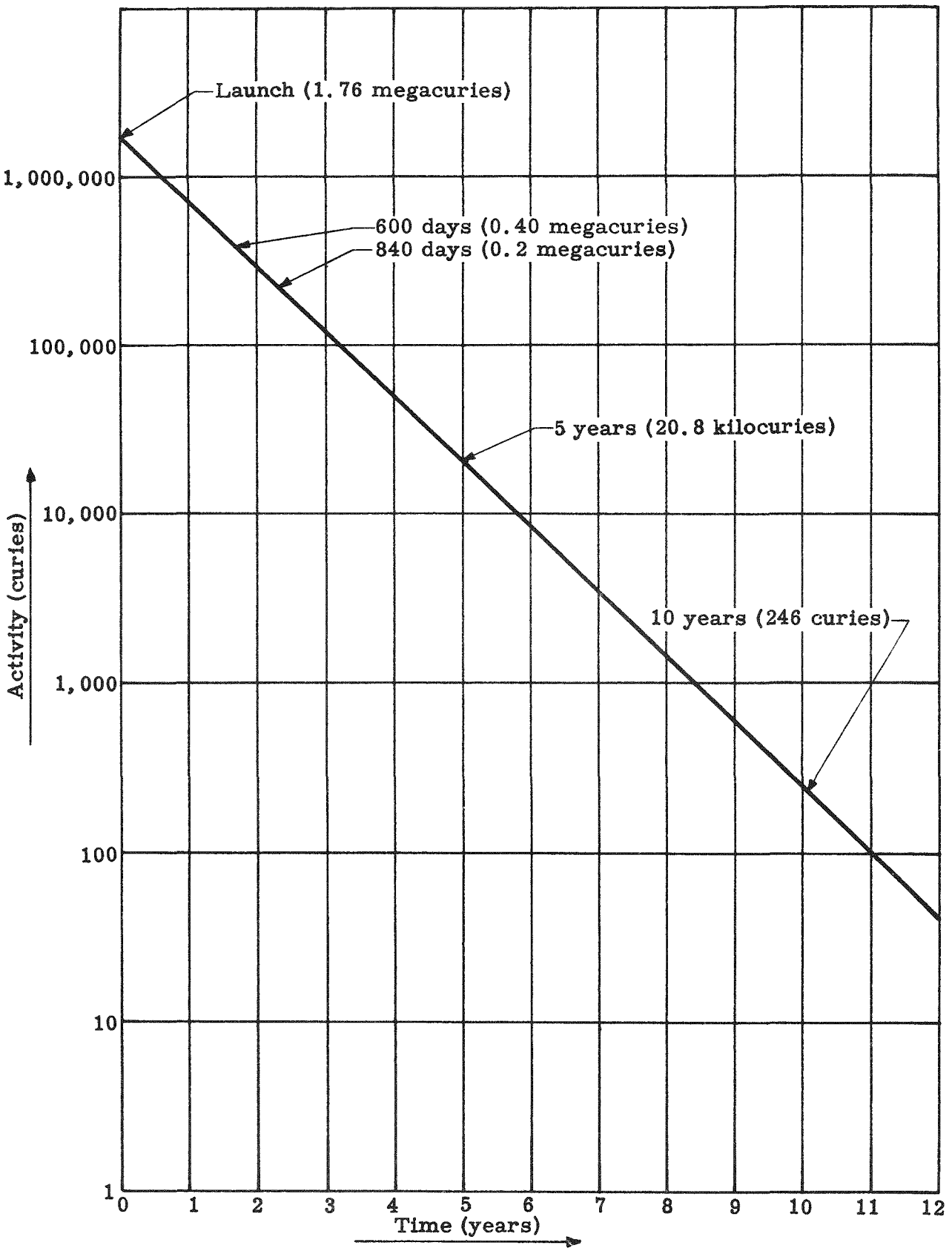

Fig. 22. Radiocerium Inventory of Satellite as a Function of Time

The chronology of events occurring at our datum time of 600 days is as follows.

(1) Orbital reduction of satellite into the sensible atmosphere.

(2) Re-entry burnup begins.

(3) Separation of generators from satellite structure.

(4) Separation of fuel cores from generators.

(5) Ablation of fuel core materials.

(6) Burnup and dispersion of fuel.

Aerodynamic retarding forces are experienced by a satellite immediately after it is injected into an orbit. The retarding forces are dependent on the orbital altitude and the aerodynamic shape of the orbiting body. The velocity of the satellite is gradually decreased which results in a decrease in altitude. This process is continuous and, when the sensible atmosphere is reached, the aerodynamic forces become significant. This will result in a more rapid re-entry and the initiation of aerodynamic heating.

The separation of the generators from the satellite will occur early in the heating cycle. Precise calculations of the separation mechanism have not been made because a general case has been considered. However, the aerodynamic heating calculation considers an additional thickness of aluminum around the generators to account for satellite structure. Figure 23 shows the re-entry trajectory and the aerodynamic heat generated by friction on the surface of the unit. The generator shells and the accompanying satellite structure will be completely consumed at an altitude of 280,000 feet. The centrifugal forces resulting from the spinning or tumbling of the unit will assist in the release of the free floating Min-K insulation. Immediately upon fuel capsule exposure to the atmosphere, aerodynamic heat will cause a temperature rise and will continue until the melting point of the capsule is reached. At an altitude of 234,000 feet, the fuel capsule is completely ablated. Originally, the study was performed with cerium metal considered as the fuel. Cerium metal, with a melting point less than that of the capsule material, will be molten upon its release. Experimental plasma jet tests were conducted, and it was satisfactorily shown that particle sizes less than 10 microns in diameter will result.

The present fuel form, ceric oxide and silicon carbide, has a melting temperature higher than the capsule material and will be released at 234,000 feet and above in a solid form. Figure 23 shows the aerodynamic heat that will be experienced by the fuel forms. Estimates

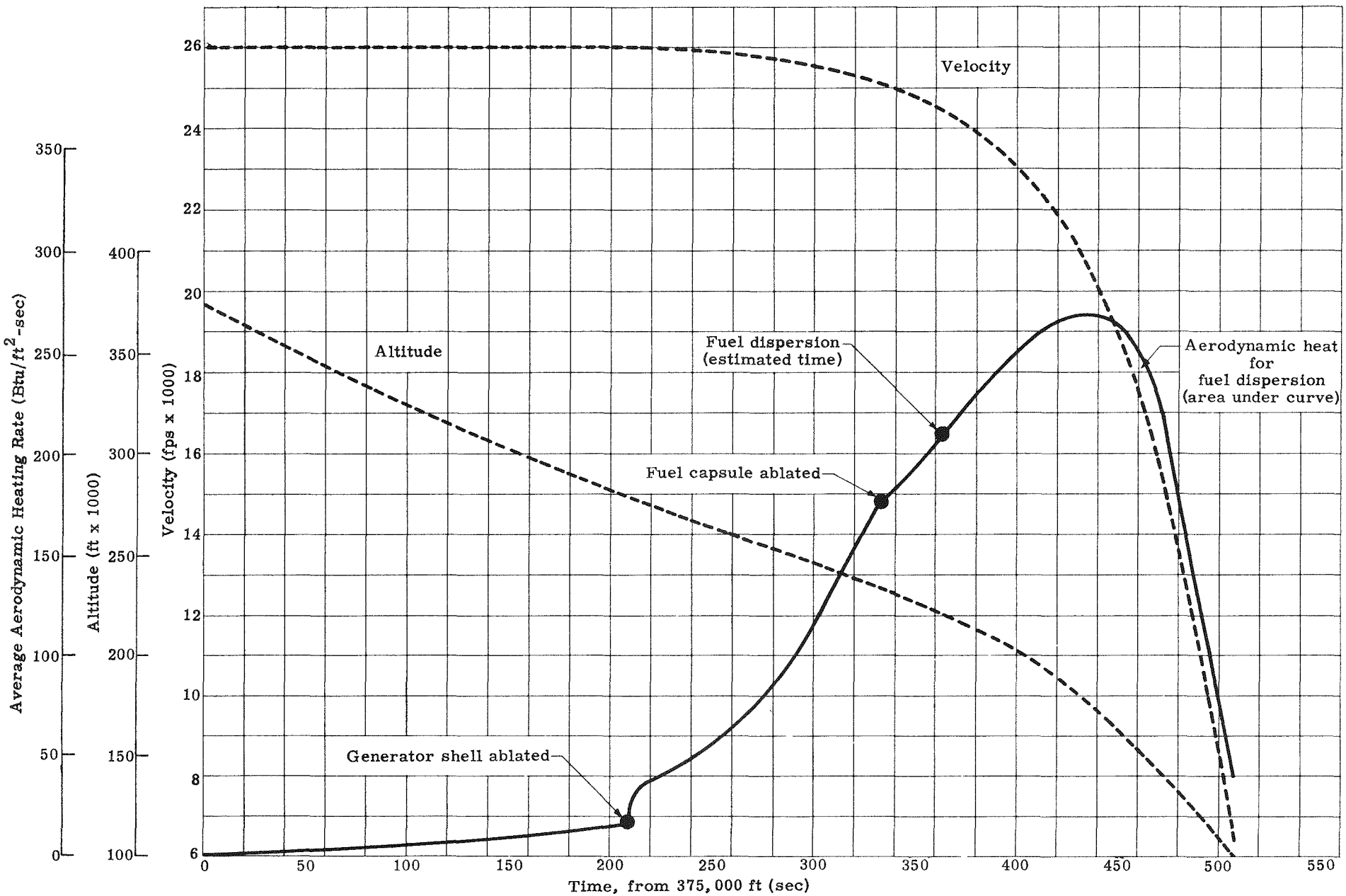

Fig. 23. Postorbital Re-entry

indicate that only 30 seconds of exposure will be required for complete melting of the fuel materials[15]; this corresponds to an altitude of 220,000 feet. Plasma jet tests have again conclusively shown that the fuel will be dispersed to submicron sizes.

The fate of the fuel is discussed in Chapter X which compares the consequences of both successful and aborted missions.

page blank

IX. ABORTED MISSIONS

This chapter will define aborted missions, describe the forces imposed on the Task 2 thermoelectric generators by the vehicle malfunctions defined, and demonstrate the resulting trajectories and aerothermodynamics associated with high altitude failures. One must reiterate here that the generators and their fuel are designed to burn up above 100,000 feet altitude on re-entry following orbital decay. Aborted missions are of four types:

(1) Launch failures.

(2) Ascent failures.

(3) Final stage failures.

(4) Orbital decay and re-entry before the design lifetime of the satellite of 600 days.

The first three points above will be covered in detail. However, orbital decay and re-entry before 600 days will yield the same conditions as those described for successful missions, with the exception of the Cerium-144 inventory, which will decrease with orbital lifetime. The satellite will circle the earth 16 times in one day and 9600 times in 600 days. Failures on the first orbit will result in an injection of 1.76 megacuries of Cerium-144, and the 600-day injection inventory will be 0.409 megacurie. Therefore, failures of Type 4 will yield ground concentrations of Cerium-144 ranging between those resulting from successful missions and those resulting from prompt aborted missions as covered by Type 3 failures.

A. DEFINITION OF ABORTED MISSIONS

Definition of the type of potential malfunctions of the launching vehicle has been derived by an analytical comparison of failure of past missile and satellite vehicles with the characteristics of the typical system examined here. The examination included a detailed study of the design characteristics of the launching vehicle and a postulation of the type of failure that might result. A series of experiments has been conducted to simulate actual destructive forces to which the generator will be exposed during failures.

1. Definition of Launch Failures

Launch failures are broadly defined as those failures which occur either on or directly above the launch pad. This will span a time period of several minutes prior to liftoff to approximately 15 seconds after the vehicle is airborne. This specifically excludes minor electronic and mechanical failures which merely interrupt the countdown. The vehicle will be at an altitude of approximately 1000 feet 15 seconds after launch, the maximum height considered for the launch failures. The trajectory calculations and the location of the dispersion area of vehicle remnants, in case of launch abort, are greatly simplified as the velocity vector of the vehicle is vertical throughout this period. Launch failures are subdivided into propellant tank, propulsion and guidance failures.

Propellant tank failure. A propellant tank failure results from either overpressurization or spontaneous structural failure of the propellant tanks. Two failure mechanisms are possible. First, there is a possibility that rupture of the bottom of the liquid oxygen tank of the booster and of the top of the RP-1 tank can cause the propellants to mix within the missile. Second, the most probable failure is side seam failure of the tanks and resultant mixing of the propellants on the launch pad.

The mixture of liquid oxygen and RP-1 fuel can be ignited by sparks, by hot engine components, or scintilla. The liquid oxygen will vaporize rapidly and some of the RP-1 fuel will soak into the launch pad or drain into the flame bucket of the launch pad. Any likely fire will be gravity fed until the collapse of the missile structure allows it to reach the unexpended fuel in the tanks.

In failures of two-stage missiles, two distinct fireballs have been observed. These have resulted from the combustion of the first stage fuel and the subsequent ignition and combustion of the second stage fuel. The second stage is assumed to be fueled with unsymmetrical dimethylhydrazine (UDMH) and the oxidizer is inhibited red fuming nitric acid (IRFNA). This mixture is hypergolic, that is, it ignites spontaneously upon mixing. Consequently, combustion of the second stage is quite probable, but subsequent to, rather than simultaneous with, the first stage combustion.

Propulsion failures. A propulsion failure can occur throughout the entire thrusting period. The vehicle is tied down by explosive bolts for approximately 10 seconds after thrust is first initiated for a final check of the propulsion system. The check includes valve settings, propellant flow, thrust buildup, and other pertinent subsystems. The vehicle will be released only when thrust is near or at full power. When the required performance is achieved, the tiedown bolts will be automatically detonated and fractured, allowing the vehicle to lift off. This is considered time zero in the launch chronology.

Failures during the launch period can be attributed to restricted fuel flow, pump failure, incomplete combustion of propellants, or other malfunctions of the booster engines. Such a failure will cause the vehicle or its remnants to impact on or near the launch pad. Two specific types of events are possible. First, very low altitude fallback failures will cause the vehicle structure to be crushed on the launch pad, releasing propellants en masse at that location followed by a major conflagration. Second, and perhaps the least serious of the two failures, is the airborne ignition of the propellants. Due to poor mixing, diffusion of propellants, and selective separation of missile components and propellants by drag, destruct charges, and gravity forces, a midair fire yields less energy than fallback. The propulsion failure of the booster engine will cause the final stage propellants to ignite due to their hypergolic characteristics.

Guidance failures. Guidance failures during the launch sequence are infrequent because the vehicle is in a vertical climb during this period. A destruct capability is incorporated in boosters to enable the range safety officer to destroy the vehicle if its performance is significantly different from the desired vertical trajectory, and inflight correction is impossible. The range safety destruct signal detonates explosive charges which rupture the propellant tanks and cause immediate thrust termination and destruction of the vehicle. Combustion of the propellants will result, producing a fire of very short duration which will be comparable to the midair fire described previously for propulsion failures. Debris from vehicle destruct will be scattered over an area within the range safety impact zone described in Chapter VI.

2. Definition of Ascent Failures

Definitions of ascent failures will be limited to those malfunctions that can occur during booster-sustainer stage operation from 1000 feet altitude up to, but not including, final stage ignition. The period of time under consideration will then be limited to 15 to 585 seconds after launch, the time of ignition of the final stage. Upon termination of the thrust of the booster-sustainer, 285 seconds after launch, a coasting time of 300 seconds is required to achieve the desired orbital altitude.

Ascent failures to be considered are at those critical points on the ascent trajectory where significant events occur. They are: failures at pitchover, maximum dynamic pressure, booster engine separation, sustainer burnout, and during the entire coasting period. Failures at points intermediate between these points will be governed by the maximum conditions of the next ascending point on the trajectory and the minimum conditions of the preceding critical point. Throughout the ascent phase, range safety destruct capability will be present in case of significant deviations from the prescribed trajectory.

Failure at pitchover. Pitchover is the point in the ascent trajectory at which the vehicle departs from the vertical climb to begin its downrange travel and acceleration to orbital speed. The time of initiating pitchover for this configuration is 15 seconds after liftoff and the conditions at this time are: altitude of 1000 feet, flight path angle of 90°, a velocity of approximately 200 feet per second, and a downrange distance of zero. If the pitch program is not initiated or if a propulsion failure occurs at that point, the missile or its debris will subsequently impact at a range of essentially 0 miles.

Failure at maximum dynamic pressure. Maximum dynamic pressure occurs approximately 60 seconds after launch at an altitude of 38,000 feet and a velocity of approximately 1000 feet per second. At this point maximum aerodynamic loads are imposed on the missile, this being one of the critical points on the ascent trajectory. After a failure, the main body of the vehicle will coast to an apogee of approximately 41,000 feet and will impact downrange a distance of approximately 2 nautical miles, still in the range safety impact zone.

Failures at booster engine separation and sustainer burnout. The booster engines of the vehicle, attached outboard of the sustainer, are assumed to deliver thrust for 140 seconds. The booster and sustainer engines draw propellant from common tankage, and the burning time for each stage is determined from an ascent optimization study. After 140 seconds, the booster engines and the skirt about them are separated and tumble away from the vehicle. This occurs at an altitude of 250,000 feet, at a velocity of approximately 10,000 feet per second, at a flight path angle of 23°, and at a downrange distance of 60 nautical miles. A complete propulsion failure at this time would cause the vehicle to coast to an apogee altitude of approximately 586,000 feet and then impact 780 nautical miles downrange.

The sustainer engine will terminate thrusting at 285 seconds after liftoff. At this time, the spent booster, the injection stage, and the payload will be at an altitude of 860,000 feet, at a velocity of approximately 18,500 feet per second, and at a flight path angle of 14.8°. The remaining portion of the booster is separated from the injection stage and will coast to an apogee of approximately 1,584,000 feet and then impact downrange a distance of 2500 nautical miles.

Failure during coast*. A coast phase is used to align the satellite stage and adjust the trajectory to proper conditions for final stage ignition. When two stages are separated as described previously, it is possible for the stages to interfere, or "bump," imparting disturbing moments to the final stage. During the separation and coasting sequences of the vehicle system, the attitude of the vehicle is defined by gyro references

*C. D. Waring

which energize the altitude control system if the vehicle deviates from the prescribed conditions. These systems have response times in milliseconds. Aside from any physical damage incurred by the injection stage during separation, it is possible that the magnitude and acceleration of the disturbing moment may be sufficiently great to drive the gyro references of the vehicle to their limits. Although this condition can occur, it is doubtful that it would go unnoticed since the gyro position is telemetered back to the range control center. If the impact prediction is such that potential vehicle impact point would endanger life and property, the vehicle would be destroyed on command.

If damage is incurred by the injection stage during separation, this may or may not be detected via telemetered information during coasting flight. Damage to the final-stage propulsion system would probably not be detected (since no propellants are flowing and the engine is not thrusting) unless the damage is of such a nature as to cause a drop in propellant tank pressures. Damage to the pitch and yaw servoactuators for engine gimbaling likewise would probably go unnoticed until ignition of the final stage engine. Damage to the gas-operated attitude control system would probably be detected immediately, since the vehicle would fail to respond to guidance signals or would respond improperly.

Just prior to final stage engine ignition, ullage rockets are fired to provide a small positive acceleration to the final stage and maintain a positive head on the propellants. These ullage rockets are canted outward and are arranged 180° apart. If either fails to fire, a slight pitch or yaw disturbance will be imparted to the vehicle. Since the angle of cant is small, this displacement can probably be easily counteracted by the operation of either the pitch or yaw gas jets. If neither rocket fires, the chances that upper stage ignition would be achieved are poor and the vehicle would continue along a ballistic trajectory, identical to that described for sustainer engine burnout failure. The projected impact point of the final stage would be 2500 nautical miles downrange in this case.

Definition of final stage failures. Failures during final stage operation can also be caused by malfunctions in propulsion, propellant feed, and guidance systems. At the point of ignition, the probability of a vehicle malfunction is relatively high since a complicated sequence of events must take place. It has been determined that for 3% of the cases in which the ascent trajectory is within 3-sigma performance limits, successful orbital injection may not be achieved because of engine ignition failures[16]. The engine injector starting characteristics could be such that high frequency instability occurs, which will cause the engine failure.

After steady-state engine operation, the probability that thrust termination or malfunction will occur is considerably reduced to 1.5%. A chamber failure could result in having the thrust vector acting at various angles to the flight path, creating a disturbing moment on the vehicle. Such failure over a finite period of time and of sufficient magnitude will cause the vehicle to tumble. Under a tumbling situation, the engine would probably shut down since propellants would be intermittently available to the propulsion system and chamber pressure could not be maintained. Other malfunctions such as ruptured propellant tanks or turbopump failure would result in a sudden termination of thrust, with a possible propellant fire.

Failures in guidance and supporting systems will cause the greatest deviation from the planned trajectory. The probability of an autopilot failure during final stage operation was determined to be 2%. The result of any guidance failure would be either to shift the gyro reference plane (resulting in a vehicle deviation in pitch or yaw from the planned trajectory) or to prevent the servos from correcting the vehicle motions as indicated by the guidance system. This condition will allow the vehicle to drift off trajectory, the extreme case being lateral drift yielding impact away from the prescribed launch azimuth.

The injection vehicle has a redundant destruct system (weighing about 25 pounds) which has a reliability factor of nearly 100 percent. This system is energized by ground command whenever it is shown by impact predictions that the vehicle will travel beyond the limits where a safe impact will be unobtainable.

Though the destruct system is highly reliable, it was decided to investigate all probable re-entries that can originate from malfunction of the injection stage. Shown on the map in a later section is an outline of the maximum dispersion that could result for failures of this stage. Failures at random times after final stage ignition were assumed in this study, with maximum dispersion simulated by placing the thrust vector at various angles to the velocity vector. Thrust misalignments were analyzed for positive and negative pitch and yaw deviations. The resulting trajectories duplicate actual re-entry trajectories experienced by the vehicle under final stage abort conditions.

Propulsion failures. Propulsion failures considered were final stage engine failures after various burning times. The net effect of final stage engine failure is to give to the injection stage various velocities short of orbital velocity at the time of failure. Velocity increments of 400 (Case 5a), 600 (Case 5b), 2000 (Case 5c), 4000 (Case 5d), 6000 (Case 5e*), and 7242 feet per second less than planned orbital velocity were considered for the points of thrust termination.

*These cases are summarized in Chapter X.

The parameters* used for the final stage rocket and flight conditions are:

Weight of Propellants Consumed (lb)	6640
Specific Impulse (lb/lb-sec)	266.43
Burning Time (sec)	106.4
Initial Flight Path Angle (deg)	2
Initial Altitude (ft)	1,524,000
Initial Velocity (fps)	17,781
Initial Longitude (deg)	121.67 W
Initial Latitude (deg)	16.37 N

Guidance failures. The final stage was analyzed for pitch and yaw misalignments during stage operation as a means of duplicating actual re-entry trajectories caused by vehicle aborts. The method of analysis used was to instantaneously deflect the thrust vector at various angles to the velocity vector, after which thrusting of the engine is continued for the total programmed period of thrust at the deflected orientation. The cases considered were as follows. The parameter ΔV is the velocity less than orbital velocity where the thrust vector was deflected.

Case	ΔV (fps)	δp (deg) (pitch deflection)	δy (deg) (yaw deflection)
1a, 1b, 1c	600	+5, +45, +90	0
6a, 6b, 6c		0	±5, ±45, ±90
2a, 2b, 2c	2000	+5, +45, +90	0
7a, 7b, 7c		0	±5, ±45, ±90
3a, 3b, 3c	4000	+5, +45, +90	0
8a, 8b, 8c		0	±5, ±45, ±90
4a, 4b, 4c	6000	±5, +45, +90	0
9a, 9b, 9c		0	±5, ±45, ±90
5f, 5g, 5h	7242*	-5, -30, -90	0

* This value corresponds to velocity at final stage ignition.

The deviations considered were the most conservative conditions that could be imposed, since deflection angles greater than 10 degrees are not credible. Figure 24 shows the method of analytical procedure employed for final stage failures.

* Estimated from available final stage data.

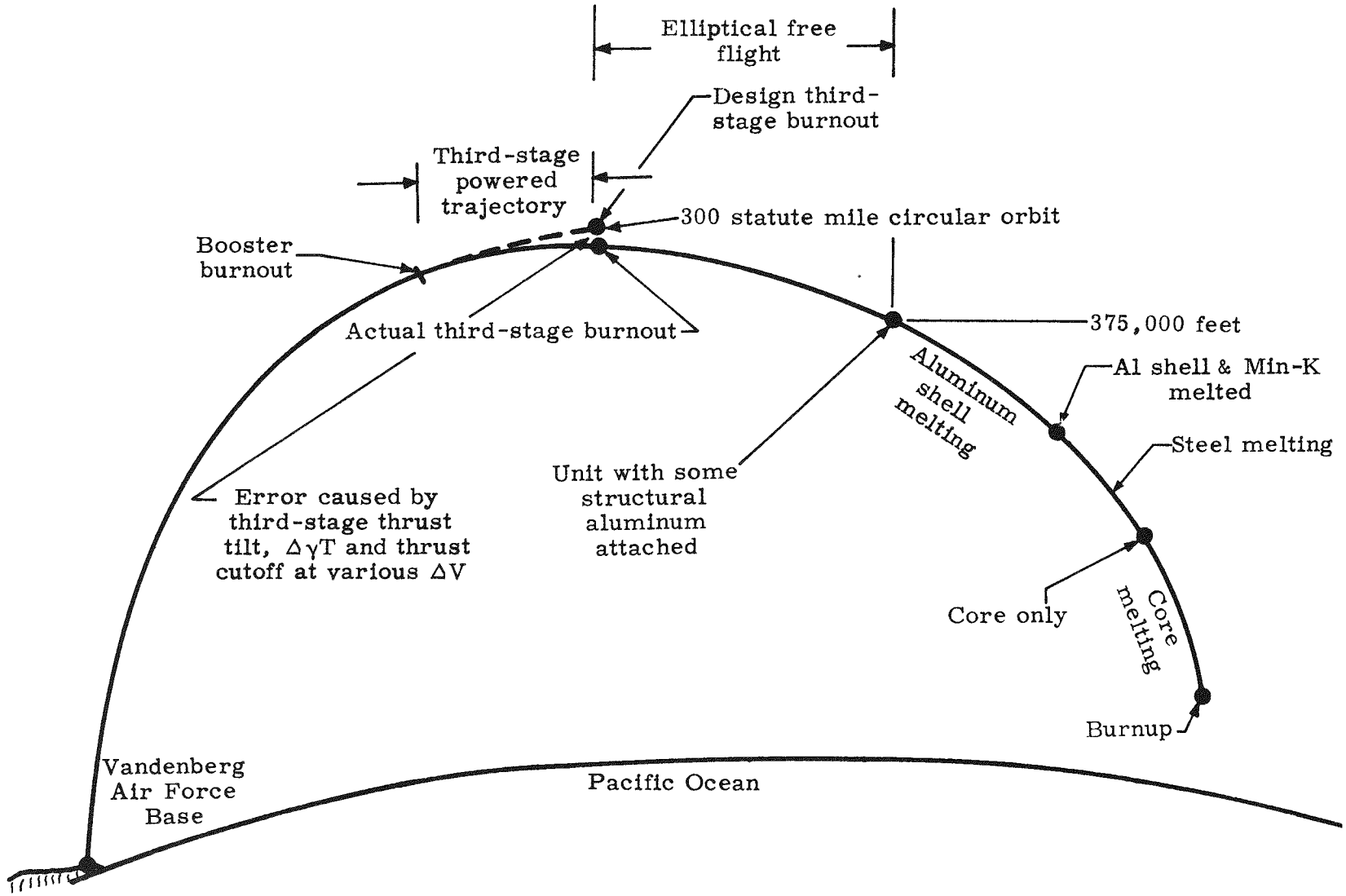

Fig. 24. Steps of Analytical Procedure

B. DEFINITION OF FORCES IMPOSED BY ABORTED MISSIONS

The forces imposed on the Task 2 thermoelectric generator by the launch, ascent and final stage aborts previously described are logically categorized as thermal, mechanical and chemical. The nature of these forces was determined from past histories of missile failures by analytical methods and through experimentation. Appendix A explains the details of pertinent experimentation conducted for the Task 2 program.

1. Forces Imposed by Launch Failures

Thermal forces. Failure of the typical vehicle described in Chapter V, below an altitude of 1000 feet, will result in a massive release and ignition of propellants of both stages on or above the launch pad with the generators intimately located in the conflagration. Initially, two successive superimposed fireballs, one from LOX-RP-1 and the other from UDMH-IRFNA (separated by an interval of several seconds), will form and be followed by a persistent propellant and metal fire. Each fireball will have a lifetime of about 6 seconds and a diameter of from 100 feet (UDMH-IRFNA) to 250 feet (LOX-RP-1). The peak fireball temperature of 5600° F lasts for only milliseconds. The initial condition of a typical propellant fire is shown in Fig. 25. The thermal energy imparted to the generators by the fireballs is relatively insignificant since they are short lived and rise 15 to 20 feet per second by convection. The violence of the fireball will serve to disperse propellants and decrease the amount of residual propellants available for combustion in the sustained fire that will follow.

However, the persistent nature of the propellant fire following the fireballs is indicative of a large source of total integrated thermal energy. Here the RP-1, metals and UDMH burn at a steady but decreasing rate after the liquid oxygen has evaporated and diffused. Of the 83,000-pound RP-1 inventory at launch, several thousand pounds would remain to feed the fire. For example, 5000 pounds of RP-1 would have a potential heat value of 10^8 Btu (18,600 Btu per pound). The 700 pounds of magnesium in the satellite would have a potential heat value of 7×10^6 Btu when reacting exothermically. Half of the UDMH inventory (~900 pounds) has a potential heat value of 10^7 Btu. Therefore, about 10^8 Btu will be potentially available from the sustained fire. Of this energy, a fraction will go into the missile structure and ground, and the rest will be carried off by radiation and convection.

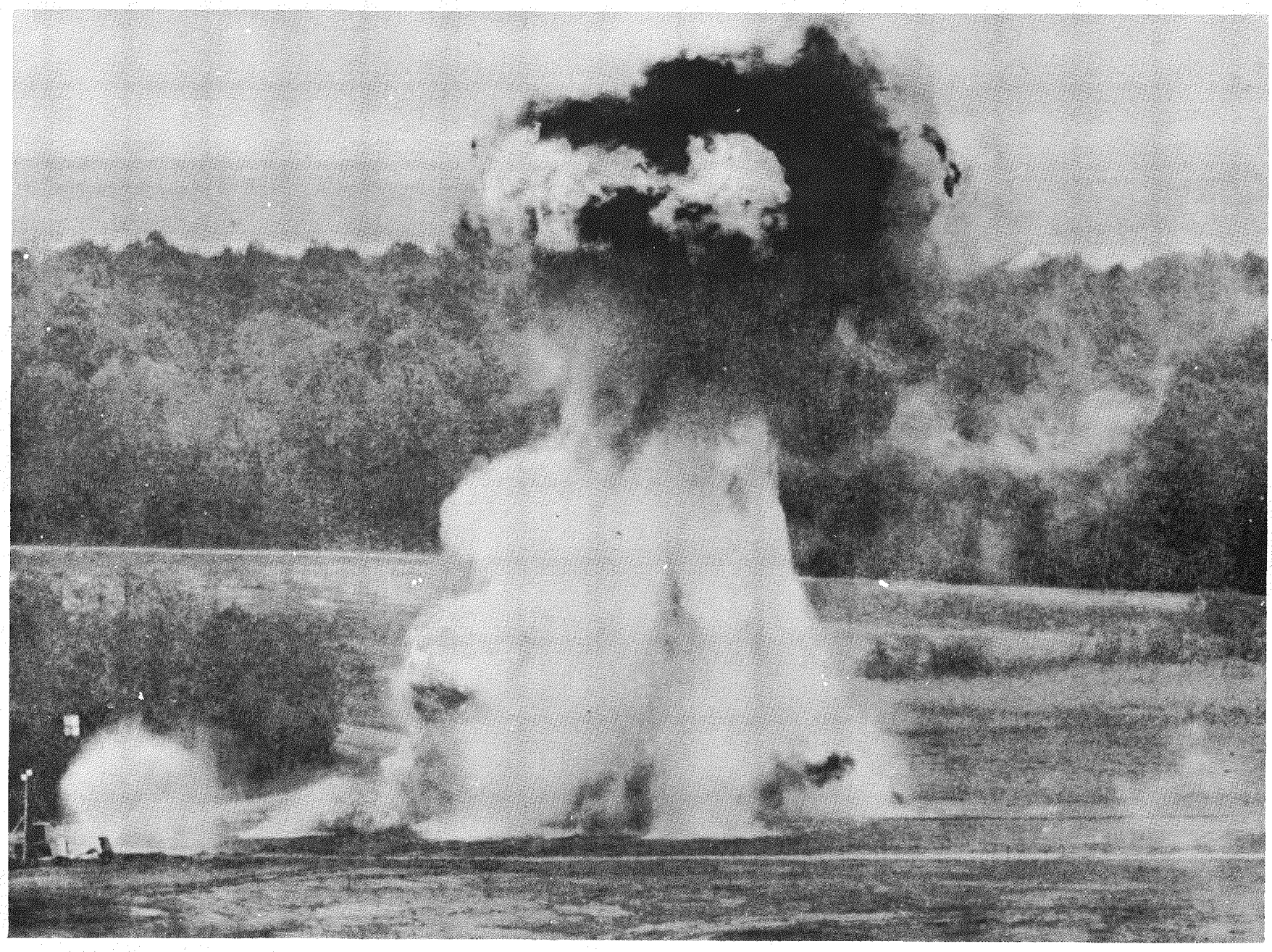

Fig. 25. Full-Scale Missile Failure Experiment

Examination of the fuel core shows that 19,500 Btu are required to raise the core from operating temperature (1670° F) to its melting point (2600° F). The isotope is providing an internal heat of 6 Btu per second. In a propellant fire, the core is insulated against the external heat by the Min-K outer shell. Therefore, throughout the fire the internal heat of the isotope is the governing factor. The core would have to be completely insulated for approximately 80 minutes before meltdown of the core could occur. The propellant fire temperature would provide a thermal barrier producing insulation for no more than four minutes, after which the temperature of the fire is less than 2600° F.

On the other hand, if the fuel core is immediately exposed to the fire at operating temperature, a comparable time (four minutes) would exist in which external heat could be transferred into the core. After this time, the core can radiate heat to the fire, since the fire temperature is below the core temperature.

Since a very rigorous heat transfer analysis involving a multitude of variables was, at best, an order of magnitude estimate of the problem, it was decided to conduct field tests to determine (1) the thermal forces imparted by the propellant fire, and (2) the effects of these forces upon the generator and fuel core. The missile failure was simulated in full scale at Aberdeen Proving Ground. Bare fuel core specimens and one full-scale generator were immersed in the center of the thermal environment. The two fireballs are shown in Fig. 25. Figure 26 is a plot of temperature versus time in the fire with bare fuel core temperatures superimposed. No appreciable thermal damage was imposed upon the cores by the tests, and simulated fuel was retained by the thermal integrity of the encapsulation.

Mechanical forces. The two mechanical forces applied to the generators by a launch failure are impact and shock overpressures. The impact of the fuel cores on or near the launch pad would occur from 70 to 1000 feet altitude, yielding maximum impact velocities of 62 to 250 feet per second, respectively. Impact forces of this magnitude can readily be dismissed, since the fuel cores are designed to withstand impact at a terminal velocity of 500 feet per second.

Early in the Task 2 program, the magnitude of shock overpressures from exploding propellants was not clearly known. The first analyses conducted indicated that, if LOX-RP-1 propellants were spilled on the launch pad, mixed, and detonated, explosive yields up to 77%* TNT equivalent could result.[17] Subsequent to this investigation the Space Technology Laboratory developed certain empirical formulae from observed missile failures.[18] These formulae were employed to determine personnel safety distances for launch complexes. They are:

*From tests of 1/10-scale missiles.

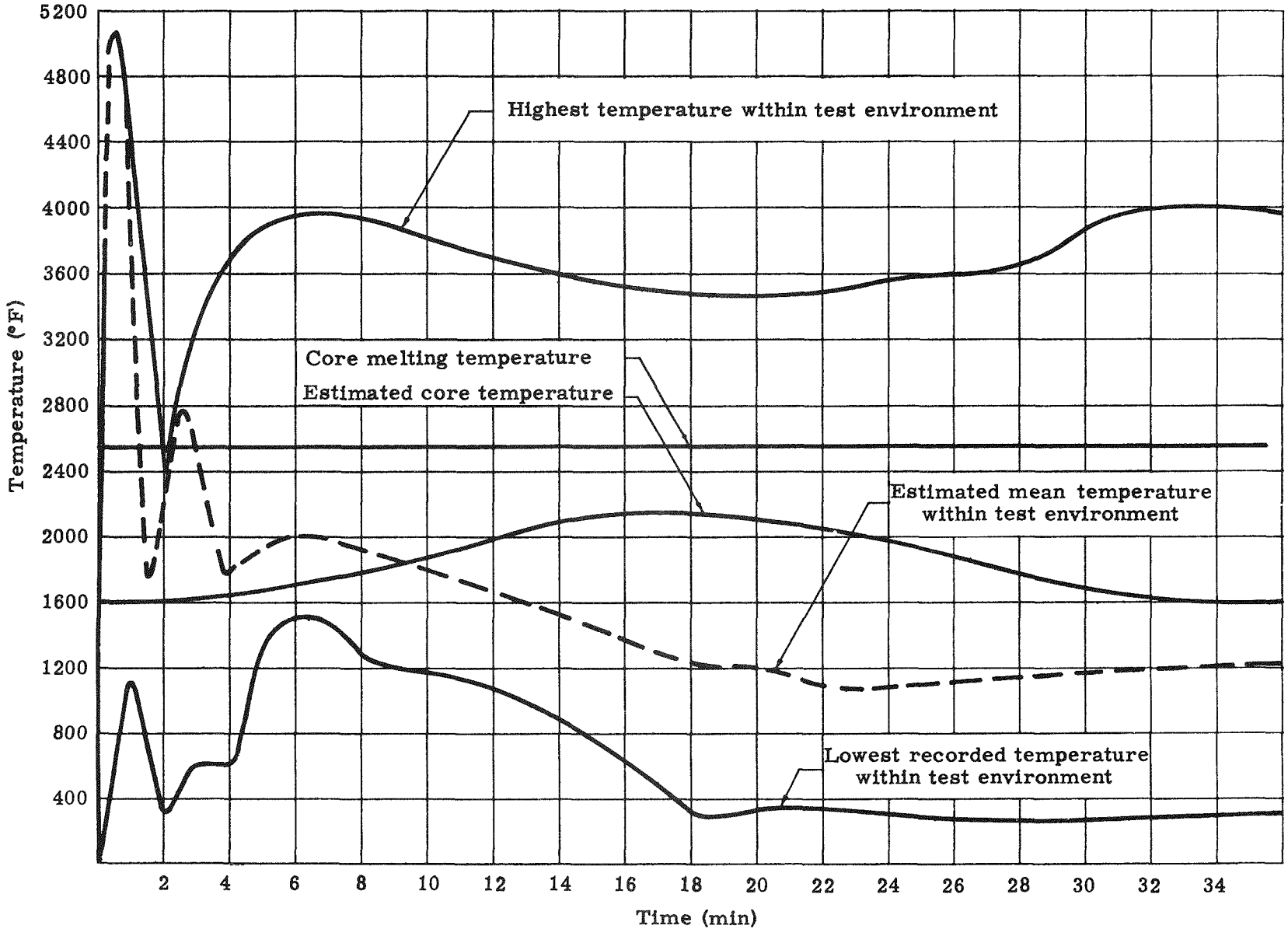

Fig. 26. Temperature Profile of Propellant Fire

Predicted average pressure

$$P = \frac{593}{Z^3} - \frac{28.8}{Z^2} + \frac{20.7}{Z}. \qquad (1)$$

At the upper 98% confidence limit

$$P = \frac{9862}{Z^3} - \frac{187.9}{Z^2} + \frac{52.8}{Z} \qquad (2)$$

where

P = peak side-on overpressure (psi)

$Z = \frac{R}{W^{1/4}}$

R = distance from explosion (feet)

W = total weight of propellants (pounds).

Using the Task 2 values and substituting into Eq (1),

R = 35 feet (distance of generator from source of explosion)

W = 260,000 pounds (weight of booster propellants)

P = 166 psi.

Using the Task 2 case and substituting into Eq (2),

P = 2568.7 psi.

Calculations performed by the Army Ballistics Research Laboratory indicated that the Task 2 generators would receive a peak overpressure of 1020 psi. Scale model tests conducted by BRL demonstrated that fuel cores would not fail at these pressures.[19] The ultimate tensile strength of Inconel X at operating temperature is over 20,000 psi.

Turning from the explosive potential of booster propellants, the injection stage propellants (UDMH-IRFNA) were investigated. Preliminary data indicated that the energy yield from these propellants was entirely thermal (i.e., no shock waves). This was verified in the full-scale failure test conducted at Aberdeen Proving Ground. Thus, the problem of shock overpressure from final stage propellants was eliminated.

Chemical forces. Since the launch abort restricts the ultimate location of fuel cores to the vicinity of the launch pad, the only possible chemical forces expected were those imposed by the immersion of fuel cores in, or contact of fuel cores with, propellants. Liquid oxygen and inhibited red fuming nitric acid were the propellants of interest. Immersion of cores in propellants is not likely because of the protection afforded the cores by the shell of the generator. Immersion in liquid oxygen, even if it occurred, would be for a very limited period because the liquid oxygen will evaporate, burn and disperse rapidly during any significant vehicle failure. Inconel X cores at operating temperatures were immersed in liquid oxygen for exposure times exceeding those of expected missile failures without any appreciable oxidation or thermal shock damage to the cores.

Corrosion of the cores by nitric acid would proceed at an estimated maximum rate of 2.5 inches per year if the cores were completely immersed and maintained at 250 to 300° F. With a core wall thickness of 0.3 inch, it would take 41 days to expose the radiocerium fuel. This time is far greater than a credible exposure time of the cores following launch aborts.

2. Forces Imposed by Ascent Failures

Though ascent aborts cover a wide variation of conditions, the forces imposed upon the generators are still intermediate between those of launch failures and final stage failures. As we pass along the ascent trajectory, the effect of propellant ignition becomes less significant as booster propellants diminish and aerodynamic heating becomes more severe with increasing velocity. Beyond an altitude of 10,000 feet, the generators or fuel cores will impact at their constant terminal velocity at impact points which range from the launch pad to a point at sea 2500 miles downrange.

Thermal forces. The maximum release of thermal enery from propellants ignited en masse was shown to occur during the launch failure. The available propellants from the booster decrease until they are completely expended at sustainer burnout (285 seconds after launch). However, during the period from 15 to 285 seconds, their ignition can be induced by missile destruct from the range safety officer if the vehicle is off course. The final stage is dormant during the entire ascent period (15 to 585 seconds), and its propellants remain as a potential source of thermal energy. The nature of the airborne propellant fire is such that the generators would only be exposed to the initial fireball and would be immediately separated from the thermal environment by drag forces as the vehicle disintegrates. Because of these factors, the thermal forces from ascent fires would not be as severe as those experienced in launch fires, and their effects upon the fuel core need not be considered further.

Aerothermodynamic forces are insignificant from trajectories resulting from aborts in the booster period including pitchover, maximum dynamic pressure, and booster engine separation. For example, failure at booster engine separation will result in re-entry from an apogee of 586,000 feet with insufficient heat to melt the outer shell of the generator. An abort at sustainer thrust termination or at final stage ignition will produce sufficient aerodynamic heat to melt the shells of the generators, exposing the core. The point at which the core is exposed is well below the altitude where the peak heating rate is imposed by aerodynamic forces so that no damage to the core will occur. However, as will be shown below, the aerothermodynamic effects on the generator of the late ascent aborts will determine the impact velocity of the fuel core.

Mechanical forces. Potential shock loads from booster propellants will decrease as they are expended in a similar manner as the thermal energy described above decreases. In addition to this factor, the intimate mixing of propellants will not occur due to the motion of the vehicle and confining surfaces. Therefore, the mechanical energy yield will decrease on a pound-for-pound basis from ground to airborne detonations. It has also been shown that the final stage propellants are not a source of mechanical energy. During the period of potential shock energy (15-285 seconds) there is a possibility of damaging the outer shell of the generator and releasing the core to the air stream. However, throughout this period, aerothermodynamic forces are not significant and would not damage the exposed core.

Impact loads imposed by cores impacting on the earth at terminal velocity are the most severe forces experienced during ascent failures. The terminal velocity of the generator is 210 feet per second; the core impact velocity is 460 feet per second. Consequently, as long as the generator shell is present at impact, the core will receive a negligible impact pressure of about 250 psi. At 460 feet per second, the terminal velocity of the core, the impact pressure is about 20,000 psi on rigid target media, and at operating temperature the core has an ultimate tensile strength of 23,000 psi. This relationship is shown in Fig. 27.

An examination of potential impact media is warranted. During pitchover aborts, the generator would impact well below its terminal velocity near the launch pad. At maximum dynamic pressure, a failure would result in terminal velocity impact approximately two nautical miles downrange. These cases would result in impact on nonrigid media consisting of unconsolidated dune sand, alluvium and terrace sediments of Quaternary age. Bare cores impacting at terminal velocity would penetrate 6 feet or so of this material. Impact pressures would be only a fraction of those previously stated for rigid media.

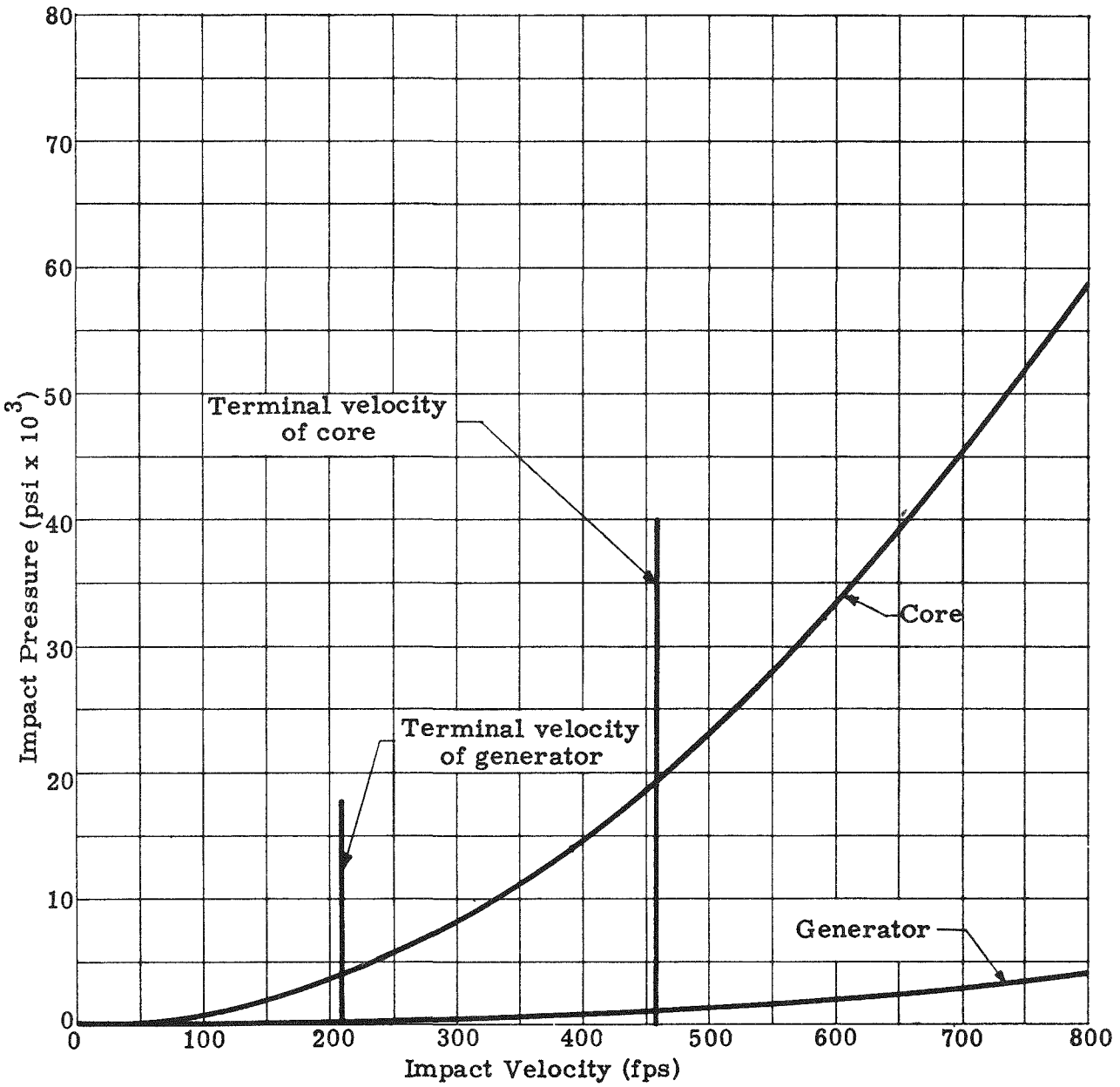

Fig. 27. Impact Pressure of Fuel Capsule and Generator on Rigid Target Media

Aborts at booster engine separation would provide impact at sea 780 miles downrange. Aborts at sustainer burnout and final stage ignition would result in impact of the fuel cores at sea 2500 miles downrange. Since impact would occur on a nonrigid medium, fuel core integrity would be maintained.

Chemical forces. Aborts at pitchover and maximum dynamic pressure could conceivably result in cores being exposed to nitric acid. However, due to the breakup characteristics of the vehicle, the fuel cores could not become immersed in nitric acid from residual propellants in the ground wreckage.

Exposure to saline solution is quite possible, since sea impact will result from aborts occurring from 100 to 585 seconds after launch, a substantial period of time. The pitting rate of sea water on Inconel X is 0.0236 inch per year acting on a core wall thickness of 0.3 inch. At this maximum corrosion rate, the fuel would become exposed after 12.8 years, when the initial Cerium-144 inventory of 1.76 megacuries has decayed to 20 curies. Therefore, effective chemical core integrity is achieved.

3. Forces Imposed by Final Stage Failures

The forces imposed by final stage failures are primarily those of aerodynamic heating and terminal velocity impact of bare fuel cores or their remnants. This framework of failures contains the grey area that must exist for all devices designed to burn up on re-entry following post-orbital decay. Fortunately, this grey area has spatial and temporal characteristics which place it in a favorable uninhabited geographical zone.

Thermal forces. The final stage propellants are the only source of in situ thermal energy amounting to an energy potential of about 10^7 Btu before final stage ignition. Again, the breakup characteristics of the injection vehicle through spontaneous or range safety-induced destruct would result in a very short exposure of the generators; the generator shell would probably not be removed.

Aerodynamic heating is very severe with the minimum case being thermal destruction of the generator shell for all final stage failures. Examination of the least complicated failure, premature thrust termination, shows a wide re-entry heating spectrum. These failures are designated Cases 5a through 5 e. For Case 5e, Fig. 28 shows the heating rate for a final stage thrust cutoff at 6000 feet per second short of orbital velocity. In this case, the generator shell is consumed and 28% of the fuel core is ablated and dispersed. Case 5b, shown in Fig. 29,

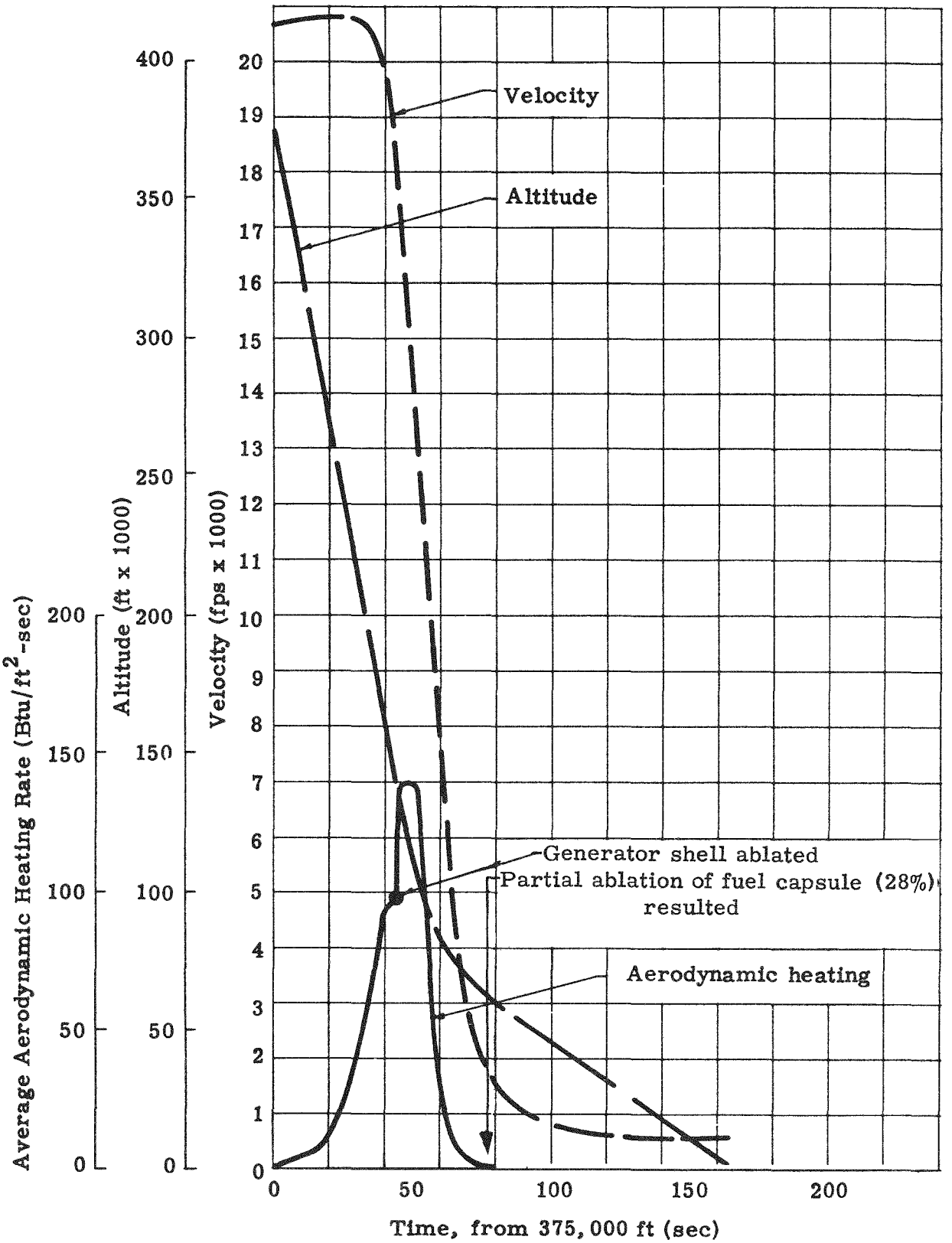

Fig. 28. Abort Early in Final-Stage Operation--Re-entry (Case 5e)

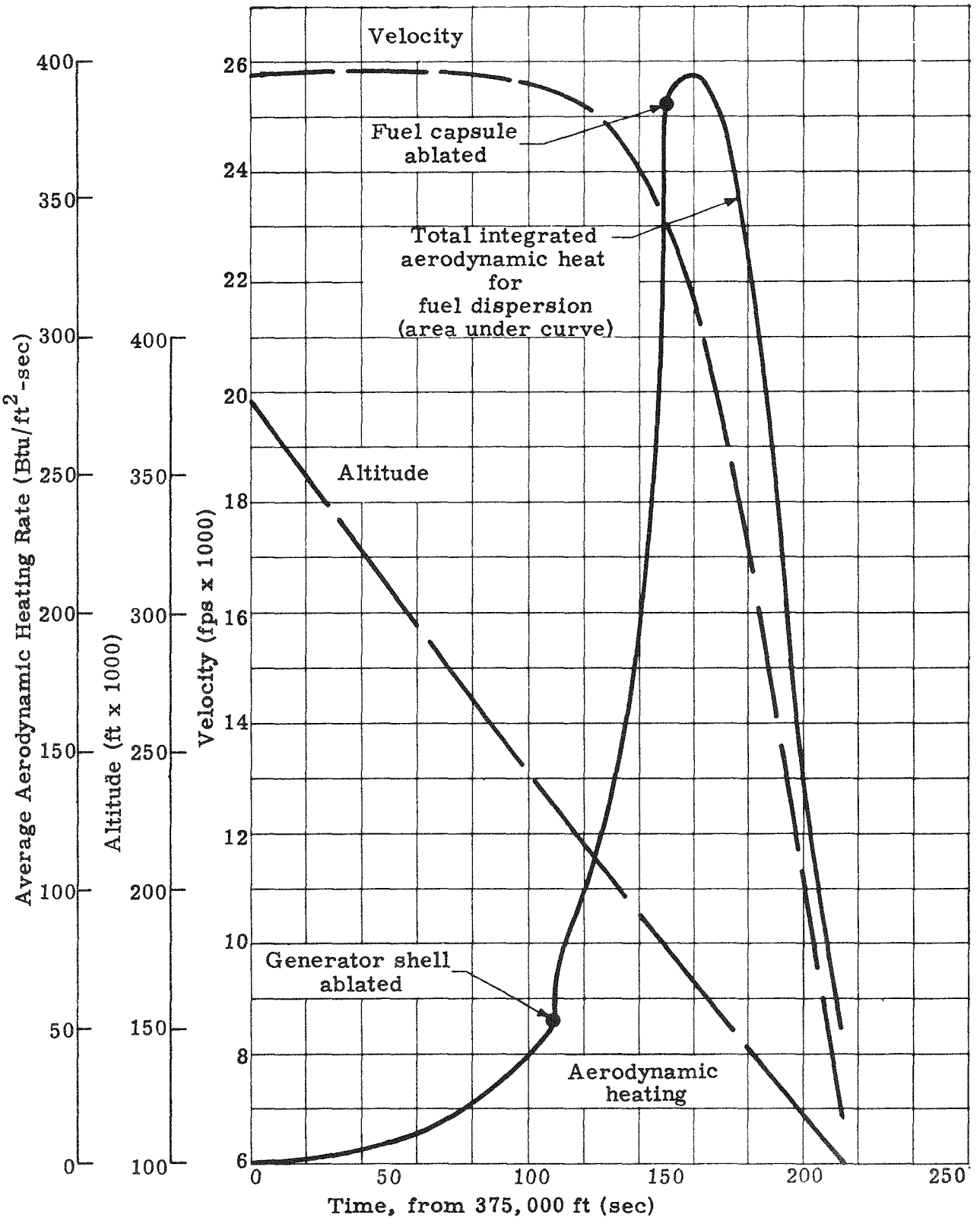

Fig. 29. Abort Late in Final-Stage Operation--Re-entry (Case 5b)

shows the heating rate for a thrust cutoff failure at 600 feet per second short of orbital velocity. High altitude burnup of the core occurs at 180,000 feet over Antarctica. The consequences of high altitude injections of Cerium-144 will be discussed in Chapter X. Of the six cases of thrust cutoff considered, three burned up at altitude, two were partially consumed and one impacted intact.

Failures in pitch yielded a complete spectrum of conditions. Of 15 failure cases considered, six went into a short lifetime orbit, three were burned up at high altitude, two were partially burned up with remnants impacting and four re-entered intact.

Twelve failures in yaw were considered. Of these, five went into a short lifetime orbit, five burned up at high altitude, and two were partially ablated at impact.

Mechanical forces. Of the 33 general cases* considered, impact of partially consumed cores or intact cores occurs in 11 cases. Ten impact at sea, of which five are not ablated and five are partially consumed. One case, a pitch misalignment failure occurring at 6000 fps short of orbital velocity, results in 10% of the core impacting near the South Pole at a temperature of 3000° R. This is indicative of a limited dispersion of material at impact on ice, a semirigid medium.

Chemical forces. Corrosion of Inconel X has been described previously. Of interest is sea water corrosion of ceric oxide in the five cases where core remnants impact with the fuel exposed. After the remnants settle to the bottom of the sea, the ceric oxide will generate 1.96 watts per gram to heat up the exposed surfaces. Ceric oxide is insoluble in hot water and, therefore, would not be appreciably disseminated in the marine environment. Further, cerium does not readily enter the biological cycle in significant amounts. Solution of praseodymium salts may occur, but this effect is minimized by its short half life of 17 minutes.

*Actually 46 specific cases were treated.

X. SUMMARY AND CONCLUSION

This chapter presents a summary of the immediate and ultimate fate of the fuel for both successful and aborted missions. Since successful missions and many of the aborted missions result in stratospheric injections of Cerium-144, a rather detailed discussion of fallout is included.

A. SUCCESSFUL MISSION

The fate of the radiocerium following a successful mission is clearly defined. The fuel will be ablated in the upper stratosphere at an altitude of 234,000 feet or more and dispersed as particles less than 10 microns in diameter. Re-entry will occur at random above the earth's surface, and the mean residence time of fallout at the altitude of release is thought to be five years or more. To obtain a conservative estimate of the consequences of this release, a mean residence time of eight months was employed in the fallout estimates.

After 600 days, the satellite inventory of Cerium-144 will be 0.4 megacurie, and this amount will be injected into the stratosphere at random as fallout, with a mean residence time of 240 days. It is assumed that 75% of this material is uniformly deposited in the Temperate Zone, corresponding to a release above this region. The resultant peak ground concentration will be 2.5 millicuries per square mile and will occur 271 days after the injection (871 days after launch). The dose rate in the fallout field corresponding to the peak concentration is 450 micromicrorad per hour. This level of radiation will be completely masked by nuclear weapons debris already residual in the Temperate Zone. The mechanism of fallout is further discussed in detail later in this chapter.

B. ABORTED MISSIONS

The statistics for aborted missions are meaningful in terms of their expected frequency over an operational cycle, the type of abort anticipated and the probable consequence. The following overall statistics are presented for operational failures.

		Type of Failure		
Statistic	Overall	Launch	Ascent	Final Stage
Probability	0.160	0.021	0.075	0.065
Percent	16.1	2.1	7.5	6.5

This shows that the ascent failure and final stage failure are roughly of equivalent probability whereas the launch failure is the least probable. Tables 4, 5 and 6 summarize all aborted missions, and Fig. 30 shows the terminal locations of the fuel following the aborts tabulated. Figure 31 presents a summary altitude-range profile of aborts.

1. Launch Failures (Table 4)

A summary of launch failures shows that the fuel cores will come to rest on or near the launch pad. Analysis of past failures indicates that the generators will probably be entangled in the vehicle wreckage. Observation of the abort test also indicated that the fuel cores would probably be enclosed within the partially breached generator shell. The fuel cores will be intact in all cases, precluding widespread contamination of the launch complex and environs. The range destruct capability would ensure that impact is confined to properly controlled areas.

The only radiation hazard presented is the direct radiation of the fuel cores. If the abort results in wreckage on the launch pad, the dose rate outside of the blockhouse, 1000 feet away, would be 80 milliroentgens per hour, and, within the blockhouse, it would be negligible. On the other hand, if the wreckage came to rest directly on the blockhouse, the dose rate inside would be 1 milliroentgen per hour. In either event, sufficient time would be available to permit retrieval of the cores without overexposure of operations personnel.

The Missile Accident Emergency Team would initiate recovery operations after the ensuing fire by (1) separating the generators from the wreckage, (2) separating the cores from the generator, and (3) providing shielding of the cores. The second operation may be bypassed if the fuel cores cannot be extricated from the crushed generator. In this case, the cores would be placed into a shield in situ. The recovery operation is a complex one, but could be accomplished without personnel overexposures if special retrieval equipment were made available. The probability of this failure is 2.1%.

2. Ascent Failures (Table 5)

Ascent failures are statistically more probable than any other type considered. However, the consequences of these failures do not pose problems of uncontrolled radiation exposure. Further, the redundant range safety destruct capability serves to constrain impact points to the range safety zone. In all cases, fuel cores will remain intact for the effective lifetime of Cerium-144. Three distinct possibilities exist for the ultimate fate of the fuel following ascent aborts; they are:

TABLE 4

Summary of Aborted Missions--Launch Failures

A. Launch Failures	Time of Failure (seconds)	Altitude of Failure (feet)	Cause	Failure Mechanism	Location of Debris	Forces Imposed By Abort: Thermal	Forces Imposed By Abort: Mechanical	Chemical	Condition and Location of Core	Primary Radiological Hazard	Counter-Measures	Ultimate Fate of Fuel
Summary of launch failures	-2000 to +15	0 to 1000	1. Propellant tank 2. Propulsion 3. Guidance	Atlas disintegrates exposing agena propellant fire	On or near launch pad	Propellant fire 2 fireballs, sustained propellant and metal fire	Shock loads Impact loads	Possible minor attack by IRFNA	After fire, core will be in missile debris; core will be intact	Direct radiation	Exclusion, shielding	Retrieved by maet with containment of fuel in all cases, safe disposal
1. Propellant tank failure	-2000 to 0	0 to 10	1. Seam failure 2. Over-pressurization	Collapse of vehicle into propellant fire	On launch pad	Release of 10^8 Btu fireball pulse to 6000° F, sustained fire 4500° F to 100° F in 30 minutes	Shock load of 2500 psi maximum Impact load of 1000 psi maximum	Minor attack by IRFNA if core is immersed for long period	Among missile debris intact	Direct radiation	Exclusion, shielding	Retrieved for safe disposal, fuel contained
2. Propulsion failure	-10 to +15	0 to 1000	1. Restricted fuel flow 2. Incomplete combustion	Collapse of vehicle, airborne fire, fallback	On or near launch pad	Same as above or airborne fire with exposure to fireball for 3 sec	Shock load of 2500 psi maximum Impact load of 1500 psi maximum	Same as above but less probable in case of airborne accident	Among missile debris intact or separated from debris	Direct radiation	Same as above	Same as above
3. Guidance failure	0 to +15	0 to 1000	1. Thrust misalignment 2. Gyro failure	Command destruct fallback	On or near launch pad	Same as above or less exposure for command destruct	Same as above	Same as above	Same as above	Direct radiation	Same as above	Same as above

TABLE 5

Summary of Aborted Missions--Ascent Failures

B. Ascent Failures	Cause of Failure	Time of Failure (seconds)	Initial Conditions at Time of Failure: Altitude (feet)	Attitude (degrees)	Velocity (fps)	Range (naut mi)	Apogee Altitude (feet)	Impact Point (naut mi)	Forces Imposed by Aborts: Thermal	Mechanical	Chemical	Immediate Fate of Fuel Core: Location	Condition	Counter-measures	Ultimate Fate of Fuel
1. Failure at pitch over	1. Guidance 2. Structural 3. Propulsion	+15	1,000	90	200	0	1,100	0	Airborne propellant fire with exposure to fire ball for 3 sec; possible exposure to debris fire	Shock 1000 psi max Impact 1500 psi	Very minor IRFNA attack possible	Near launch pad, on base	Intact in debris or buried	Command destruct	Retrieved by MAET for safe disposal
2. Failure at maximum dynamic pressure	1. Structural 2. Guidance 3 Propulsion	+60	38,000	54	1,000	1	41,000	2.0	Same as above	Shock 1000 psi max Impact loads 6000 psi max	Same as above	1 mile down-range	Intact in debris or buried	Command destruct	Same as above
3. Failure at booster engine separation	1. Poor separation 2. Guidance 3. Propulsion	+140	250,000	23	10,000	60	586,000	780	Airborne propellant fire minimal; very minor aerodynamic heat	Shock load minimal Impact load 6000 psi max	Salt water corrosion of Inconel	In Pacific in deep water	Intact	Command destruct	Left to decay; exposure of fuel in 12.8 years (20 curies)
4. Failure at sustainer burnout	1. Poor separation 2. Guidance	+285	860,000	14.8	18,500	340	1,584,000	2500	Aerodynamic heat will destroy generator shell	Impact load 6000 psi max	Salt water corrosion of Inconel	In Pacific in deep water	Intact	Command destruct	Same as above
5. Failure during coast	1. Guidance	+285 to +585	860,000 to 1,524,000	14.8 to 2.0	18,500	340 to 1,000	1,584,000	2500	Same as above	Same as above	Same as above	Same as above	Intact	Command destruct	Same as above
6. Failure at final stage ignition	1. Propulsion 2. Guidance	+585	1,524,000	2.0	18,500	1,100	1,584,000	2500	Possible propellant fire. Aeroheat melts shell	Same as above	Same as above	Same as above	Intact	Command destruct	Same as above

TABLE 6

Summary of Aborted Missions--Final Stage Failures

Final Stage Failures (probability 6.5%)	Case Number*	Time of Failure After Launch (sec)	Failure Characteristics: Probable Cause of Failure	Misalignment of Failure (deg)		Velocity Decrement at Failure, ΔV (fps)	Probability of Failure (%)	Immediate Fate of Core: Geographical End Points: Latitude (deg)	Longitude (deg)	% Consumed Aerodynamically	Altitude of Dispersal (ft)	% to Impact	Impact Temperature (°R)	Immediate Location of Radiocerium After Abort	Ultimate Fate of Radiocerium	Summary of Consequences
				Pitch	Yaw											
Propulsion failures	Summary	+585 to +691					4.5									
At final stage ignition	General	+585	Failure to ignite.	0	0	7242	3.0	3.3S	122.4W	0		100	2060	Intact at bottom of Pacific	Exposure after 12.8 yrs	Corrosion of 20 curies Ce^{144}, near equator
After final stage ignition	5e	+610	Failure of propellant feed system, pressurization system or thrust chamber.	0	0	6000	1.5	11.4S	124.5W	28	~100,000	72	3000	In Pacific and stratosphere	Marine exposure, fallout	Corrosion most of fuel, limited fallout
	5d	+644		0	0	4000		20.0S	125.1W	70	~100,000	30	3000	In stratosphere and Pacific	Fallout, marine exposure	Fallout S. Temp. Zone, corrosion of fuel
	5c	+671		0	0	2000		36.0S	125.3W	100	121,000	0		Stratospheric injection	Fallout, mean res 8 mo	Fallout S. Temp. Zone (1.7 mc** injected)
	5b	+686		0	0	600		80.0S	127.9W	100	180,000	0		Stratospheric injection	Fallout, mean res 8 mo	Fallout S. Temp. Zone (1.7 mc injected)
	5a	+688.5		0	0	400		47.9S	49.0E	100	234,000	0		Stratospheric injection	Fallout, mean res 5 yr	Fallout S. Temp. Zone (1.7 mc injected)
Guidance failures	Summary	+585 to +691					2.0									
Vehicle unstable	General		Poor separation.				1.0									Similar to propulsion failure
Pitch failure (vehicle stable)	5f	+585	Failure to control disturbing moments.	-5	0	7242	0.5	Into orbit						Into orbit	Re-entry after 10 days	Fallout at random (1.7 mc injected)
	5g	+585		-30	0	7242		6.2S	124.0W	20	~100,000	80	3000	In Pacific and stratosphere	Marine exposure	Corrosion of fuel, very limited fallout
	5h	+585	Shift of gyro.	-90	0	7242	Very improbable	5.9N	123.3W	0		100	2060	Intact at bottom of Pacific near equator	Exposure after 12.8 yr	Corrosion of 20 curies
	4a	+610	Reference.	±5	0	6000		Into orbit						Into orbit	115 days (+) Re-entry after 10 days (-)	Fallout at random (1.3 mc injected)
	4b	+610	Failure of servos.	+45	0	6000		88.7S	49.3E	90	~100,000	10	3000	Impact near S. Pole	Fallout, dispersion in ice	Limited contamination by 200,000 curies eventual ice burial
	4c	+610		+90	0	6000	Very improbable	35.4S	127.5W	0		100	2940	Intact at bottom of Pacific	Exposure after 12.8 yr	Corrosion of 20 curies Ce^{144}
	3a	+644		+5	0	4000		Into orbit						Into orbit	Re-entry after 220 days	Fallout at random (0.8 mc injected)
	3b	+644		+45	0	4000		77.0S	49.8E	100	118,000	0		Polar stratospheric injection	Fallout mean res 8 mo	Fallout in S. Polar, Temp. Zone (1.7 mc injected)
	3c	+644		+90	0	4000	Very improbable	46.6S	127.4W	0		100	2270	Intact at bottom of Pacific	Exposure after 12.8 yr	Corrosion of 20 curies Ce^{144} at sea
	2a	+671		+5	0	2000		Into orbit						Into orbit	Re-entry after 240 days	Fallout at random (0.8 mc injected)
	2b	+671		+45	0	2000		53.0S	48.7E	100	163,000	0		Stratospheric injection	Fallout mean res 8 mo	Fallout in S. Temp. Zone (1.7 mc injected)
	2c	+671		+90	0	2000	Very improbable	63.9S	128.8W	0		100	2900	Intact at bottom of Pacific	Exposure after 12.8 yr	Corrosion of 20 curies Ce^{144}
	1a	+686		+5	0	600		Into orbit						Into orbit	Re-entry after 230 days	Fallout at random (1 mc injected)
	1b	+686		+45	0	600		Into orbit						Into orbit	Re-entry after 12 days	Fallout at random (1.7 mc injected)
	1c	+686		+90	0	600	Very improbable	76.9S	50.5E	100	172,000	0		Stratospheric polar injection	Fallout mean res 8 mo	Fallout S. Polar, Temp. Zone (1.76 mc injected)
Yaw failure (stable)	Summary						0.5									
	9a	+610	Failure to control disturbing moments.	0	±5	6000		Into orbit						Into orbit		
	9b	+610		0	±45	6000		44.3S	143.3W 106.2W	100	133,000	0		Stratospheric injection	Fallout mean res 8 mo	Fallout in S. Temp. Zone (1.7 mc injected)
	9c	+610	Shift of gyro reference.	0	±90	6000	Very improbable	11.3S	135.7W 112.5W	44	~100,000	56	3000	In Pacific and stratosphere	Marine release, fallout	Corrosion most of fuel, limited fallout
	8a	+644		0	±5	4000		Into orbit						Into orbit	Re-entry after 220 days	Fallout at random (1 mc injected)
	8b	+644	Failure of servos.	0	±45	4000		56.5S	141.1W 110.0W	100	169,000	0		Stratospheric injection	Fallout mean res 8 mo	Fallout in S. Temp. Zone (1.7 mc injected)
	8c	+644		0	±90	4000	Very improbable	20.5S	135.6W 113.4W	80	~100,000	20	3000	In stratosphere and Pacific	Fallout, marine release	Fallout (1 mc injected), corrosion (0.7 mc)
	7a	+671		0	±5	2000		Into orbit						Into orbit	Re-entry after 220 days	Fallout at random (1 mc injected)
	7b	+671		0	±45	2000		70.4S	140.3W 104.7W	100	178,000	0		Stratospheric injection	Fallout, mean res 8 mo	Fallout S. Temp. Zone (1.7 mc injected)
	7c	+671		0	±90	2000	Very improbable	36.2S	135.2W 114.1W	100	105,000	0		Stratospheric injection	Fallout, mean res 8 mo	Fallout S. Temp. Zone (1.7 mc injected)
	6a	+686		0	±5	600		Into orbit						Into orbit	Re-entry after 220 days	Fallout at random (1 mc injected)
	6b	+686		0	±45	600		Into orbit						Into orbit	Re-entry after 13 days	Fallout at random (1.7 mc injected)
	6c	+686		0	±90	600	Very improbable	64.5S	150.3W 104.1W	100	185,000	0		Stratospheric injection	Fallout mean res 8 mo	Fallout in S. Temp. Zone (1.7 mc injected)

* Refers to machine run and map plot points.
** mc = megacuries.

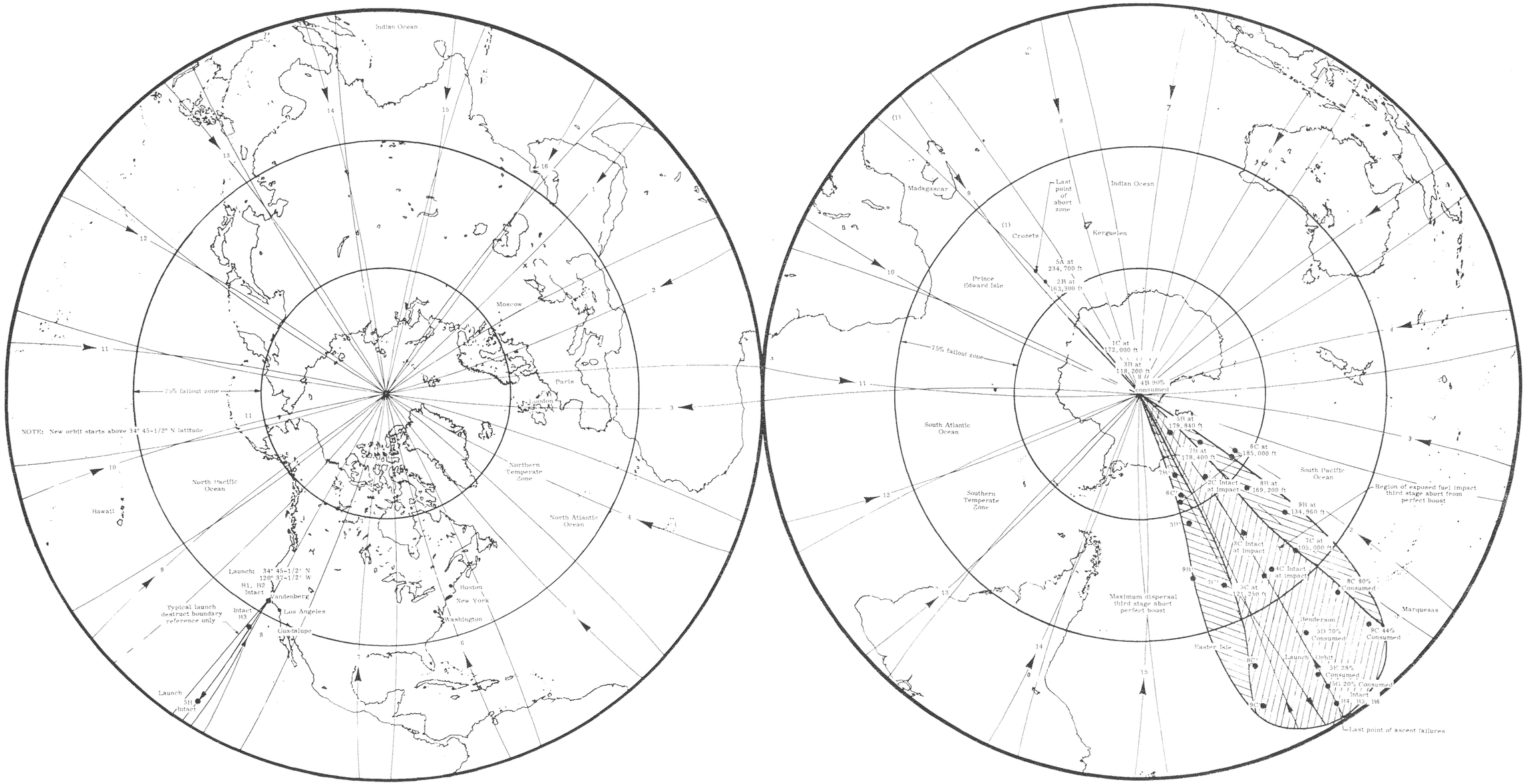

Fig. 30. Polar Projection of Abort Zones

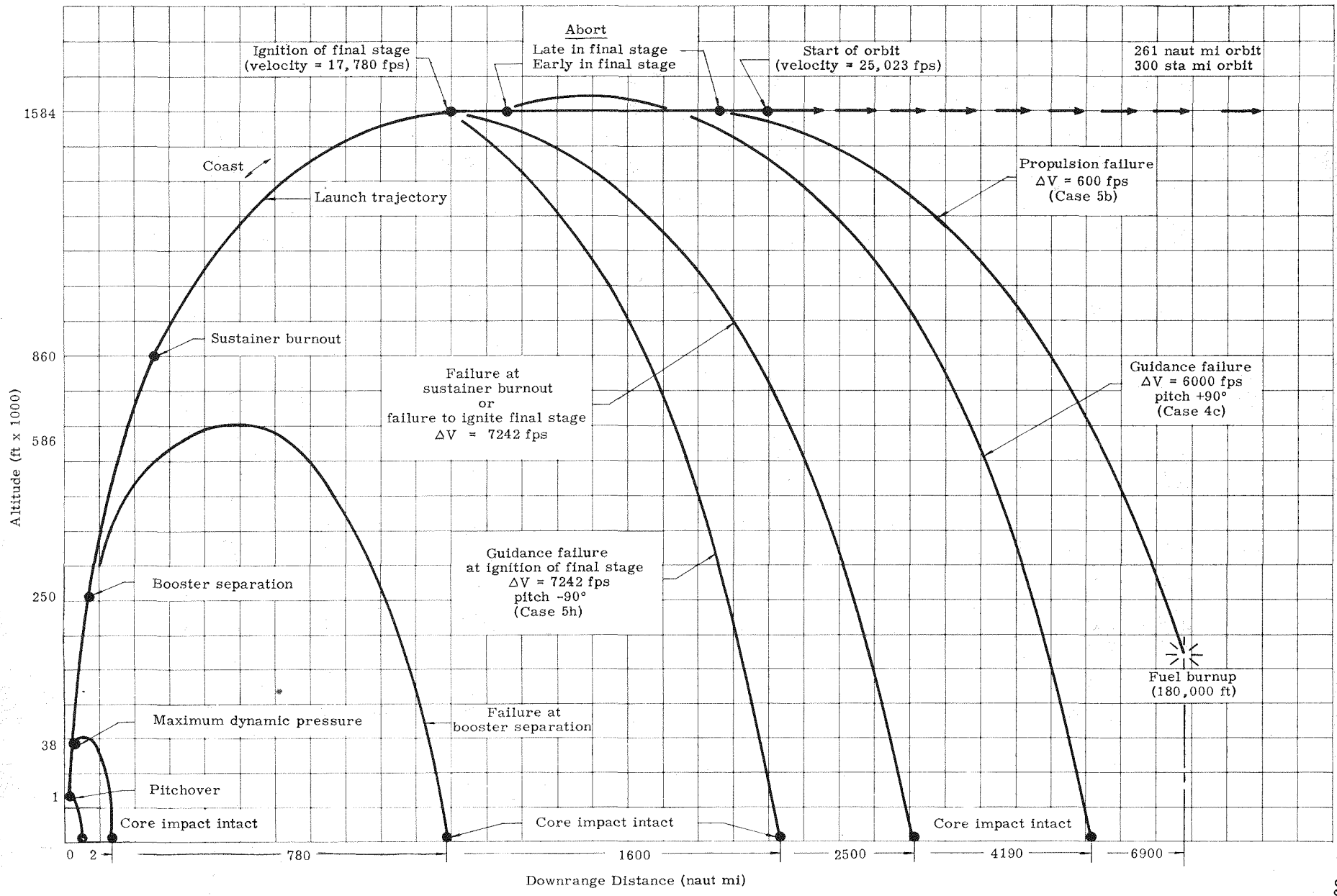

Fig. 31. Profile of Abort Trajectories

(1) Impact on land--This will occur zero to five miles from the point of launch for pitchover failures (0 miles), failures at maximum dynamic pressure (2 miles), and for failures occurring immediately after the point of maximum dynamic pressure (2 to 5 miles). The consequences will be essentially those described for launch failures earlier (i.e., recovery by MAET).

(2) Impact in shallow water offshore--After the point of maximum dynamic pressure is passed on the ascent trajectory, subsequent vehicle failure could result in impact of cores in shallow water offshore (5 to 10 miles downrange). This would make recovery operations safer by providing shielding, but would require considerable time to separate the cores from the wreckage. The probability of the occurrence is quite low because a very narrow band of flight time is available in which the vehicle can malfunction.

(3) Impact in deep water downrange--Failure at booster separation would provide core impact 780 miles downrange in deep water. Failures at sustainer burnout, during coast, and a final stage ignition would result in core impact 2500 miles downrange. In these cases, there would be no attempt to recover the cores and they would come to rest in the bottom of the Pacific in relatively deep water. The radiocerium would be exposed through the mechanism of marine corrosion after a minimum of 12.8 years when the total source strength is 20 curies.

If the flight time available for ascent failures is any criterion (50 seconds for failures resulting in land impact versus 520 seconds for failures resulting in impact at sea), it appears that the majority of ascent failures would result in water impact. The sea provides an ideal resting place for a radiation source sealed in a corrosion resistant container.

3. Final Stage Failures (Table 6)

The final stage failures (33 general cases) yield a wide spectrum of consequences varying from high altitude burnup of the fuel to impact of the fuel core intact at sea. The terminal locations for the fuel for the majority of the cases considered are shown in Fig. 29. Excluded from this plot are the cases where the satellite enters an eccentric orbit and re-enters at random. Four distinct possibilities exist for the ultimate fate of the fuel following final stage aborts. They are as follows:

Into orbit (11 cases). Guidance failures in pitch and yaw result in 11 cases in which the satellite goes into orbits of short or intermediate lifetimes. Pitch failures occurring with minor angular deviations to the planned trajectory (± 5°) characteristically produce orbits at all velocity decrements. One pitch failure at 45° late in the final stage operation (Δ V = 600 fps) produced an orbit. The orbital lifetime varied from 10 to 240 days for all pitch cases.

Failures in yaw yielding orbits were five in number; four were due to minor deviations to the flight path (± 5°) at all velocity decrements, and one was due to a ± 45° deviation late in final stage operation (ΔV = 600 fps). The orbital lifetimes varied from 13 to 220 days for all cases.

It is concluded that failures yielding very minor pitch and yaw deviations from the prescribed trajectory will result in orbital injection of the satellite. Similar failures occurring late in the final stage operation (ΔV = 600 fps, trajectory deviation = 45°, t = 686 seconds) will also result in orbital injection.

Since the generator and fuel are designed to be burned up from orbital decay, the consequence of these failures will be world-wide fallout, and re-entry will occur at random above the earth. The Cerium-144 inventory injected, however, will vary from an amount approaching that injected from a successful mission to that injected by the prompt re-entry and burnup case considered next.

Prompt re-entry and total burnup (11 cases). Prompt re-entry of the satellite and high altitude burnup and dispersal of the radiocerium occurs subsequent to some thrust cutoff, pitch and yaw failures. Thrust cutoffs on trajectory, occurring intermediate and late in final stage operation (ΔV = 2000, 600, 400 fps) will yield high altitude burnup of the fuel in three cases. Case 5a is the key case since the fuel burns up at 234,000 feet, between Antarctica and Madagascar, the most distant point downrange where prompt re-entry and burnup occurs.

Three cases of pitch failures yield prompt re-entry and burnup. Two cases occur early in final stage operation (ΔV = 4000, 2000 fps) where a positive pitch of 45° is induced. The third occurs late in final stage operation with a large pitch deviation (ΔV = 600 fps, +90°).

Five cases of yaw failures yield prompt re-entry and burnup. Three of these cases occur early in final stage operation (ΔV = 6000, 4000, 2000 fps) at deviations of ± 45°. Another case occurs at ΔV = 2000 fps at a deviation of ± 90°. The last case is a ± 90° deviation late in final stage operation (ΔV = 600 fps).

The consequence of prompt re-entry and burnup is the injection of 1.76 megacuries of Cerium-144 into the stratosphere above the Southern Temperate Zone. The altitude of burnup varies from 105,000 to 234,000 feet.

Partial ablation--impact of remnants (6 cases). Partial burnup and dispersion of the fuel will occur at high altitudes, and core remnants will subsequently cool to below melting temperatures and impact. The distribution of this type of failure is even between thrust cutoff, pitch and yaw failures. Early thrust cutoffs (ΔV = 6000, 4000 fps) will yield partial ablation in two cases. Very early pitch failures (ΔV = 7242, 6000 fps) with significant deviations (-30°, +45°) will yield partial burnup. Yaw failures occurring early in final stage operation (ΔV = 6000, 4000 fps) with extreme deviations (± 90°) will also yield this consequence.

Five of the six cases will result in exposed fuel impacting in the Pacific Ocean 6 to 20 degrees south of the Equator in the Western Hemisphere. It can be shown that 1.7 megacuries of Cerium-144 would contaminate only 6 cubic miles of ocean above acceptable levels if all of it were dissolved. However, ceric oxide is insoluble and would remain exposed at the bottom of the Pacific until neutralized by radioactive decay.

One case results in impact of 10% of the fuel (176 kilocuries) on the Antarctic Continent near the South Pole. Though this would represent a nuisance, it would not constitute a significant biospheric injection.

The fuel released in the case of partial ablation would fall out in the Southern Temperate Zone.

Impact of core intact at sea (5 cases). When the mode of failure yields a low re-entry velocity, fuel cores will not be ablated and will impact at sea downrange. A characteristic case is failure of the final stage to ignite (ΔV = 7242 fps). The remaining four cases occur due to pitch failures early and intermediate in final stage operation (ΔV = 7242, 6000, 4000 and 2000 fps) with 90° pitch deviations. The downrange impact points vary from 5.9° N latitude to 63.9° S latitude.

The immersion of the fuel in deep water as a sealed source is probably the most desirable fate of the fuel following an abort. Using the maximum corrosion rate of Inconel X capsules, the fuel would become exposed on the floor of the Pacific 12.8 years when it has decayed to 20 curies.

4. Summary

The safety analysis and evaluation has screened a large number of vehicle failures in order to narrow the multiplicity of consequences into seven broad categories. Table 7 shows this relationship. The importance of the mechanism of fallout of the fuel manifests itself in all cases not resulting in fuel containment and is discussed next.

TABLE 7

Fate of Fuel

Category	Type of Failure	Fate of Fuel	Fuel Recovery
Impact on land	Launch, ascent	Contained	Yes
Impact in shallow water	Ascent	Contained	Yes
Impact in deep water	Ascent, final stage	Contained effectively	No
Partial ablation--remnant impact	Final stage	Stratospheric dissemination Hydrospheric exposure*	No
Prompt re-entry--burnup	Final stage	Stratospheric dissemination	No
Into orbit	Final stage	Stratospheric dissemination	No

* Hydrosphere includes water and ice

C. FALLOUT PATTERN

The world-wide fallout from combined U.S., UK and USSR bomb tests serves as a basis upon which the relative importance of the fallout derived from an injection of radiocerium into the stratosphere can be evaluated.

From the total yield of 174 megatons from bomb tests to date, 92 megatons are due to fission of heavy nuclei. Due to the fission, 140 pounds or 9.2 megacuries of Strontium-90 have been produced.[20] Of this amount, approximately 6 megacuries were injected into the stratosphere and 3.2 megacuries had already come down to earth by October 1958 (2.4 megacuries in the Northern Hemisphere and 0.8 megacurie in the Southern Hemisphere).[21] Figure 32 shows the present and predicted soil levels of Strontium-90.

Based upon the measurements of activity from various bomb tests in the Northern and Southern Hemispheres, the material injected into the stratosphere above the higher latitudes of a given hemisphere will deposit almost entirely in that hemisphere, as shown in Fig. 32.

Weapons debris injected into the stratosphere will fall out in an average time of 1 to 3 years, depending upon the latitude of injection. More specific data based upon a recent report indicates that in the lower stratosphere (below 125,000 feet) injections at temperate and polar latitudes will remain in the stratosphere for less than one year. A mean residence time of 8 months has been selected as applicable to both polar and temperate injections in the vicinity of 100,000 feet. The estimated mean residence time for equatorial injections is approximately 2 years for an altitude of 100,000 feet. For injections at and above 200,000 feet, the mean residence time is equal to or greater than 5 years.[22]

The Joint Committee report of 1958 indicates that a total of 40 megatons of fission occurred during the 1957 to 1958 bomb tests. Of this debris, 31 megatons were injected into the atmosphere; this amount produced 3.1 megacuries of Strontium-90. Based upon the fact that the initial proportion of one fission product to another is about the same in each nuclear explosion and that the independent yields for Strontium-90 and Cerium-144 are nearly the same, 111.0 megacuries of Cerium-144 would have been injected during this period.

1. Correlation of Theoretical Approach and Actual Measurements*

Actual measurements of Cerium-144 fallout deposition have been made by Argonne National Laboratory from soil samples by gamma ray

---

* E. Divita

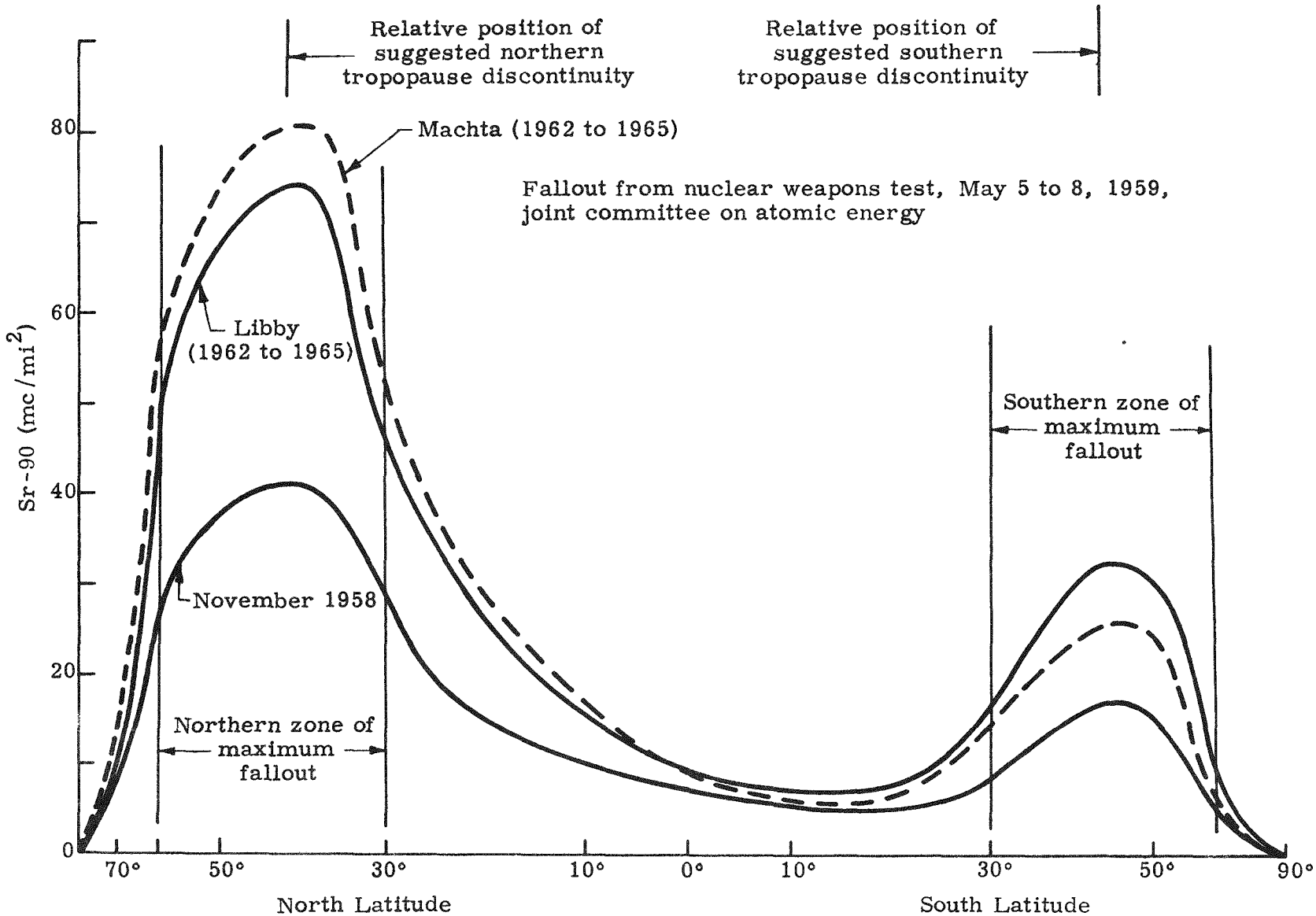

Fig. 32. Present and Predicted Soil Levels of Sr-90

spectroscopy. The samples were collected at ANL, which is located at about 42° N latitude. The data is listed as follows.

Ce-144 Activity in Soil (ANL)[24]

Month	Activity (mc/sq mi)	Estimated Dose Rate (mrad/hr)
September 1958	270	0.05
March 1959	1127	0.21
April 1959	1450	0.27
May 1959	1533	0.28
June 1959	1704	0.31
July 1959	1812	0.33

In an attempt to correlate a theoretical analysis with the measurements, it was necessary to make several general assumptions:

(1) The fission yields from the U.S. and Soviet bomb tests during 1957 to 1958 are the major contributors.

(2) The U.S. and Soviet bomb bursts were concurrent and totally released during the fall of 1958.

(3) The total source of Cerium-144 is 111.0 megacuries.

(4) The effects of weather conditions over the zone of measurement might result in an increase of theoretical values by as much as a factor of 2.5.

(5) A factor of 2 was included in the theoretical calculation to allow for precipitation effects.

Computation of U.S. and Soviet contributions were made separately. This is due mainly to the difference in mean residence time. For the Soviet tests, the mean residence time assumed is 4 months; that assumed for the U.S. tests is 1 year. The results of the theoretical approach, the measurements, and the semiempirical estimate are presented in graphic form in Fig. 33 for comparative purposes.

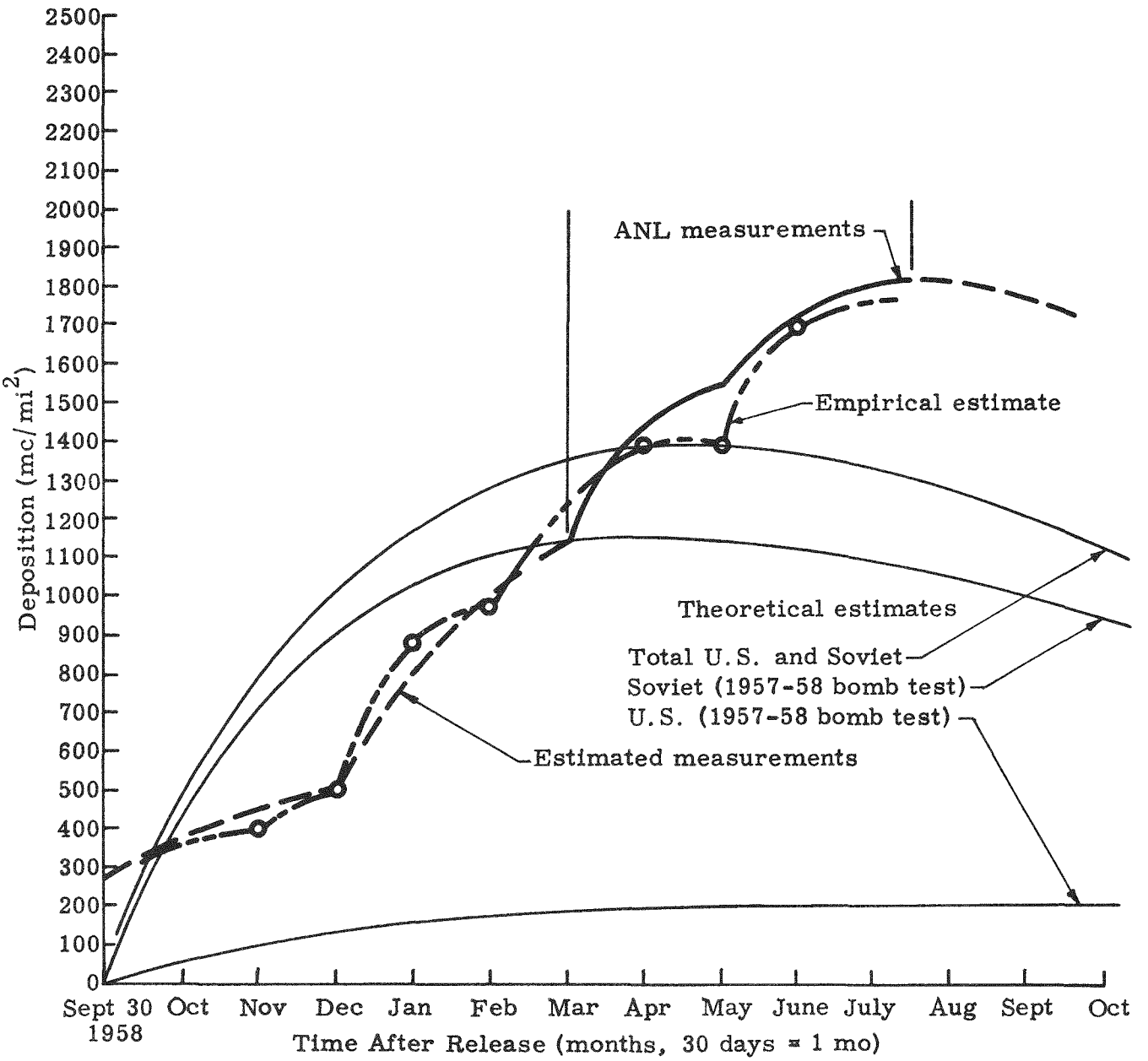

Fig. 33. Predicted Levels of Ce-144

The stratospheric fallout from Soviet tests was greatly influenced by the peculiarity of the tropopause. Due to exchange of air between the two atmospheric regions, the Soviet fallout injected into the lower stratosphere could have been carried by the movement of stratospheric air through the tropopause gap into the troposphere, where vertical mixing would bring it fairly rapidly to earth. Soviet tests have been carried out north of a latitude of 50°; therefore, substantially all of the fallout they have produced has remained in the Northern Hemisphere. This has been confirmed by measurements in both hemispheres. The total fission yield from the Soviet tests during 1957 to 1958 was 21 megatons. For the computations, the total yield was assumed to be injected into the lower stratosphere. That portion of the fission yield having particle sizes less than 5 microns accounts for more than 2/3 of the total fission yield. The total Ce-144 inventory due to the Soviet tests amounted to 75 megaeuries.

Fallout from U.S. high yield tests, all of which have taken place near the Equator, has been evenly distributed over the world. The U.S. tests injected approximately 50% of their 1957 to 1958 total fission yield of 19 megatons[25] into the upper stratosphere above 100,000 feet; the remainder fell out in the vicinity of the test site. Particles less than 5 microns in size account for more than 2/3 of the total fission yield, disregarding that portion which fell fairly rapidly over the test site area. The total Ce-144 radioactivity due to the U.S. tests amounted to 30 megacuries.

Data on precipitation in the region where the measurements were taken is presented in Table 8 to give the reader an indication of why the theoretical values were either increased or decreased.

TABLE 8

Precipitation over Lemont, Illinois[25]

Month	Precipitation (in.)
September 1958	1.86
October 1958	2.12
November 1958	1.58
December 1958	0.57
January 1959	1.97

February 1959	2.36
March 1959	3.94
April 1959	3.94
May 1959	3.94
June 1959	5.91
July 1959	4.72

It is to be noted that the areas under the measurements curve and the semiempirically determined curve are slightly lower ut in fair agreement with the area under the theoretically determined curve. This may be an indication that the theoretical equation attempts to smooth out the rate and presents a theoretical average.

2. Direct Fallout From Aborted and Successful Missions

Aborted missions. Following final stage high altitude aborts, radiocerium is injected directly into the stratosphere above the Southern Hemisphere. Where partial burnup occurs and results in a release of some fuel as very large particles, fallout will be prompt over uninhabited regions of the Southern Hemisphere (i.e., over South Pacific and Indian Oceans and Antarctica where population density is essentially zero).

A conservative analysis has been made which assumes all the radiocerium to be released as fine particles above an altitude of 100,000 feet at 53° S and 49° E above the Indian Ocean.* Figure 34 shows the Cerium-144 deposition in the Southern Hemisphere as a function of time after release due to either failure of final stage or orbital abortions. The zone of deposition is shown in Fig. 30.

Computations of ground concentration from stratospheric fallout were performed with the following formula, which expresses total deposition, X_o, in units of millicuries per square mile.

$$X_o = \frac{N_o Z}{A} \left[e^{-\lambda_r t} \right] \left[1 - e^{-\lambda_f t} \right]$$

where

N_o = number of millicuries released initially

Z = fraction deposited in zone 30° to 60° S latitude

A = area of zone, square miles

* Final stage failure, Case 2b

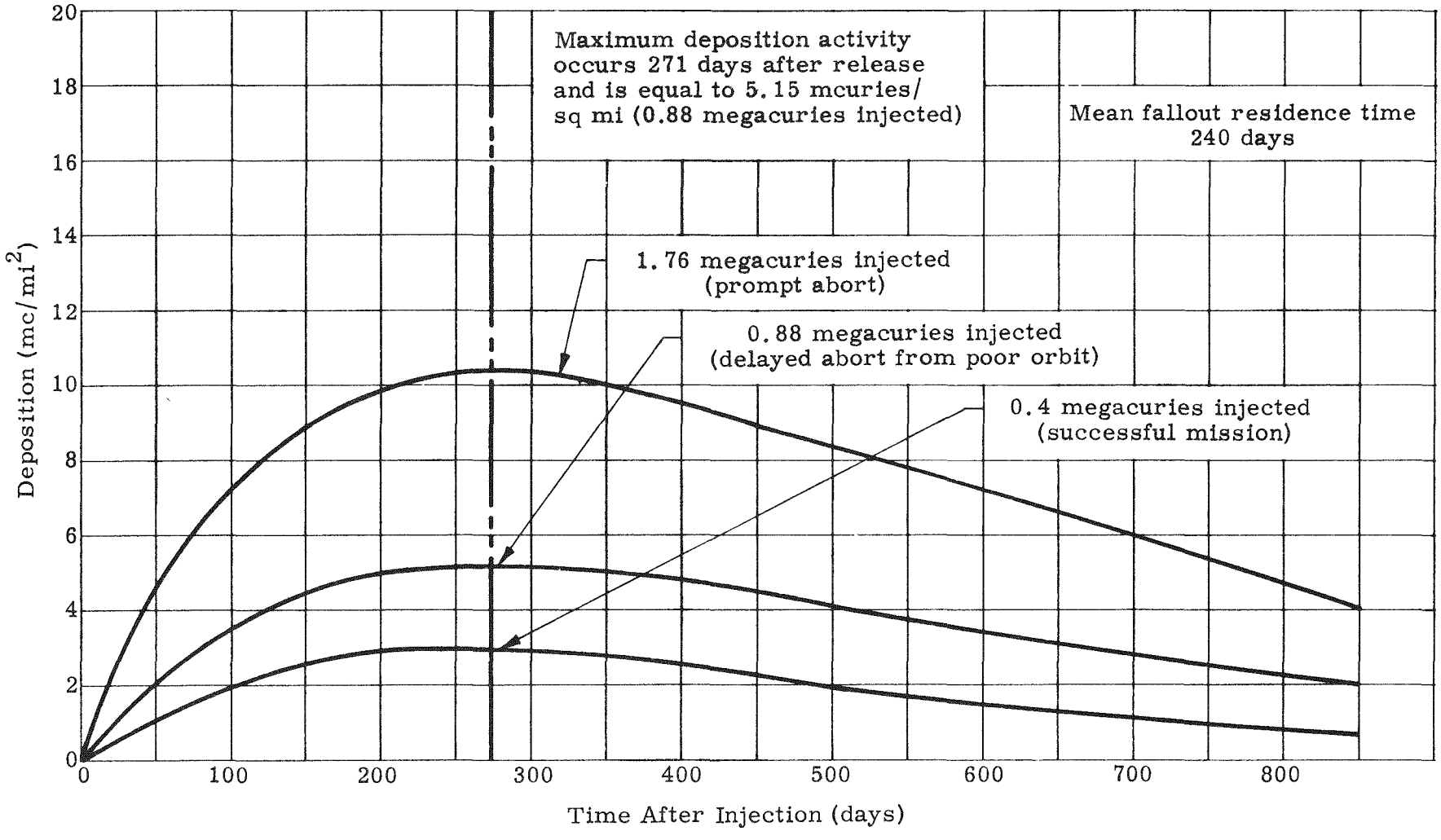

Fig. 34. Cerium-144 Deposition in Southern Hemisphere (30° to 60°) from A Stratospheric Fuel Injection

λ_r = radioactive decay constant of cerium, day^{-1}

λ_f = mean residence decay constant, day^{-1}

t = time after release, days.

The injections separately considered were 1.76, 0.88 and 0.4 megacuries of Cerium-144. Other parameters necessary for the computation of total deposition are presented below:

$Z = 0.75$

$A = 3.6 \times 10^7$ square miles

$\lambda_r = 2.43 \times 10^{-3}\ day^{-1}$

$\lambda_f = 2.885 \times 10^{-3}\ day^{-1}$.

The maximum deposition occurs when $\frac{d}{dt}(X_o) = 0$; by utilization of the resulting equation, the maximum deposition and a corresponding value of time after release was determined.

In consideration of the maximum dose that an individual might receive while in the fallout zone, an estimated exposure dose was determined by using the following formula[22]:

$$I = CE_\gamma \; F_d^T(t)$$

where

I = exposure rate, millirads/year

C = conversion factor, $0.1 \frac{(mrad)\ (km^2)}{(yr)(mcurie)(mev)}$

E_γ = average gamma energy, 0.2 mev for Ce-144 - Pr-144

$F_d^T(t) = \int_0^T X_o \, dt$ = total activity of the deposit, millicuries/ km^2 per time unit

X_o = total deposition, millicuries/km^2

T = time of exposure, years

By use of the above equation, an exposure dose of 0.031 millirad for the first year was determined for individuals in the above ground fallout zone. The 30-year exposure dose is 0.087 millirad. These doses were

computed for the 0.88-megacurie injection. The corresponding doses for a 1.76-megacurie injection are 0.06 millirad for the first year and a 30-year exposure of 0.17 millirad.

The following table compares the exposure dose from Cerium-144 injections with the doses received from various natural and man-made sources of radiation[23].

Estimated Dose from Different Radioactive Sources

	30-Year Genetically Significant Dose (millirads)
Natural sources	3000
Fallout from nuclear weapons	50
Medical sources	500 to 5000
From 1.76-megacurie Ce-144 injection postulated	0.17

Having estimated the 30-year genetically significant dose, there remains the potential internal hazard from the entry of Cerium-144 into food chains and man. This can best be evaluated by using the known amounts of Cerium-144 produced in weapons tests as a tracer and actually measuring the amounts present in foods and human tissues. A pilot sampling program has been designed, but is not yet under way.

Successful missions. The successful mission would amount to an injection of 0.4 megacurie with a 240-day mean residence time. The peak ground concentration would be 2.5 millicuries per square mile 271 days after the injection. This would be equivalent to a one-year dose in the temperate zones of 0.015 millirad and a 30-year dose of 0.04 millirad.

XI. REFERENCES

1. Dix, G. P., "Preliminary Operational Hazards Summary Report for the Task 2 Thermoelectric Generator," MND-P-2184, December 1959. SECRET-RESTRICTED DATA

2. Dix, G. P., Kelly, V., and Dobry, T., "Cerium-Fueled Thermionic Generator Radiological Safety Analysis, " MND-P-2182, November 1959.

3. "SNAP-1A Fuel Core Materials Development Summary," MND-P-2349, June 1960.

4. The Martin Company, "Radioisotope-Fueled Auxiliary Power Unit, Quarterly Progress Report No. 14," April to June 1960, in preparation.

5. "Report of Committee II, International Commission on Radiological Protection on Permissible Dose for Internal Radiation," 1959, prepublication.

6. Burnett, T. J., "Reactors, Hazards Versus Power Level," Nuclear Science and Engineering, Vol. 2, No. 3, May 1,1957.

7. Bomhardt, W., "Elevated Temperature Properties of Metals for Aircraft," The Martin Company, September 1954.

8. May, T., "Materials Evaluation for SNAP-1A Re-entry," The Martin Company, May 1960.

9. International Nickel Company Literature.

10. Harley, J. H., Personal Communication, HASL, June 1960.

11. Knapp, H. A., "Cost and Safety Considerations in the Transport of Radioactive Materials," unpublished.

12. Reilly, M. J., "Preliminary Technical Manual--Loading, Shipping and Testing Procedures for Task 2 Isotopic-Powered Thermoelectric Generator," MND-P-2316, March 24, 1960.

13. Pacific Missile Range Headquarters, Information Brochure on Pacific Missile Range, April 10, 1959.

14. Air Force Special Weapons Center, "Recovery of the Nuclear Auxiliary Power Source of a Missile After a Launch Abort," SWC-9S-47115, October 1959. SECRET-RESTRICTED DATA

15. Oehrli, R., Hagis, W., and Milewski, C., "Summary Report Aerodynamic Re-entry Analysis--Task 2 Thermoelectric Generator," MND-P-2291, The Martin Company, February 1960. SECRET-RESTRICTED DATA

16. Lockheed Aircraft Company, "Time and Place Impact Probabilities for SNAP--Equipped Vehicles," LMSD 446096, December 30, 1959. SECRET-RESTRICTED DATA

17. Broadview Research Corporation, "An Investigation of the Integrity of Certain Test Assemblies Under Missile Failure Forces--Explosive Shock, Temperature and Oxidation Test Program," RD-58-2, 1035-9, July 1958.

18. Smalley, W. M., and Anderson, D. E., "The Explosive Potential of Liquid Oxygen and RP-1 Missiles," GM-TR-59-0000-00579, January 30, 1959. CONFIDENTIAL

19. Baker, W., Army Ballistics Research Laboratory, Personal Communication, May 1960.

20. Joint Committee on Atomic Energy, "Fallout from Nuclear Weapons Tests," August 1959, p 41.

21. Arnold, J. R., and Martell, E. A., "The Circulation of Isotopes," Scientific American, September 1959, Vol. 201, No. 3, pp 84-93.

22. Eisenbud, M., Personal Communication.

23. Supplement No. 17 (A/3838), "Report of the United Nations Scientific Committee on the Effects of Atomic Radiation," 13th Session, New York, 1958, p 101.

24. Joint Committee on Atomic Energy, "Fallout from Nuclear Weapons Tests," May 1959, Table IV, p 40.

25. "Quarterly Statement of Fallout by the U.S. Atomic Energy Commission," October 1959, Table I, p 5.

26. Hardy, E. P., and Klien, S., "Strontium Program, Quarterly Summary Report," HASL-65 Analytical Division, Health and Safety Laboratory, USAEC, New York Operations Office, May 29, 1959.

APPENDIX A

SAFETY TEST PROGRAM*

A. TEST SPECIMENS

1. Fuel Cores

The selected Inconel X core design is represented in test specimen Types 1 and 8 in Table A-1. They reflect material requirements necessary to support all maximum operating forces without structural failure. Core Design 8 includes a fuel core and an impact depressor on each end. The impact depressors are utilized to diminish forces resulting from impact on a rigid target.

The impact depressor is 2.125 inches long. A cavity 1.750 inches deep is machined to a diameter which permits a press fit of the depressor onto the fuel core end. The depressor is welded to the core side wall after it is positioned to the core end so that a 0.750-inch air gap exists between the two surfaces.

The function of the depressor is to reduce impact forces on the fuel core. The depressor, in theory, assimilates impact energy by:

(1) Breaking welds along the circumference of the core.

(2) Compressing out the air between it and the core.

(3) Deforming structurally.

If it is designed properly, little impact energy will be imparted to the core, diminishing the possibility of structural failure. The probability of end impact of the assembly with two depressors is maximum; however, if the core did impact on the sides, the depressors would still provide a reduction of impact force as compared to the discrete core.

The test specimen fabricated for this program included a single depressor, since the nature of the test rendered a second cap unnecessary.

2. Other Test Specimens

Another type of test specimen was used in this test program. It was represented by specimen Type 12 in Table A-1. This specimen was a simulated one-third scale model of the fuel core. A total of four speci-

*T. Dobry

TABLE A-1

Detail Specifications of Test Specimens Used to Evaluate Unit Integrity--Task 2 Generator

Specimen Type	Specification No.	Shape	Average Diameter (in.)	Length (in.)	Weight (lb)	Material	Test Environment	Remarks
1	1	Right cylinder	3.75	11.003	24.17	Inconel X	Impact	Multitubular core with seven fuel channels drilled parallel to axis. CeO_2 fuel simulated by lavite pellets. Each channel is fitted with a 0.49-inch thick threaded closure weld at the chamber top and bottom.
	2		3.746	11.000	24.06		Impact	
	3		1.2709	3.679	1.245		Shock	
	4		1.2715	3.676	1.283		Shock	
	5		3.7518	11.003	25.027		Fire	
	6		3.7495	11.003	23.814		Fire	
	7		3.7486	11.000	23.98		Fire	
	8		3.75	11.000	25.4		LOX immersion	
8	1	Right cylinder with impact depressor	4.2707 dep 4.752	12.104 2.125	38.147	Core--Inconel X Cap--SAE 1020 carbon steel	Impact	Essentially same design as Type 1 except for larger walls of fuel channels and impact depressor.
	2		4.269 dep 4.7508	12.018 2.125	38.312		Impact	
	3		4.2718 dep 4.754	12.095 2.125	38.036		Impact	
10	1	Complete Task 2 generator			158.84	--	Fire	--
12	1	Right cylinder, graded aluminum	1.2488	3.6775	0.342	Aluminum	Shock	Used to grade shock damage.
	2		1.250	3.675	0.3416		Shock	
	3		1.2517	3.670	0.3428		Shock	
	4		1.2518	3.680	0.3534		Shock	

mens were fabricated using four different structural strengths of aluminum. The function of these specimens was to measure, by comparison, the difference of structural damage to a simulated Task 2 fuel core of varying strengths. The method utilized to generate a test force was mechanical. The four specimens were exposed to a shock overpressure generated by the detonation of 1650 pounds of TNT and later analyzed to grade structural damage.

The specimen was a right cylinder 3.6750 inches long by 1-1/4 inches in diameter. Seven holes were drilled parallel to the longitudinal axis. Six were equally spaced on an 0.823-inch diameter circle, and the seventh was located in the center of the core. The holes were drilled through the block with a 1/16-inch diameter and 1/4-inch diameter to a depth of 3.3 inches. Materials and tested ultimate strengths fabricated into the four test specimens were as follows:

	Ultimate Tensile Strength (psi)
1100-F Aluminum Alloy Bar	10,000
2014-0 Aluminum Alloy Rod	20,000
7075-0 Aluminum Alloy Rod	30,000
6061-T6 Aluminum Alloy Rod	40,000

A single conversion system design was fabricated for this test program. It was not a complete unit, in that the thermoelectric elements were not included. However, it was used to investigate the safety protection it afforded to the energy source system when the entire unit was subjected to an intense thermal environment. This is designated as Type 10 in Table A-1.

B. TEST DEVELOPMENT

Five test programs were developed to analyze the nuclear safety of the Task 2 generator:

(1) High velocity impact.

(2) Mechanical shock.

(3) Missile fire.

(4) Thermal shock.

(5) Corrosion.

A sixth test was developed to determine the extent of a nuclear hazard, should the radiocerium fuel be released to the biosphere during some unforeseen situation of sabotage or combinations of conditions not likely to occur. Since this test was associated with the missile fire test, it was included in the fire test development and is referred to as a fallout test.

The following discusses the development of these tests. It was assumed that the specimens utilized in this program are functionally adequate and that each can be burned up upon re-entry under conditions previously stipulated.

1. High Velocity Impact Test

Since it was necessary to appraise the integrity of the Task 2 generator when subjected to impact forces, a high velocity impact test was developed. The primary purpose of this experiment was to determine the degree of damage and possible mode of failure of test specimen designs being considered for the Task 2 generator system. This was accomplished by actually impacting full-scale specimens at a specific velocity into media of varying rigidity. Twelve specimens were tested on three different impact media. Generalizations for the selection of test specimens, velocities and impact media are given below.

Test specimens. Theoretical calculations indicated that impact pressures on a fuel core are greater than those on a complete generator by a factor of about 12 at corresponding impact velocities. Based on these calculations and the terminal velocities of the fuel cores compared to the complete generator, it can be seen that impact forces are greater when the fuel core is separated and impacts alone. Therefore, the specimens used to examine structural integrity of the Task 2 generator system when subjected to impact forces were the separate fuel cores. If integrity is demonstrated on these specimens, it is logically demonstrated for the entire system. Since material strength is a function of temperature, the test specimens were preheated before impact.

Impact velocities. The terminal velocities of the various core designs average approximately 464 feet per second. The maximum terminal velocity of the complete generator, if impacted as an integral unit, is approximately 210 feet per second. The impact pressures on the discrete

core are greater in magnitude by a factor of 100 than those imposed on the complete generator. The fuel core impacting at core terminal velocities, therefore, represents the most severe test conditions. Since the average terminal velocity is about 464 feet per second, a datum velocity of 500 feet per second was established for the purpose of test planning. This velocity was obtained by employing the supersonic Ballistic Research Track at the Aberdeen Proving Ground.

Impact media. Three impact media representative of the earth's surface fabric were utilized in this test. These were granite, unconsolidated rock, and water.

Granite is a typical rigid material on which a fuel core might impact. Since little momentum is transferred to the granite from the impacting core, almost all energy is available to deform the specimen. This creates the most severe impact force possible. This medium was selected because it represented a rigid target from which damage of impacted specimens was measured as a maximum.

The use of unconsolidated rock as an impact medium served a twofold purpose. First, since it is not rigid, some of the impact energy is transferred and can be measured. This permits the determination of a degree of specimen deformation which, when compared to the maximum condition, could be used to establish configuration impact strength equations for future core designs. Second, the burial depth can be measured. This information can be utilized to determine radiation shielding afforded to the core by the medium should a fuel capsule meet with this fate.

Water is a typical nonrigid medium upon which the Task 2 fuel cores are most likely to impact in cases of missile failures. It was included in this test to determine structural deformation of the impacted specimens and to analyze the effects of cold water on a thermally hot core when it is instantaneously quenched upon impact. Since it is not possible to measure energy transfer, no comparison can be made to damage sustained during impact with the other media.

2. Mechanical Shock Test

Shock forces originating from missile propellant explosions on the launch pad appeared to be of sufficient magnitude to warrant experimental verification of core integrity to shock overpressures. Shock overpressures imposed on a generator enclosed in the payload package of a satellite system were studied and a fuel core shock integrity test was developed.

The primary purpose of this test was to determine structural deficiencies of core designs subjected to an atmosphere of intense shock forces generated by missile fuels exploding on a launch pad. Absence of deficiencies will vindicate theoretical core design parameters. Generally, the test was devised to support design conjectures for two different core configurations in a shock environment equivalent to that produced by a liquid oxygen and RP-1 fueled missile explosion. Duplication of the shock environment, specimen function and justification of this shock integrity test are described below:

Shock environment. Since it was not economically feasible to explode a full-scale missile, it became necessary to develop a simulated shock environment which could be used to determine structural integrity of isotopic fuel capsules. However, before this environment could be planned, the mechanics of a missile explosion had to be understood. Recent work by Smalley and Anderson of The Space Technology Laboratory yielded a reliable method of predicting the blast overpressures expected from a liquid oxygen-RP-1 missile explosion.

Assumptions made to derive equations for the expected overpressures from a liquid oxygen-RP-1 explosion are as follows:

(1) The missile tanks must be ruptured in a manner to permit a mass spill of the propellants.

(2) The entire weight of propellants in the missile at the time of the spill is the effective weight.

(3) An ignition source must be present.

(4) Once the blast wave forms a clean shock front, the resulting peak overpressure will decay with distance in the same manner as that from a TNT explosion.

Experience has shown that release of the propellants en masse will occur when the fuel tanks are ruptured by tank overpressurization prior to liftoff, or upon fallback after liftoff of the missile. Ignition sources are flame from the engine exhaust and/or impact of the missile structure. The empirical equations developed from 1/10 and 1/18 scale missile tests and full-scale operational vehicle failures to calculate expected overpressures as a function of the weight and distance involved are:

$$P = \frac{593}{Z^3} - \frac{28.8}{Z^2} + \frac{20.7}{Z}$$

and $$P = \frac{9862}{Z^3} - \frac{187.9}{Z^2} + \frac{52.8}{Z}$$

where

$$Z = \frac{R}{W^{1/4}}$$

P = average side on overpressure (psi)

R = distance from explosion (feet)

W = total weight of propellants (pounds).

The first equation is the predicted average pressure and the second is at the upper 98% confidence limit.

Since data were available to calculate overpressure, it was decided to simulate the test shock environment by employing TNT as the shock source. Dr. W. Baker of the Ballistic Research Laboratory at the Aberdeen Proving Ground compared maximum overpressure as a function of distance for a typical launching missile to compiled data on Pentolite explosives. This comparison indicated that an explosive weight of 22,400 pounds was required to produce the same peak overpressures over a large range of distances as the worst expected accident. This weight represents the weight of explosive detonated in free air (not near a reflecting surface such as the ground). However, the thermoelectric generator, in the launch configuration, might be subjected to both an initial shock wave from the fuel explosion and a relatively strong shock reflected from the ground. To compensate for this reflection, the maximum possible reinforcement of the incident shock was increased by doubling the effective explosive weight, giving a total weight of 44,800 pounds of TNT.

If it were feasible to detonate a TNT charge of 44,800 pounds, shock environment equivalent to that of a maximum missile explosion containing 260,000 pounds of fuel could be created. However, test facilities and funds limited to this program would not permit the detonation of such a charge. Therefore, it became necessary to investigate the possibility of scaling down the charge weight to a reasonable quantity.

The maximum charge weight was dictated by facility requirements. Safety personnel at the Aberdeen Proving Ground, where the charge was detonated, agreed to a maximum of 2000 pounds of TNT with the reservation that the time of detonation should be dependent on meteorological conditions.

Experiments by Dr. W. Baker and staff at BRL showed that the dynamic response of structures to blast loading from explosive charges can be scaled. The scaling factor is a function of the structure's linear dimensions, distance from the blast, and the weight of explosive charge producing the blast. Tests showed that the dynamic responses of structures to blast loadings were the same at scaled distances for any linear scale of the structure if the charge weight producing the blast was altered by the cube of that linear scale. That is to say, if the test specimen linear dimensions were scaled down by a factor of one-third, the charge weight required to produce the same dynamic response in the full-scale specimen from a missile blast must be scaled down by a factor of $(1/3)^3$. Therefore, shock integrity of the generators could be determined by utilizing a TNT charge of 44,800 x $(1/3)^3$ or 1650 pounds if the test specimens and distances were scaled down by a factor of one-third. Now, the charge weight was within test facility requirements, and the test was performed when meteorological conditions were favorable. Hence, the shock environment was generated by employing just 1650 pounds of TNT.

Test specimens. As with the impact tests, shock forces on a fuel core are greater in magnitude than those on a complete generator. Thus, this test was developed to investigate integrity of a Task 2 fuel core without the generator structure. The two different core configurations tested represent minimum core requirements; therefore, test confirmation of integrity in these cores inferred integrity in all configurations. The fuel cores representing identical material configurations were preheated to operating temperatures so that the blast effect simulated actual operating conditions. Simulated configurations of different materials were tested cold to measure, by comparison, structural damage of cores with varying structural strengths.

The position of the test cores with respect to the blast center was determined by scaling down the distance of the generator in the satellite package to the missile area where an explosion is likely to originate. This information was obtained from STL. According to this group, a blast is more likely to originate in the area between the LOX tank and RP-1 tank, a distance of 36 feet from the satellite package. Therefore, using the scaling factor, the test specimens were located 12 feet from the blast center.

To determine the effects of a shock front on generator-to-missile attachments, the test specimens were secured in the test shock environment by two different fastening schemes. These were: (1) rigid attachment and (2) loose attachment. The function of the rigid system was to contain the test specimen in the shock front for a time of sufficient duration to permit the shock wave to cycle at least once through the

structural material of the simulated core. The loose connection was to free the specimen so that the shock front could eject it without passing through the structure. Test specimens were analyzed after the test to determine which connection was more effective against shock overpressures resulting from missile propellant explosions.

Test justification. Since a theoretical approach for investigating blast effects on fuel cores was too complex, a mechanical shock test was necessary to establish the safety of an isotopic generator system. It has been demonstrated by tests that blast effects resulting from a LOX-RP-1 explosion could be duplicated by a TNT blast. Laws for elastic response and permanent deformation of model structures subjected to blast loadings have been developed and tested.

In estimating charge weight, conservative assumptions and maximum possible blast effects were used. The scaled loading on the specimens is undoubtedly considerably greater than would be experienced in a launch accident. Therefore, the shock test described was more than adequate to prove the safety of the generator system.

Summary. The mechanical shock test was developed to determine the effects of shock overpressures generated by exploding missile propellants on a Task 2 generator system. Effects were measured on eight test specimens exposed to a shock blast induced by detonating 1650 pounds of TNT. The samples represented fuel core configurations being considered for the Task 2 thermoelectric generator.

The TNT blast simulated a missile exploding on the launch pad. It generated shock overpressures equal to those to which a generator system would be exposed if it were aboard a missile that exploded on the launch pad.

3. Missile Fire and Fallout Tests

The basic goal of this test was to simulate a temperature profile equivalent to that of a missile burning on the launch pad and to create a known quantity of contaminated atmosphere of simulated radioactive cerium particles. The thermal environment generated was utilized to expose test specimens so that a thermal integrity evaluation could be established on the various generator configurations being developed for the Task 2 system. The contaminated atmosphere was used to determine a fallout profile and air concentrations of a nuclear release from the launch pad.

Modes of developing the simulated temperature profile and the contaminated atmosphere are presented below. Also, selection of test specimens and justification of these selections are given.

Temperature profile. As in the shock test, it was economically prohibitive to intentionally set fire to a missile. Therefore, a simulated test environment was developed. To accomplish this, theoretical calculations and data from previous missile fires were studied to determine temperature and heat profiles of a burning missile. These investigations revealed the following: (1) the splatter of liquid propellants issuing from the missile tanks is distributed over an area which forms a base for a fireball with a diameter of approximately 175 feet; (2) winds and the normal rise of the hot gases cause the entire fireball of combustion products to drift entirely clear of the launch point within five seconds; (3) about 6% of the available liquid oxygen enters into combustion; the remainder is either burned in the rocket motor or evaporated off; (4) the fire left burning consists of surface pools of fuels supported by combustion very similar to any surface oil fire; and (5) about 16% of the missile structure is consumed.

With these facts, a temperature profile was established. This profile is given in Table A-2.

TABLE A-2

Theoretical Temperature Profile of a Burning Missile

Temperature (°F)	Duration (sec)	Time (sec)	Time (min)
6000	Few micro-seconds.	0	0
4500	4	4	0.067
3000	3	7	0.12
2000	490	497	8.3
1500	700	1197	20

Using these data, calculations indicated that a thermal environment equivalent to a burning missile would be approximated by completely burning the following:

(1) 1500 pounds of aniline.

(2) 8500 pounds of RP-1.

(3) 4000 pounds of magnesium.

From this information, an environment for a fuel core thermal integrity test was developed. The test environment was generated by burning the materials indicated above. Red fuming nitric acid was utilized as the oxidizer for the aniline. Since these materials are hypergolic, the fire was ignited by releasing the two propellants from containers over a simulated missile structure.

The missile structure was simulated by utilizing scrap metal of various materials from which missile components are fabricated. This scrap metal consisted of steel, aluminum and magnesium. These were zoned in layers to simulate distribution of materials in the missile. The zoning also simulated heat distribution throughout the burning missile structure.

Atmospheric contamination. To generate a known quantity of contaminated atmosphere for fallout evaluations, a measured quantity of simulated radioactive fuel material was disposed in the missile structure. The material was released to the atmosphere spontaneously. Therefore, mischmetal was selected for this experiment because of its pyrophoric property. Also, it contains 50% cerium metal which was detected chemically on fallout trays and air sampler filters in quantities as small as 10 micrograms.

Since this material was pyrophoric, complete combustion of the entire mass occurred instantaneously as soon as the fire temperature reached 1500° F to trigger the reaction. The ensuing cloud provided an excellent environment from which a fallout profile could be determined.

Fallout field layout. The fallout field was designed to collect fallout data from the contaminated atmosphere. Field provisions, for the most part, limited the layout to a 60-degree wedge. Thus, the execution of the test was restricted to days when meteorological conditions were favorable. These conditions were dependent upon the fallout field's orientation.

The field was a wedge originating at the simulated missile structure. It was 90 degrees wide for the first 100 meters and 60 degrees wide to 1000 meters. The field was staked off at distances indicated in Fig. A-1 with an area of 4.4×10^5 square meters (4.73×10^6 square feet).

During the test, fallout trays, air samplers and cascade impactors were positioned in the fallout area. The fallout trays were located on 12 different radii throughout the field. Air samplers and cascade impactors were located on three radii at distances of approximately 3 degrees between each other. After the test, these were recovered, and the collecting medium of each was analyzed to determine necessary fallout information.

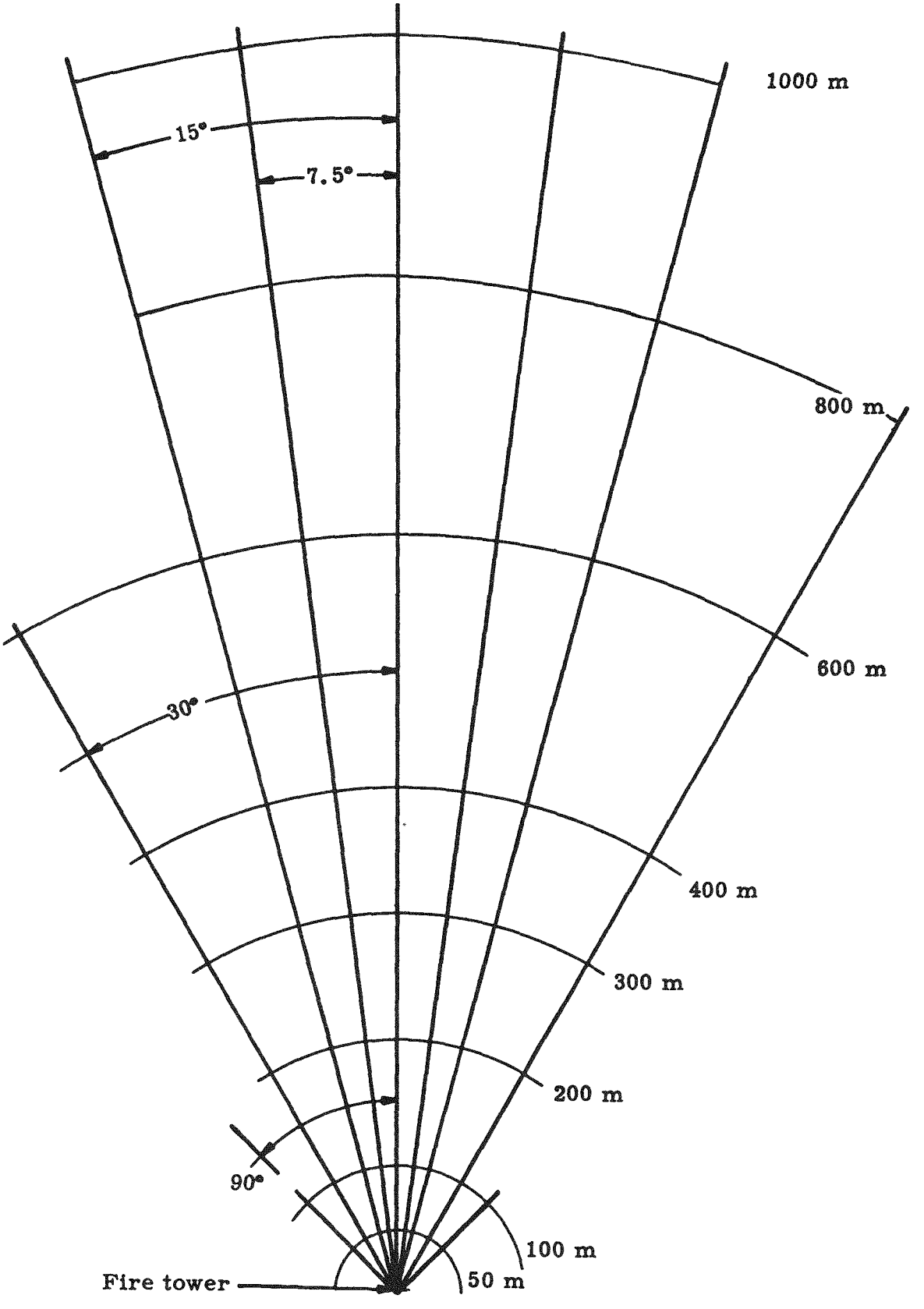

Fig. A-1. Fallout Field Layout

The fallout trays were gummed polyethyline of the type utilized by the Atomic Energy Commission. They were one square foot in area. The high volume air samplers were of the Staplex type, developed in the laboratories of the New York Office of the Atomic Energy Commission. The collecting media were of the Staplex filter PFA No. 41 type. This medium was rated to retain 25% of particles with a minimum size of 0.3 micron. The low volume samplers consisted of plastic sampling heads which retained filter media 0.750 inch in diameter. The filter medium utilized in these samplers was of the type Whatman No. 41 rated to retain 15% of particles with a minumum size of 0.3 micron. Suction for three of these heads was provided by a single vacuum ump of 17 liters per minute capacity. The cascade impactors were of the type manufactured by C. F. Casella Company, Ltd., London. These were designed for quantitative and qualitative sampling of windborne clouds of dust in the size range of 200 to 1/2 microns. A vacuum pump of 17 liter per minute capacity was utilized as a source of suction for each of these units.

Test specimens. Thermal effects on test specimens representing three different configurations were evaluated. Two of the three represented fuel cores, and the third represented a fuel core surrounded by a Task 2 generator structure. The generator structure was included in this experiment to determine the magnitude of thermal shielding it afforded the fuel core in the test environment.

Several test specimens were preheated to operating temperatures. Thermal effects on the hot and cold specimens were correlated to establish differences of heat input to the cores from the thermal environment.

Since specimens reflected minimum requirements, design verification of these structures was demonstrated for all configurations.

4. Thermal Shock and Corrosion Tests

Materials used for the containment structure of the Task 2 generator system are constantly being deteriorated by the operational environment. The magnitude of this deterioration depends upon the resistance of the structural materials to the environmental elements the unit will encounter during its life. Since these elements and exposure durations could be determined when investigating the nuclear safety of the unit, a corrosion time schedule could be established. Thus, containment materials were chosen on the basis of desirable physical properties for resisting the corrosive action of a select group of possible environments for a specific length of time.

For the Task 2 space unit, investigations were only directed to requirements previously outlined, that is, compatibility of containment structural materials with the various fuel forms, air, sea water, mercury and the various missile propellants.

Since all present day satellite booster engines employ cryogenic oxidizers and because a generator could be quenched in the missile oxidizer in certain accidents on the launch pad, it is important not only to investigate the corrosive action but to determine thermal shock effects of these materials on a thermally hot generator system.

The Corrosion Unit of the Martin Nuclear Division Materials Section developed a series of corrosion and thermal shock tests.

Test environment. A test environment for the thermal shock experiment was provided by liquid oxygen. This material was selected because it represents a typical cryogenic missile propellant and is one of the corrosive environments to which the Task 2 generator could be subjected in the particular missile program being evaluated for nuclear safety.

Test environments for corrosion studies were provided, for the most part, in laboratory scale experiments. Corrosion rates were based on test results of scaled exposure times in a simulated corrosive environment. For the Task 2 system, these environments included:

(1) High temperature air.

(2) Ceric Oxide (CeO_2).

(3) Sea water.

(4) Mercury.

(5) Liquid oxygen.

(6) Red fuming nitric acid.

Test specimens. In the thermal shock test, a single specimen was evaluated. A bare core was used for it reflected the most severe thermal shock condition imposed on the entire system. That is, if the complete system were subjected to a cryogenic substance, the generator shell would afford sufficient thermal protection to the fuel core so as to cause little if any shock to the containment material. Only one of the possible containment materials was evaluated since preliminary investigations indicated that all would possess similar thermal properties if exposed to a cryogenic substance. The test specimen was preheated to simulate actual accident conditions.

Specimens used in the corrosion studies were typical laboratory-weighed test bars of each of the materials evaluated.

C. TEST PROCEDURES AND RESULTS

This section summarizes procedures and results of all the tests developed to optimize design configurations of the Task 2 space generator. Since these tests have been justified as to requirements, the procedure of each includes only details of facilities and setup.

1. High Velocity Impact Test

These tests were conducted on the Supersonic Ballistic Research Track at the U.S. Army Chemical Center, Edgewood, Maryland. Specimens were preheated, propelled by rocket sleds and impacted against simulated earth media. Description of test equipment, procedures and results are presented.

Supersonic ballistic track. The ballistic track utilized in this test is a dual rail track, 2448 feet long. The cold-rolled steel rails are 2 inches by 1 inch in cross section with a two inch separation between rails. Sleds are mounted by metal shoes designed to lock between the rails.

The track is designed to achieve varying velocities with a payload of from 1.5 to 590 pounds. Maximum acceleration is 110 g.

Sleds can be affixed to any position along the length of the track. The impact velocity is dependent upon position, sled weight and rocket thrust (see Fig. A-2).

Rocket sled. To obtain the desired impact velocity of 500 feet per second on each test specimen, a rocket sled propelled by two FFAR rocket engines was employed. Specifications for these engines are as follows:

Engine weight	12.1 pounds
Length	32 inches
Diameter	2.75 inches
Thrust	520 pounds
Propellant weight	6.4 pounds
Burning time	1.7 seconds
Lot number	ALN-RMHA-10 C-52

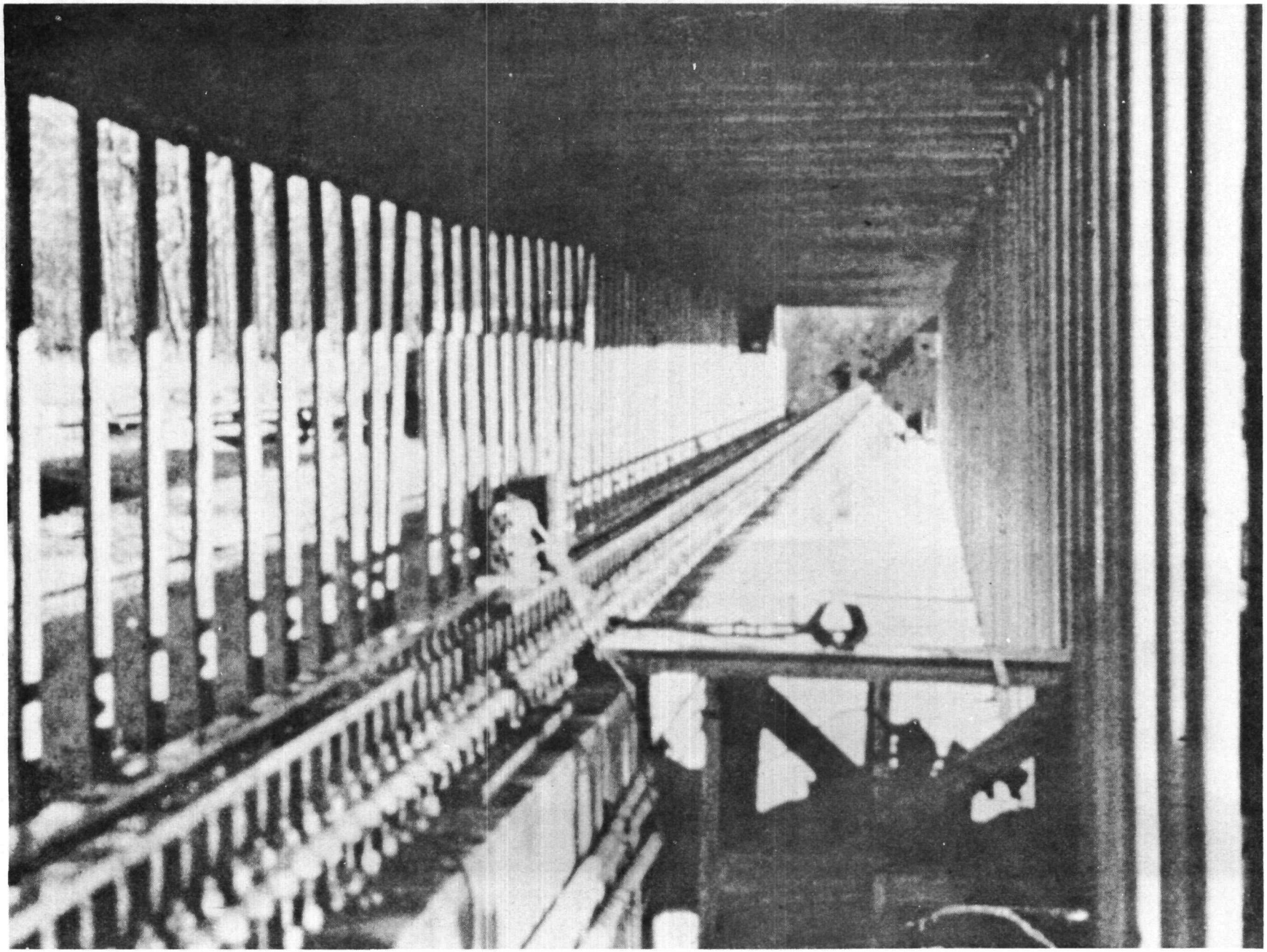

Fig. A-2. Supersonic Track

A specially designed insulated cradle was mounted in front of the rocket engine cluster on a massive steel structure. The cradle was used to contain the heated test specimen in the sled vehicle. The massive structure was used to prevent sled debris from impacting the target after specimen separation. Sled specifications and track distances are given in Table A-4. Figure A-3 shows a view of this sled.

Separation technique. To separate the test specimen from the rocket sled, a unique impact system was employed. A large vertically mounted steel plate, 10 feet square and 8 inches thick, was located approximately 5 feet, 8 inches beyond the end of the track. An 8-inch diameter aperture in this plate was directly in the path of the specimen-bearing vehicle. Upon leaving the track, the sled vehicle impacted the steel plate. The test specimen entered the aperture, separated from the sled and impacted the target medium. The vertically mounted steel plate restrained the rocket engine and sled debris from impacting the target. Figures A-4 and A-5 show views of this separation plate. Figure A-6 shows a typical sequence of separation.

Test specimens. Core configurations were tested to evaluate core impact integrity. Data for these specimens are given in Table A-1 (detailed specimen specifications), Table A-4 (detailed test data) and Table A-5 (Test results).

The specimens were preheated to temperatures as indicated in Table A-4 in a Harper electric furnace rated at 10 kva. Power for this furnace was supplied by a portable generator furnishing 220-volt, 60-cycle, single-phase service. To assure good specimen temperatures, the cores were not removed from the furnace until furnace temperature remained stable for 1/2 hour. Since it required between 10 to 40 seconds to remove the core from the furnace and impact it, the specimens were preheated to a temperature higher than that desired at impact. This allowed for the loss of heat due to radiation during this period of time.

After impact, specimen penetration was measured, and photographs were taken to record core conditions.

Impact media. Specifications and containment details of the three impact media are given in Table A-3. All three media were positioned aft of the vehicle separation plate in the path of impacting specimen. These setups are shown in Figs. A-7, A-8, and A-9. Table A-4 gives the position of each.

Data recording. Physical data recorded during this test is summarized in Table A-4. Also, documentary and Fastax 16-mm films of the impacts were taken. These have been given a careful examination to verify impact velocities and check overall results.

Test results. Test results are shown in Table A-5.

TABLE A-3

Specifications and Containment of High Velocity Impact Media

	Target Medium		
	Granite	Unconsolidated Rock (tamped earth)	Water
Containment	Solid rectangular block backed up by 10 tons of earth	Steel framed rectangular plywood box (1 inch thick) with open front and top.	Watertight rectangular plywood box (1 inch thick) with reinforced steel bands. Water inlets were two 4-inch diameter holes in the top.
Length (ft)	4.5	20	12
Width (ft)	2	4	4
Breadth (ft)	2	4	4
Volume (ft^3)	18	320	192
Density (lb/ft^3)	168	76	62.4
Weight (lb)	3024	24,320	11,980
Compressibility (psi)	~30,000	~300	--
Remarks	Abrasive hardness similar to that of steel (Rockwell hardness (C-53))	Earth was partially frozen during first series of tests.	

TABLE A-4

Summary of Test Data--High Velocity Impact Test

Date of Firing	Specimen Type	Specimen Number	Configuration Design Number	Vehicle Weight (lb)	Track Distance (ft)	Free Flight Before Separation (in.)	Free Flight After Separation (in.)	Specimen Preheat Temperature (°F)	Time from Furnace to Impact (sec)	Impact Velocity (ft/sec)	Impact Medium	Penetration Depth (in.)
12/1/59	1	1	A-I_{CeO_2}	102.8	425	68	109	1726	30.6	519	Granite	None
12/2/59	1	2	A-I_{CeO_2}	102.9	425	68	168	1800	16.0	492	Unconsolidated rock	120
3/11/60	8	1	D-I_{CeO_2}	117.67	425	65	137	1500	35.7	497	Granite	3 visible cracks
3/11/60	8	2	D-I_{CeO_2}	119.70	425	65	137	1600	20.4	495	Granite	None
3/11/60	8	3	D-I_{CeO_2}	119.48	425	65	137	1600	32	521	Water	Through box

TABLE A-5

Summary of Test Results--High Velocity Impact Test

Specimen Type	Specimen Number	Specimen Impact Temperature (°F)	Impact Pressure (psi x 10^3)	Energy of Impact (ft-lb x 10^4)	Force of Impact (lb x 10^4)	Energy Lost to Impactor (ft-lb x 10^4)	Force Acting on Specimen (lb x 10^4)	Number of Fuel Tube Plugs Lost	Number of Fuel Tubes Fractured	Dimensions of Impacted Specimens: Maximum Diameter (in.)	Average Length (in.)	Deformed Average Length (in.)	Simulated Fuel Released (%)	Description of Impacted Target	Description of Impacted Specimens and Analysis of Its Mode of Failure
1	1	1626	25.5	10.11	28.4	0	28.4	0	4	6.50	9.05	2.65	~15	No change	Impacting face expanded and fractured to a depth of 3 in. (see Fig A-10). Impact plane requires more material or less cross-sectional area
1	2	1750	23.5	9.04	26.2	5.5	16.4	0	0	No change	No change	0	0	30 in. of soil disarranged at impact face (see Fig. A-14)	No measurable damage (see Fig A-11)
8	1	1485	22.3	14.6	39.5	~10	22.2	0	0	Depressor 6 Core 5.4	Assembly ~10.4 Core ~10.2	Assembly 8.6 Core ~8.4	0	3 cracks from impact point. Approximate cross section of crack = 200 in.^{2} (see Fig A-15)	Core diameter expanded for a length of 8 in. from impacted face. No fractures in core or depressor (see Fig. A-12). Cracks in target medium had definite bearing on core condition, as compared to Specification 2 of this design
8	2	1530	22.0	14.6	39.0	0	39.0	0	1	Depressor 5.8 Core 5.0	Assembly ~10.47 Core ~10.25	Assembly ~3.8 Core ~3.6	0	No change	Core diameter expanded for a length of 4 in. from impacted face. Impact depressor fractured at edge for a distance of 6 in. Core has a small fissure under fracture in depressor (see Figs. A-12 and A-13). Depressor impact area should be designed smaller
8	3	1495	25	16	4.43	--	--	0	0	No change	Assembly 11.6 No change	0	0	Side and top blown off by pressure of impact (see Fig. A-16)	Impact depressor welds around core wall fractured. No damage to core or depressor (see Fig. A-12)

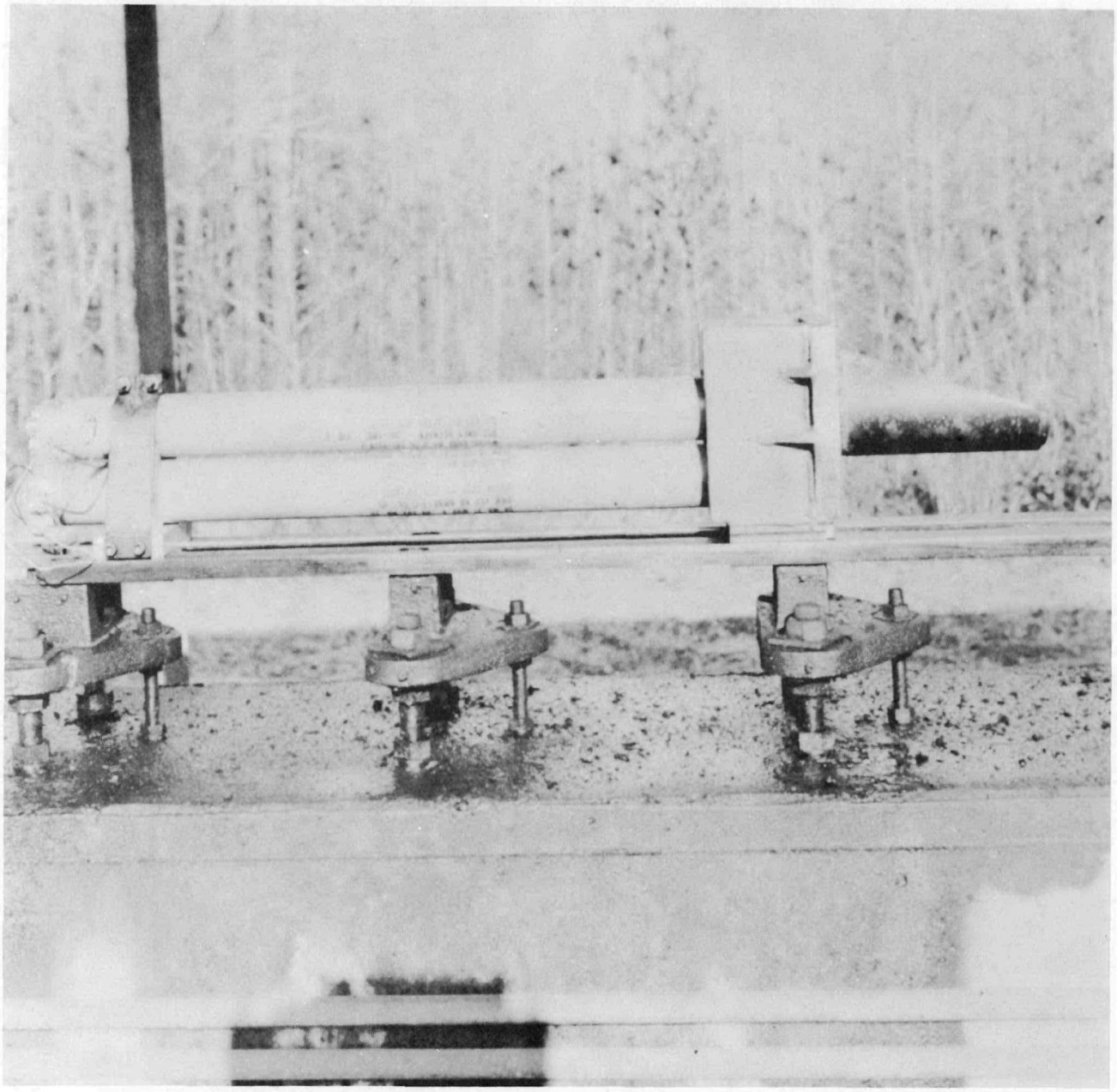

Fig. A-3. Rocket Sled--High Velocity Impact Test

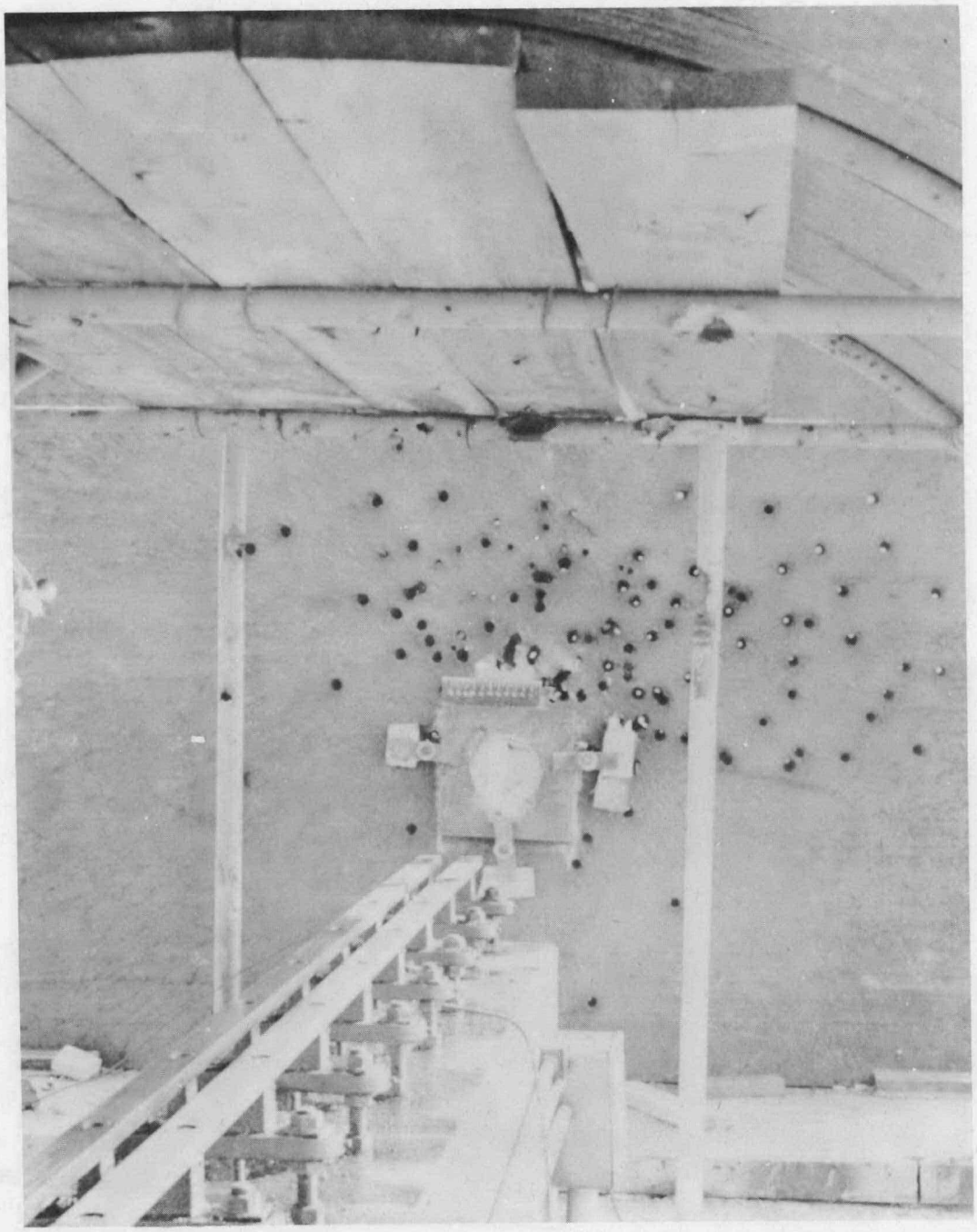

Fig. A-4. Vertical Separation Plate, Sled View

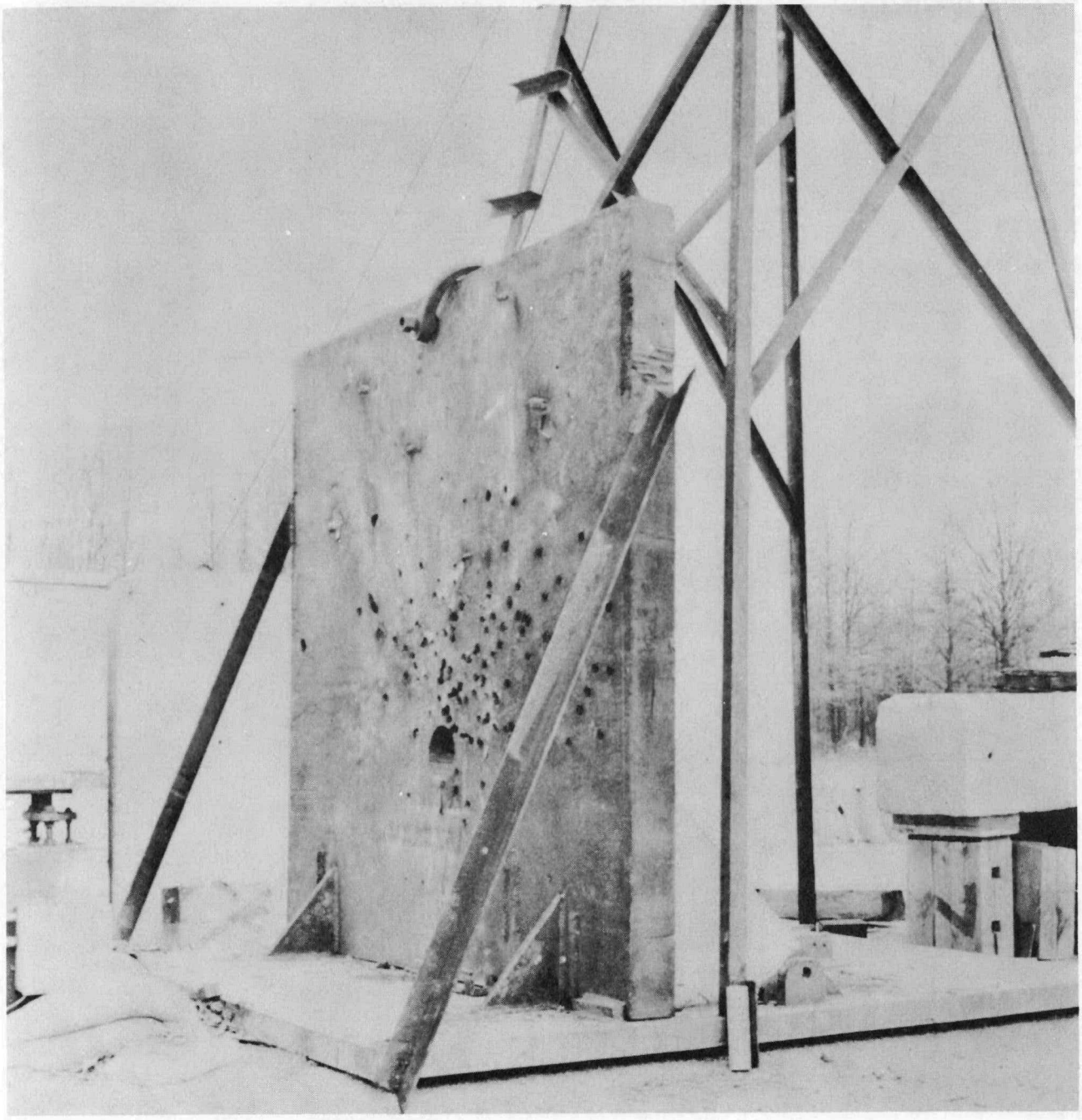

Fig. A-5. Side View of Vertical Separation Plate

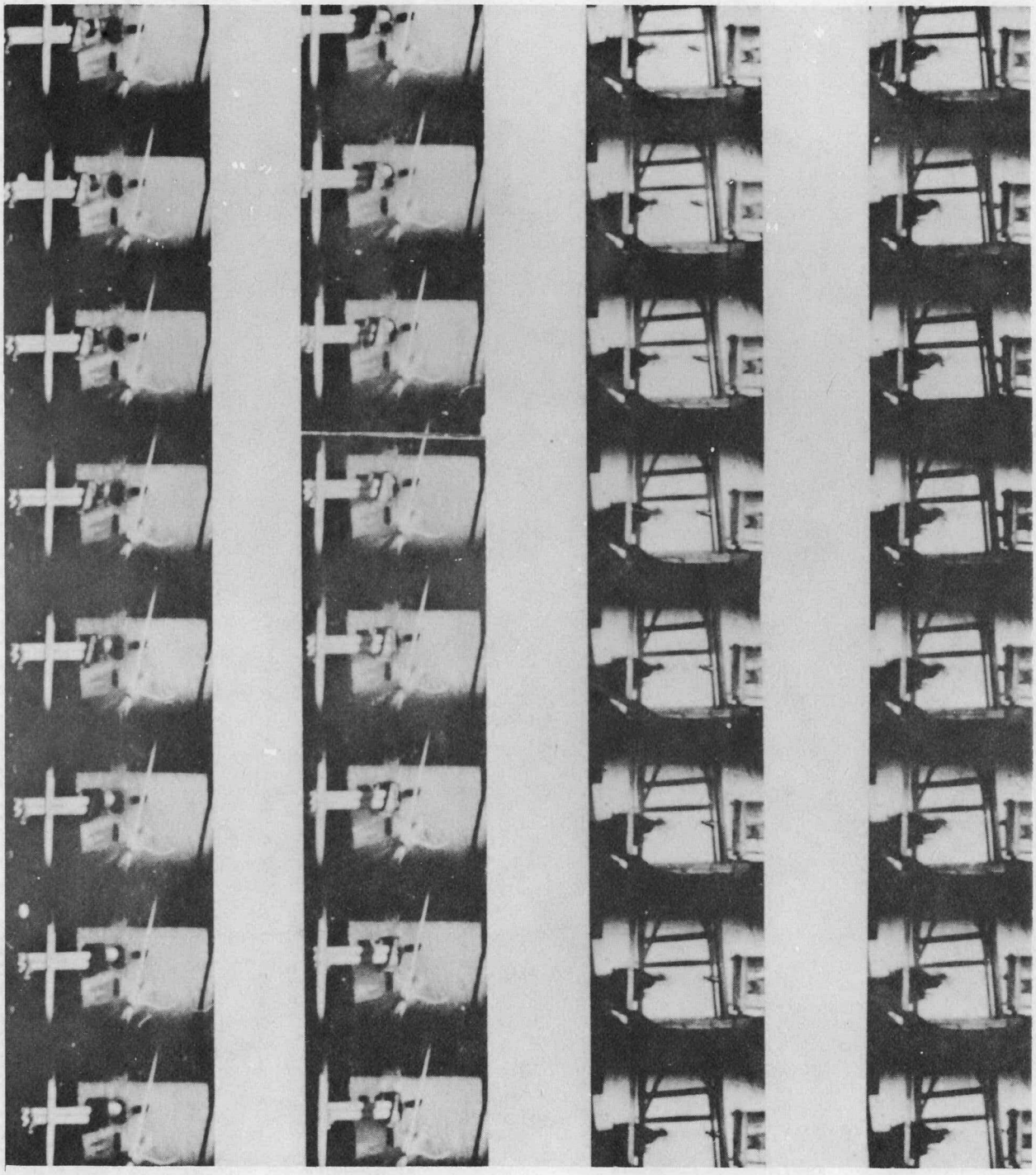

(1) (2) (3) (4)

(1) Sled leaves track
(2) Sled impacts separation plate
(3) Test specimen in free flight
(4) Test specimen impacting medium

Fig. A-6. Rocket Sled and Test Specimen Separation Sequence

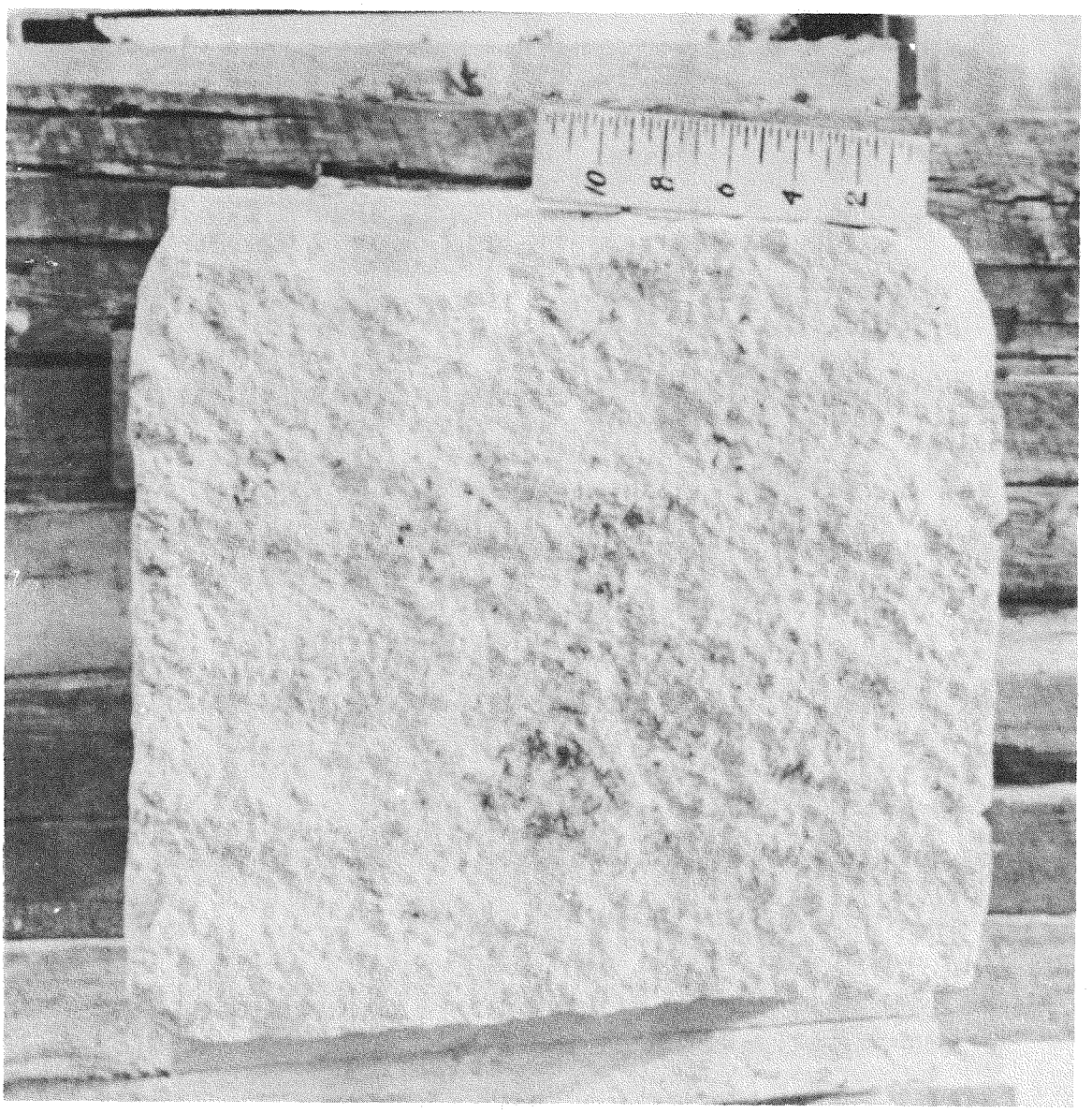

Fig. A-7. Granite Impact Medium

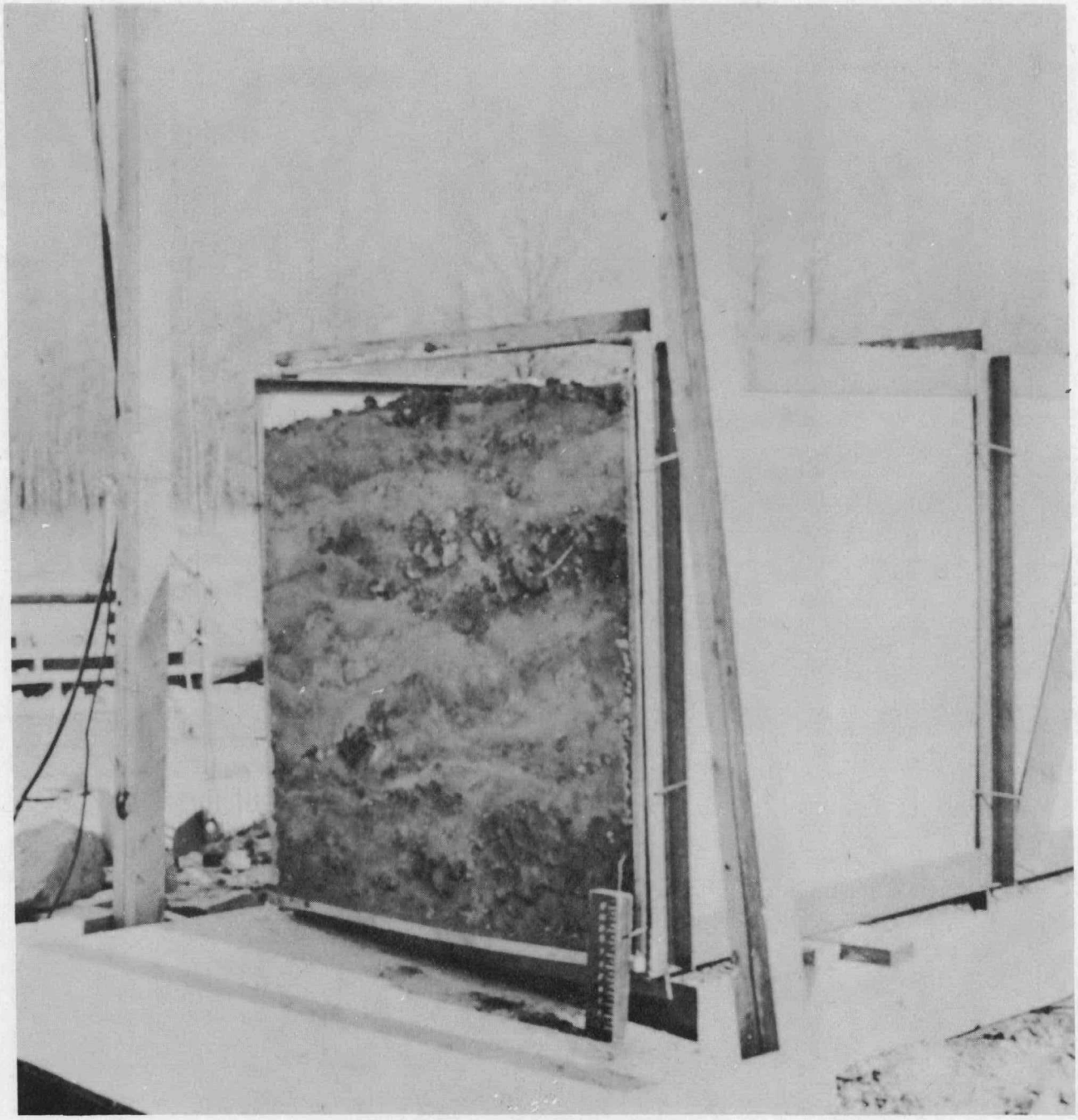

Fig. A-8. Unconsolidated Rock Impact Medium

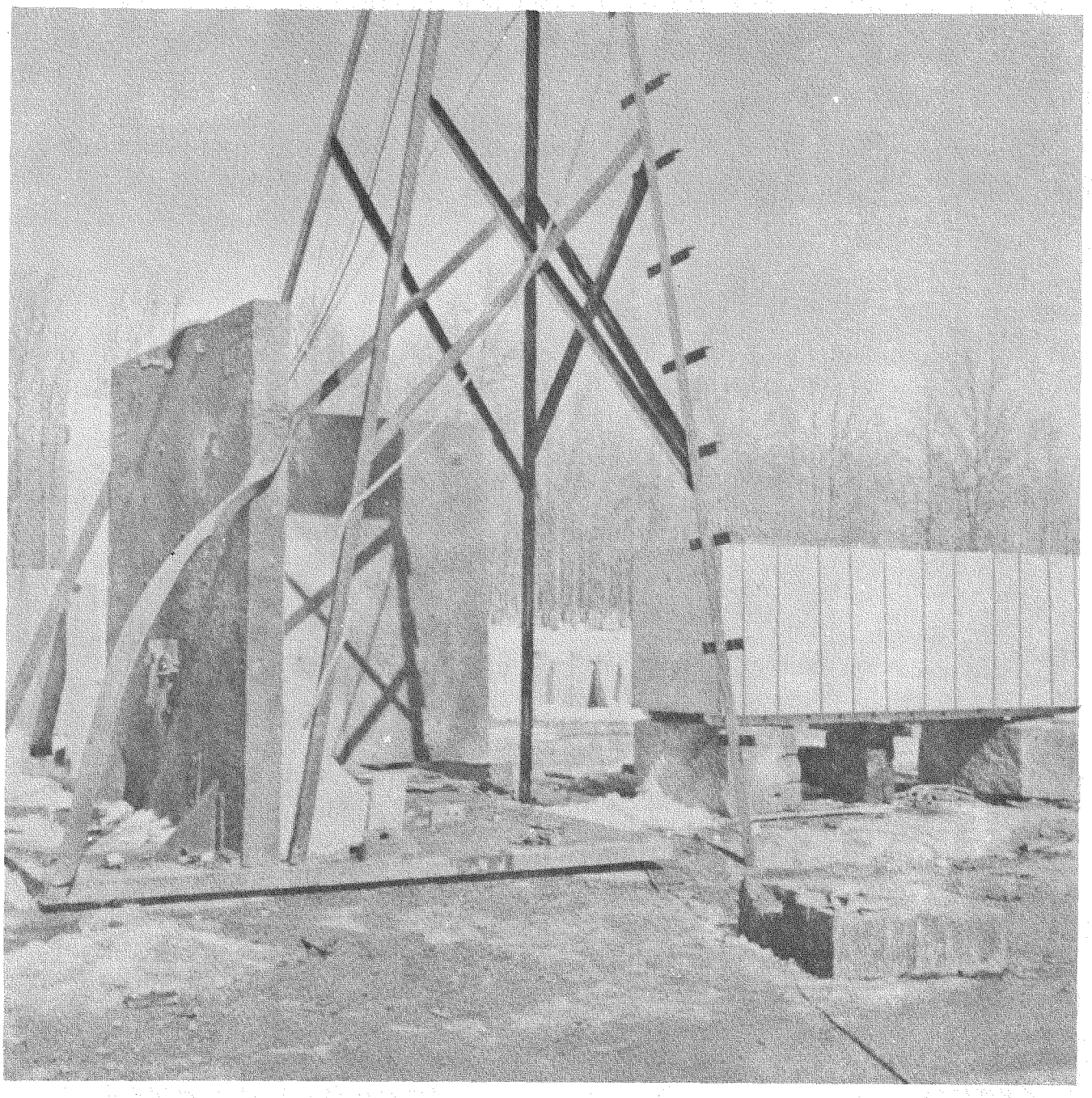

Fig. A-9. Water Impact Medium

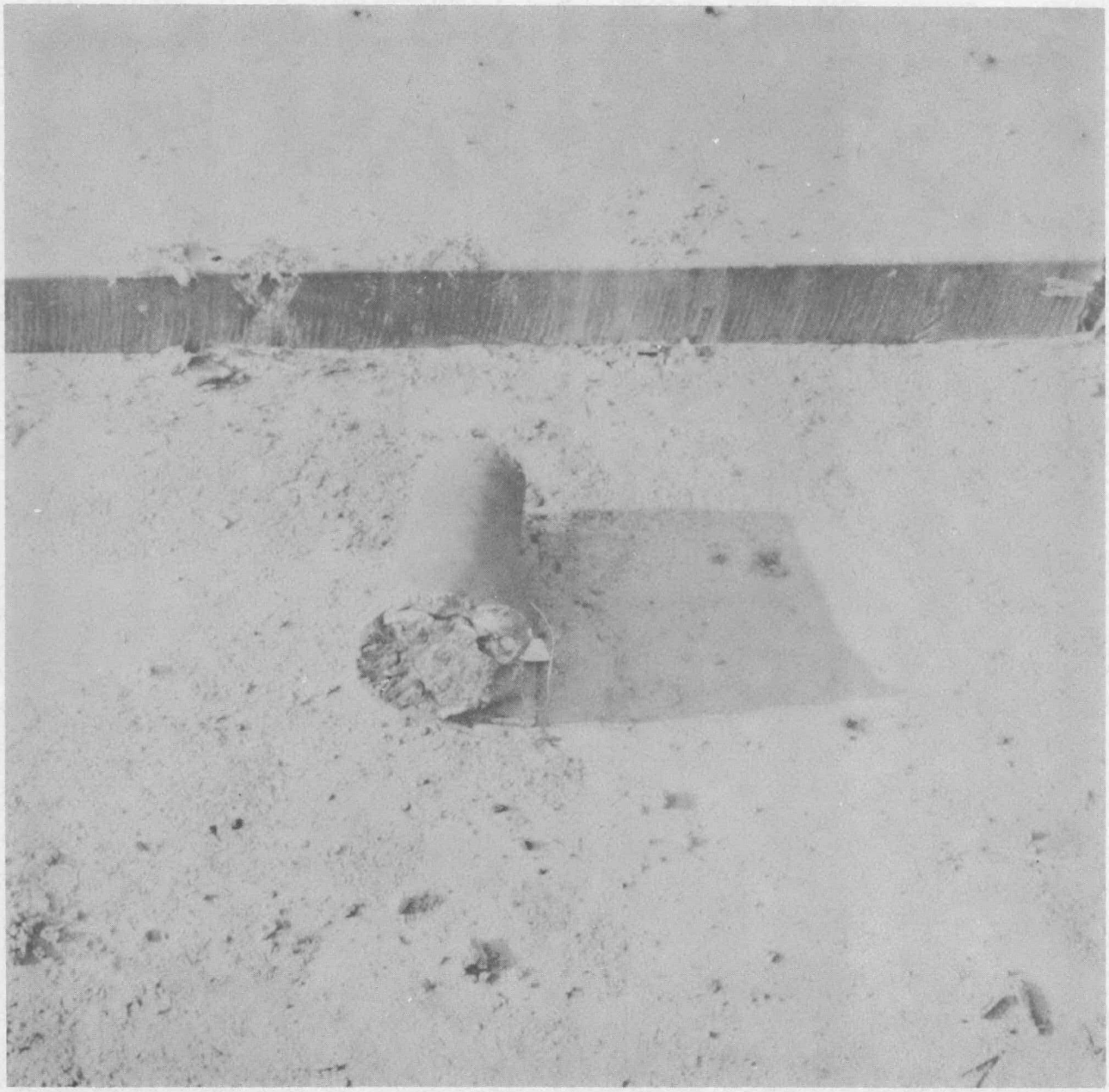

Fig. A-10. Fuel Core Impacted on Granite--Type 1, Number 1, Design A-I, CeO_2

Fig. A-11. Fuel Core Impacted on Unconsolidated Rock--Type 1, Number 2, Design A-I, CeO_2

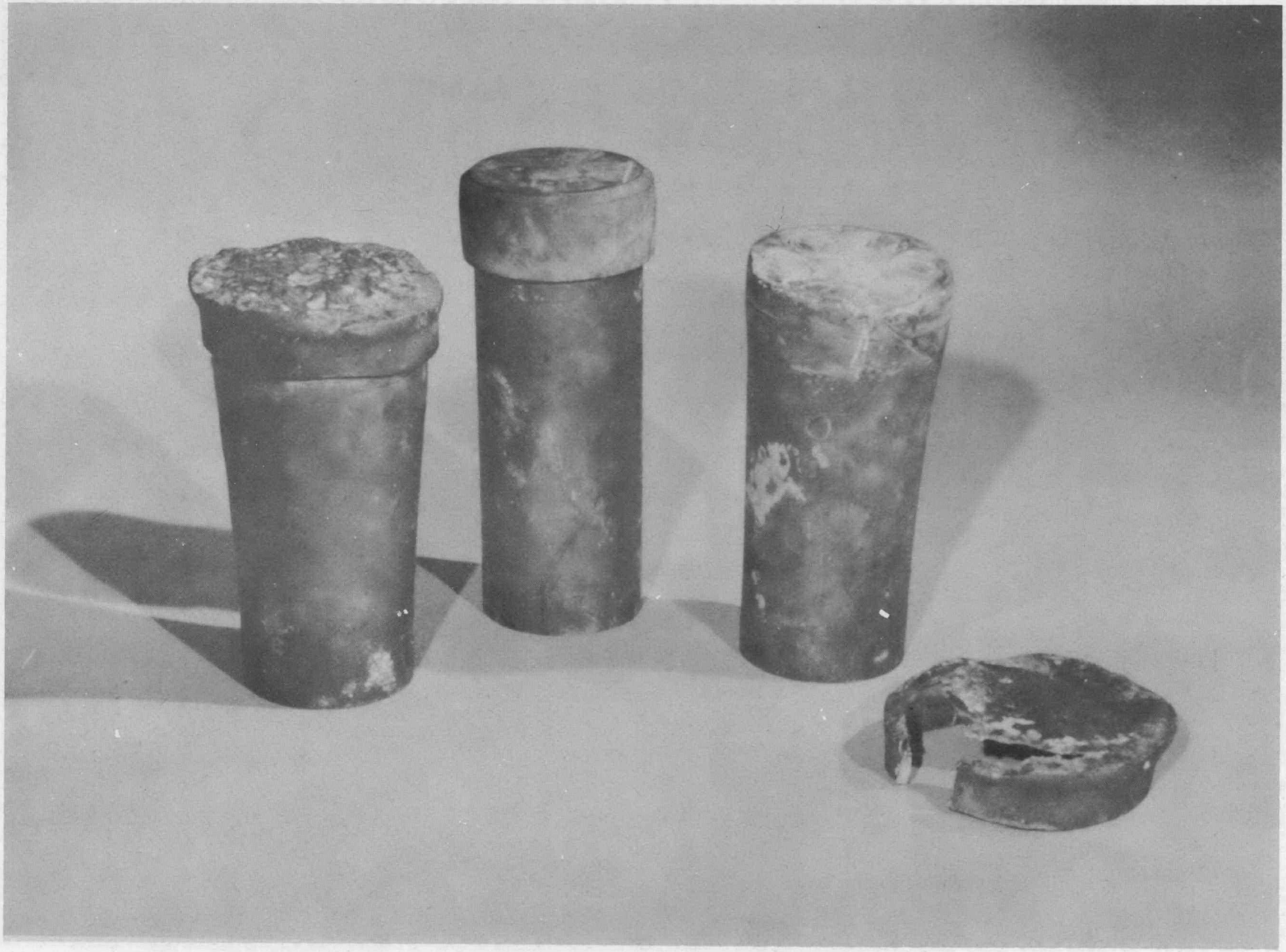

Fig. A-12. Fuel Cores Impacted on Granite and Water--Type 8, Numbers 1, 2 and 3, Design D-I, CeO_2

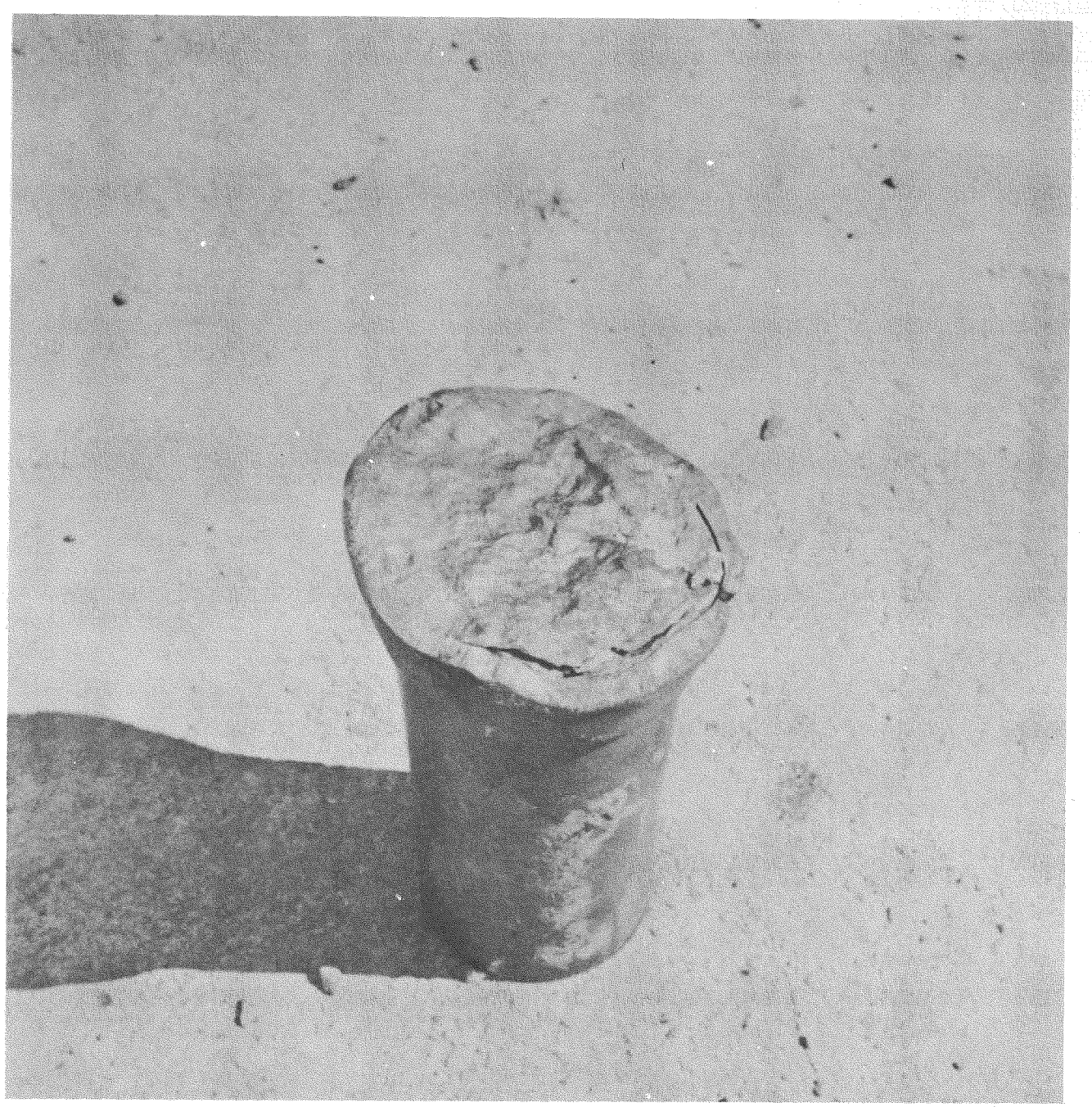

Fig. A-13. Fuel Core Impacted on Granite--Type 8, Number 2, Design D-I, CeO_2

Fig. A-14. Unconsolidated Rock Medium After Specimen Impact

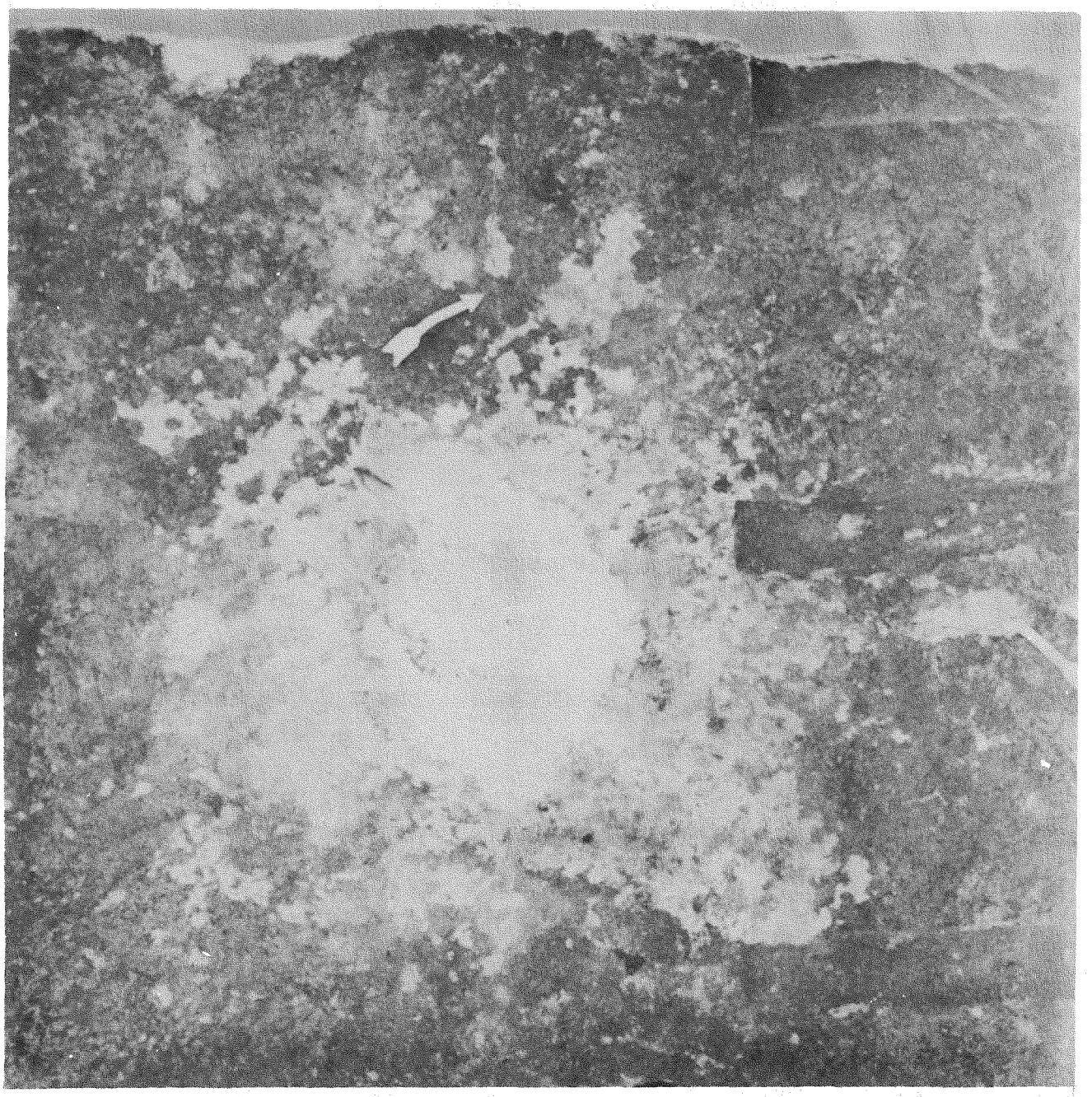

Fig. A-15. Granite Medium After Impact of Specimen--Arrows Indicate Position of Fissures Resulting from Impact Forces

Fig. A-16. View of Water Medium After Specimen Impact

2. Mechanical Shock Test

This test was conducted 23 March 1960 on "M" Field at the U.S. Army Chemical Center, Edgewood, Maryland. Specimens were preheated in some cases and exposed to a shock wave produced by the detonation of 1650 pounds of TNT.

Test site. The site utilized for this test is a bomb test field located on a peninsula in the Chesapeake Bay at the entrances of the Bush and Gunpowder Rivers. A massive concrete wall approximately 50 feet high and 75 feet long protected equipment. Thickness of the wall varied from 14 feet at the base to 5 feet at the top. The test blast was 200 feet from the wall in an east-northeast direction. A personnel bunker with an observation port was located approximately 1000 feet from the blast in a southeast direction. Figure A-17 is an aerial view of this site after conclusion of the test.

Shock energy source. To obtain the desired shock overpressures, 1650 pounds of TNT were employed. This gives an energy release of 1.8×10^9 foot-pounds. This charge was contained in 25 wooden crates, each containing 66 one-pound blocks of TNT. All 25 crates were positioned in a five-layer pyramid on a wooden stand. This stand was leveled about 3 feet above the ground and rested on a steel plate 4 inches thick by 12 feet square. The charge configuration was designed to reproduce a geometric form as near to a hemisphere as possible. This geometry was required to obtain a symmetrical shock wave in all directions. The pyramid satisfied this requirement very effectively.

The TNT was primed and detonated by an experienced demolition engineer from the Aberdeen Proving Grounds. It was set off from the personnel bunker, 1000 feet from the charge.

Test specimens. Eight specimens, representing two fuel core configurations, were tested in this shock environment. Data for these specimens are given in Table A-1 (detail specimen specifications), Table A-6 (detail test data) and Table A-7 (test results).

Four of the specimens were preheated to 750° F. This is the operating temperature of the core at the time when the generator might be exposed to a shock environment on the launch pad. Since the specimens are 1/3 scale, and preheating had to be accomplished remotely, electric pencil-type heaters were employed. These were energized by a 110-volt, 60-cycle, single-phase power source, which was located behind the concrete barrier, 200 feet from the specimens. The remaining four specimens were graded strength simulated cores of aluminum, which were exposed to the shock at ambient temperatures.

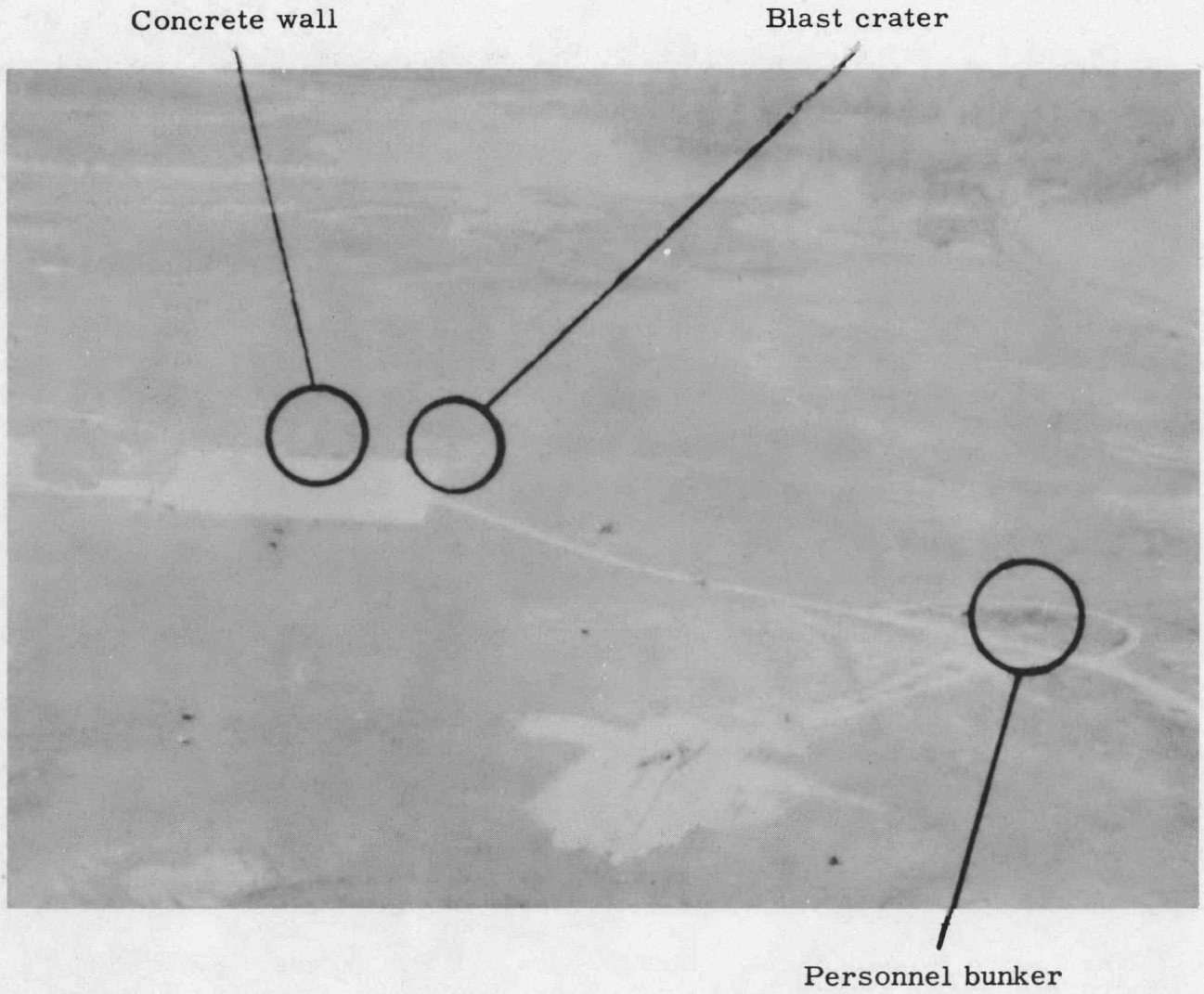

Fig. A-17. Aerial View of Mechanical Shock Test Site

TABLE A-7

Summary of Test Results--Mechanical Shock Test

Specimen Type	Specimen Number	Configuration Design Number	Specimen Side-on Overpressure (psi)	Shock Force (lb) Max.	Shock Force (lb) Min.	Minimum Time for Shock Front to Traverse Specimen (microseconds)	Ultimate Tensile Strength of Material (psi)	Description of Tested Specimens	Assumed Mode of Retention or Release of Test Specimens
1	3	$A\text{-}I_{Ce\,02}$	1020	7,400	1,200	19.7	148,000	No visible or measurable change (see Fig A-24) Lanyard ring ultimate tensile force = 4080 lbs. Yield force = 2700 lbs.	1 Shock front released specimen from its loose mounting 2 Force carried specimen until it was restrained by rope 3 Force = 1200 lbs Ultimate strength of rope = 7500 lbs 4 Conclusion Specimen returned by nylon rope and no deformation resulted in lanyard ring; yield strength = 2700 lbs 5 Test verifies assumptions.
1	4	$A\text{-}I_{Ce\,02}$	1020	7,400	1,200	19.7	148,000	Not recovered.	1 Shock front sheared post with specimen attached. 2. Force carried assembly from blast center 3 Force on assembly = 700,000 lbs, ultimate tensile force on hardware - 6500 lbs 4 Conclusion Force carried assembly, attaching hardware failed freeing specimen from assembly Force on specimen caused rope to fail freeing specimen completely Possible recovery location > 3000 feet from blast center
12	1	Graded Aluminum	1020	7,400	1,200	18.5	30,000	Lanyard ring failed in tension, U T. force = 828 lbs. Surface damaged by impinging particles, penetration depth-max. 0.07 in (see Fig A-25)	1 Loose mounting permitted specimen to be released 2 Force = 1200 lbs 3 Rope would have retained specimen, but lanyard ring broke 4 Conclusion Specimen lanyard ring failed in tension, releasing it from rope 5 Slight damage by impinging particles
12	2	Graded Aluminum	1020	7,400	1,200	18.5	40,000	Lanyard ring failed in tension, U.T force = 1104 lbs. Surface damaged by impinging particles, penetration depth-maximum 0 01 in (see Figs. A-25 and A-26)	1 Shock front sheared post with specimen attached 2 Nylon rope pulled specimen out of its attaching hardware 3 Force of 1020 lbs caused lanyard ring to fail; however, rope continued to retain specimen 4 Conclusion· Specimen retained by rope; ring failed in tension and attaching hardware still attached to post 5 Damage by impinging particles minor--highest strength material
12	3	Graded Aluminum	1020	7,400	1,200	18.5	10,000	Not recovered	1 Loose mounting permitted specimen to be released 2 Force of 1020 lbs caused lanyard ring to fail; ultimate force on ring = 276 lbs 3 Specimen continued away from the blast Approximate recovery location > 3000 ft from blast center
12	4	Graded Aluminum	1020	7,400	1,200	18.5	20,000	Lanyard ring failed in tension U.T. force = 552 lbs. Surface damaged by impinging particles, penetration depth--maximum 0.10 in (see Fig A-25)	1 Same as specimen 1, Type 4, rigid attachment Specimen found about 3000 ft from blast center 2 Damage by impinging particle most severe of the 3 graded strength specimens recovered

TABLE A-6
Summary of Test Data--Mechanical Shock Test
Specimen Data

Specimen Type	Specimen Number	Configuration Design Number	Identification	Post Position (from true north) (deg)	Attachment	Specimen Preheat Temperature (°F)	Specimen Recovery Data
1	3	$A\text{-}I_{CeO2}$	2	65	Loose	750	Retained by nylon rope
1	4	$A\text{-}I_{CeO2}$	2	65	Rigid	750	Not recovered
12	1	Graded aluminum	1	353	Loose	Ambient	1000 ft, 353 degrees from blast center
12	2	Graded aluminum	1	353	Rigid	Ambient	Retained by nylon rope
12	3	Graded aluminum	2	65	Loose	Ambient	Not recovered
12	4	Graded aluminum	2	65	Rigid	Ambient	~3000 ft, 65 degrees from blast center

Fire Ball Data

Shape	Maximum Dimensions Horizontal (ft)	Maximum Dimensions Vertical (ft)	Maximum Rise (ft)	Time Measurements (sec) Develop Maximum Ball	Time Measurements (sec) At Ground Level	Time Measurements (sec) Dispersal	Temperature (maximum) (°F)
Mushroom (see Fig. A-21)	~175	~100	~100	~0.1	~0.71	~2.7	~7000

Crater and Pressure Data

Shape	Crater Dimensions (ft) Diameter	Crater Dimensions (ft) Depth	Crater Volume (ft^3)	Weight of Earth Moved (lb)	Detonation (psi)	Pressure Side-on Overpressure (psi) At 130 ft	Pressure Side-on Overpressure (psi) At 190 ft
Spherical segment (see Fig. A-23)	26	6	1600	144,000	9×10^5	5.02	2.95

Specimen setup. The eight specimens were positioned 12 feet from the blast center on two posts 1 foot above the bottom layer of the TNT. These were anchored in the ground to a depth of 10 feet. The points were 4-inch diameter steel tubing, located on the circumference of a 24-foot diameter circle. The posts were located 65° and 353°, respectively, from true north.

Two types of specimen attachments were utilized. A rigid attachment was made by securing the specimens to 0.75-inch thick steel plates with oversize hardware. The steel plates are welded to the steel mounting posts. The nonrigid attachment was made by securing the specimens to the steel plates with pins. These pins were 0.064 inch in diameter and 1 inch long. Holes were provided in the plates and specimens to accommodate the pins. There were four specimens on each post, two rigidly attached and two merely pinned. Figures A-18 and A-19 show core attachments on Posts 1 and 2, respectively. Methods of attachment used on the test specimens are given in Table A-1. The heated specimens were covered with insulation to reduce heat losses during the preheating operation.

To recover the specimens after the test, 0.75-inch diameter nylon rope with a 7500-pound tensile strength was secured to each specimen by a lanyard ring welded to the core. These ropes were anchored on the ground 75 feet behind each setup. They were covered with earth for about 10 feet from each post. The function of the earth cover lines was to contain the test specimens within a 200-foot diameter circle (see Fig. A-20 for the complete setup).

Two beam-type pressure gauges were positioned at 130 and 190 feet from the center of the charge. These were utilized to measure side-on overpressures. These data are given in Table A-6.

Data recording. Physical data recorded during this test are given in Table A-6. In addition, four cameras were covering the action of the test. Films have been screened in order to obtain visual test data. Data collected from these films are also given in Table A-6.

Test results. Test results are summarized in Table A-7. A detailed analysis of the explosion, setup and test specimens is presented below.

Explosion. The 1650-pound charge was detonated at time 1404 hours. A mushroom fireball, 175 feet in diameter by 100 feet high, developed 0.1 second after detonation. It remained on the ground for 0.7 second and then rose to a maximum altitude of 100 feet. At this point and at a time of 2.7 seconds after detonation, the ball dispersed into a black cloud and moved downwind. Figure A-21 shows the blast sequence.

Fig. A-18. View of Mechanical Shock Test Specimen Attachment--Post 1

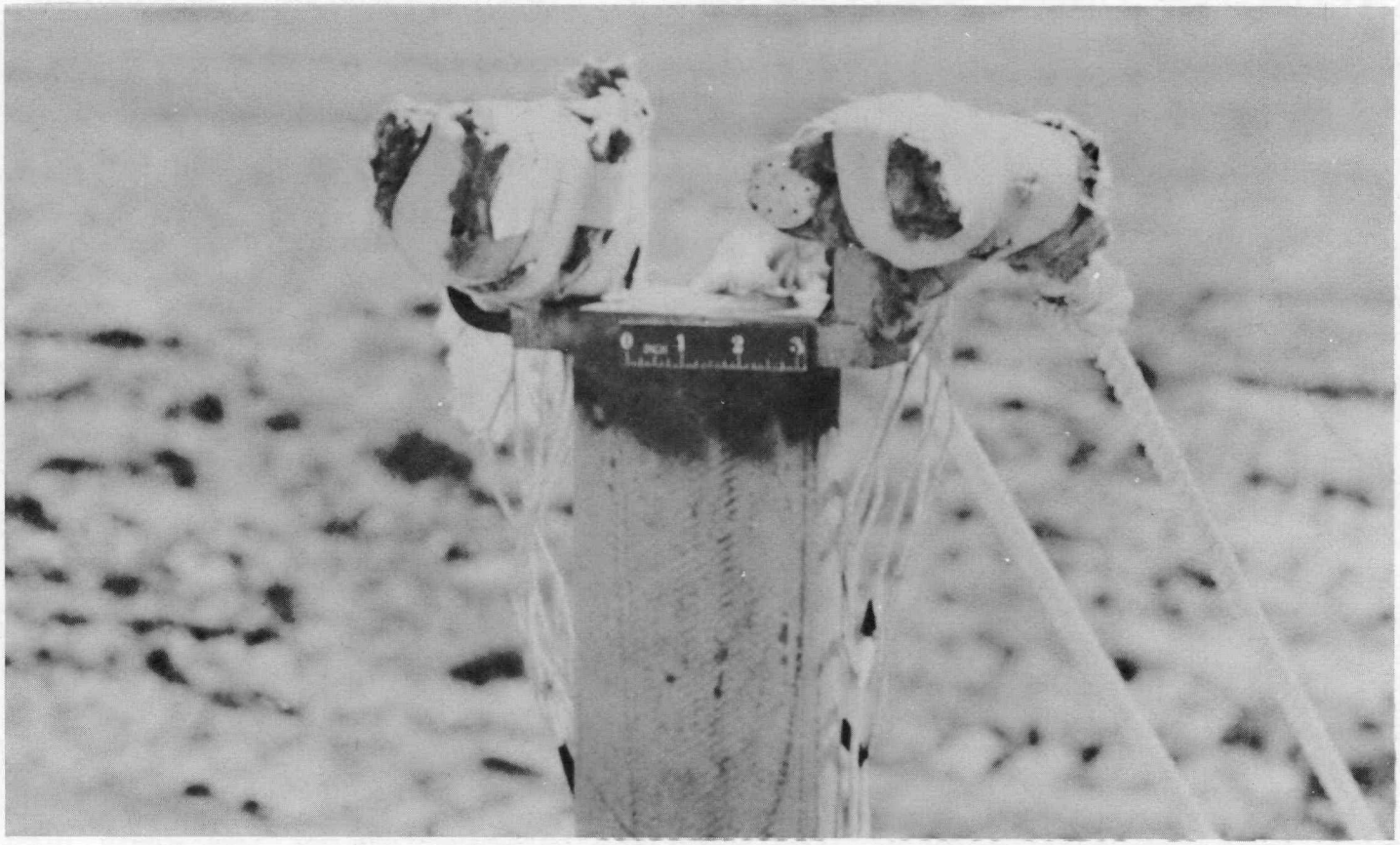

Fig. A-19. View of Specimen Attachment--Post 2

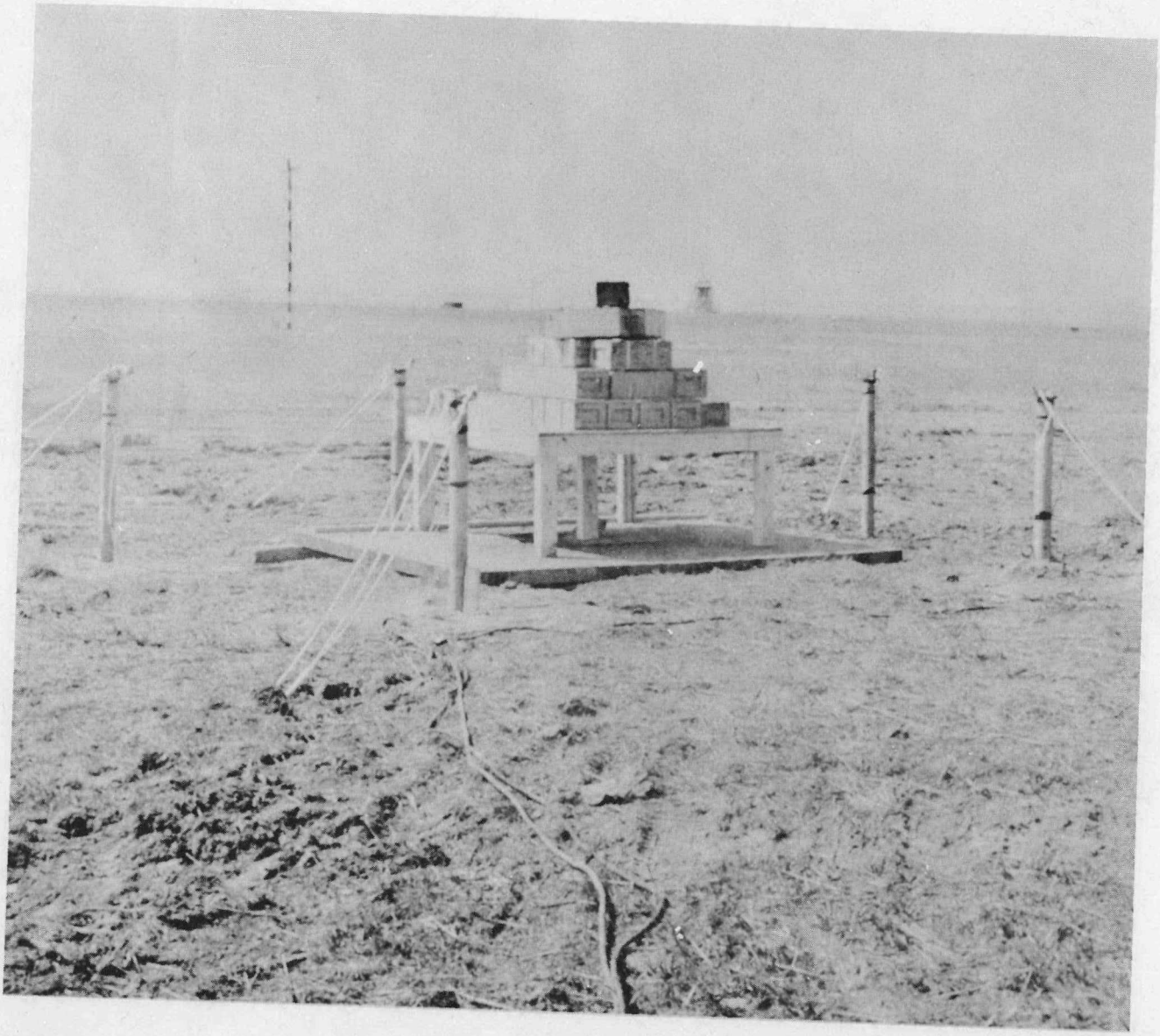

Fig. A-20. View of Complete Mechanical Shock Test Setup

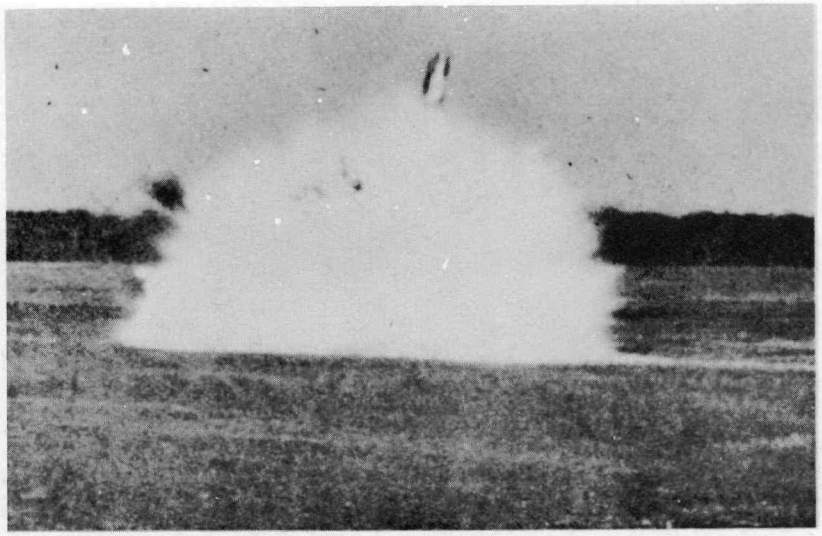

t = 0.00

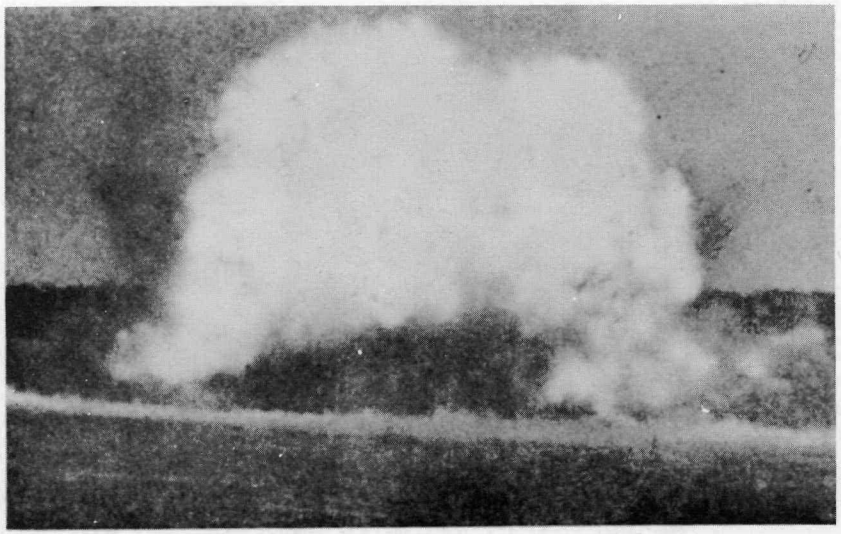

t = 0.10 second

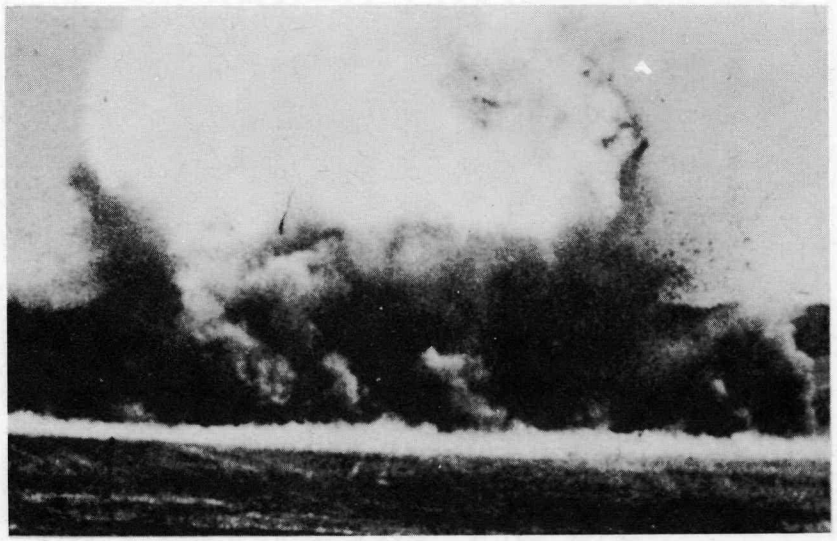

t = 0.71 second

Fig. A-21. View of Blast Sequence--Mechanical Shock Test

As the fireball moved off the ground, a cloud of dust and white smoke issued from the blast area. This condition remained for approximately three minutes and prevented the cameras from recording specimen behavior in the blast. There were no indications on the film as to when or how the specimens left the test area.

Setup. After the debris cleared, the blast area was examined to determine all possible effects of the explosion. The area inspected was within a 3000-yard diameter circle. Field notes of this investigation revealed the following.

The wooden stand on which the charge was resting and the wooden crates in which the TNT was packed were completely obliterated. Not even a splinter of wood was found in the area inspected.

The two posts, which were located on a 24-foot diameter circle about the blast center, were sheared off at ground level. Post 1 was found approximately 2000 feet from and radially behind its original position. Post 2 was also found radially behind its original position at approximately the same distance as Post 1. This indicated, assuming equal strengths and weights in each post structure, that the shock front was of equal magnitude at these two points. Both posts were permanently deformed structurally as indicated in Fig. A-22. Both had holes punctured through them perpendicular to the shock front. These holes showed indications of being burned through the metal rather than being sheared. Therefore, it was assumed that the impinging projectile was at a temperature higher than the melting point of the steel tubing (2500° F).

The rigid specimen attaching hardware was sheared off the posts in three of the four setups. On Post 1, the attaching hardware for specimen Type 12, No. 2, remained on the post structure. All others were missing.

A crater, 26 feet in diameter and 6 feet deep, was formed at the blast site. Calculations indicate that approximately 144,000 pounds of earth were moved out of the crater. The steel plate on which the TNT charge was resting was found at the bottom of the crater. There was no indication of damage to the plate by the blast.

Test specimens. Of the specimens tested, four were recovered. Two were retained by the nylon ropes and were found in a 200-foot diameter circle about the blast center. The other two were recovered at distances of 1000 and 3000 feet from the blast site. Each was found directly behind the post on which it was originally attached. Table A-7 describes the assumed behavior of each of the specimens in the blast and the conditions of the tested specimens.

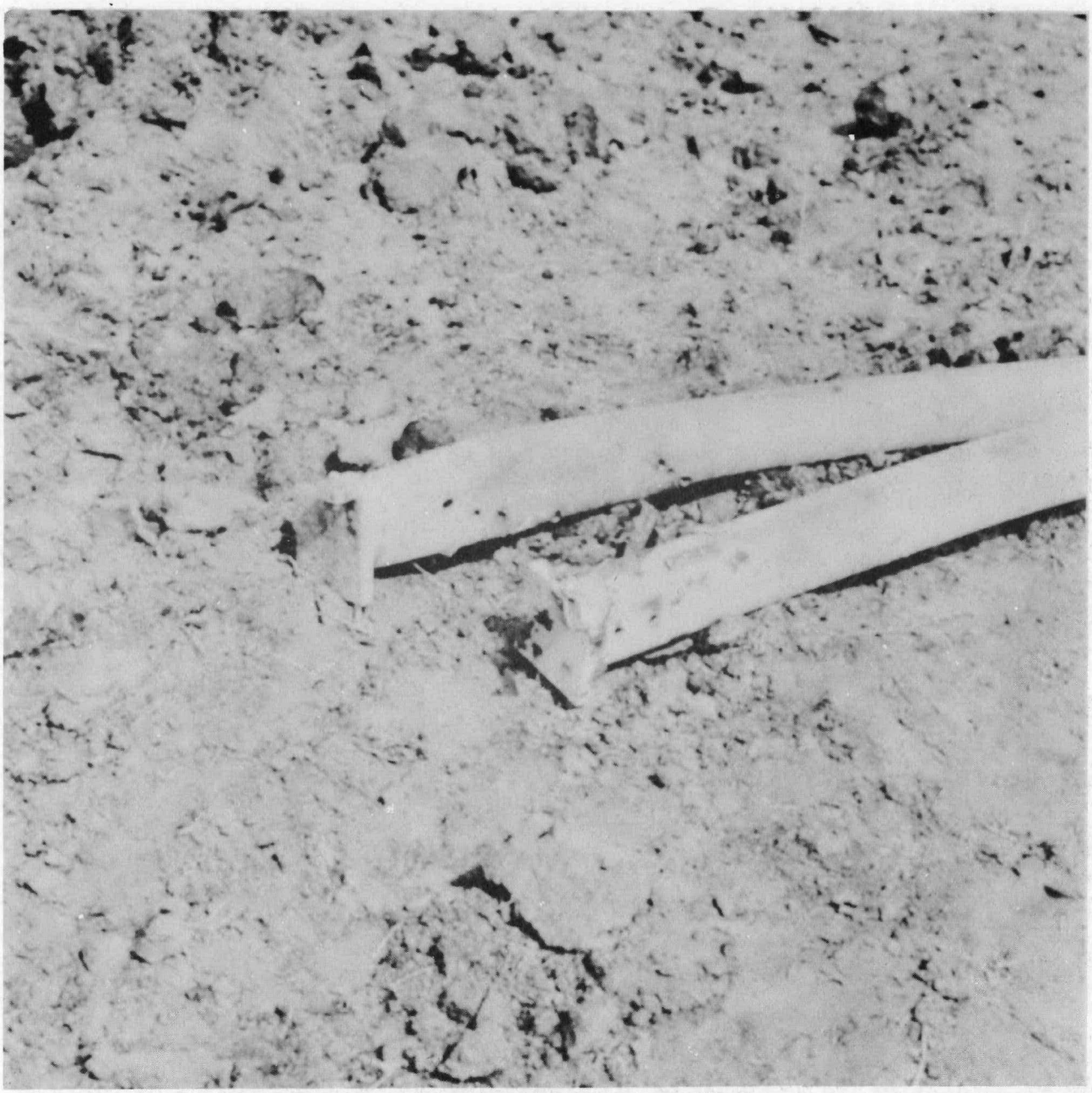

Fig. A-22. View of Post After Detonation

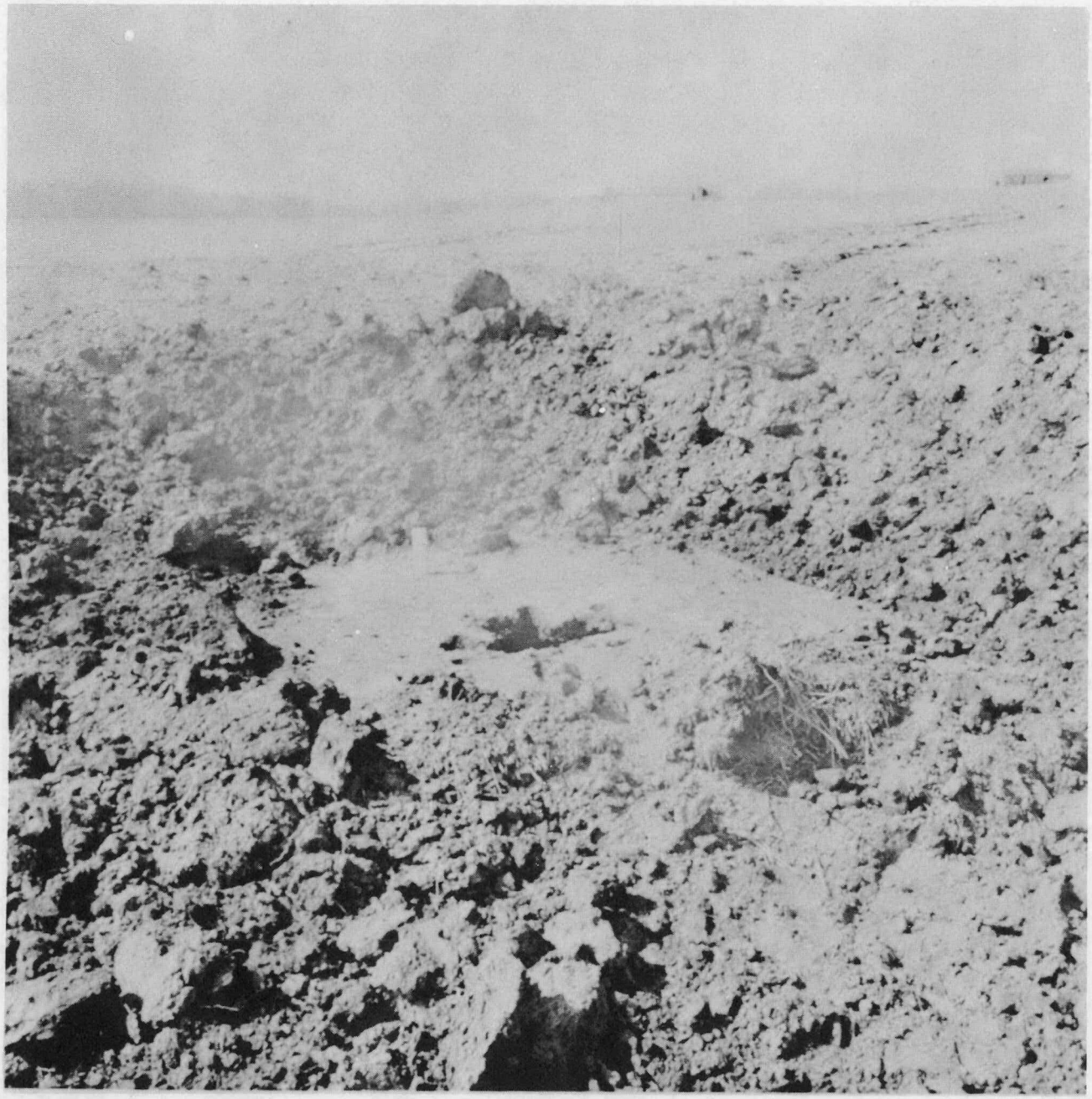

Fig. A-23. View of Ground Crater After Detonation

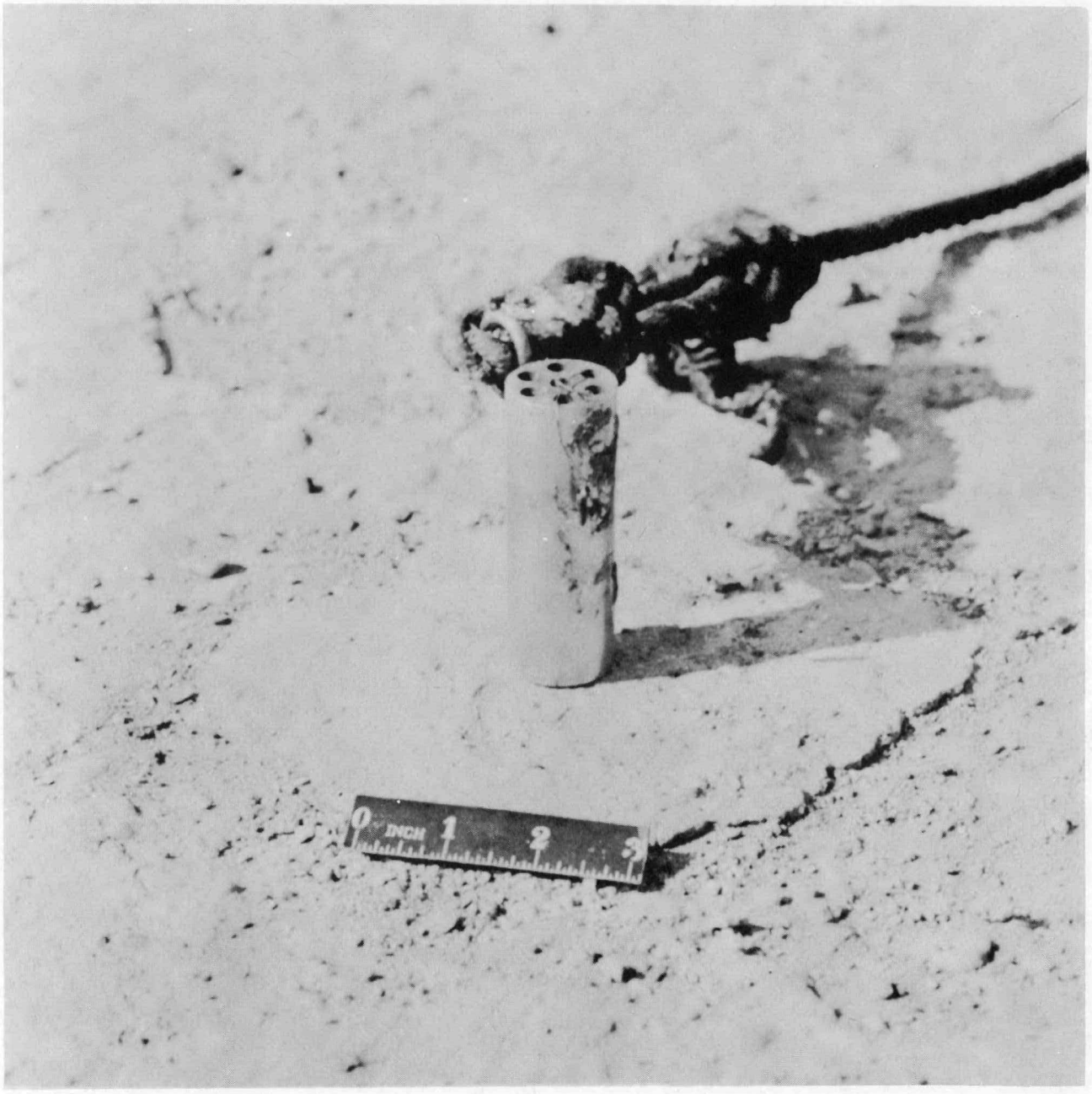

Fig. A-24. Tested Fuel Core--Type 1, Number 3, Design A-I, CeO_2

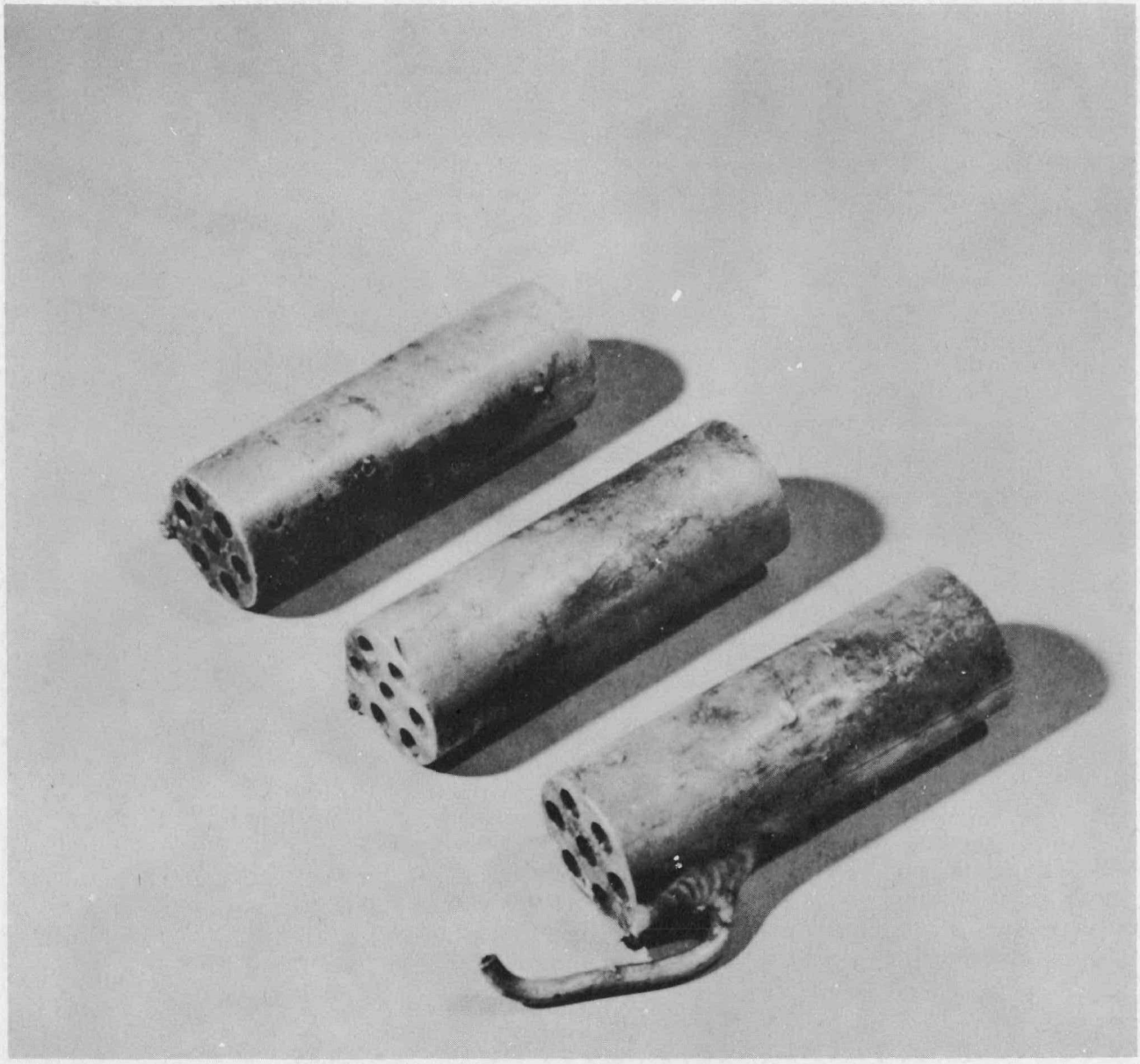

Fig. A-25. Tested Graded Strength Simulated Fuel Cores--Type 12, Numbers 1, 2 and 4

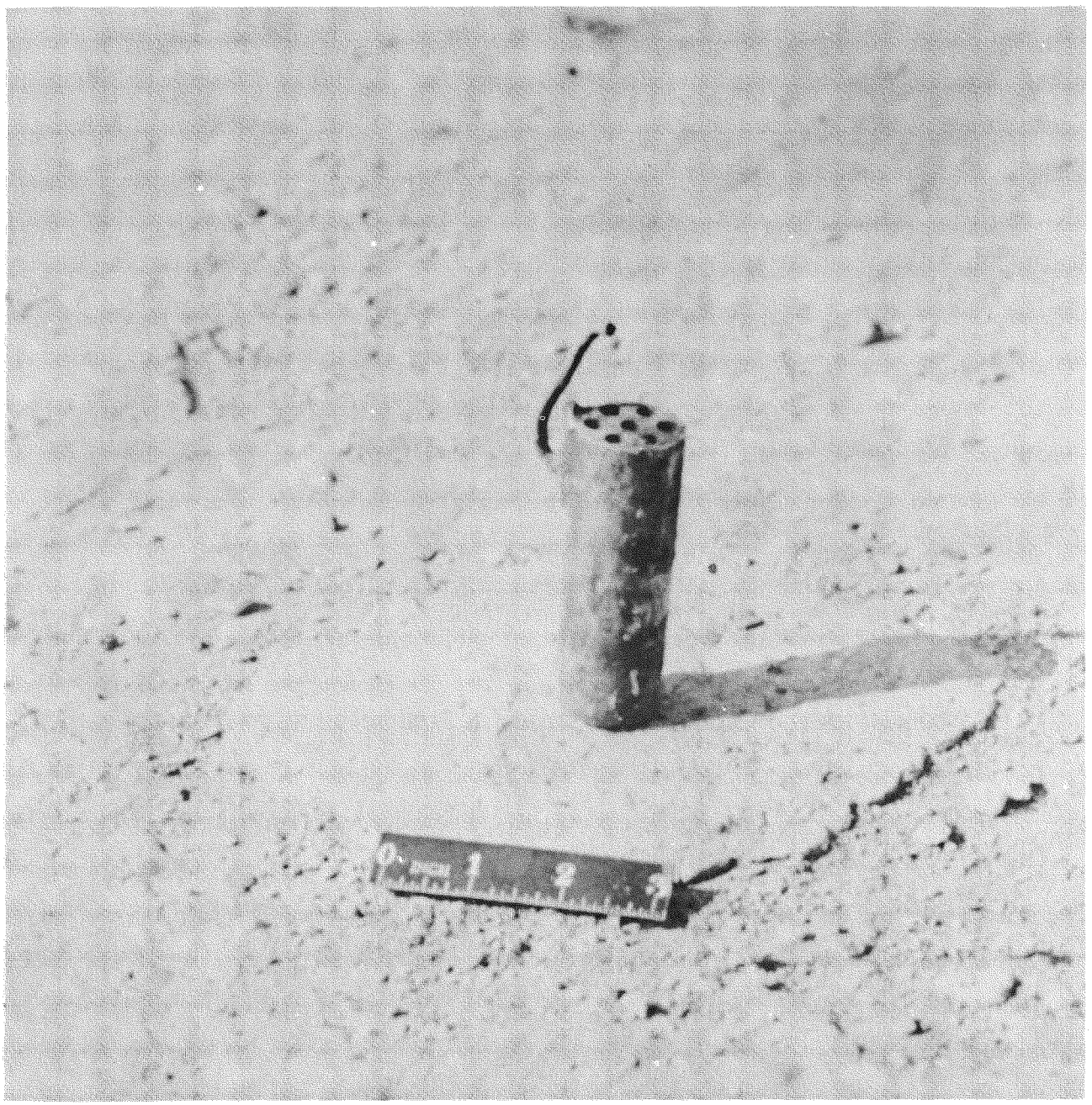

Fig. A-26. Tested Graded Strength Simulated Fuel Core--Type 12, Number 2

3. Fire and Fallout Tests

The test was conducted April 27, 1960 on "M" Field at the U.S. Army Chemical Center, Edgewood, Maryland. A thermal environment typical of a missile fire on a launch pad was generated to evaluate thermal integrity of Task 2 fuel capsules and one Task 2 generator system. Also, the environment was utilized as an energy source to release a cloud of cerium particles which were used to determine a fallout and air concentration profile.

Test site. The site utilized for this test is the same bomb test field described in the mechanical shock test. Figure A-27 shows an aerial view of this site.

Test environment setup. A test environment duplicating a missile fire and producing a contaminated atmosphere was generated by burning aniline, RP-1, mischmetal and magnesium metal in a simulated missile structure. Red fuming nitric oxide was used as the oxidizer and igniter, since it is hypergolic with aniline.

A 30-foot wooden tower supported the simulated missile structure. It was fabricated by bracing four creosote treated poles, 12 inches in diameter, with a wooden truss designed to support 25,000 pounds of metal. Scrap metal was contained in the tower by steel mesh wire. Horizontal dimensions of the tower were 11 feet square at the base and 6 feet square at the top. The entire structure was bolted to a 2-inch thick, 14-foot square steel plate. The tower is shown in Fig. A-28.

The fuels, scrap metal, mischmetal and test specimens were distributed throughout the tower from the bottom to the top and zoned as follows:

(1) 8500 pounds of RP-1 in a plastic tank.

(2) 4000 pounds of scrap steel.

(3) 2000 pounds of magnesium metal.

(4) 6000 pounds of aluminum sheet.

(5) 2000 pounds of magnesium metal.

(6) 2000 pounds of aluminum metal fittings.

(7) 4000 pounds of magnesium metal.

(8) Ten Task 2 test specimens supported by two wooden beams.

(9) Aluminum sheets over the specimen support beams.

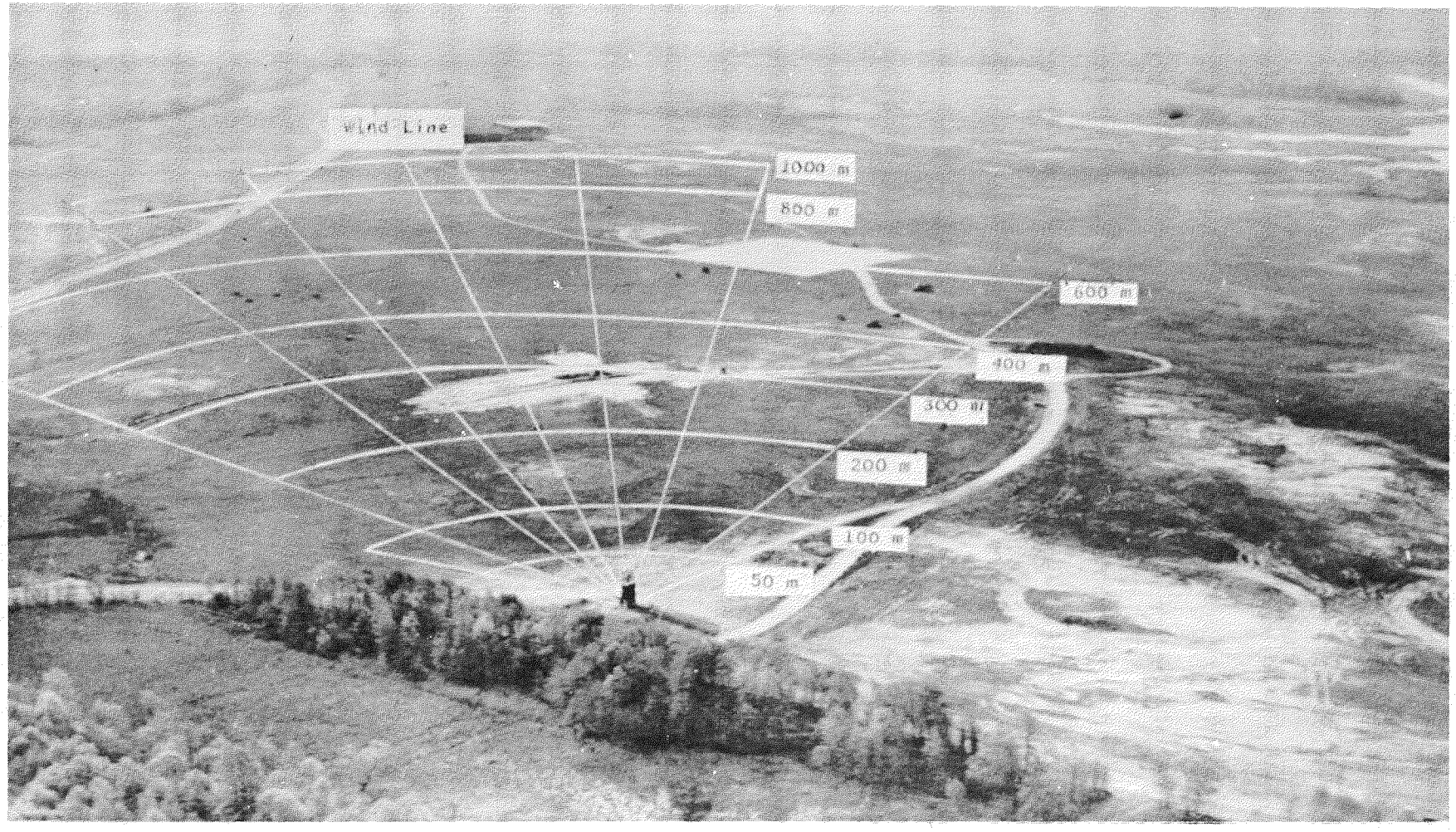

Fig. A-27. Aerial View of Fire and Fallout Test Setup

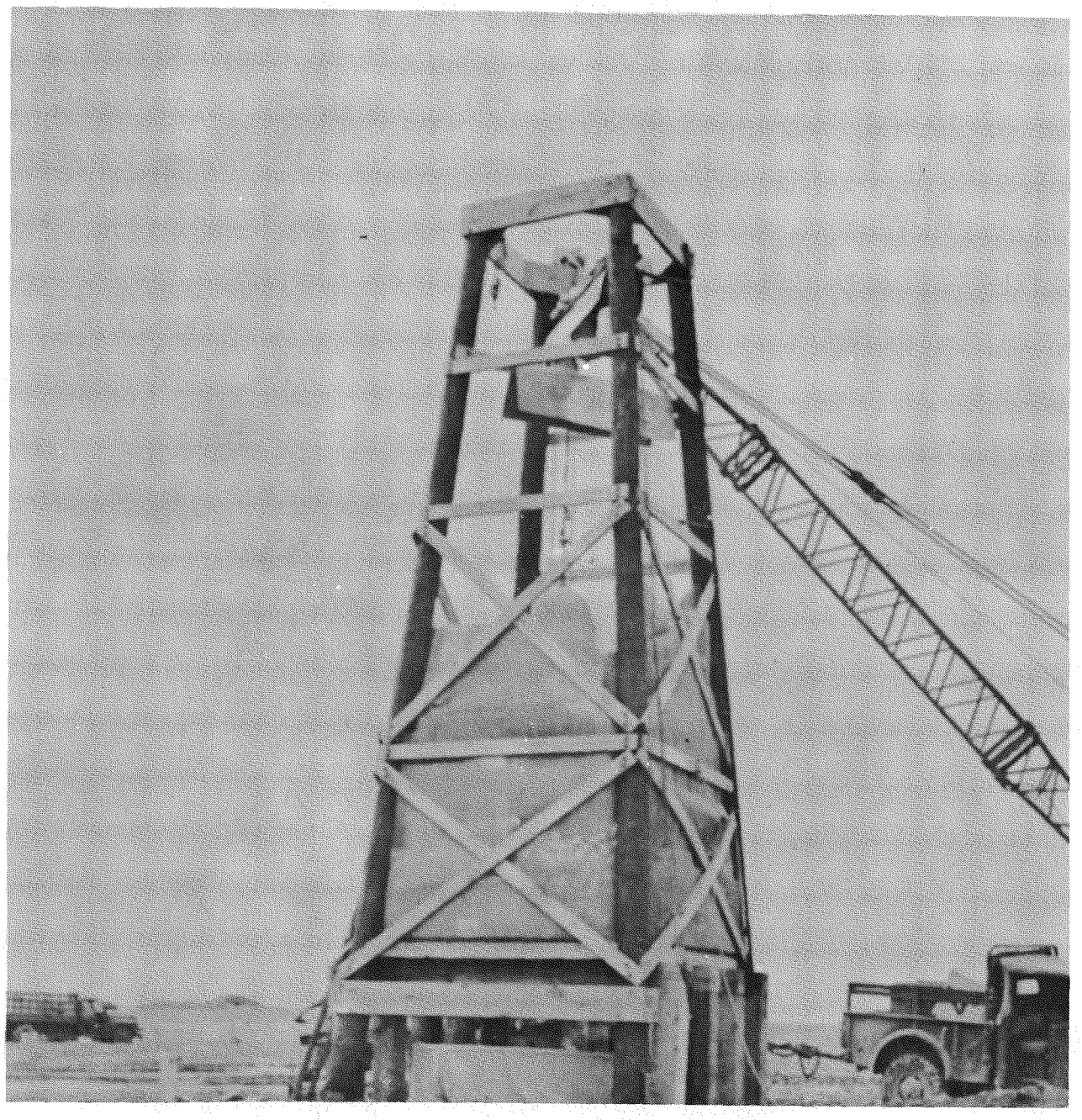

Fig. A-28. Fire Test Tower Showing The Position of Test Specimens and Metal Fuels

(10) 200 pounds of mischmetal in eight polyethylene bags.

(11) 3500 pounds of red fuming nitric acid contained in 13 aluminum drums.

(12) 1500 pounds of aniline in three steel drums.

Items (1) through (10) were within the limits of the tower, while the last two were positioned atop the tower on a portable steel and wooden pallet.

A semicircular retaining wall of earth 2 feet high was erected on the downhill side about 24 feet from the center of the tower to retain the fuel in the vicinity of the tower. This concentrated the heat of the burning fuels in the tower structure.

The aluminum metal sheets in the tower were positioned to permit maximum airflow through the tower structure, for calculations indicated that 196,000 pounds of air were required for the complete burning of the fuels and metals, not counting the aniline.

The test specimens were positioned on two wooden beams located diagonally across the tower's support legs at distances of 22 feet and 28 feet from the ground. The bottom beam was located in a northeast line, while the top beam was 90° to the bottom in a northwest direction. The specimens were supported by chain hoops rigidly fastened to the two beams. Specific positions of each specimen are listed in Table A-9.

The function of the aluminum sheets over the test specimens was to protect the specimens against direct contact with the burning fuels. This simulates the installation of the Task 2 generator in a missile structure.

The mischmetal was encapsulated in polyethylene containers to delay the release of the cerium cloud so that photographic recordings could distinguish between it and the propellant cloud. The propellant cloud should be dark yellow as compared to the cerium cloud which should be white to yellow in color. The mischmetal was in the form of 8-mesh granules. Its chemical composition was:

	(%)
Cerium	50
Rare earths	47.65
Magnesium	2.0
Iron	0.3
Silicon	0.025
Aluminum	0.02
Nickel	0.005

The nitric acid and aniline were secured to the pallet by 1/4-inch diameter steel cables and wooden blocking. Thirteen aluminum drums of nitric acid and one dummy drum were banded and blocked together on the pallet's floor panel about a central lift column. The aniline, in three steel drums, was placed on top of the nitric acid. These drums were wired to support braces which were welded to the lift column. Details and dimensions of the pallet were: (1) floor panel, 7.5-foot square by 1-inch thick steel plate, reinforced by steel angle iron and perforated to permit fuel flow to the tower structure and (2) central lift column, steel tube 6 inches in diameter by 10 feet long, welded to the floor and support structure.

Two shaped charges were installed on each of the drums. These were wired to an electrical firing circuit designed to detonate individual charges. Total explosive weight, including squibs, was 15 pounds. The function of this setup was to rupture the fuel drums so that the hypergolic fuels could mix and ignite the fire. Two charges on each drum were required to equalize forces on the drums, allowing them to remain in position on the pallet when the fuel was released.

Fallout field layout. Since the fallout collecting area was limited for the most part to a 60° wedge, meteorological studies were made of the test area to determine a field orientation which would effect maximum data. These studies indicated that the seasonal prevailing winds during this test program are from the northwest. Therefore, the fallout field was surveyed for a wind from this direction, in concurrence with the wedge described in the test development section of this report. Each of the eight arcs and the nine radii shown in Fig. A-1 were delineated with lime.

Instrumentation and equipment setup. Data recorded during this test included:

(1) Temperature measurements in tower.

(2) Air concentration measurements.

(3) Fallout measurements.

(4) Particle size measurements.

(5) Photographic coverage.

Temperature measurements were recorded in the tower to establish a temperature profile. Air concentration, fallout and particle size measurements were taken all over the field layout. Photographic coverage included the recording of specimen data in the fire, time measurements of cerium release, temperature measurements by color comparison and cloud measurements in the fallout field.

Tower temperature measurements. There were five thermocouples equally spaced in the vertical plane and approximately in the center of the tower in the horizontal plane. Figure A-29 shows a diagram of the approximate locations of these couples.

The first 18 inches of each couple were protected by heat resistant ceramic tubing. The tubing end opposite the junction was sealed into a 1-3/8-inch diameter steel pipe. This pipe terminated in a drum buried in the ground at the base of the tower. The drum served as a cold junction. The leads were continued, in a covered trench, to a recorder approximately 500 feet away. Wiring in the steel tubing was protected from the intense heat by water forced through the tubes under pressure. The water was supplied from a reservoir and the pressure from a 1500-psi air tank, both of which were buried in the ground near the tower. The couples were of chromel-alumel and platinum-platinum-10% rhenium types, located as indicated in Fig. A-29. Continuous temperature readings were recorded in millivolts on a Visicoder for 58 minutes.

Fallout measurements. Equipment setup to measure fallout data included fallout trays, high and low volume air samplers and cascade impactors. Throughout the field, there were 45 fallout trays, a cascade impactor, 12 high volume air samplers and 27 low volume samplers. Positions of these were as shown in Fig. A-30. In this figure, equipment is identified as follows:

(1)	Fallout trays	FT x
(2)	High volume air samplers	HA x
(3)	Low volume air samplers	LA x
(4)	Cascade impactors	CI x

Table A-11 gives detailed information from the samplers and impactors, and Table A-12 lists fallout tray data.

The fallout trays were positioned on 12 different radii of the field wedge. Since theoretical calculations indicated that somewhat higher concentrations should occur between 300 and 600 meters, fallout trays were positioned every 50 meters on the test wind-direction line in this area.

Air concentration and particle size measuring equipments were positioned on three of the radii in the wedge, 200, 400 and 800 meters. Power for this equipment was supplied by five 110-volt, single-phase gasoline generators. The first and second lines were operated remotely, and the third line manually.

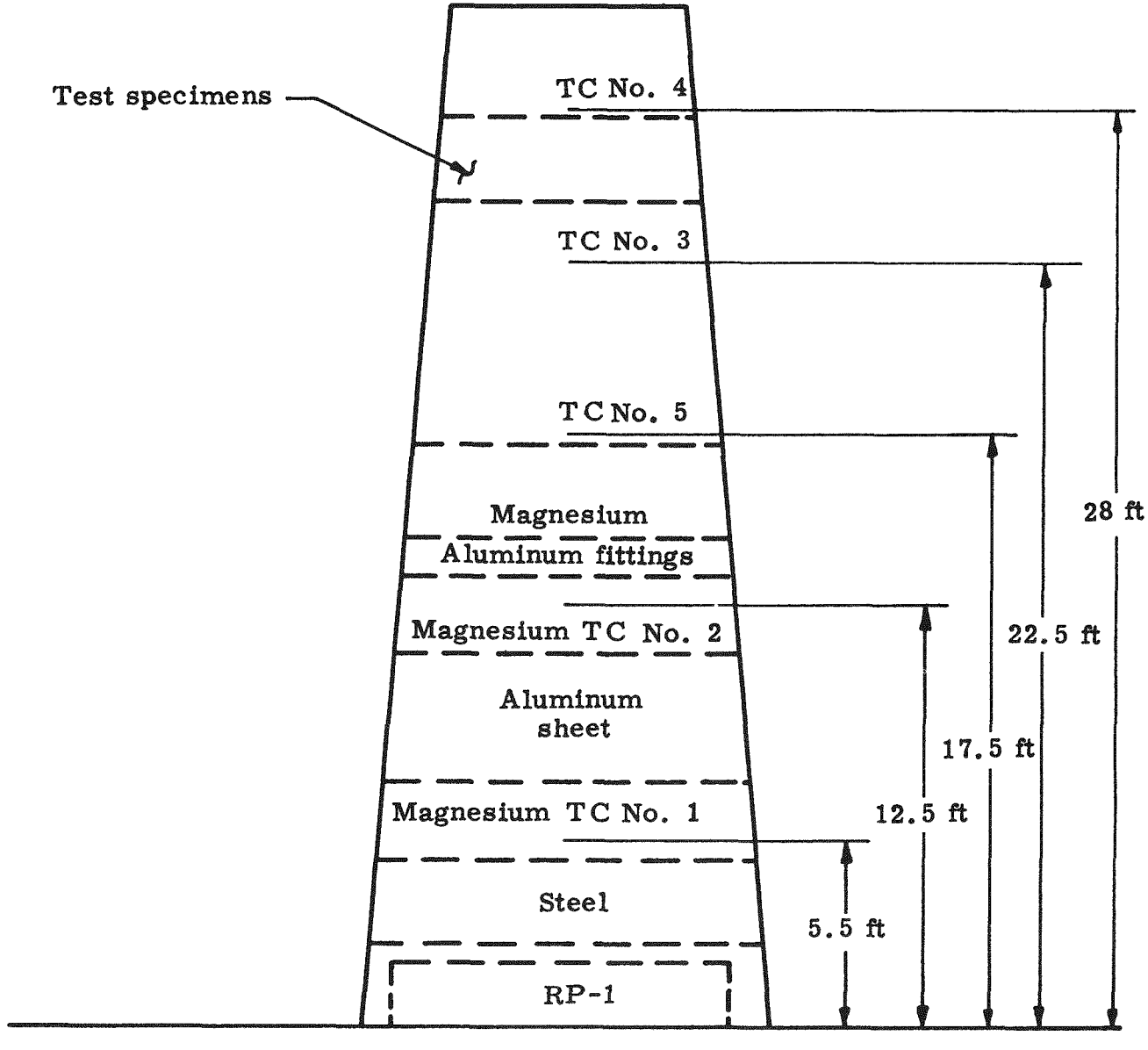

Fig. A-29. Fire and Fallout Test, Tower Temperature Instrumentation

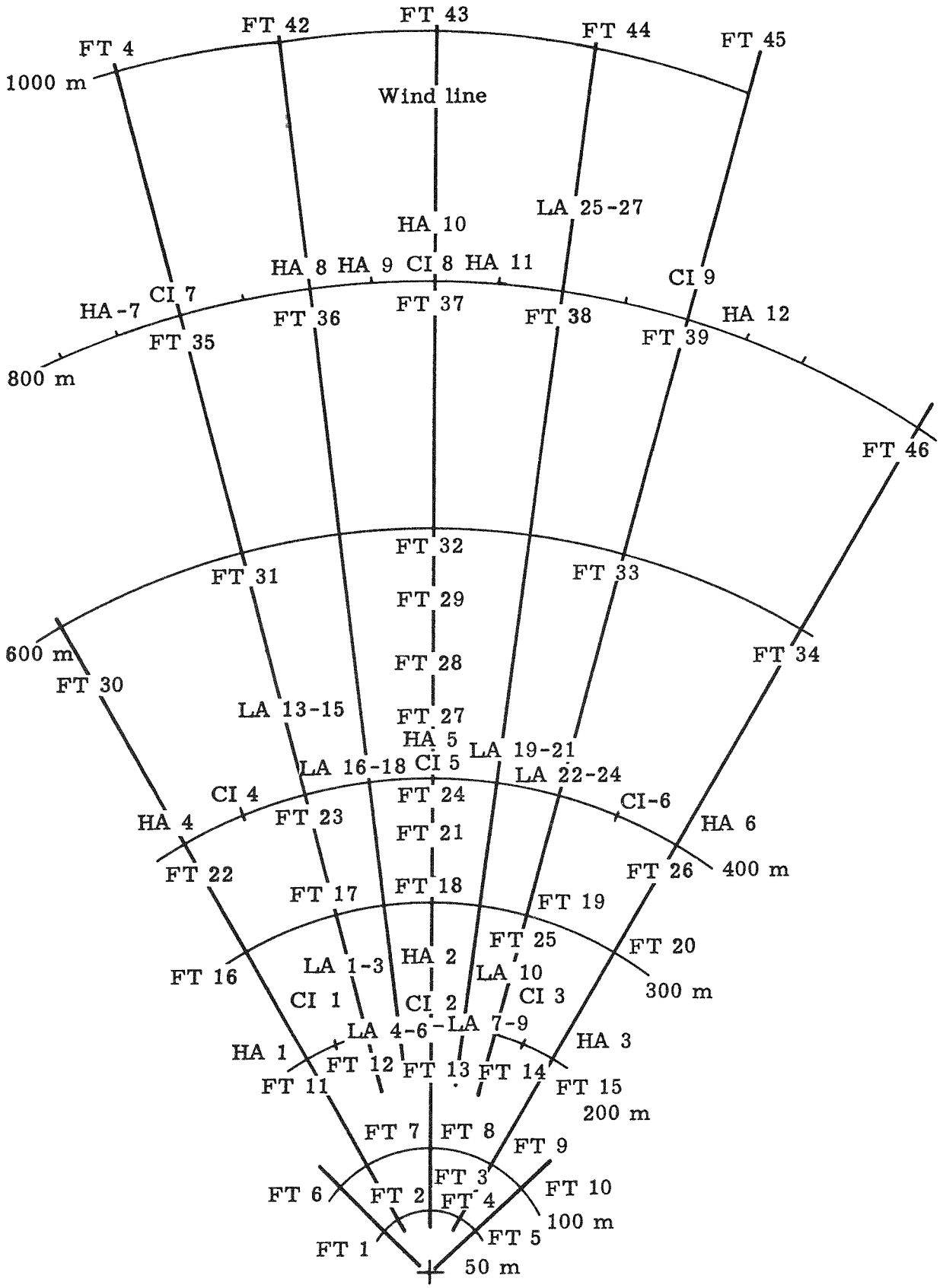

Fig. A-30. Detailed Fallout Field Layout, Fire and Fallout Test

Photographic coverage. Camera setup, film, film speed, location, function and other pertinent information utilized during this test are listed in Table A-8. There were 11 cameras strategically positioned to record data.

Test specimens. The configurations included two fuel cores and a full-scale generator structure. The latter was included to measure the magnitude of thermal shielding afforded by this structure to the core. Data for these specimens are given in Table A-1 (detailed specimen specifications), Table A-9 (detailed test data) and Table A-14 (test results).

Of the specimens, two were preheated to core operating temperatures indicated in Table A-9. This was accomplished by utilizing 220-volt electrical heaters encapsulated in the core structure. Power was supplied by a portable generator furnishing 220-volt, 60-cycle, single-phase service. Temperature was controlled by regulating voltage through a control panel wired between the specimens and the power source. Temperatures were measured by utilizing chromel-alumel thermocouples welded to the test specimen. Temperatures were manually recorded until 10 seconds before ignition. In order to maintain temperatures in the cores, each was insulated with 4 inches of Cerafelt material packed into a 12-inch diameter by 20-inch long steel drum.

4. Test Procedures

Prior to the test date, the following setup procedures were completed:

(1) Fallout field surveyed and staked out.

(2) Tower and fuel pallet constructed and erected on test site.

(3) Scrap metal placed in tower.

(4) Test specimens and mischmetal positioned in tower.

(5) Wiring for heating test specimens set up and checked out.

(6) Tower temperature instrumentation installed.

(7) Field wiring for air samplers installed and checked out.

(8) Camera positions and towers erected.

(9) Fallout field delineated with lime.

(10) Fuel retaining wall around tower erected.

(11) Two safety practice runs conducted on hypergolic fuel pallet.

On the test date, determined by meteorological conditions, a test countdown was initiated. This countdown began 2 hours prior to ignition. The following work was accomplished during this period:

Time: 0 minus 2 hours

(1) Air samplers positioned and tested.

(2) Cameras positioned and checked out.

(3) Hypergolic fuels moved into test area (on separate vehicles).

(4) Electrical heaters in test specimens energized.

Time: 0 minus 1 hour

(1) Fallout trays positioned in field.

(2) Local meteorological conditions checked and recorded.

(3) Radio silence established and maintained for the remainder of the test.

(4) Roadblocks in test area set up and maintained.

(5) Demolition charges installed to fuel containers, and firing wires extended to control center where they were shorted and grounded.

Time: 0 minus 20 minutes

(1) Area within 20 feet of the tower cleared of all personnel except operating crew.

(2) RP-1 fuel tank under tower filled.

Time: 0 minus 15 minutes

(1) Crane operator, wearing high temperature suit, positioned fuel pallet atop of tower.

Time: 0 minus 10 seconds

(1) Time indicated by green flare.

(2) Final specimen temperature readings recorded.

(3) Cameras started.

(4) Air samplers started.

(5) Instrumentation recorder turned on.

Time: 0--demolition (1404 hours, April 27, 1960)

(1) Explosive charges energized.

(2) Pertinent data recorded.

Time: 0 plus 30 minutes

(1) Fire extinguishing operation begun.

Time: 0 plus 58 minutes

(1) All equipment turned off.

5. Data Recording

Data collected during this test are given in figures and tables as indicated below:

(1)	Photographs of fireball	Figures A-31 through A-36
(2)	Specimen test data	Tables A-1, A-9 and A-14
(3)	Tower temperature measurements	Table A-10
(4)	Fallout field elevation profile	Figure A-37
(5)	Air sampler and cascade impactor measurements	Table A-11
(6)	Fallout tray measurements	Table A-12
(7)	Meteorological data	Table A-13, Figs. A-38 and A-39
(8)	Effect on specimens	Figures A-41 through A-44

TABLE A-8

Camera Setup--Fire and Fallout Test

Camera No.	Camera Type	Film Speed (fps)	Film Running Time (min)	Lens	Camera Location	Remarks
1	16 mm Cine.	24	Manual Control	1 inch 3 inch wide angle		General documentary of test setup, test and post-test including preparation and damage. Also general site scenes.
2	16 mm Mitchell	24	33	1 inch	1000 feet from fire tower on windward side	Fixed camera position with target pole 20 feet high, 2 x 2 foot target located 100 feet in front of camera. Positioned off center of subject tower to show cloud drift.
3	16 mm Bell and Howell	24	30 for tracking	6 inch	On 150-foot tower 3000 feet from fire tower, leeward side	Tracking camera, to record fire test, secondary ignition and cerium cloud
4	Hulcher camera with frame rate sequence	Intermittent	30	Tele-photo	On 150-foot tower as above	For complete coverage of test data collections of cloud movements and size
5	16 mm Bell and Howell	24	Manual control	6 inch	Test control center	To record any unforeseen events at the fire tower
6	16 mm Cine.	24	Manual control	Zoom lens	Test control center	General documentary of test. Target pole to be used to determine cloud rise and size.
7	16 mm Model K	2	33.3	1 inch	In marinite box on 20-foot tower 150 feet from fire tower	Field of view: 19.25 feet in horizontal and 14.42 feet in vertical planes. To record action of test specimens in fire.
8	16 mm Model	2	33.3	2 inch	In marinite box on 20-foot tower 100 feet from fire tower	Field of view, 19.25 ft. horizontal 14.42 feet invertical planes. To record action of test specimens in fire.
9	16 mm Cine.	24	6.12, ran intermittent-ly	1 inch	Same as No. 7	Same as No. 7
10	16 mm Cine.	24	6.12, ran inter-mittently	6 inch	Same as No. 8	Field of view: 6.33 feet in horizontal and 4.75 feet in vertical planes. To record action of test specimens in fire.
11	16 mm	1500	5 sec	Fastax	At control center	To record first 5 seconds of fire ball.

NOTE: All remotely operated cameras are started 10 seconds before start of test.

TABLE A-9

Summary of Specimen Test Data--Fire and Fallout Test

Specimen Type	Specimen Number	Position in Fire Tower	Preheat Temperature (° F)	Description of Action on Specimen During Test	Recovery of Specimen Position and Date
1	5	Upper layer, edge of tower, northwest from center.	1550	Exposed to excessive misch-metal burning. Fell into burning debris during first 10 minutes of fire.	Sifted from debris 5/4/60.
1	6	Upper layer, between specimens 4-4 and 3-4.	Ambient	Remained on tower structure, support partially fell after 20 minutes.	On tower structure, recovered 5/2/60.
1	7	Lower level, edge of tower, northeast from center.	Ambient	Remained on tower structure, support partially fell after 20 minutes.	On tower structure, recovered 5/2/60.
2	1	Upper layer, between specimens 4-4 and 1-5.	Ambient	Remained on tower structure, support partially fell after 20 minutes.	On tower structure, recovered 5/2/60
2	2	Lower level, between specimens 10-1 and 1-7.	Ambient	Remained on tower structure, support partially fell after 20 minutes.	On tower structure, recovered 5/2/60.
2	3	Lower level, between specimens 10-1 and 3-5.	Ambient	Fell into burning debris during first 15 minutes of fire.	Sifted from debris 5/4/60.
3	4	Upper layer, edge of tower, southeast from center.	1611	Remained on tower structure, support partially fell after 20 minutes.	On tower structure, recovered 5/2/60.
3	5	Lower level, edge of tower, south-west from center.	Ambient	Remained on tower structure, support partially fell after 20 minutes.	On tower structure, recovered 5/2/60.
10	1	Center of tower, 15 feet from ground.	1612	Fell into burning debris during first 10 minutes.	In front of tower, recovered 4/28/60.

TABLE A-10

Summary of Tower Temperature Data--Fire and Fallout Test

Time (sec)	Time (min)	Thermocouple No. 1	Thermocouple No. 3	Thermocouple No. 4	Thermocouple No. 5	Highest Temperature Film (° F)	Time (sec)	Time (min)	Thermocouple No. 1	Thermocouple No. 3	Thermocouple No. 4	Thermocouple No. 5	Highest Temperature Film (° F)
0		Ambient	Ambient	Ambient	Ambient	Ambient	420	7	1543	1628	1519	1472	3970
10		Ambient	Ambient	Ambient	Ambient	3600	450		1510	1565	1455	1375	3960
20		230	1757	1578	165	5000	480	8	1418	1502	1389	1278	3940
25		340	4200	1610	1670	5100	510		1370	1460	1550	1240	3920
30		450	1700	1649	2592	5000	540	9	1332	1413	1312	1205	3900
40		824	2464	1442	831	4720	570		1325	1404	1306	1195	3860
50		1045	1874	1229	736	4540	600	10	1319	1395	1300	1186	3800
60	1	1198	1779	1133	1288	4200	660	11	1259	1327	1238	1123	3750
70		1124	1413	917	704	4000	720	12	1191	1260	1182	1060	3700
80		1144	1121	701	514	3200	780	13	1121	1186	1124	977	3650
90		1140	860	1473	374	1720	840	14	1054	1112	1062	904	3600
100		1150	670	1596	301	1960	900	15	1028	1060	926	863	3550
110		1182	707	438	920	2160	960	16	958	1014	710	809	3500
120	2	1054	590	330	444	2300	1020	17	917	977	673	587	3500
130		1067	584	747	501	2440	1080	18	885	937	327	533	3480
140		1102	559	1920	552	2500	1140	19	853	916	312	514	3460
150		1108	415	1735	650	2800	1200	20	837	906	330	533	3460
160		1131	1284	1389	777	3040	1260	21	645	436	340	577	3480
170		1204	1812	1272	806	3160	1320	22	645	452	343	634	3500
180	3	706	989	485	872	3240	1380	23	645	492	340	546	3520
190		965	1204	494	920	3400	1440	24	623	476	309	492	3560
200		1428	1275	299	964	3540	1500	25	613	485	290	470	3560
210		1322	1091	593	495	3620	1560	26	597	476	290	428	3600
220		1565	1597	932	1110	3660	1620	27	581	476	290	428	3600
230		1460	1511	1025	1117	3720	1680	28	572	492	266	444	3650
240	4	1418	1398	1327	634	3760	1740	29	454	504	269	444	3700
270		1428	1521	1287	1015	3860	1800	30	460	492	269	482	3900
300	5	1514	1628	1445	1364	3920	1920	32	454	492	272	666	4000
330		1565	1653	1544	1475	3940	2160	36	470	507	278	634	3980
360	6	1572	1674	1550	1513	3960	2400	40	480	492	278	508	3800
390		1555	1645	1535	1490	3980	3480	58	150	169	161	419	--

Notes·

Thermocouple numbers 1 through 4--chromel-alumel

Thermocouple number 5--platinum-platinum +10% rhenium

Thermocouple number 2 was destroyed before test

Film temperatures were estimated by flame color comparison

Ambient temperature 67° F

TABLE A-11

Summary of Air Sampler Data--Fire and Fallout Test

Sampler No.	Distance from Tower (m)	Position Left or Right of Wind Line (deg)	Datum-Tower Elevation (ft)	Sampler Serial No.	Sampler Source	Measured Flow Rate (cc/min)	Operating Time (min)	Total Air Flow (cc x 10^5)	Cerium Deposit (μgm)	Magnesium Deposit (μgm)	Cerium Concentration (μgm/cc x 10^{-7})	Cerium Concentration (μc/cc)
HA-1	200	30-L	-2	1789	Maryland	1.3×10^6	58	655	<10	400	< 1.55	
LA-1	200	17-L	3	--	CWL	5000	58	2.9	--	22.7	--	
LA-2		15-L	3	--	CWL	7000	58	4.1	--	9.0	--	
LA-3		13-L	3	--	CWL	6000	58	3.48	< 2.5	--	< 72	
LA-4		9-L	4	--	CWL	6000	58	3.48	--	17.4	--	
LA-5		7.5-L	5.5	--	CWL	7000	58	4.1	< 2.5	--	< 61	
LA-6		6-L	6	--	CWL	6500	58	3.77	--	74.1	--	
HA-2		WL	8	3178	Maryland	1.5×10^6	58	870	<10	3,350	< 1.15	
LA-7		6-R	8	--	CWL	7500	58	4.35	--	47.0	--	
LA-8		7.5-R	8	--	CWL	7500	58	4.35	--	47.5	--	
LA-9		9-R	8	--	CWL	7500	58	4.35	--	64	--	
LA-10		13-R	8	--	CWL	5000	58	2.9	< 2.5	--	< 86	
LA-11		15-R	7.5	--	CWL	5000	58	2.9	--	118	--	
LA-12		17-R	8	--	CWL	5000	58	2.9	--	118	--	
HA-3	200	30-R	10	2	Baltimore City	1.27×10^6	58	737	20	28,000	2.72	5.25×10^{-12}
HA-4	400	30-L	0	1	Baltimore City	1.98×10^6	45	890	<10	50	< 1.13	
LA-13		17-L	4	--	CWL	5000	45	2.25	< 2.5	--	<111	
LA-14		15-L	4	--	CWL	5000	45	2.25	--	19.5	--	
LA-15		13-L	4	--	CWL	5000	45	2.25	--	38.6	--	
LA-16		9-L	9	--	CWL	5000	45	2.25	< 2.5	--	<111	
LA-17		7.5-L	9	--	CWL	5000	45	2.25	--	37	--	
LA-18		6-6	9	--	CWL	5000	45	2.25	--	34.2	--	
HA-5	400	WL	21	2-79	Taft	1.13×10^6	45	509	<10	5,300	< 1.96	

TABLE A-11 (continued)

Sampler No.	Distance from Tower (m)	Position Left or Right of Wind Line (deg)	Datum-Tower Elevation (ft)	Sampler Serial No.	Sampler Source	Measured Flow Rate (cc/min)	Operating Time (min)	Total Air Flow (cc x 10^5)	Cerium Deposit (μgm)	Magnesium Deposit (μgm)	Cerium Concentration (μgm/cc x 10^{-7})	Cerium Concentration (μc/cc)
LA-19	400	6-R	13	--	CWL	7000	45	3.15	< 2.5	--	< 79	
LA-20		7.5-R	13	--	CWL	6500	45	2.9	--	32.0	--	
LA-21		9-R	13	--	CWL	6000	45	2.7	--	9.2	--	
LA-22		13-R	14	--	CWL	5000	45	2.25	< 2.5	--	<111	
LA-23	400	15-R	14	--	CWL	5000	45	2.25	--	49.5	--	
LA-24	400	17-R	14	--	CWL	4500	45	2.03	--	106	--	
HA-6	400	30-R	30	3066	Taft	9.9×10^5	45	446	2.5	24,200	0.56	1.08×10^{-12}
HA-7	800	19-L	14	3067	Taft	9.9×10^5	53	525	<10	2,300	< 1.9	
HA-8		7.5-L	16	570	Taft	1.42×10^6	53	753	<10	1,250	< 1.33	
HA-9		4-L	18	3069	Taft	1.27×10^6	53	673	<10	1,760	< 1.48	
HA-10		WL	20	714	Taft	1.13×10^6	53	599	<10	400	< 1.67	
HA-11		4-R	17	--	APG	1.7×10^6	58	986	<10	4,950	< 1.04	
LA-25		6-R	13.5	--	CWL	7000	58	4.1	--	32.0	--	
LA-26		7.5-R	13	--	CWL	7500	58	4.35	--	19.5	--	
LA-27		9-R	12.5	--	CWL	7000	58	4.1	< 2.5	--	< 61	
HA-12	800	19-R	-3	ME 36910	Martin	9.9×10^5	58	574	<10	1,400	< 1.74	

TABLE A-12

Summary of Fallout Tray Data--Fire and Fallout Test

Tray No.	Distance from Tower (meters)	Location Left or Right of Wind Line (deg)	Cerium Deposit (micrograms)	Magnesium Deposit (micrograms)	Radiocerium Concentration (curies/ft^2)
1	50	45-L	<10	4,650	$<1.94 \times 10^{-4}$
2	50	30-L	50	11,500	9.7×10^{-4}
3	50	WL	580	11,480	1.1×10^{-2}
4	50	30-R	9,850	31,300	0.19
5	50	45-R	20,750	15,450	0.402
6	100	45-L	10	1,750	1.94×10^{-4}
7	100	30-L	<10	2,450	$<1.94 \times 10^{-4}$
8	100	WL	<10	3,640	$<1.94 \times 10^{-4}$
9	100	30-R	625	27,900	1.2×10^{-2}
10	100	45-R	4,400	28,000	8.54×10^{-2}
11	200	30-L	<10	2,250	$<1.94 \times 10^{-4}$
12	200	15-L	<10	960	$<1.94 \times 10^{-4}$
13	200	WL	Lost	6,680	--
14	200	15-R	<10	8,280	$<1.94 \times 10^{-4}$
15	200	30-R	4,050	16,850	7.85×10^{-2}
16	300	30-L	<10	50	$<1.94 \times 10^{-4}$
17	300	15-L	<10	8,800	$<1.94 \times 10^{-4}$
18	300	WL	10	6,040	1.94×10^{-4}
19	300	15-R	50	6,200	9.7×10^{-4}
20	300	30-R	<10	9,920	$<1.94 \times 10^{-4}$
21	350	WL	50	750	9.7×10^{-4}
22	400	30-L	<10	6,960	$<1.94 \times 10^{-4}$
23	400	15-L	<10	1,040	$<1.94 \times 10^{-4}$
24	400	WL	25	5,700	4.85×10^{-4}
25	400	15-R	50	6,100	1.94×10^{-4}
26	400	30-R	10	3,300	1.94×10^{-4}
27	450	WL	<10	1,400	$<1.94 \times 10^{-4}$
28	500	WL	<10	8,100	$<1.94 \times 10^{-4}$
29	550	WL	<10	4,080	$< 1.94 \times 10^{-4}$
30	600	30-L	75	6,850	1.45×10^{-3}
31	600	15-L	<10	3,400	$<1.94 \times 10^{-4}$
32	600	WL	<10	5,720	$<1.94 \times 10^{-4}$
33	600	15-R	<10	Lost	$<1.94 \times 10^{-4}$
34	600	30-R	<10	7,550	$<1.94 \times 10^{-4}$
35	800	15-L	365	5,780	7.1×10^{-3}
36	800	7.5-L	260	3,000	5.04×10^{-3}
37	800	WL	<10	1,600	$<1.94 \times 10^{-4}$
38	800	7.5-R	<10	6,360	$<1.94 \times 10^{-4}$
39	800	15-R	<10	6,480	$<1.94 \times 10^{-4}$
40	800	30-R	<10	6,480	$<1.94 \times 10^{-4}$
41	1000	15-L	<10	250	$<1.94 \times 10^{-4}$
42	1000	7.5-L	<10	11,040	$<1.94 \times 10^{-4}$
43	1000	WL	<10	--	$<1.94 \times 10^{-4}$
44	1000	7.5-R	<10	5,840	$<1.94 \times 10^{-4}$
45	1000	15-R	<10	--	$<1.94 \times 10^{-4}$

These data represent information recorded and observed with instruments and photographic equipment previously described. All cloud information and time intervals were recorded. Detailed analysis of this data is given in the test results.

6. Test Results

Test results are summarized in Tables A-9 through A-14. A detailed results analysis of the fireball, specimens, tower temperature, fallout cloud, fallout field, air concentration, fallout, meteorological data and setup are presented below.

Fireball. The hypergolic fuels were ignited at time 14 04 hours. Two mushroom fireballs, each approximately 150 feet in diameter, developed in the following manner. At ignition, the original fireball was 50 feet in diameter and 30 feet off of the ground, as seen in Fig. A-31. One second after ignition, the fireball proceeded to expand in all directions. At this time, the ball was approximately 90 feet in diameter, with its lower surface 12 feet above the ground. The upper extremity was 72 feet from the ground. A color comparison temperature reading indicated temperatures as high as 5000° F. Figure A-32 shows the fireball 1 second after ignition. At 2 seconds after ignition, the fireball rose to an altitude of 140 feet. Its diameter was about 100 feet, and it ejected a white cloud downward over an area of approximately 8000 square feet (see Fig. A-33). At 3 seconds after ignition, the original fireball reached its maximum diameter of 120 feet. At this point, it rose to an altitude of 200 feet, and the downward cloud was over an area of 12,000 square feet, as shown in Fig. A-34. The second fireball developed 5 seconds after ignition. As the first began to disperse into a dark yellow to black cloud at an altitude of 250 feet, the second fireball exploded about 30 feet and encompassed the entire tower. Temperatures were as high as 5500° F (see Fig. A-35). At 8 seconds after ignition, both fireballs were completely dissipated into a dark yellow to black cloud. This cloud proceeded downwind from an altitude of approximately 200 feet (see Fig. A-36).

Specimens. The positions of each specimen before, during and after the test are given in Table A-9. Conditions of the specimens are summarized in Table A-14. All specimens were recovered. Two of these were found on the tower structure and recovered when the tower was dismantled on May 2, 1960. One was found in the debris on May 4, 1960. The generator specimen was recovered April 28, 1960 on the ground.

Tower temperatures. Temperature recordings as a function of time are given in Table A-10.

Fallout cloud. During the test, the wind was shifting from north to northwest. An estimate of its average direction was 25° off the planned northwest. Therefore, the fallout cloud moved downwind 25° off the desired direction throughout most of the test.

Table A-13

Summary of Metorological Data-Fire and Fallout Test

Time (hr:min)	Altitude (ft)	Wind Direction (deg)	Wind Velocity (mph)	Temperature (°F)	Relative Density
12:14	0	335	12.0	71.6	0.985
12:15	1,110	342	13.0	63.2	0.997
12:16	2,250	327	14.8	58.3	1.002
12:17	3,390	325	16.5	54	1.006
12:18	4,545	322	16.4	50	1.007
12:19	5,775	306	13.4	46	1.011
12:20	6,630	283	16.5	44.5	1.010
12:21	8,070	272	21.4	39	1.014
12:22	9,240	257	23.7	36	1.012
12:23	10,470	253	31.3	33	1.011
13:15	0	330	5.0	71.1	0.986
13:16	1,140	338	15.9	64	0.997
13:17	2,160	333	16.9	57.3	1.004
13:18	3,210	322	17.5	54	1.008
13:19	4,260	313	18.3	51	1.007
13:20	5,430	307	15.0	49	1.008
13:21	6,645	287	12.5	45	1.008
13:22	7,830	278	13.9	41	1.011
13:23	8,940	274	16.6	36	1.015
13:24	10,155	290	22.4	34	1.010
14:16	0	330	10 to 16	66.2	0.997
14:17	885	341	23	59.0	1.008
14:18	1,800	337	17.9	56.0	1.008
14:19	2,700	324	9.7	55	1.007
14:20	3,705	301	9.8	53.5	1.004
14:21	4,680	298	14.6	51	1.007
14:22	5,625	301	14.7	48	1.007
14:23	6,615	308	15.3	44	1.011
14:24	7,590	307	15.6	39	1.013
14:25	8,625	290	11.0	37	1.015
14:26	9,660	245	14.2	33	1.015
14:27	10,680	237	26.8	33	1.011

Fire ignition time--14:04

Surface Data (ignition time)

Sky--overcast Temperature--67° F Relative Humidity--78%

Wind Direction--320° Visibility--6 miles, haze S.L. Pressure--29.86

Relative Density--0.994 Wind Speed--5 mph, gusts to 16

TABLE A-14

Summary of Specimen Test Results--Fire and Fallout Test

Specimen Type	Specimen Number	Exposure Temperatures °F Maximum Fireball	Exposure Temperatures °F Maximum Burning Metals	Exposure Temperatures °F Average (30 min)	Exposure Temperature Time (sec) Fireball	Exposure Temperature Time (sec) Burning Metals	Description of Test Specimen and Test Analysis
1	5	5060	4000	2000	8	600	Specimen exposed to burning cerium metal which was placed in fire test fixture to facilitate fallout measurements. Resulting corrosion caused about 15% of simulated fuel to release from 3 of 7 fuel channels. Analysis of specimen indicated no damage by melting.*
1	6	5060	4000	1400	8	0	No damage. See Fig. A-41.
1	7	5060	4000	1400	8	0	No damage. See Fig. A-41.
316 S/S	--	5060	4000	1400	8	0	No damage. See Fig. A-41.
316 S/S	--	5060	4000	1400	8	0	No damage. See Fig. A-41.
316 S/S	--	5060	4000	2000	8	600	No damage. See Fig. A-41.
Hastelloy B	--	5060	4000	1400	8	0	No damage. See Fig. A-41.
Hastelloy B	--	5060	4000	1400	8	0	No damage. See Fig. A-41.
Hastelloy B	--	5060	4000	1400	8	0	No damage. See Fig. A-41.
10	1	5060	4000	2000	8	600	Approximately 20% of the aluminum shell was burned off. See Figs. A-42 and A-43. No damage to core. See Fig. A-44.

* This particular specimen was heavily damaged whereas the other Inconel X specimens were completely undamaged. Test films and visual observations showed that this specimen was (1) immersed in burning cerium metal (used for fallout measurements) for 10 minutes, (2) fell into burning magnesium and remained there for 20 minutes, and (3) remained in the debris for 8 days, during which time it was exposed to lime, a 5% solution of soda ash and 0.38 inches of rainfall. It was concluded that the combined agents, cerium metal, lime and soda ash provided this damage rather than nitric acid exposure alone. Cerium metal has been found to attack Inconel X in an accelerated manner. Therefore, this anomaly is to be disregarded for purposes of evaluation.

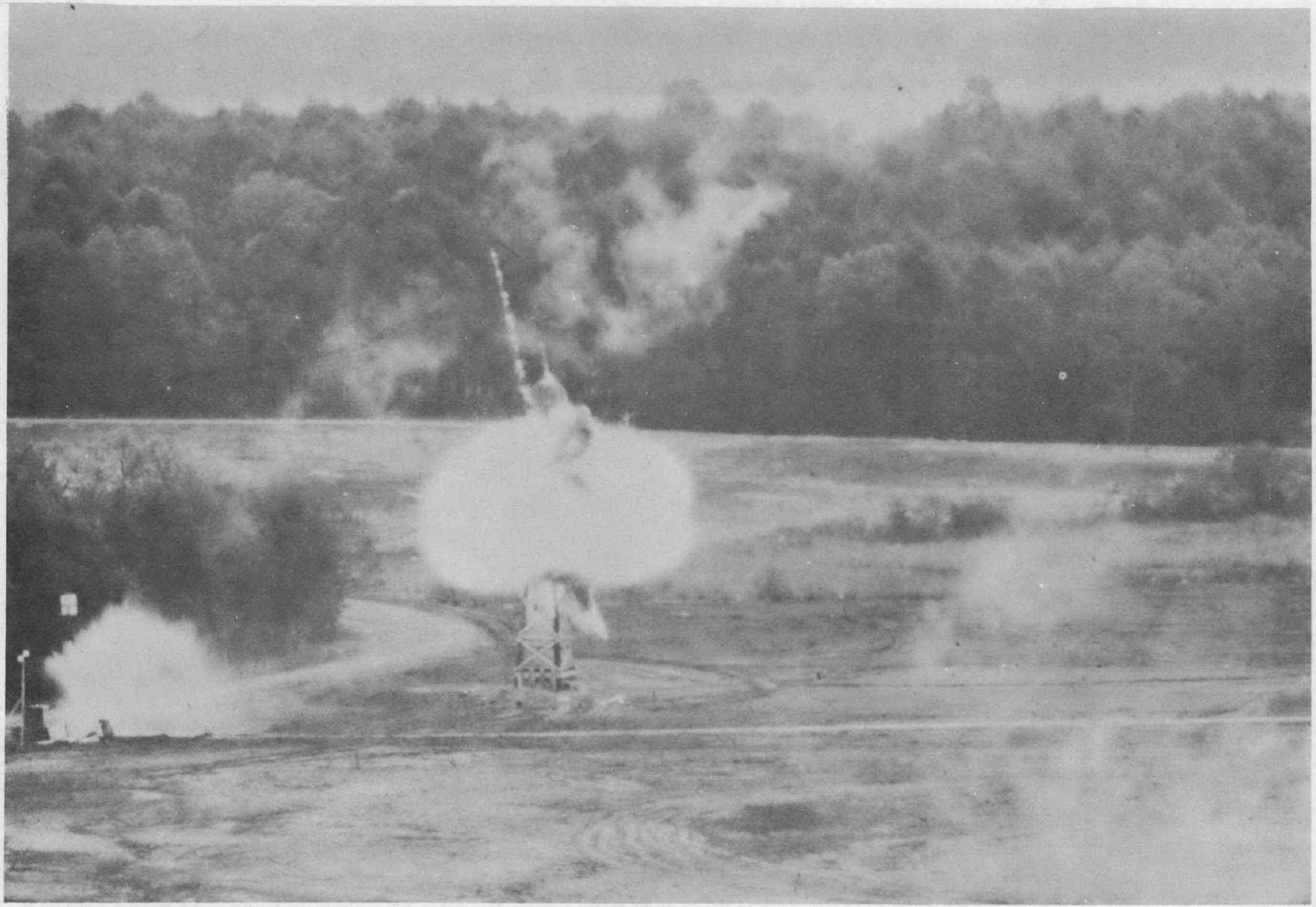

Fig. A-31. Fireball at Ignition

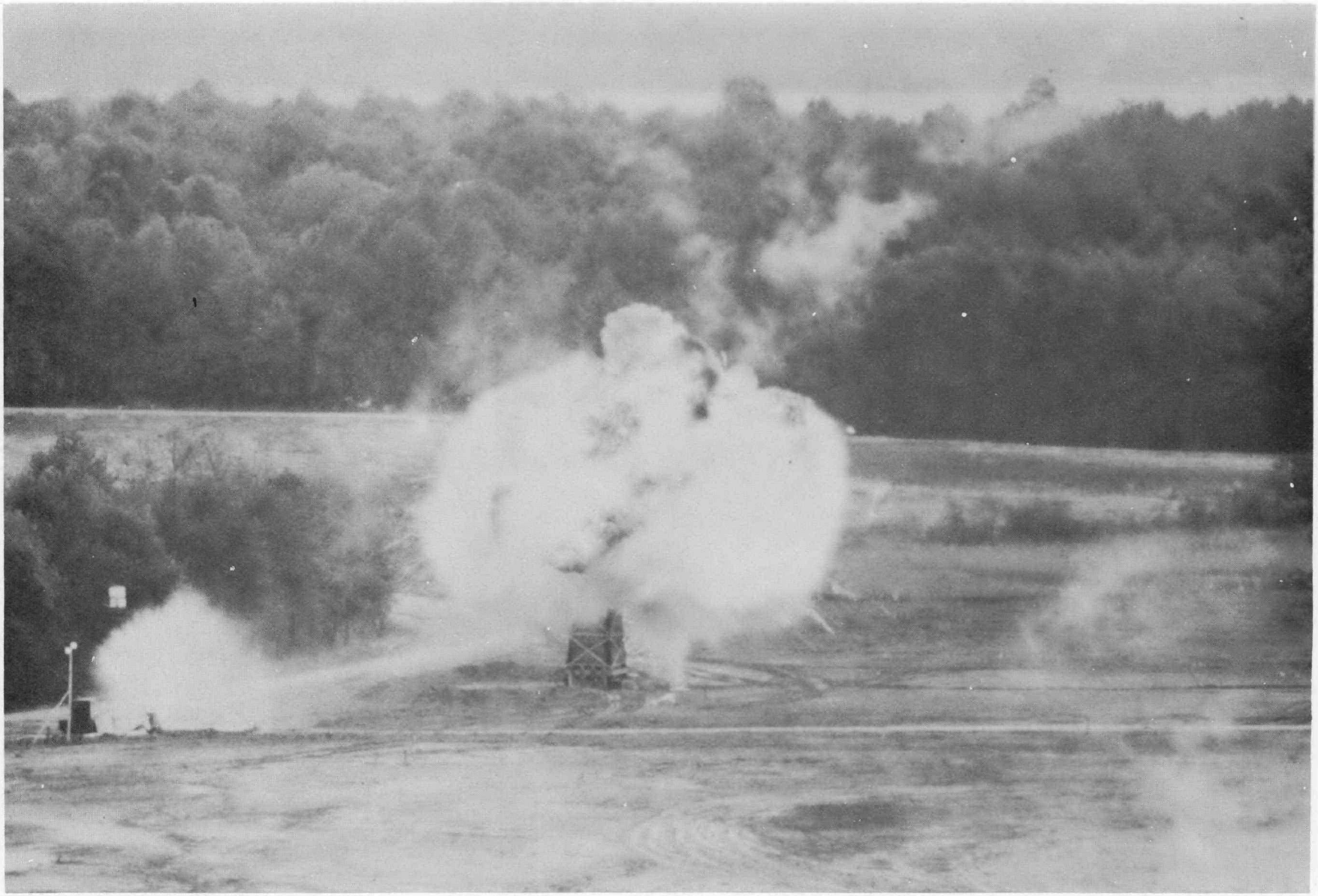

Fig. A-32. Fireball 1 Second After Ignition

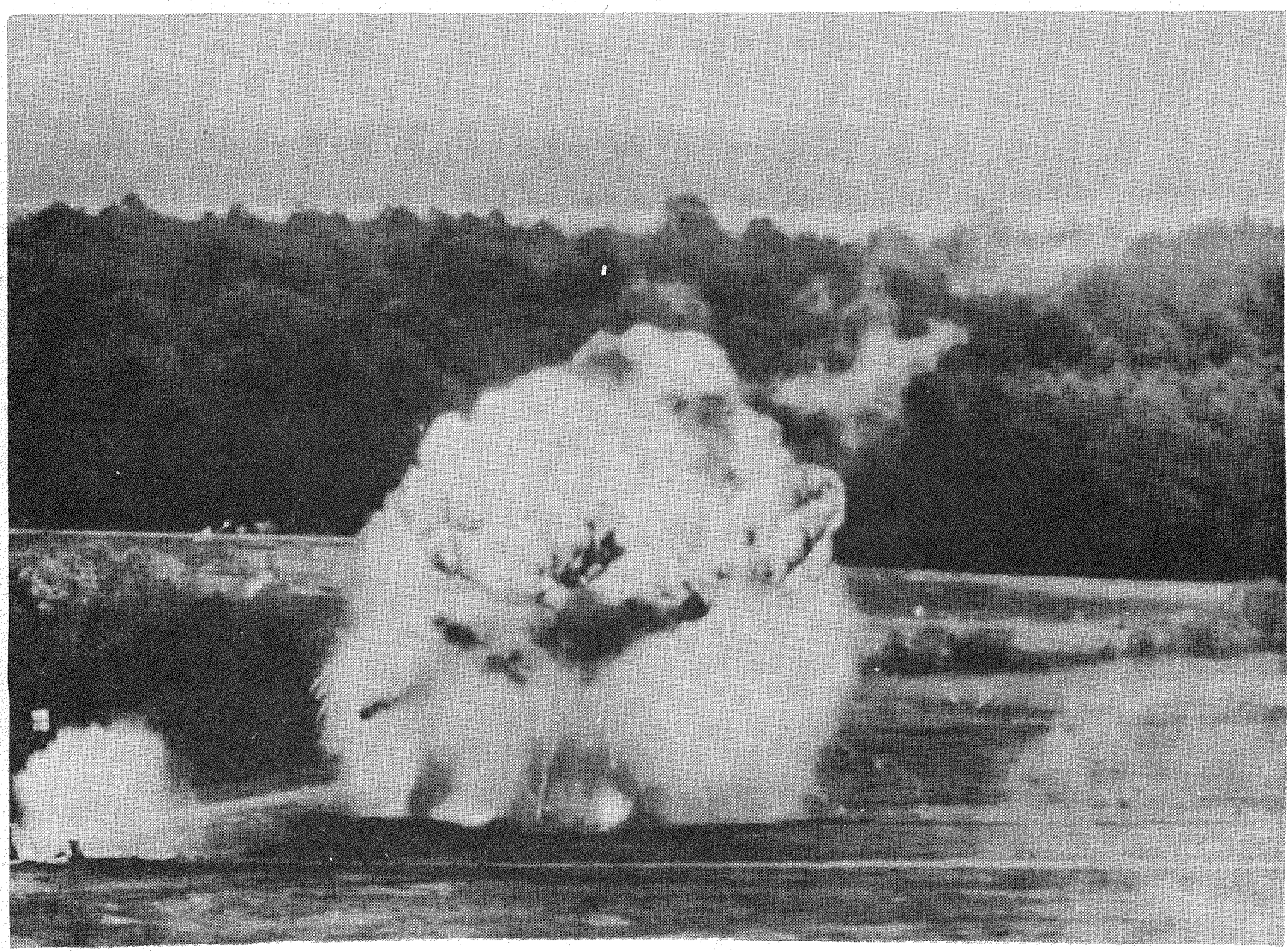

Fig. A-33. Fireball 2 Seconds After Ignition

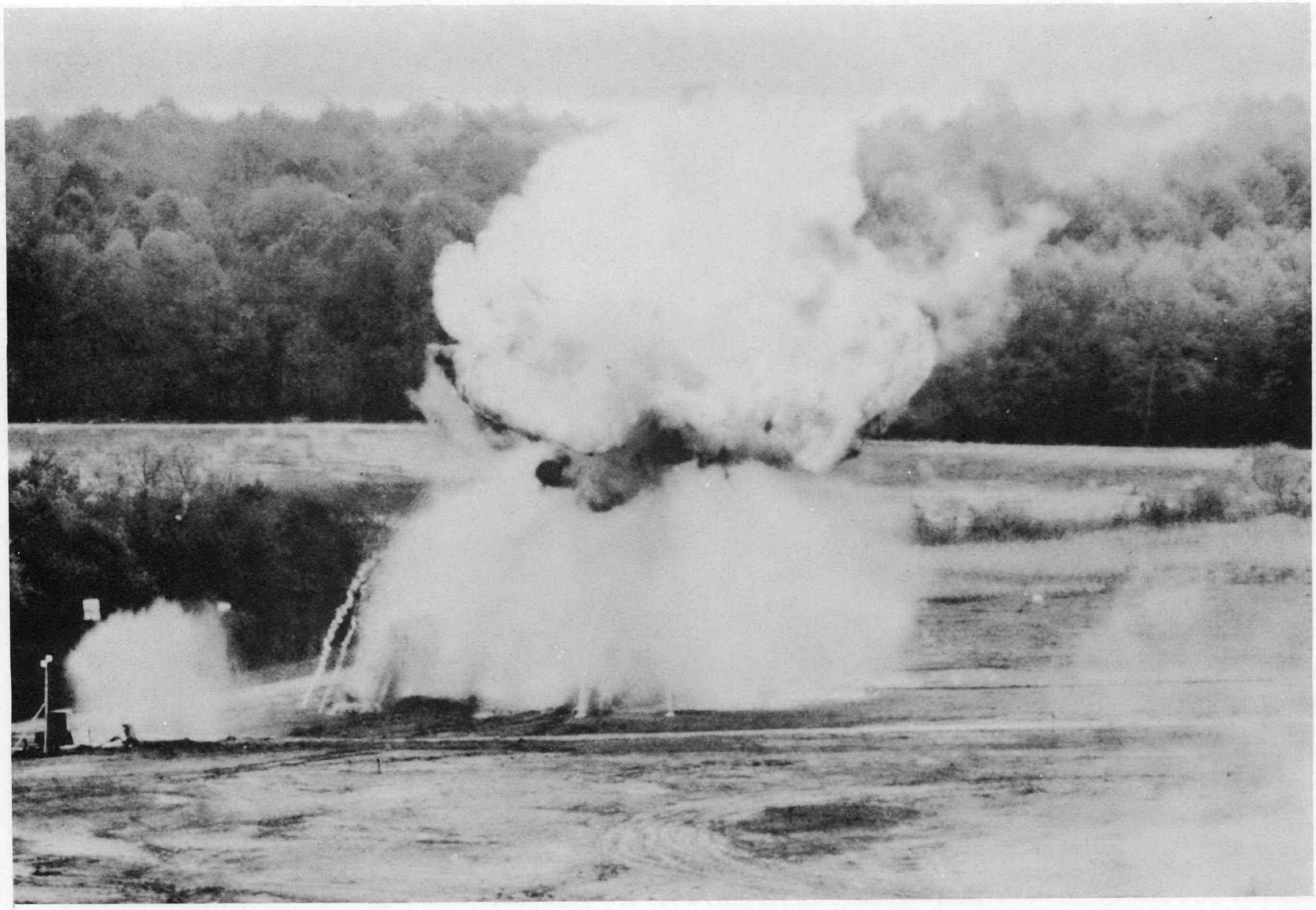

Fig. A-34. Fireball 3 Seconds After Ignition

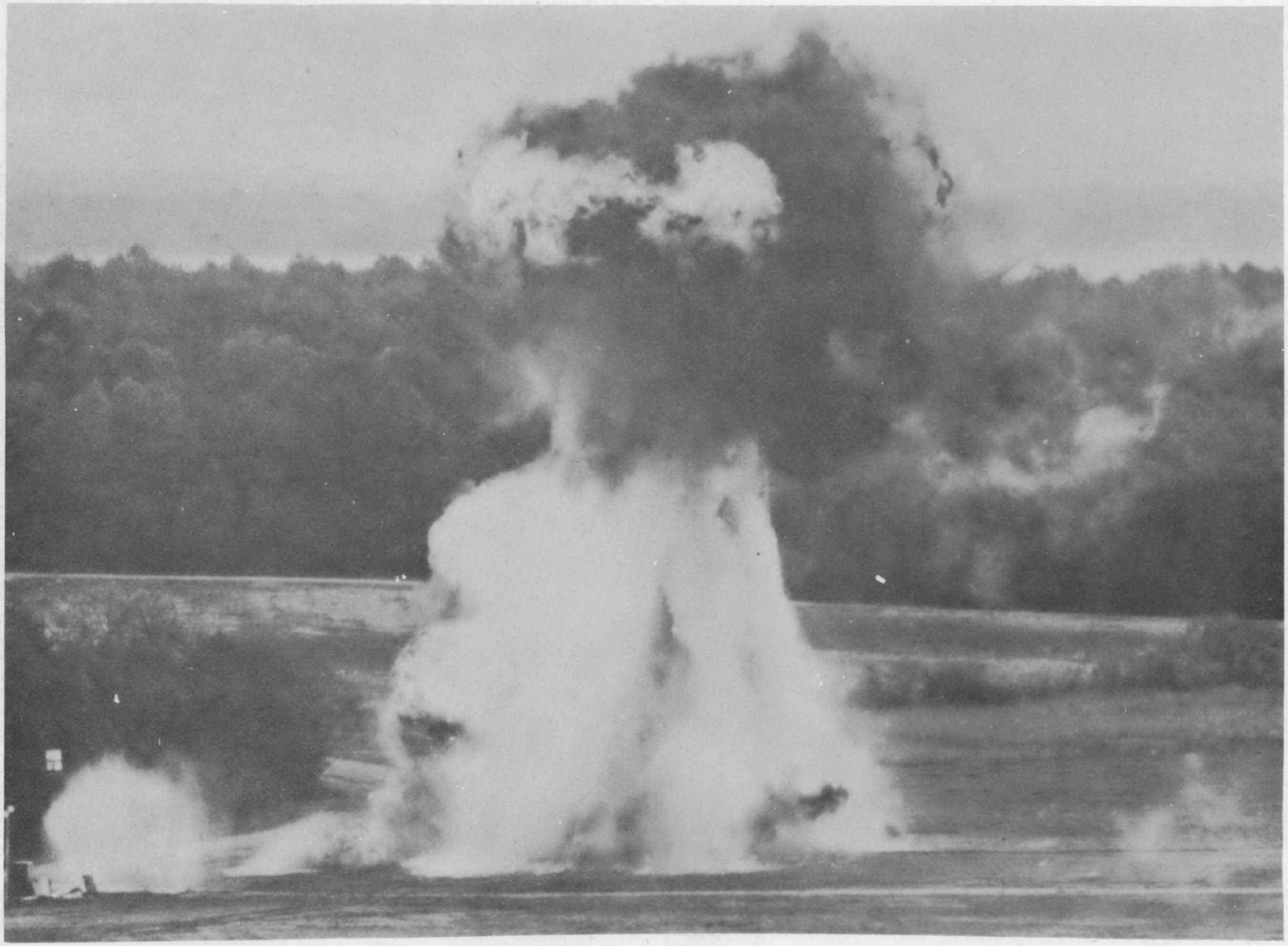

Fig. A-35. Development of Second Fireball 5-Seconds After Ignition

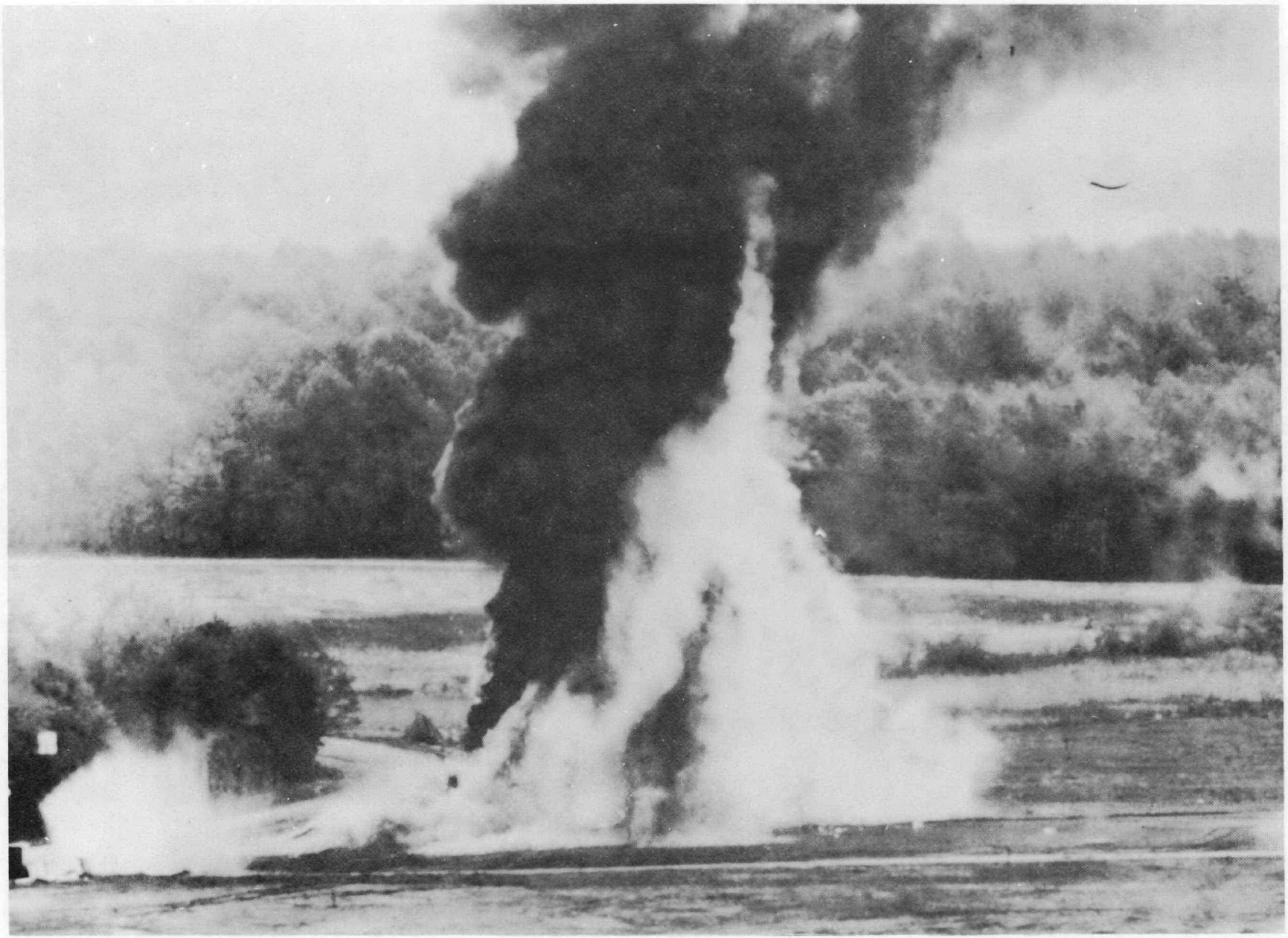

Fig. A-36. Dispersal of Fireball 8 Seconds After Ignition

Closeups of the tower recorded on film indicated that most of the cerium was burned during the first 78 seconds of the fire. Based on a wind speed of 10 miles per hour, the contaminate-bearing cloud passed over the last line of fallout-collecting instruments approximately 300 seconds after ignition of fire. However, since the winds were variable, the contaminated cloud could have remained in the area of the fallout field for a much greater time. In fact, the 400-meter line of air samplers recorded contamination in the cloud 13 minutes after ignition.

After the fireball dissipated, the cloud issuing from the tower developed into a plume which shifted in direction as indicated above. In the fallout field, the cloud never rose more than 200 feet from the ground. In fact, the lower surface of the plume was at ground level, between 400 and 800 meters, during most of the test.

Fallout field. Elevation profile of the fallout field is shown in Fig. A-37. Generally, the field was higher in elevation than the base of the tower. The fallout trays were located on the ground. Air samplers were positioned on platforms which were at least 3 feet from ground surface.

Air concentration data. The degree of contamination in the air as a function of distance away from the release is given in Table A-11. The sampling equipment at the 400-meter distance was inoperative during the first 13 minutes of the test. This condition resulted from a failure of the power generator. The condition was corrected as fast as possible; however, 13 minutes of sampling time were lost.

The cascade impactor collector slides were analyzed for cerium particles with a microscope. Since the operating time of the impactor could not be regulated due to the nature of the test, only an estimate was made of the percent of particle sizes collected. These were:

	(%)
(1) At the 200-meter distance:	
Particle size, 0 to 1 micron	0
Particle size, 1 to 5 microns	35
Particle size, 5 microns and larger	65
Maximum particle--70 microns.	
(2) At the 400-meter distance:	
Lost due to power failure.	

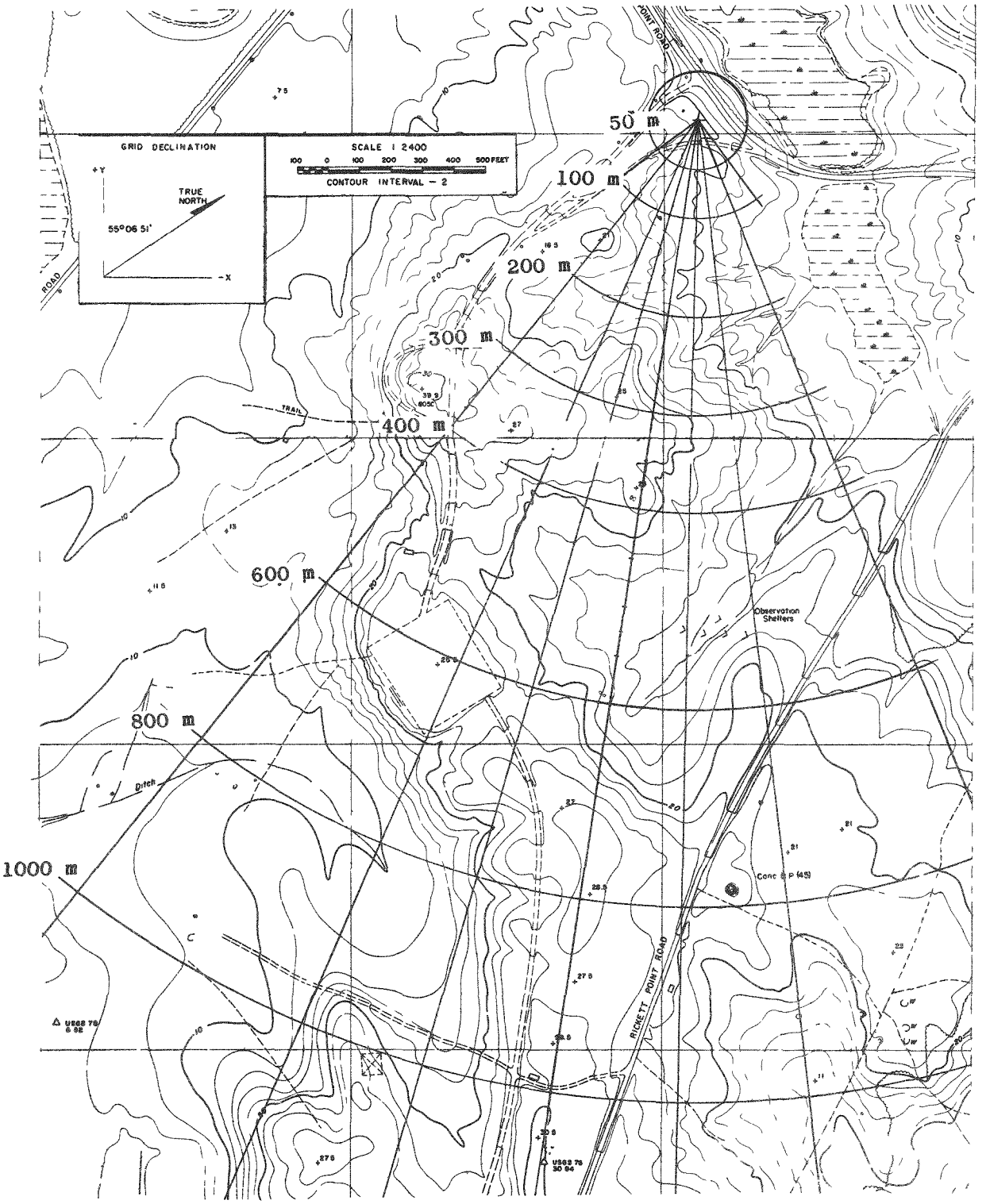

Fig. A-37. Elevation Profile of Fallout Field

	(%)
(3) At the 800-meter distance:	
Particle size, 0 to 1 micron	50
Particle size, 1 to 5 microns	35
Particle size, 5 microns and larger	15
Maximum particle--10 microns.	

Fallout data. Fallout data collected on the trays are summarized in Table A-12. Maximum fallout occurred at the 50-meter distance. It decreased greatly at the 300-meter distance, but increased somewhat at the 800-meter distance.

Meteorological data. A portable meteorological trailer was located 400 meters downwind from the test tower. The trailer contained instruments to measure and record the wind velocity and direction before, during and after the test. These data are shown in Figs. A-38 and A-39. The figures show data for the first 7 minutes of the test. Wind velocity varied between 10 and 16 miles per hour, and wind direction shifted from 360 to 310° measured from 360° true north.

Three balloon runs, to record wind direction, velocity, temperature and density at altitudes up to 10,000 feet, were made at the Meteorological Station at Aberdeen Proving Ground. These runs were made at 1214, 1315 and 1416 hours, and the recorded data are contained in Table A-13.

Setup. After the fire had burned for 30 minutes, the APG Fire Department pumped water on the test area until 1600 hours. At this time, the fire was nearly extinguished. The mass was still smoking, however, and there was definite evidence of nitric acid fumes. The tower was still standing (see Fig. A-40). Two days after the test, the debris was still hot and there was still evidence of nitric acid fumes. More water was pumped on and around the test area. Five bags (400 pounds) of lime were spread around the test area to neutralize the acid and decontaminate the area. During the next two days, the test area, including the specimens, was exposed to 0.38 inch of rain. On the fifth day after the test, 350 gallons of a 5% solution of soda ash were sprayed over the debris. On this day, the tower was dismantled and two specimens were recovered. The last specimen was recovered by sifting the debris on the seventh day, May 4, 1960.

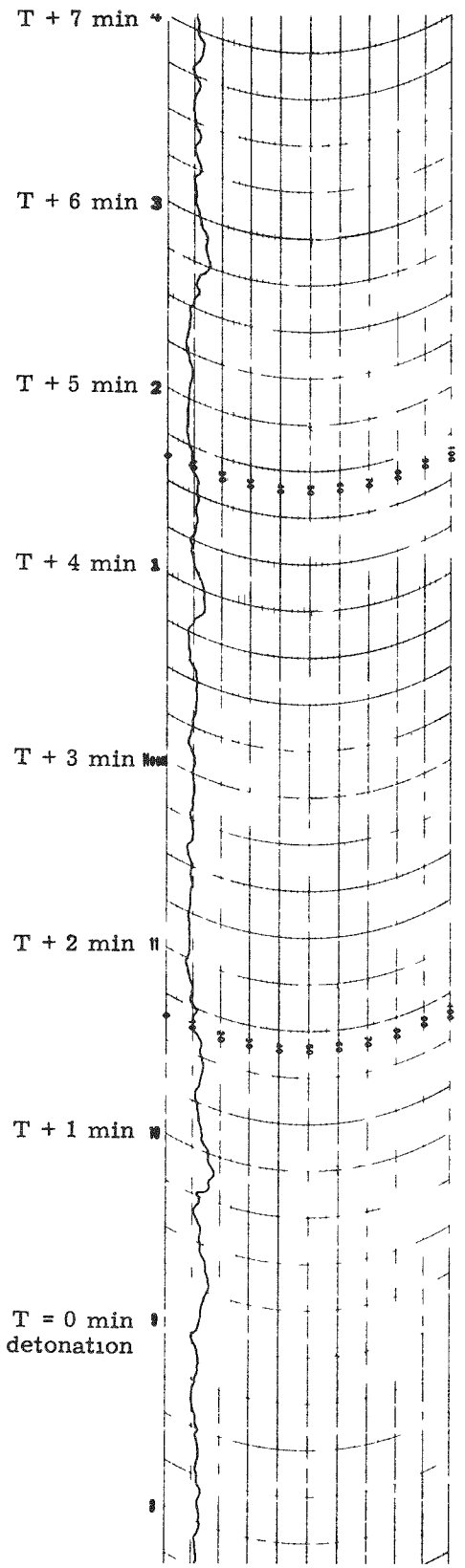

Fig. A-38. Wind Velocity as a Function of Time--Fire and Fallout Test

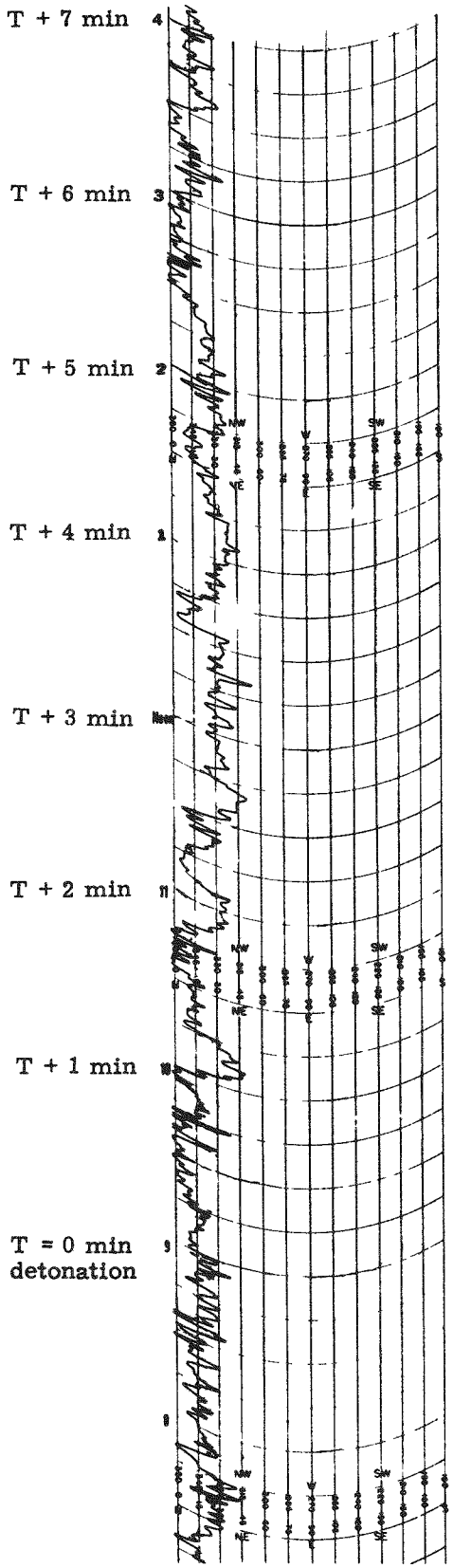

Fig. A-39. Wind Direction as a Function of Time--Fire and Fallout Test

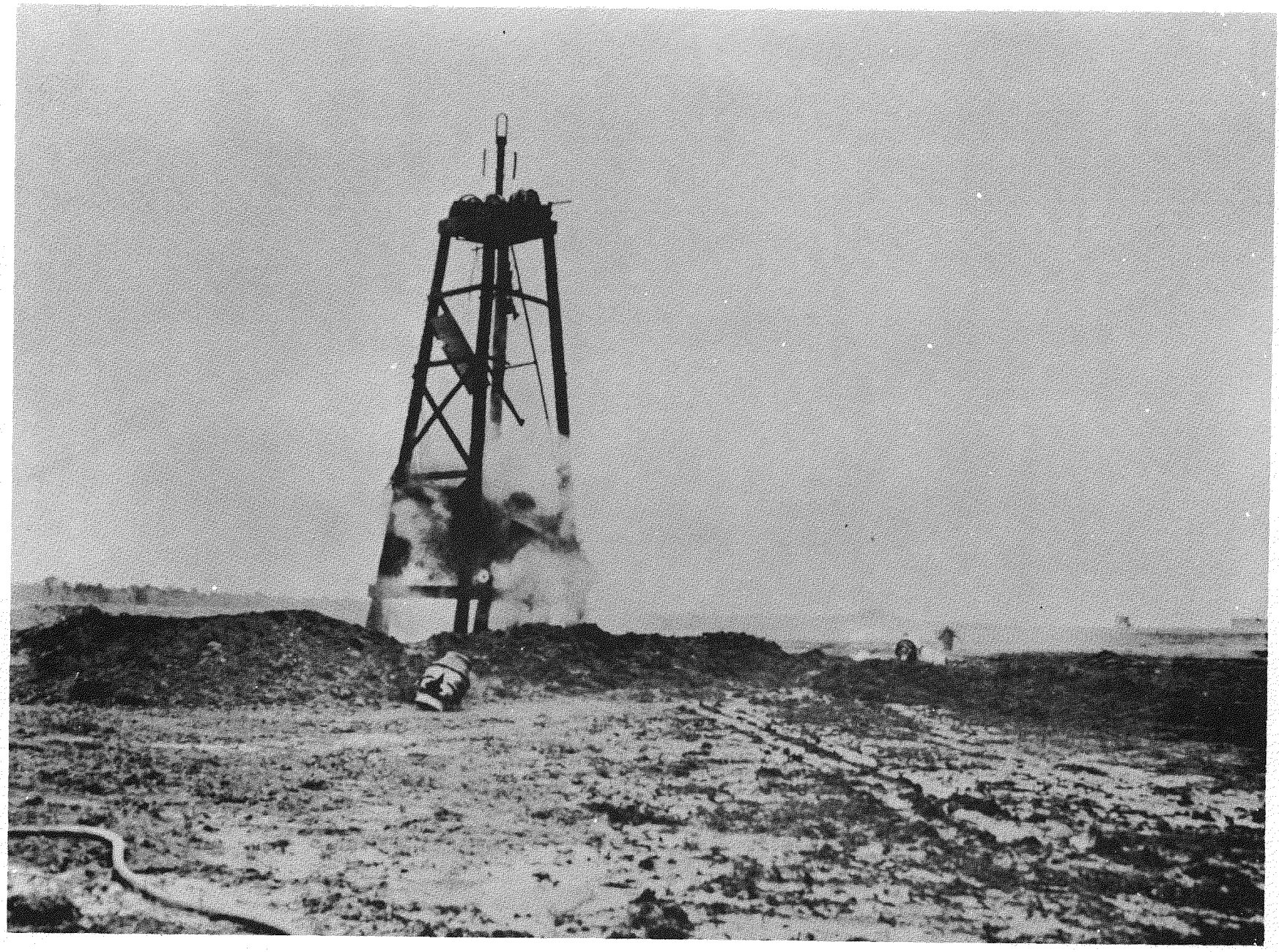

Fig. A-40. Fire Tower After Test

D. THERMAL SHOCK AND CORROSION TESTS

These tests were conducted by the Martin Nuclear Division Materials Unit. A single specimen was tested for thermal shock and corrosion tests were performed on five different materials.

1. Thermal Shock Test

This test was conducted on May 4, 1960 at the Martin airport revetment facility.

Procedures. A stone crock containing 40 liters of liquid oxygen was utilized as a test receptacle. This container was positioned below a tube furnace. The furnace, which was set up with its major axis in a longitudinal plane, was provided with two insulated doors, one at the top and the other at the bottom.

The top door was opened and the test specimen was inserted into the furnace. After heating to 1200° F, the specimen was lowered through the bottom door and quenched in the crock of LOX. All operations were performed remotely with the aid of a pulley system.

Temperatures of the specimen in the LOX were recorded periodically. After one hour of cooling, the test sample reached ambient air temperatures (73° F) and the test was terminated.

Test specimen. The specimen utilized in this test was specimen Type 1, No. 8 and its Design Number was A-I_{CeO_2}. Specifications for this specimen are given in Table A-1.

Test results. Boundary turbulence and boiling of the LOX were not excessive. The core retained its metallic luster and only a slight bluish iridescent oxide film formed at the top of the block. There was no change in weight and no cracking (or crazing) of the surface was noted. The core was not affected by extreme thermal shock.

2. Corrosion Tests

Corrosion tests were conducted in the laboratory under simulated operating conditions whenever possible. Results of these tests are given in Table A-15; procedures are detailed below.

Air oxidation test. Six degreased weighted specimens of each material, Hastelloy B and Inconel X, were exposed to air at 1700° F. The specimens were secured in Vycor holders to avoid contamination from the pot furnaces. One specimen of each material was removed after each hour of exposure for six hours. Metallographic examination was made on each of the specimens.

TABLE A-15

Summary of Corrosion Test Results

Test	Material	Test Time (hr)	Corrosion Rate (mdd)*	Penetration Rate (mpy)**	Control Corrosion Rate (mdd)	Control Penetration Rate (mpy)
Air oxidation at 1700° F	Inconel X	6	255	44	--	--
Fuel compatibility CeO_2	Inconel X Tantalum	72 72	*** SA****		nil	nil
Fuel compatibility Ce metal	Inconel X Tantalum	72 72	SA nil			
Sea water at 110° F	Inconel X	980	0.7	0.1	nil	nil
Mercury at 600° F	Inconel X	30	nil	nil		
Red fuming HNO_3 at 77° F	Inconel X	96	1.2	0.02		
Red fuming HNO_3 at 125° F	Inconel X (refluxed)	96	55	9.6		
Red fuming HNO_3 at 1500° F and quenched	Inconel X	96	6.4	1.1		

NOTE:

* Milligrams per square decimeter per day

** Mils per year

*** Formed tightly adherent, protective oxide film which could not be removed with normal reagents

**** SA--severely attacked.

One specimen of each material was exposed to air at 1700° F for six hours and evaluated as follows:

(1) Loose corrosion products were removed by brushing in soapy water.

(2) Specimens were rinsed in demineralized water and acetone, thoroughly dried in a desiccator and weighed.

(3) Oxide film was removed by treating the specimen in a 10% sodium hydroxide-5% potassium permanganate solution at 200° F, and finally in a 5% oxalic acid solution.

Vanadium and tantalum were not tested because available data show poor resistance to air oxidation.

Fuel compatibility. Fuel compatibility of the container materials was measured for cerium metals and ceric oxide fuel forms. About 9 to 15 grams of the two fuel forms were encapsulated into chemically cleaned crucibles fabricated from the container materials. These crucibles were sealed into containers which were evacuated and heated to 1700° F in pot furnaces. After 72 hours, the test specimen crucibles were descaled and corrosion rates were determined from weight losses.

Sea water corrosion tests. Calculations indicated that a fuel core immersed in the ocean would attain an outside surface temperature of approximately 120° F above ambient. Hence, the sea water corrosion tests were developed to measure corrosion rates at this temperature. The condition was simulated in the laboratory by heating tubular test specimens immersed in sea water. Hot water at 180° F was circulated through the weighed, chemically cleaned specimen by a centrifugal pump. The sea water was contained in a plexiglas container and was maintained at a 70° F temperature by employing a stainless steel cooling coil. A control specimen for each material was exposed to the sea water at ambient temperature. After exposure of between 30 and 41 days, the specimens were removed from the bath and evaluated. Photomicrographs were used in this evaluation.

Mercury tests. To determine corrosion resistance of the container materials to mercury, actual operating conditions were simulated. Type 316 stainless steel test containers, with a hollow central tube into which an electric heater was inserted, were utilized. Weighed test specimens were inserted into the mercury-filled container in contact with the hot central tube. The test container temperature was adjusted to 600° F on the outside surface. After 30 minutes, the test specimens were reweighed and a corrosion rate established.

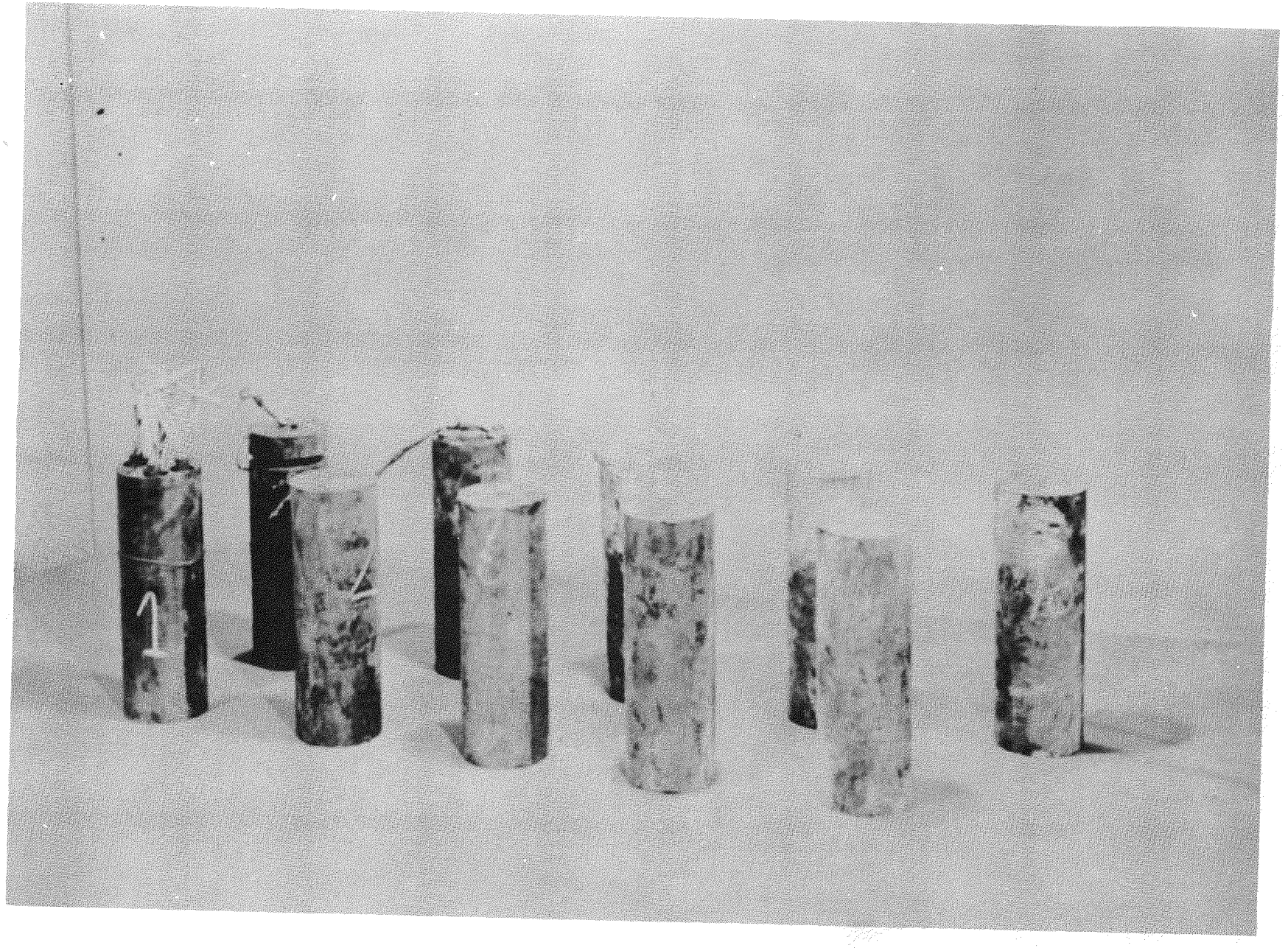

Fig. A-41. Fire and Fallout Test Fuel Cores

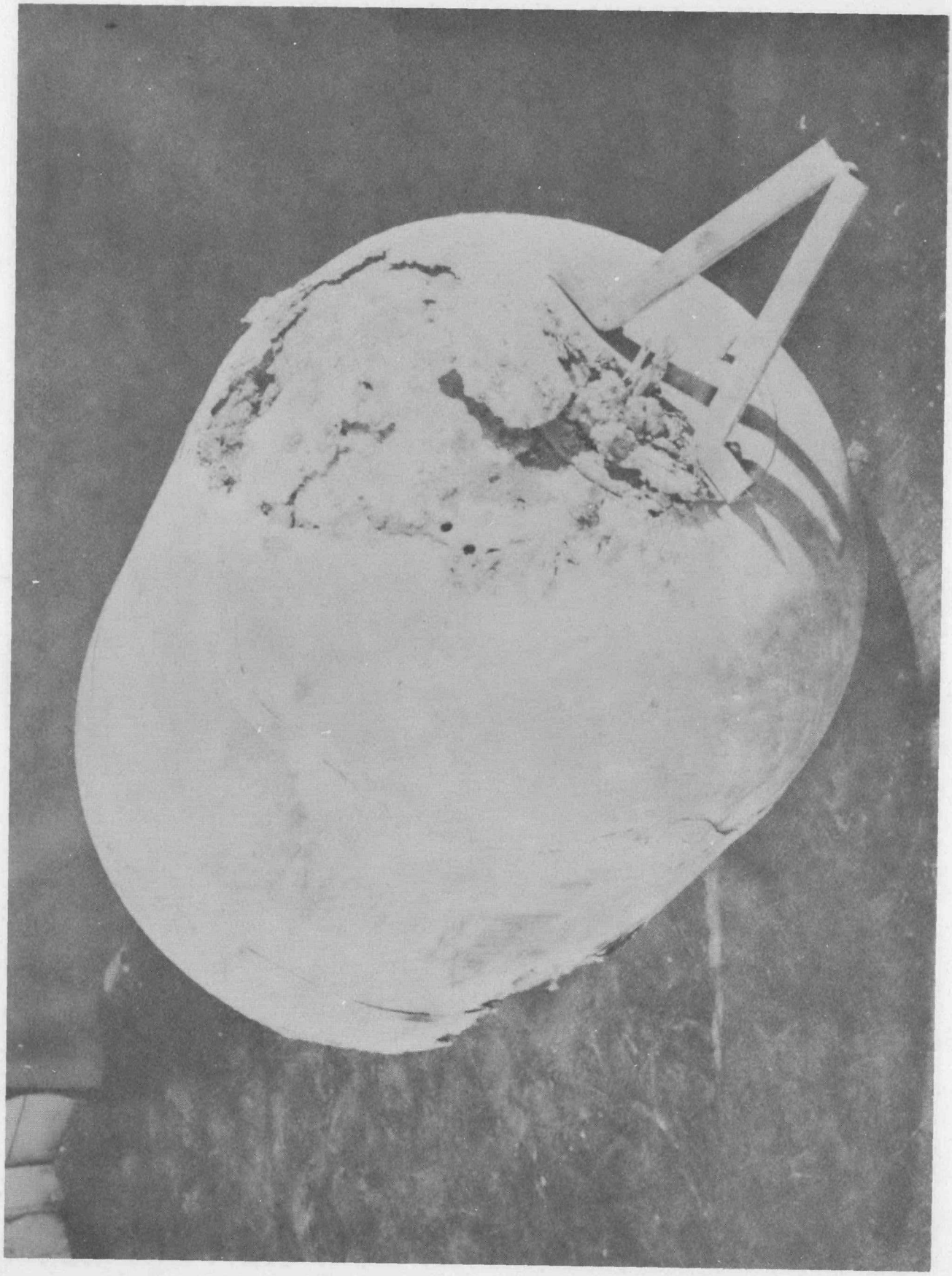

Fig. A-42. Tested Task 2 Generator--Top View

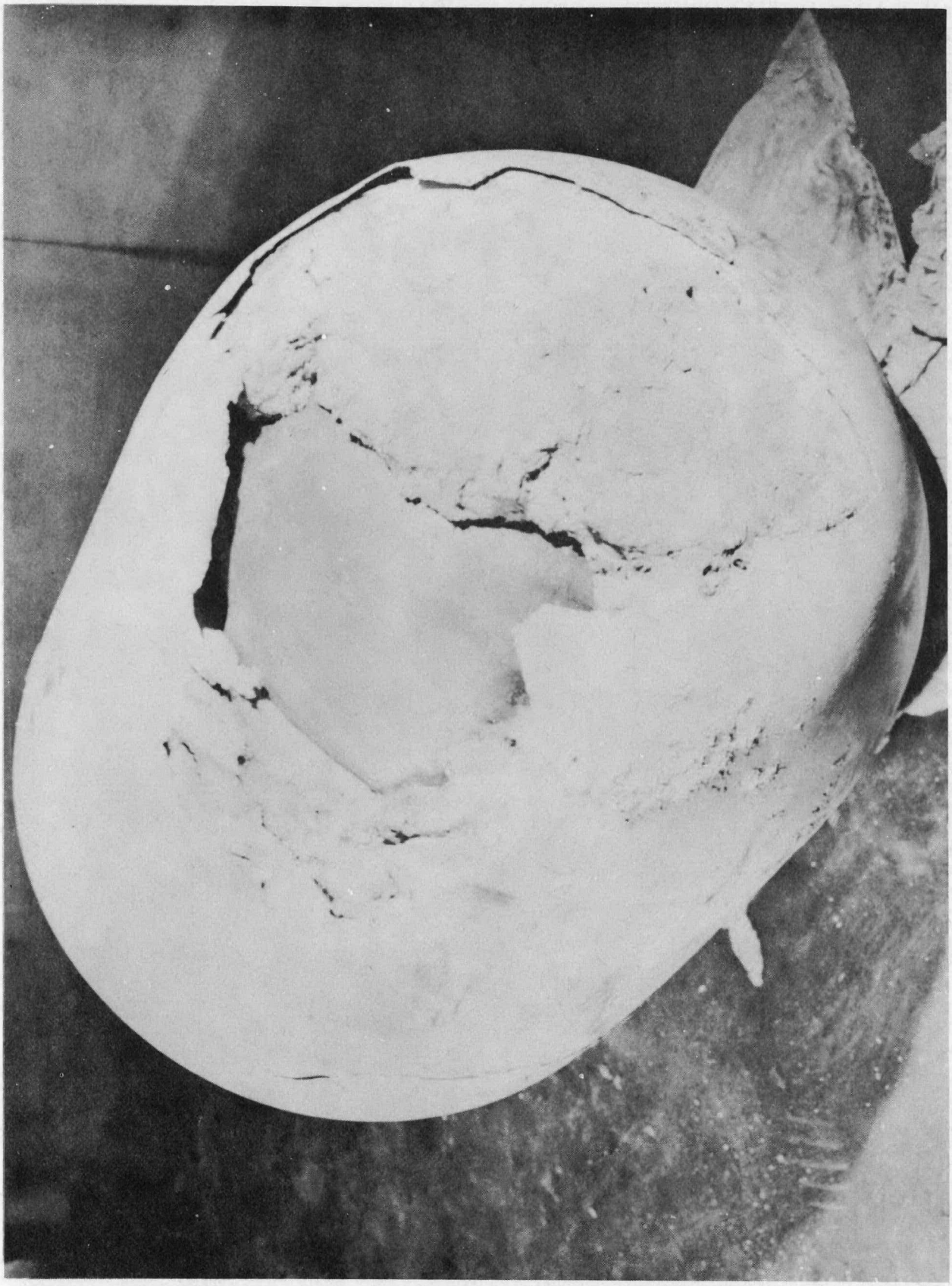

Fig. A-43. Tested Task 2 Generator--Bottom View

Fig. A-44. Fuel Core of Tested Task 2 Generator

APPENDIX B

AERODYNAMICS*

Analytical methods used for the computation of trajectories, aerodynamic heating rates generated on re-entering bodies and ablation rates of the bodies are presented. Computer programs are used extensively in this analysis and are modifications of those that were initiated on past operational projects.

The scheme for the analytical procedure carried out in this study is as follows. Essentially, the final stage is ignited at such an altitude and flight condition that if the stage fires successfully, the satellite would enter a 300-mile circular polar orbit. If the thrust is prematurely cut off or misaligned during this stage of injection, an undesirable flight altitude will be obtained. Depending upon the degree of error, the satellite will enter into an elliptical orbit or immediately re-enter the atmosphere. The case history of the thermoelectric generator then becomes of concern. In particular, the location and condition of the isotopic fuel and its containment must be determined. Aerodynamic forces become significant at an altitude near 375,000 feet and the thin outer shell of the satellite vehicle will fail. As the isotope unit with some structural aluminum attached is released, the aluminum outer wall and steel inner wall of the generator shell are subsequently melted and the core is exposed to the atmosphere. The fuel core then finally melts and burns up at altitude. A change in ballistic coefficient between the less dense complete unit and heavier core is noted. For purposes of determining final terminal velocities, these ballistic coefficient values are increased when the velocity becomes subsonic. Methods used for this analysis are described below.

A. TRAJECTORY PROGRAMS

There are several types of IBM 709 trajectory programs available especially designed for versatility in handling other than normal ascent and re-entry flight paths.

Among the most commonly used is the N-Stage Two-Dimensional Powered Trajectory Program. The following summarizes the equations and coordinate system used in the program. This program is used to compute normal ascent and re-entry trajectories, but can also be used to compute misalignments of thrust in the pitch direction (directly upward and downward). A spherical earth is considered, but any launch azimuth or position can be handled. Coast phases may be integrated where aerodynamic effects are desired, but where thrust is not available. The trajectory can also be computed as an elliptical path when external forces are not present.

---

* W. Hagis

The coast phase of an ascent or re-entry trajectory is an integrated sequence where the aerodynamic drag and the missile's weight are the only forces affecting the flight path. This maneuver is normally used during the ascent portion to enable the missile to reach a prescribed altitude and flight path angle (γ). Currently, all re-entries are flown with the coasting maneuver.

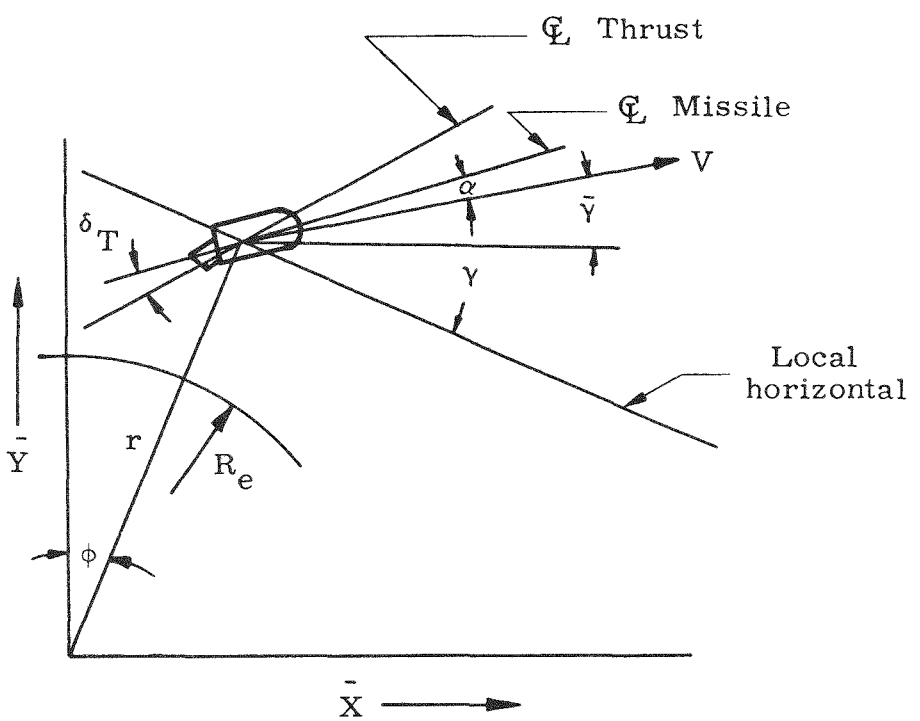

$\bar{X}$, $\bar{Y}$	Inertial axis
R_e	Radius of earth
r	Radius of vehicle from center of earth
ϕ	Range angle
α	Vehicle angle of attack
γ	Local flight path angle
$\bar{\gamma}$	Inertial flight path angle

δ_p	Thrust alignment in pitch
μ	Earth's gravitational constant
m	Mass of vehicle

Equations

$$\ddot{\bar{X}} = -\left[\frac{T \sin(\alpha + \delta_p) + L}{m} - \frac{\mu}{r^2} \cos \gamma\right] \sin \bar{\gamma}$$

$$+ \left[\frac{T \cos(\alpha + \delta_p) - D}{m} - \frac{\mu}{r^2} \sin \gamma\right] \cos \bar{\gamma}$$

$$\ddot{\bar{Y}} = \left[\frac{T \sin(\alpha + \delta_p) + L}{m} - \frac{\mu}{r^2} \cos \gamma\right] \cos \bar{\gamma}$$

$$+ \left[\frac{T \cos(\alpha + \delta_p) - D}{m} - \frac{\mu}{r^2} \sin \gamma\right] \sin \bar{\gamma}$$

The free flight method of analysis solves the elliptical equations of motion and is used when the vehicle or re-entry body is above the significant atmosphere where the flight path is determined only by gravitational and centrifugal forces. These calculations are normally used for determining the flight path from orbital departure altitude to the re-entry altitude (approximately 375,000 to 400,000 feet). The re-entry altitude is defined as the altitude where aerodynamic forces become significant.

Three-Dimensional Trajectory Programs are available for more complicated maneuvers where vehicle motion can be calculated for lateral displacement. These programs are usually too detailed for advanced design calculations and are reserved for checkout of preliminary calculations, or are used when three-dimensional trajectories dictate no other choice. Two such programs are available at The Martin Company. One is just a refinement of the original program to enable additional application of guidance laws. The Basic Three-Dimensional Trajectory Program can be easily modified to account for

specific missions. An oblate, rotating earth is assumed, with provisions to launch at any point on the earth's surface and at any launch angle. Ground traces are printed continuously, giving the vehicle's latitudinal and longitudinal coordinates, altitude, and velocity.

B. AERODYNAMIC HEATING

On a blunt nose the aerodynamic heating becomes a function of nose shape, Mach number, atmospheric pressure and nose radius. The relations used are shown in Fig. B-1.

For the present shell analysis, the laminar hemispherical values were used. An integration of the value around the entire nose indicates that an average value of 0.35 of the stagnation value would be applicable for the tumbling outer sphere. This method is somewhat conservative since no turbulent flow heating was used. (Fig. B-1 shows that a considerable amount of heating could be derived from this source.) In general, on a roughened spherical nose, turbulent flow will be obtained back of the 40-degree total central arc.

For the round cylindrical core analysis, the two-dimensional equivalent of K_1 and K_3 must be used. These are also shown in Fig. B-1.

Figure B-2 shows a typical re-entry heating rate as a function of time.

C. HEAT TRANSFER

The Martin Company digital program for ablation has a method of analysis similar to that used by ABMA. With the trajectory and aerodynamic heating methods established it becomes necessary to calculate the heat transfer through the unit. It is an empirical approach and is primarily a function only of the melting temperature and heat of fusion of the materials under consideration. Flexibility in the procedure is achieved by being able to vary the above two values. The method is essentially the solution of a series of simultaneous equations for calculating heat flow rates through materials. A body of revolution, such as the cylindrically shaped fuel element, will be treated as a series of concentric cylindrical shells. The transfer of heat through each layer will be determined so that the outermost layer (number 1) will conduct heat to the next layer (number 2). The applied heat will pass through number 2 and be applied to the next layer and so on. As sufficient heat is applied to the first layer to completely melt it, the program will Ablate this layer. The number of simultaneous heat transfer equations and layers that the fuel cylinder specimen need be reduced is a function of its shape, type of material, etc. Figure B-3 shows the scheme for analysis and a summary of equations.

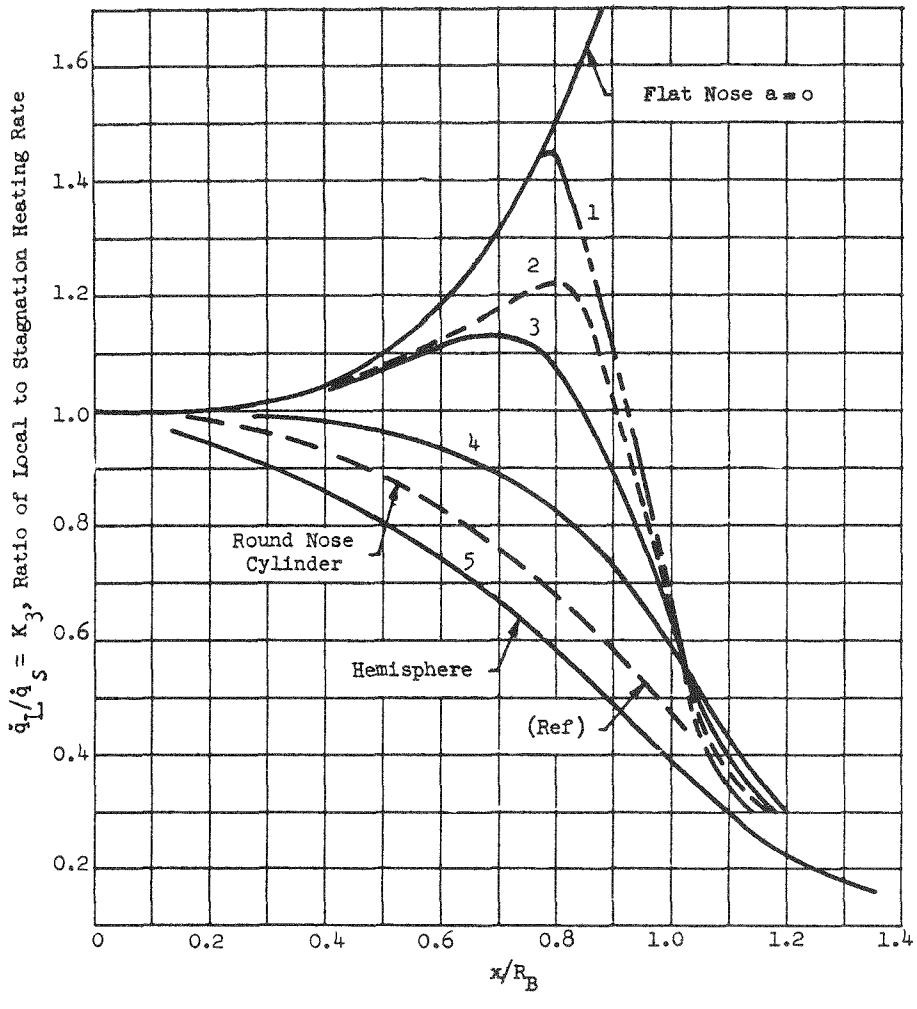

$$\frac{z^2}{a^2} + y^2 = R_B^{\,2}$$

1 a = 0.037
2 a = 0.333
3 a = 0.5
4 a = 0.666
5 a = 1.0

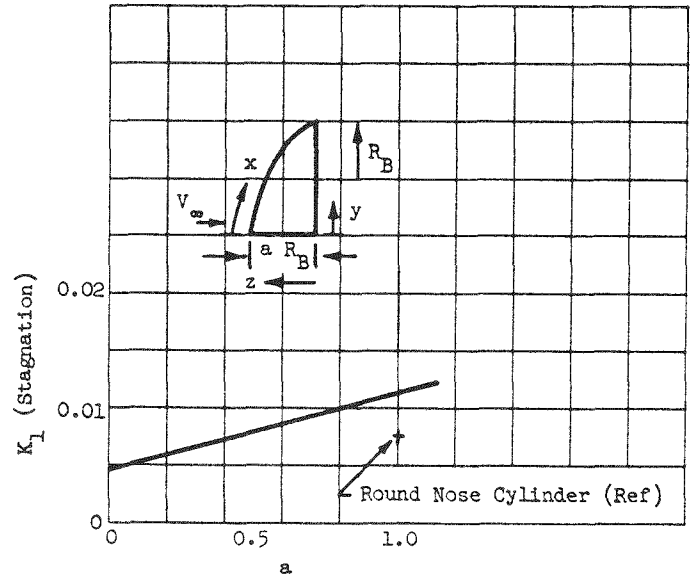

$$\dot{q}_L = K_1 K_3 M_\infty^{3.34} \left(\frac{P_\infty}{R_B}\right)^{1/2} \left[1 - 0.0137\, M_\infty\right] \text{ Btu/sq ft-sec}$$

Fig. B-1. Axially Symmetric Nose Aerodynamic Heating

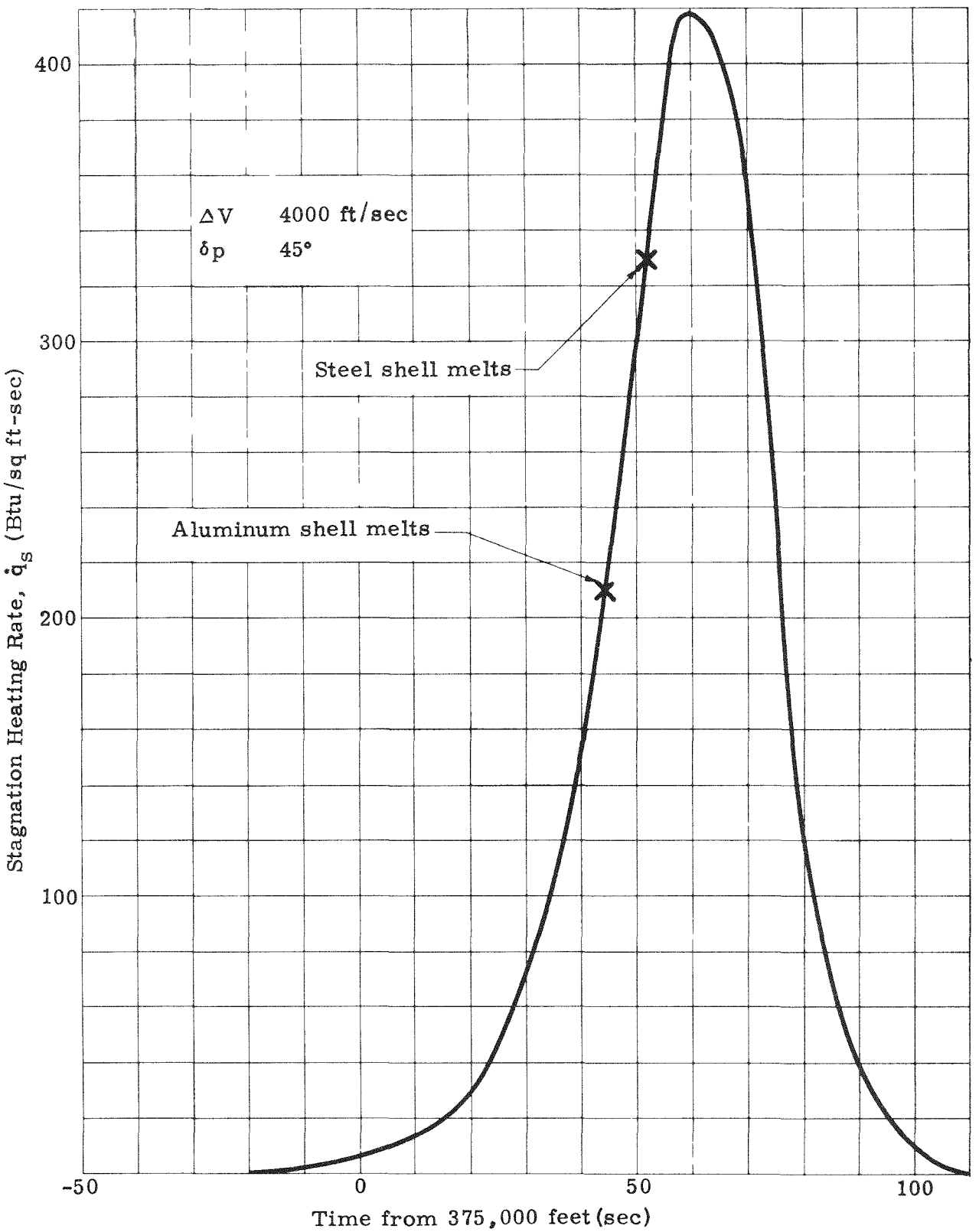

Fig. B-2. Shell Stagnation Heating Rate

Element	Aerodynamic Heat In	- Heat Radiated Out	+ Heat Conducted In-Out	= Heat Stored + Phase Change
1	$\dot{q}_{in}$	$- \sigma\epsilon \quad T_1^4 - T_\infty^4$	$- \frac{k}{\Delta x}(T_1 - T_2)$	$= \frac{\rho C_p \Delta x}{\Delta t} \Delta T_1 + \frac{\rho \Delta x}{\Delta t} L_F = \frac{\rho C_p \Delta x}{\Delta t}\left(\Delta T_1 + \frac{L_F}{C_p}\right)$
2			$+ \frac{k}{\Delta x}(T_1 - T_2) - \frac{k}{\Delta x}(T_2 - T_3)$	$= \frac{\rho C_p \Delta x}{\Delta t}(\Delta T_2)$
3			$+ \frac{k}{\Delta x}(T_2 - T_3) - \frac{k}{\Delta x}(T_3 - T_4)$	$= \frac{\rho C_p \Delta x}{\Delta t}(\Delta T_3)$

etc.

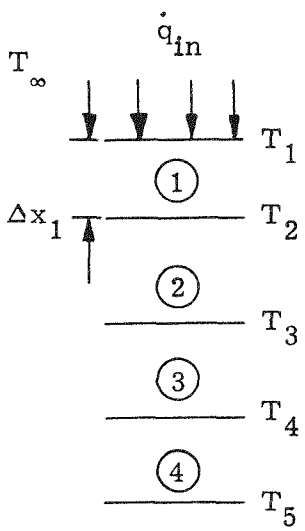

ΔT_1 = increment of temperature T_1 for a time increment Δt

For initial values of T_1, T_2, etc., a step by step solution of a series of set of simultaneous equations is performed. T_1 increases until $T_1 = T_{melt}$; at this time the heat balance (T_2, T_3, etc.) is held until T_1 increases an amount L_F/C_p. At this time the outer element (1) is melted and the old element (2) now becomes new element (1) and the process is repeated. For a sphere or cylinder, the heating rate is increased for a decrease in radius.

Fig. B-3. Heat Transfer Scheme (per unit area)

First, an equivalent heat transfer configuration for the basic thermoelectric generator was established as shown in the sketch.

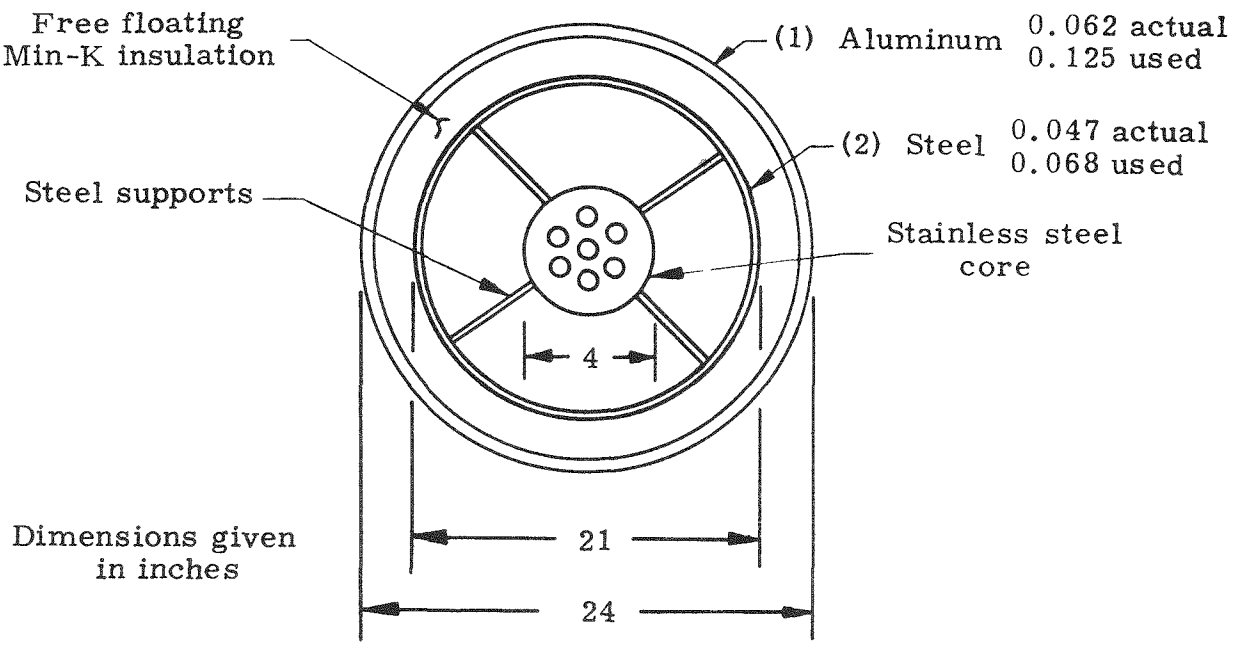

(1) To represent the effect of light aluminum satellite structure, the outer shell of the generator was increased to 0.125 from the actual value of 0.0625.

(2) An additional five pounds of steel were distributed both to the outer steel shell and the stainless core. The five pounds represent 1/6 of the support structure weight. This increased the stainless steel shell from the actual value of 0.047 to 0.068 and the core diameter from 3.75 to 4.0 inches.

The following material properties were used.

Outer Shell	Aluminum	Steel
C_p, Specific heat--Btu/lb-°F	0.226	0.150
T_m, Melting temperature--°R	1670	3000
L_F, Heat of fission--Btu/lb	167	117
ρ, Density--lb/cu ft	169	496

Core. Since the heating elements are already molten, it is assumed that this liquid has no effect on the heat balance and serves only to maintain shape.

C_p = 0.105 at 100° F
0.120 at 1000° F

*k = 3.3 at 100° F
6.35 at 1000° F

T_m = 3000° R

L_F = 117 Btu/lb

*ρ = 0.126 lb/cu in.

Using this information and heat input data from curves similar to Fig. B-2, the heat balance equation for a number of elements may be calculated as shown in Fig. B-3.

Outer shell. To further illustrate the use of the method, consider the outer shell with its thin walls.

For the outer aluminum shell

Heat In - Heat Radiated = Heat Stored + Phase Change

$$(\dot{q}_{in} - \sigma\epsilon T_w^4)\ \Delta t = W\ C_p\ \Delta T + L_F\ W$$

$$= W\ C_p \left(\Delta T + \frac{L_F}{C_p}\right)$$

For a time increment, Δt, the temperature increases an amount ΔT. The heat of fusion is equivalent to a temperature increase L_F/C_p. The material of a thin element can therefore be considered to be removed at $T = T_{melt} + L_F/C_p$. For aluminum, T_{melt} is 1670° R and the radiation is small.

---

* Forty-four percent of the core volume is steel, hence k = 0.44 k steel and ρ = 0.44 ρ steel.

$$\dot{q}_{in} A = \frac{\rho A \ \Delta x}{\Delta t} \Delta T$$

$$\Delta T = \frac{\dot{q}_{in}}{\rho \Delta x \ C_p} \Delta t$$

Δx,	shell thickness--feet	0.0104
Δt,	time increment--seconds	10
$\dot{q}_{in}$,	0.35 stagnation heating rate	Fig. B-2

$$T_{final} = T_m + \frac{L_F}{C_p} = 1670 + \frac{167}{0.226} = 2404° \text{ R}$$

$$\Delta T = 8.85 \ \dot{q}_{in_{stagnation}} \quad \text{for 10-second interval}$$

t	$\dot{q}_{in}$	$\dot{q}_{av}$	ΔT	T (°R)
-20	0			400.0
		1.0	8.9	
-10	2			408.9
		3.0	26.5	
0	4			435.4
		7.0	62.0	
10	10			497.4
		18.0	159.0	
20	26			656.4
		48.0	425.0	
30	70			1081.4
		110.0	975.0	
40	150			2056.4
		225.0	1990.0	
50	300			4046.0

Aluminum is considered melted at t = 44 seconds and 2404° R.

Steel shell

Δx,	shell thickness--feet	0.00566
Δt,	time increment--seconds	1
L_F,	heat of fusion--Btu/lb	117

$$T_{final} = 3010 + \frac{117}{0.150} = 3790° \text{ R}$$

$$\Delta T = 0.835 \, \dot{q}_{in_{stagnation}}$$

For the steel inner wall of the outer shell, radiation is no longer negligible.

$$\Delta \dot{q}_{radiation} = \sigma \epsilon T_w^{\,4} \text{ or } \Delta \dot{q}_R = \left(\frac{T}{1230}\right)^4$$

t	$\dot{q}_{in}$	$\dot{q}_{av}$	$\Delta \dot{q}_R$	$\Delta \dot{q}_c$	ΔT	T
44	210					2060
		217.5	- 8.0	209.5	174	
45	225					2234
		232.5	-10.5	222.0	185	
46	240					2419
		247.5	-15.0	232.5	193	
47	255					2612
		262.5	-20.0	242.5	202	

t	$\dot{q}_{in}$	$\dot{q}_{av}$	$\Delta\dot{q}_R$	$\Delta\dot{q}_c$	ΔT	T
48	270					2814
		277.5	-32.0	245.5	204	
49	285					3018
		292.5	-35.0	257.5	214	
50	300					3232
		307.5	-35.0	272.5	227	
51	315					3459
		322.5	-35.0	287.5	240	
52	330					3699
		337.5	-35.0	302.5	252	
53	345					3951
		352.5	-35.0	317.0	264	
54	360					4215
		367.5	-35.0	332.5	278	
55	375					

∴ Steel is consumed at 52 seconds.

Upon the complete melting of the outer aluminum and steel shells, the insulating materials and the thermoelectric elements are separated. The remaining aerodynamic heat is applied to the fuel core. Utilization of the Ablation Program is initiated at this time.

Thus, by the simultaneous use of trajectory analysis, aerodynamic heating rates generated during re-entry, and the Ablation Heating Program, it is possible to determine the rate of ablation of the generator components and the geographical location of impact or of altitude of burnup.